AUS DEM LEHRSTUHL
FÜR NEUROLOGIE
PROF. DR. MED. ULRICH BOGDAHN
DER FAKULTÄT FÜR MEDIZIN
DER UNIVERSITÄT REGENSBURG

The Influence of Metformin and TGF-β_2 on Proliferation and Migration of Glioblastoma Cells

Inaugural – Dissertation
zur Erlangung des Doktorgrades der Medizin

der
Fakultät für Medizin
der Universität Regensburg

vorgelegt von
Anne-Louise Meyer

2016

AUS DEM LEHRSTUHL
FÜR NEUROLOGIE
PROF. DR. MED. ULRICH BOGDAHN
DER FAKULTÄT FÜR MEDIZIN
DER UNIVERSITÄT REGENSBURG

The Influence of Metformin and TGF-β_2 on Proliferation and Migration of Glioblastoma Cells

Inaugural – Dissertation
zur Erlangung des Doktorgrades der Medizin

der
Fakultät für Medizin
der Universität Regensburg

vorgelegt von
Anne-Louise Meyer

2016

Dekan:	Prof. Dr. Dr. Torsten E. Reichert
1. Berichterstatter:	Prof. Dr. med. Peter Hau
2. Berichterstatter:	Prof. Dr. med. Martin Proescholdt
Tag der mündlichen Prüfung:	19.04.2017

Selbstständigkeitserklärung

Ich, Anne-Louise Meyer, geboren am 25.12.1988 in Itzehoe, erkläre hiermit, dass ich die vorliegende Arbeit ohne unzulässige Hilfe Dritter und ohne Benutzung anderer als der angegebenen Hilfsmittel angefertigt habe.

Die aus anderen Quellen direkt oder indirekt übernommenen Daten und Konzepte sind unter Angabe der Quelle gekennzeichnet. Insbesondere habe ich nicht die entgeltliche Hilfe von Vermittlungs- bzw. Beratungsdiensten (Promotionsberater oder andere Personen) in Anspruch genommen. Niemand hat von mir unmittelbar oder mittelbar geldwerte Leistungen für Arbeit erhalten, die im Zusammenhang mit dem Inhalt der vorgelegten Dissertation stehen.

Die Arbeit wurde bisher weder im In- noch im Ausland in gleicher oder ähnlicher Form einer anderen Prüfungsbehörde vorgelegt.

_____ _____

Ort, Datum Unterschrift

Table of Contents

Selbstständigkeitserklärung V

1 ABSTRACT 1

2 ZUSAMMENFASSUNG 2

3 INTRODUCTION 4

3.1 Glioblastoma 4

3.2 The role of metformin in diabetes and glioblastoma 10

3.3 The role of TGF-β_2 in glioblastoma 16

3.4 Possible links between metformin and TGF-β_2 22

3.5 Research aim 24

4 MATERIAL AND METHODS 25

4.1 Material 25

4.1.1 Consumables and supplies 25

4.1.2 Glioblatoma cell lines 26

4.1.3 Culture media and supplements 28

4.1.4 Additional substances and solutions 30

4.1.5 Equipment 30

4.1.6 Software 31

4.2 Methods 31

4.2.1 Cell culture 31

4.2.2 Cell Proliferation Assays 33

4.2.3 Crystal-Violet Staining 36

4.2.4 Spheroid Assay 37

4.2.5 Scratch Migration Assay 39

4.2.6 Analysis of data 40

5 RESULTS 41

5.1 The functional effects of metformin on GBM cells 41

5.1.1 Overall, high doses of metformin reliably reduced proliferation and migration 41

5.1.2 Susceptibility to metformin's anti-proliferative and anti-migratory action varied among subgroups of cells 43

5.1.3 Unique cellular reaction patterns to metformin....48
5.2 The functional effects of TGF-β_2 on GBM cells....60
5.2.1 TGF-β_2's effects were anti-proliferative and anti-migratory....60
5.2.2 Mesenchymal GBM cell lines were most susceptible to TGF-β_2....62
5.2.3 Unique cellular reaction patterns to TGF-β_2 and SD-208....66
5.3 The functional effects of metformin and TGF-β_2 on GBM cells....73
5.3.1 Metformin and TGF-β_2 were anti-proliferative and anti-migratory....73
5.3.2 The combination of 10 mM metformin and 10 ng/ml TGF-β_2 reduced proliferation and migration especially in mesenchymal cell lines....75
5.3.3 Unique cellular reaction patterns to the combination of TGF-β_2 and metformin80
5.4 Synopsis of the functional effects of metformin, TGF-β_2 and SD-208....98
6 DISCUSSION....100
6.1 The role of metformin in GBM....100
6.2 The role of TGF-β_2 in GBM....106
6.3 Possible links between metformin and TGF-β_2 in GBM....111
6.4 Outlook....119
7 LITERATURE....121
8 APPENDIX....132
8.1 Table of Abbreviations....132
8.2 Table of Figures....139
8.3 Table of Tables....143
8.4 Table of Equations....145
8.5 Acknowledgments....146

1 ABSTRACT

To this day, glioblastoma (GBM) remains a brain tumor impossible to cure. Among its tumor properties are rapid proliferation and aggressive migration, two hallmarks investigated in this study. GBM's rapid recurrence after treatment is attributed to tumor cells exhibiting stem cell properties, the so called brain tumor initiating cells (BTICs). These are targeted by the anti-diabetic drug metformin which has demonstrated its anti-glioma potential in previous studies. However, metformin's mechanisms and especially its links to transforming growth factor beta 2 (TGF-β_2) are not yet fully understood. Therefore, this study explored the effects of different doses of metformin and a single dose of TGF-β_2 on proliferation and migration of proneural and mesenchymal BTICs and their differentiated counterparts (TCs) as well as possible functional interactions. Proliferation and migration of 5 BTIC and 5 TC lines were assessed in cell counts, CyQuant assays, spheroid migration assays and scratch migration assays.

The functional investigation showed that 10 mM metformin reliably reduced proliferation and migration of primary GBM cell lines and also demonstrated that low doses of metformin may inhibit proliferation of proneural BTICs. Proneural cells were more susceptible to metformin than mesenchymal cells and BTICs were more susceptible than TCs providing possible predictors for successful metformin treatment. The low-dose effects of metformin also seem attainable in brain tissue of human cancer patients. Hence, this study sets the rationale to explore higher doses of metformin in patients who may profit from metformin treatment, especially since proneural cells respond less to standard temozolomide (TMZ) treatment.

The effects of TGF-β_2, a cytokine held responsible for GBM's proliferation, invasion, angiogenesis and immunosuppression, were also assessed. Unexpectedly, TGF-β_2 had either no effects or it decreased proliferation and migration. Generally, mesenchymal cells showed an increased sensitivity.

As TGF-β_2 has been described to increase proliferation and migration while metformin may lower both, this study investigated whether their functional effects were opposite. This was not the case. The effects of the combination of TGF-β_2 and metformin were anti-proliferative and anti-migratory. They were either as strong as those of the single agents or stronger indicating that there is no functional opposition of the two but rather uniform effects possibly potentiating each other. Thus, this study suggests that metformin and TGF-β_2 exert their functional effects independently of each other.

2 ZUSAMMENFASSUNG

Das Glioblastom (GBM) ist ein bis heute nicht heilbarer Hirntumor. Diese Studie untersuchte zwei der wichtigsten Tumoreigenschaften des Glioblastoms, seine rasche Proliferation und seine Migration. Die hohe Rezidivrate bei Glioblastompatienten wird einer Zellpopulation mit Stammzelleigenschaften zugeschrieben, den sogenannten Hirntumor-initiierenden Zellen (BTICs). Bisherige Studien zeigten, dass die Vermehrung und die Wanderung von GBM Zellen im Allgemeinen und von BTICs im Speziellen mithilfe von Metformin reduziert werden können. Allerdings sind die Wirkmechanismen von Metformin und insbesondere seine potentiellen Interaktionen mit dem Wachstumsfaktor transforming growth factor beta 2 (TGF-β_2) bisher nicht vollständig verstanden. Darum untersuchte diese Studie die Wirkung verschiedener Dosen Metformin und einer Dosis TGF-β_2 auf die Proliferation und Migration von proneuralen und mesenchymalen BTICs und den jeweiligen differenzierten Tumorzellen (TCs) sowie mögliche Interaktionen. Proliferation und Migration von 5 BTIC- und 5 TC-Linien wurden mittels Zellzählungen, CyQuant Assays, Spheroid-Migrationsassays und Scratch-Migrationsassays untersucht.

Dabei zeigte sich, dass 10 mM Metformin zuverlässig Proliferation und Migration der GBM Zelllinien senkte und dass niedrige Dosen die Proliferation von proneuralen BTICs hemmten. Proneurale Zelllinien sprachen insgesamt besser auf Metformin an als mesenchymale und BTICs sprachen besser an als ausdifferenzierte Zellen. Damit kann die Einteilung von GBM in proneurale und mesenchymale Tumore weiter als Prediktor für das Ansprechen auf eine Behandlung mit Metformin erforscht werden um in der Zukunft möglicherweise klinische Anwendung finden. Da niedrige Metforminkonzentrationen realistischerweise im Hirngewebe erreicht werden können und proneurale Tumore schlecht auf die Standardbehandlung mit Temozolomid (TMZ) ansprechen, sollten klinische Studien mit Metforminbehandlung insbesondere bei Patienten mit proneuralen GBM durchgeführt werden.

Außerdem wurde die Wirkung von TGF-β_2, einem Wachstumsfaktor, der bei GBM Proliferation, Migration, Invasion und Angiogenese fördert und das Immunsystem supprimiert, untersucht. Im untersuchten zellulären Modell zeigte TGF-β_2 entweder keine Effekte oder senkte Proliferation und Migration. Hierbei wiesen mesenchymale Zelllinien eine höhere Sensitivität auf als proneurale.

Da TGF-β_2 als Proliferations- und Migrations-fördernd beschrieben worden ist, Metformin beides zu senken vermag und zudem als Antagonist von TGF-β_2 in anderen Tumormodellen beschrieben worden ist, untersuchte diese Arbeit des Weiteren, ob die Wirkungen von TGF-β_2 und Metformin einander entgegenstehen. Dies war nicht der Fall: Die

Kombinationsbehandlung war, wenn es Effekte gab, anti-proliferativer oder anti-migratorischer Natur. Dabei war die Wirkung entweder mindestens genauso stark wie bei Einzelbehandlung oder stärker. Insgesamt kann also nicht von einer entgegengesetzten Wirkung von Metformin und TGF-β_2 auf Proliferation und Migration von GBM Zellen ausgegangen werden. Vielmehr scheinen die funktionalen Effekte von Metformin und TGF-β_2 unabhängig voneinander zu sein.

3 INTRODUCTION

3.1 Glioblastoma

Although a rare tumor entity, glioblastoma (GBM) is one of the deadliest. In the US, 3.19 per 100,000 inhabitants acquire GBM per year and only 14% survive for more than two years. Five years after diagnosis, as few as 5% of the GBM patients are still alive making the diagnosis of GBM an almost certain death sentence (Stupp *et al.* 2009, Ostrom *et al.* 2014, Weller *et al.* Glioma guideline 2014).

Men are 1.6 times more likely to develop GMB than women (Dubrow *et al.*, 2011). Also, age presents one of the main risk factors with probability to develop GBM increasing exponentially to the 4th power of age (Dubrow *et al.*, 2011). However, GBM can affect any age group (Dubrow *et al.*, 2011, SEER Cancer Statistics Factsheets 2016). Although the exact mechanisms of tumor genesis remain elusive, several other GBM risk factors have been established including ionizing radiation, syndromes such as Li-Fraumeni, neurofibromatosis 1 and 2, retinoblastoma, Turcot's, tuberous sclerosis and multiple hamartoma (Houben *et al.* 2005, Schwartzbaum *et al.* 2006, Ostrom *et al.* 2014) and Caucasian ethnicity (Dubrow *et al.* 2011, Maile *et al.* 2016).

Patients suffering from GBM may present with a variety of symptoms. Twenty to 40% present with first time seizures (Glantz *et al.* 2000). Focal signs such as hemiparesis, hemihypaesthesia or aphasia, may be due to GBM (Omuro *et al.* 2013). Headaches, especially combined with nausea, vomiting, and those worsening when bending over, might also present the first symptom of a brain tumor (Forsyth *et al.* 1993). However, it is difficult to aptly diagnose GBM from generic symptoms such as headaches, ataxia, blurred vision, or dizziness (Urbánska et al 2014). Consequently, magnetic resonance imaging (MRI) is used to diagnose brain tumors. The combination of MRI and FET-PET (*O*-(2-[^{18}F]fluoroethyl)-l-tyrosine positron emission tomography) increases specificity in glioma detection (Pauleit *et al.* 2005). However, only biopsy or primary resection with subsequent histological analysis can determine whether or not a brain tumor belongs to the group of GBM (Weller *et al.* Glioma guideline 2014).

Until 2016, Glioma was classified solely according to histological criteria defined by the 4th Edition of the WHO Classification of Tumors of the Central Nervous System (Louis *et al.* 2007). Proliferation rate, infiltration of surrounding tissue, mitotic rate and atypical mitosis, cell and nuclear atypia, microvascular proliferation, endothelial proliferation, and necrosis, are evaluated to determine the WHO grade (I-IV) of a central nervous system (CNS) tumor

(Louis *et al.* 2007). GBM is a WHO grade IV brain tumor entity which belongs to the astrocytic tumor group and is characterized by:

- high proliferation rates
- high number of atypical mitosis
- increased necrosis
- microvascular proliferation

The update on the 4th Edition of WHO Classification of Tumours of the Central Nervous System from 2016 (Louis *et al.* 2016) also accounts for genetic markers. Thus, mutations in the *isocitrate dehydrogenase* (*idh*) gene, defining whether a GBM is primary (*idh*-wildtype) or secondary (*idh*-mutant) are represented. Overall, GBM is now classified as a grade IV tumor within the group of diffuse astrocytic and oligodendroglial tumours according to mutational status (Louis *et al.* 2016):

- GBM, IDH-wildtype
    - Giant cell GBM
    - Gliosarcoma
    - Epithelioid GBM
- GBM, IDH-mutant.

Idh-mutational status, histological criteria as well as molecular and genetic markers are also considered to plan treatment and predict outcome (Riemenschneider *et al.* 2010, Weller *et al.* 2014). First, *idh* mutations can be helpful not only to differentiate between primary and secondary GBM, but also to differentiate between grade II or III glioma from grade IV glioma, because *idh*-1 and -2 mutations are found in approximately 80% of patients suffering from grade II or III glioma, but in only 5 to 10% of patients suffering from grade IV glioma (Weller *et al.* Glioma guideline 2014). The enzyme IDH catalyzes the oxidative decarboxylation of isocitrate, which is converted into α-ketoglutarate under production of NADPH (Olar *et al.* 2014). However, if an *idh*-mutation is present, isocitrate is converted to the oncometabolite 2-hydroxyglutarate (Olar *et al.* 2014). Due to its correlation with low grade tumors, but also due to other mechanisms, the presence of *idh*-mutations usually implies a better outcome (Olar *et al.* 2014). Additionally, assessing *mgmt*-methylation is useful for planning therapeutic procedures and for predicting the outcome. O^6-methyguinine-DNA-methyltransferase (MGMT) is an enzyme involved in DNA repair. If the promoter region of *mgmt* is methylated, its transcription is inhibited resulting in lower enzyme levels and consequently reduced ability of tumor cells to repair their DNA. Thus, treatment with TMZ, a DNA alkylating agent (Stupp *et al.* 2005), is more effective in patients suffering from *mgmt*-methylation positive GBM (Weller *et al.* Glioma guideline 2014).

In general, gliomas are treated according to their WHO grade. For GBM, standard treatment includes complete macroscopic resection of the tumor if possible and subsequent radio-chemotherapy (Stupp *et al.* 2005, Weller *et al.* Glioma guideline 2014). Surgery aims at cytoreduction of > 98% (Adamson *et al.* 2009). During surgery, the tumor can be stained with 5-aminolevulinic acid to enable surgeons to distinguish cancer tissue from healthy brain tissue (Stummer *et al.* 2006). Alternatively, sodium fluorescein is used as it seems to have less side effects and may be helpful in detecting metastases (Schebesch *et al.* 2012). Following partial or total resection, patients are treated with TMZ and focal radiation (Stupp *et al.* 2005). For older patients with a positive *mgmt* methylation status, radiation is renounced in favor of chemotherapy (Weller *et al.* Glioma guideline 2014). Apart from this standard regime, there are two approaches approved for treatment of recurrent glioma in the US (Swanson *et al.* 2016): bevacizumab and tumor treating fields (TTF). Bevacizumab is a vascular endothelial growth factor (VEGF) antibody designed to lower neo-vascularisation, which largely contributes to the malignancy of brain tumors (Würth *et al.* 2014). TTF are alternating electrical fields which impede mitosis and lead to reduced cell proliferation. Thus, the combination of TTF and TMZ prolongs OS from 15.6 months (TMZ treatment only) to 20.5 months (Stupp *et al.* 2015). The immune checkpoint inhibitors, ipilimumab, pembrolizumab, and nivolumab, are currently being evaluated in clinical trials (Theeler and Gilbert 2015). While ipilimumab is a humanized IgG1 monoclonal antibody against cytotoxic T lymphocyte antigen (CTLA-4), pembrolizumab and nivolumab are humanized monoclonal antibodies against programmed cell death 1 (PD-1) (Theeler and Gilbert 2015).

However, despite extensive research on and continuous improvement of GBM treatment, prognosis remains poor. The mean survival time after diagnosis equals approximately 15 months (Stupp et al 2005). However, prognosis of individual patients varies. Longer survival and higher quality of life are being reported for patients with (Louis *et al.* 2007, Adamson 2009, Verhaak et al 2010):

- lower age
- high Karnofsky index (indicating how well patients can perform everyday life tasks without external help)
- complete macroscopic primary resection (>98%)
- positive *idh* mutation status
- positive *mgmt* methylation status.

The poor prognosis of GBM is, among other factors, due to rapid recurrence after initial treatment. To explain rapid recurrence, it has been proposed that a small population of brain tumor initiating cells (BTICs) remains in the brain tissue after resection of the primary tumor

(Vescovi *et al.* 2006; Esparza *et al.* 2015). In 2006, Vescovi *et al.* proposed that these BTICs possess characteristic functional abilities:

- self-renewal
- formation of tumors in xenografts (e.g. mice)
- potency to form different subtypes of cells including non-tumerogenic end cells
- loss of proper differentiation
- genetic mutations.

In order to define brain tumor initiating cells, CD133 is widely used as a marker (Beier *et al.* 2011). However, this concept has been challenged by Chen *et al.* reporting in 2010 that $CD133^-$ brain tumor cells are also capable of forming new tumors in nude mice. These inconsistencies within the tumor stem-cell model led to alternative explanations for differences among tumor cell subpopulations such as genetic heterogeneity and micro-environment dependent plasticity (Meacham and Morrison 2013). While the tumor stem-cell model proposes a hierarchy of tumorigenic cells which can produce tumorigenic and non-tumorigenic spouses, the concept of micro-environment dependent plasticity argues that cell fates largely depend on cues from the surrounding tissue rather than on different hierarchies of tumor cells (Meacham and Morrison 2013). This study was based on the tumor stem cell model. CD133 was utilized to define stemness of BTICs along with transcription factor Sex determining region of Y (Sox2), the intermediate filament Nestin, which is highly expressed in developing neural cells, and Oligodendrocyte transcription factor 2 (Olig2) (Würth *et al.* 2014).

Tumors mostly develop *de novo*, so only approximately 10% of GBM are secondary deriving from lower grade lesions (Urbánska *et al.* 2014). Primary and secondary GBM differ in their genetic mutations indicating that there might be different mechanisms of tumor genesis. While primary glioma are distinctly characterized by over-expression of epidermal growth factor receptors (EGFR) and *phosphatase and tensin homolo*g (*pten*) mutations, they do not exhibit *idh1* mutations. Secondary glioma, on the contrary, show *idh1* mutations and *p53* mutations, but lack EGFR amplification (Riemenschneider *et al.* 2010). Examining primary glioma's specific patterns of genetic mutations, they prove to be substantially more varied than those of secondary gliomas, including alterations in Transforming growth factor beta signaling (TGF-β_1) (Tso *et al.* 2006). Genetic mutations and variant gene products present potential therapeutic targets. As over 50% of all GBM exhibit EGFR mutations, most commonly EGFR variant III (EGFRvIII), anti-EGFR therapeutic approaches are being evaluated (Francis *et al.* 2014, Furnari *et al.* 2015, Hicks *et al.* 2016). Also, compounds to inhibit TGF-β receptors and signaling have been explored (Hau *et al.* 2007, Bogdahn *et al.*

2011) and continue to be a focus of research (Nana *et al.* 2015, Herbertz *et al.* 2015, Gallo-Oller *et al.* 2016, clinical trials using the TGFR inhibitor galunisertib listed on www.clinicaltrials.gov: NCT02423343, NCT01220271, NCT01582269; Nov. 2016).

The heterogeneous group of GBM cells can be clustered into subgroups according to marker expression and genetic aberrations (Verhaak *et al.* 2010, Van Meir *et al.* 2010). In 2010, Verhaak *et al.* were able to distinguish the four subgroups of neural, proneural, classical and mesenchymal GBM cells. As experiments of the present work were conducted using proneural and mesenchymal cell lines, these are described in more detail in Table 1.

Table 1: Molecular and genetic characteristics of proneural and mesenchymal GBM cells (Verhaak 2010)

Subgroup	Marker expression	Characteristic mutations	Further frequent mutations
proneural		PDGFRA alteration, IDH-mutation	p53, LOH, PIK3CA/PI3KR1
mesenchymal	CHI3LI, MET, CD44, MERTK	NF1 deletion	High expression of TRADD, RELB, TNFRSF1A

Abbreviations: CHI3LI = Chitinase 3 like protein 1; MET = HGFR hepatic growth factor receptor; CD44 = cluster of differentiation 44; MERTK = C-Mer proto-oncogene tyrosine kinase; PDGFRA = platelet derived growth factor receptor A; IDH = isocitrate dehydrogenase; NF1 = neuro fibromatosis 1; TP53 = tumor protein 53; LOH = loss of heterozygosity; PI3KCA = phosphoinositide 3 kinase catalytic subunit alpha; PI3KR1 = phosphoinositide 3 kinase receptor 1; TRADD = gene encoding for tumor necrosis factor receptor type 1-associated DEATH domain protein; RELB = V-Rel avian reticulo-endotheliosis viral oncogene homolog B; TNFRSF1A = tumor necrosis factor receptor superfamily member 1A.

Clustering GBM cells into subgroups is helpful to predict response to treatment and survival rates, because they are different for each subgroup. While aggressive chemotherapy prolongs survival of patients with mesenchymal GBM, it does not affect survival of patients with proneural GBM (Verhaak *et al.* 2010). However, radiation treatment targets proneural cells to a greater extent than mesenchymal cells (Bhat *et al.* 2013, Nakano 2015). Importantly, different GBM subtypes are present within the same tumor (Patel *et al.* 2014). As different subtypes respond differently to treatments, intratumoral heterogeneity needs to be considered when designing new treatment approaches (Patel *et al.* 2014).

Additionally, it is important to note the altered metabolism of tumor cells. Instead of channeling all incoming glucose into the citric acid cycle, many tumor cells rely heavily on

glycolysis, a mechanism termed "aerobic glycolysis" or "Warburg effect" (Warburg 1956, Vander Heiden *et al.* 2009). In GBM cell lines, 70 to 80% of cellular adenosine 5'-triphosphate (ATP) stems from glycolysis (Sesen *et al.* 2015). Marcus *et al.* (2010) demonstrated, that the tumor environment differs significantly from healthy brain regions in the same patient regarding glucose and lactate levels, but also growth factors and proteases. While glucose levels in a healthy brain are between 2 and 5 mM, only 0 to 3 mM are found in brain tumor tissue (Marcus *et al.* 2010). Lactate levels are normally below 25 mM, but increase to 50 - 250 mM in brain tumor tissue (Marcus *et al.* 2010). These findings underline that GBM cells exhibit high metabolic activity and increased glycolysis. Thus, glycolysis seems to be a preferred mechanism to generate ATP in GBM cells. However, glycolysis only yields 2 molecules of ATP instead of 36 molecules of ATP obtainable in the citric acid cycle (Vander Heiden *et al.* 2009). This apparent waste of resources raises the question of the utility of aerobic glycolysis in the presence of oxygen. One explanation is that the needs of rapidly dividing cells exceed the mere need for ATP. Prior to cell division, lipids, amino-acids and nucleotides have to be generated which requires acetyl-coenzyme A (Acetyl-CoA) and nicotinamide adenine dinucleotide phosphate hydrogen (NAD(P)H) on top of ATP (Vander Heiden *et al.* 2009). Glycolysis results in a stable NADH production enabling proliferation. This may be one of the reasons why GBM cells engage mostly in aerobic glycolysis (DeBerardinis *et al.* 2007). Another reason might be that brain tumors are very well supplied with nutrients, thus not being at a selective advantage when producing ATP most efficiently (by channeling glucose towards the citric acid cycle), but rather when multiplying most efficiently (by building bio mass) (Vander Heiden *et al.* 2009). Due to increased lactate production, the extracellular compartment acidifies. This acidification promotes migration and invasion of tumor cells (Stock *et al.* 2009). Thus, an altered tumor cell metabolism may sustain invasiveness through creating a more acidic extracellular environment. Glucose withdrawal, on the other hand, resembles growth factor withdrawal as both result in increased apoptosis (Vander Heiden *et al.* 2001). While 70 to 80% of GBM cells' ATP stems from glycolysis (Sesen *et al.* 2015), BTICs rely more on oxidative phosphorylation for ATP production indicating that BTICs differ not only genetically and functionally, but also metabolically (Janiszewska *et al.* 2012). Thus, GBM metabolism needs to be targeted in more than one way (Kim *et al.* 2016, Sesen *et al.* 2015).

Lastly, growth factor signaling and enzyme levels in the tumor environment are crucial factors for proliferation and invasion of GBM cells. Marcus *et al.* (2010) investigated the levels of growth factors and certain enzymes such as proteases in brain tissue immediately after resection of GBM in human patients. They found interleukin 8 (IL-8), a pro-angiogenic cytokine, to be significantly elevated, hinting at the important role of angiogenesis in GBM progression. Additionally, the metalloproteinase 2 (MMP2) to tissue inhibitor of

metalloproteinase 1 (TIMP-1) ratio was found to be elevated. Thus, MMP2's net activity, enabling tumor cells to migrate through the extracellular matrix, was increased. Overall, a great variety of growth factors, enzymes and metabolic changes seems to be responsible for GBM's aggressive proliferation, migration, angiogenesis and recurrence. Many researchers have described elevated levels of TGF-β_2 in GBM (Bruna *et al.* 2007, Aigner and Bogdahn 2008, Hau *et al.* 2011, Frei *et al.* 2015). Therefore, the present work will focus on the effects of metformin and TGF-β_2 on two key properties of GBM cells, proliferation and migration.

3.2 The role of metformin in diabetes and glioblastoma

One of the agents influencing metabolism in general and tumor cell metabolism in particular is the anti-diabetic drug metformin. Metformin (N',N'-dimethylbiguanide), is the most commonly prescribed oral anti-diabetic drug to treat type 2 diabetes (T2D) (Kourelis and Siegel 2011). As metformin effectively lowers blood glucose levels and additionally diminishes vascular complications and mortality, it is considered first line medication for treatment of obese T2D patients in Germany (German National Guideline on treatment of T2D 2013). Side effects such as weight gain or hypoglycemia are only rarely observed. However, low glomerular filtration rates increase the risk for lactate acidosis (German National Guideline on treatment of T2D 2013).

At a pH of 7.4, as usually found in intra- and extracellular compartments, metformin exists in its cationic form that is unable to penetrate membranes. Thus, its cellular uptake depends on the presence of organic cation transporters, namely OCT1, 2 and 3 (Shu *et al.* 2007). If OCTs are absent in a certain tissue or morphologically different due to polymorphisms or genetic aberrations, metformin's action is impeded (Shu *et al.* 2007). In hepatocytes, metformin's blood glucose reducing action is ascribed to its anti-gluconeogenic effects. Viollet *et al.* (2012) propose that metformin decreases gluconeogenesis by impairing complex I of the mitochondrial respiratory chain. Subsequently, two different signaling pathways result in lowered gluconeogenesis. Firstly, diminished ATP levels inhibit key gluconeogenic enzymes such as fructose-1,6-bisphosphatase. Secondly, decreased ATP and increased AMP levels activate AMP-activated protein kinase (AMPK). When AMP binds to the γ-catalytic subunit of AMPK, its activator, liver kinase B1 (LKB1) can bind more easily and activate AMPK (Hardie 2006). AMPK-activation inhibits transcription of various genes leading to lower levels of gluconeogenic and lipogenic enzymes. Hence, hepatocytes conserve energy when AMPK is activated and less glucose and fatty acids are being released into the blood stream preventing microvascular damage (Viollet *et al.* 2012).

Apart from metformin's beneficial effects on blood glucose levels and blood vessels, epidemiological studies suggest that patients who are being treated with metformin are at a lower risk of developing cancer (Evans *et al.* 2005). These findings sparked an unprecedented interest in metformin as an anti-cancer drug. An epidemiological study on type 2 diabetes and GBM reveals that patients suffering from type 2 diabetes and GBM have a better outcome when taking metformin compared to all other anti-diabetic medications (Welch and Grommes 2013, Elmaci and Altinoz 2016), a result supported by Adeberg *et al.* (2015) who also found that metformin treatment prolongs survival of diabetic GBM patients. *In vitro* studies have been performed including breast, lung, pancreatic, colorectal, ovarian and brain tumors and they have shown that metformin is able to lower tumor cell proliferation; either when being administered as a single agent or in combination with other cytoreductive agents (Würth *et al.* 2014). As metformin penetrates the blood-brain-barrier (Labuzek *et al.* 2010), it may unfold anti-tumerogenic action in glioma. Studies investigating the functional effects of metformin on glioma are outlined in Table 2.

Table 2: Functional effects of metformin on glioma cells

Study	Cell lines	Media	Effects of metformin
Beckner *et al.* 2005	U87MG LN229	MEM eagle / α-MEM + 10% FCS	• inhibits migration in cells in which mitochondria were blocked with NaN_3
Isakovic *et al.* 2007	C6 (rat); U251 (h)	Hepes (20 mM)-buffered RPMI1640 + 5% FCS + 10 mM glc.	• no proliferation inhibition in primary astrocytes • 4 mM induces morphological changes either to more spindle like shape or to granular shape • cell cycle arrest in non-confluent cells • 4 mM reduces viability through caspase-mediated apoptosis in confluent cells
Sato *et al.* 2012	dnf	dnf	• 1 mM reduces sphere formation • 1 mM induces differentiation (astrocyte marker GFAP and neural marker βIII-tubulin) • 500 mg/kg/day i.p. for 5 days delays tumor formation in transplanted mice
Ferla *et al.* 2012	LN18, LN229	Low-glc. DMEM + 5% FCS	• 2-16 mM reduce proliferation in a dose-dependent manner • 2-16 mM decrease migration
Würth	GBM	DMEM-	• no effects on human stem cells from the umbilical chord

et al. 2013	1-4	F12/Neurobasal (1:1) + 10 ng/ml bFGF + 20 ng/ml EGF	• effects on TICs > differentiated cells • 5-50 mM decrease viability, proliferation, and sphere formation
Gao *et al.* 2013	U251	DMEM + 10% FCS	• 10 and 30mM decrease viability • 0.3-3 mM inhibit migration in a dose-dependent manner
Liu *et al.* 2014	T98G, A172, U87	DMEM + 10% FCS	• 10 mM reduces proliferation (cytostatic effect)

Sesen *et al.* 2015	U87, LN18, U251, SF767	DMEM + 10% FCS	• 10 mM decreases proliferation
			• in PTEN wildtype cells, proliferation decreases after 48 h, in PTEN mutated cells after 96 h
			• Timeline of death: cell cycle arrest --> death --> autophagy
			  ○ 12 h: earliest time point for cell cycle arrest in G_1 and transition into G_0-phase
			  ○ 24 h: beginning cell death as a consequence of cell cycle arrest
			  ○ 48 h: consistent observation of cell death --> autophagy
			• 300 mg/kg/day for 30 days reduces tumor volume and tumor weight in transplanted mice

Kim *et al.* 2016	TS1320 TS1588 TS0903 GSC11 U87	DMEM/ F-12 + 10% FCS	• 5 mM metformin reduces proliferation in 1/5, enhances proliferation in 1/5 and leaves proliferation unaffected in 3/5 cell lines. • 15 mM inhibits sphere formation, a key factor of stemness • decreases stemness markers to some degree in 3/5 lines • 5 mM / 15 mM metformin do not decrease migration

Abbreviations: MEM = Minimal essential media; FCS = Fetal calf serum; RPMI1640 = cell media developed at the Roswell Park Memorial Institute (USA); TIC = tumor initiating cell; dnf = data not found; GFAP = glial fibrillary acidic protein (astrocyte marker); glc. = glucose; i.p. = intraperitoneal administration; DMEM = Dulbecco's modified Eagle's medium; bFGF = basic fibroblast growth factor; EGF = epidermal growth factor; PTEN = Phosphatase and tensin homolog.

Much research has been undertaken to investigate the mechanisms of metformin's actions on non-tumor and on tumor cells. The most important pathways, which have been identified in various tumor tissues, are displayed in Figure 1.

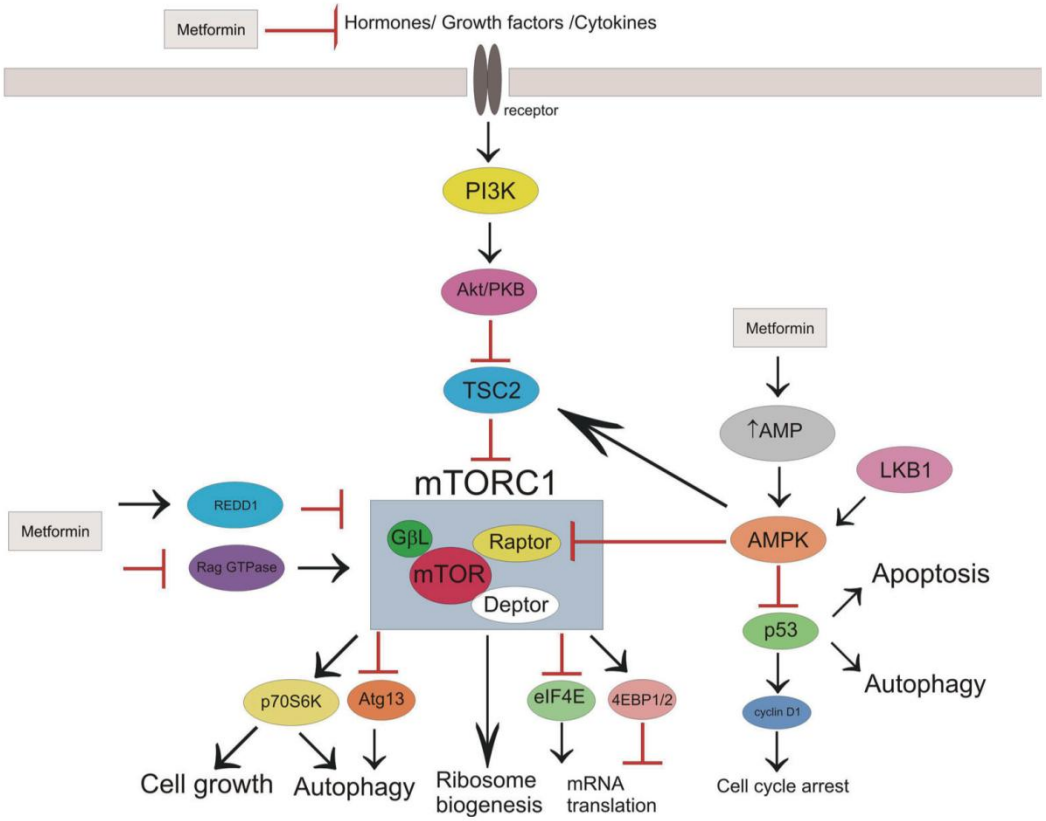

Figure 1: Potential mechanisms and sites of metformin's action in cancer cells (Republished from Kasznicki *et al.* 2014: "Metformin in cancer prevention and therapy." The Annals of translational medicine 2014, 2 (6): 57, © 2014. Republished with author's permission and permission of the editor of The Annals of Translational Medicine, Sept. 2016) Abbreviations: PI3K= phosphoinositide 3-kinase; Akt= refers to a mouse named "Ak", expressing spontaneous lymphomas and thymoma and Akt= PKB= protein kinase B; TSC2= tuberous sclerosis complex protein 2; mTORC1= mammalian target of rapamycin complex 1; raptor= regulatory associated protein of mTOR; GβL= G protein beta subunit-like; deptor= DEP domain-containing mTOR-interacting protein; REDD1= regulated in development and DNA damage responses 1; RAG GTPase= Ras-related GTPase; AMP= adenosine monophosphate; AMPK= AMP-activated protein kinase; LKB1= liver kinase 1; p53= protein 53; p70S6K= ribosomal protein S6 kinase; Atg13= autophy-related protein 13; eIF4E= eukaryotic translation initiation factor 4E; 4EBP1= eIF4E binding ptotein.

Some of the functional effects of metformin that are listed in Table 2, such as decreased proliferation via cell cycle arrest, apoptosis and viability reduction can be explained on a molecular level. To begin with, some effects of metformin on cancer cells seem similar to those on hepatocytes. Hence, AMPK is activated through the inhibition of complex I of the mitochondrial respiratory chain (Viollet *et al.* 2012). Generally, AMPK activation returns a cell to energy safe mode, thus impairing the energy consuming process of self-replication. In order to self-replicate, cancer cells need to produce amongst others fatty acids, proteins and nucleotides. AMPK mediates these biosynthetic processes via several pathways. On the one hand, AMPK inhibits acetyl-CoA carboxylase (ACC), an enzyme involved in fatty acid synthesis, thus reducing lipid production (Viollet *et al.* 2012). On the other hand, it has been proposed by several authors that *p53* and Cyclin D1 are mediated by AMPK and result in cell cycle arrest and apoptosis (Kasznicki *et al.* 2014, Würth et al 2014). In addition, metformin inhibits mammalian target of rapamycin (mTOR) signaling that regulates cell growth and

proliferation. According to Viollet *et al.* (2012) and Kasznicki *et al.* (2014), four pathways lead to the inhibition of mTOR by metformin. To begin with, AMPK phosphorylates tuberous sclerosis 2 (TSC2) which then inhibits mTOR. Secondly, AMPK impairs the association of mTOR and its regulatory associated protein (raptor) by phosphorylating raptor. Thirdly, AMPK-independent mechanisms of mTOR inhibition have been proposed such as metformin's potential to modulate a Ras-related GTPase (RAG GTPase), which subsequently leads to the inhibition of mTOR or, independently, metformin's ability to activate "regulated in development and DNA damage responses 1" (Redd1) which also entails mTOR inhibition. Last but not least, metformin can modulate the PI3K/Akt axis. Normally, insulin, insulin-like growth factor (IGF) and other growth factors bind to corresponding receptors and trigger a signal transduction cascade. Phosphoinositide 3-kinase (PI3K) catalyzes the reaction from phosphatidylinositol-4,5-bisphosphate (PIP2) to phosphatidylinositol-3,4,5-triphosphate (PIP3). PIP3 binds to Akt and facilitates its activation by kinases such as the mTOR complex 2. Once activated, Akt inhibits tuberous sclerosis complex 2 (TSC2) thus enabling the activation of mTOR. mTOR in turn up-regulates lipogenesis, glucose uptake, protein synthesis and inhibits autophagy (Schultze *et al.* 2012). This cascade is impaired by metformin at different levels. First and foremost, metformin lowers circulating insulin levels and consequently, IGF-levels also. As these substrates bind to their receptors less frequently, mTOR activation is being reduced. On the other hand, metformin can activate TSC2 via the AMPK-pathway resulting in mTOR inhibition. As mTOR regulates proliferation, inhibiting mTOR has an anti-proliferative effect, which constitutes of several aspects (Kasznicki *et al.* 2014, Würth *et al.* 2014). Cell growth is impaired, because p70S6K, normally in charge of phosphorylating the ribosome protein S6K, is not activated anymore. Autophagy is induced due to lack of p70S6K activation and lack of inhibition of autophagy-related protein 13 (Atg13). Protein synthesis is decreased as mRNA translation is diminished by decreased inhibition of eukaryotic translation initiation factor 4E (eIF4E) and by decreased activation of eIF4E-binding protein 1 (4E-BP1). The mechanisms of metformin's anti-cancer properties mentioned above have been elucidated using different tissues derived from breast, colon and prostate cancer, *et cetera*.

Regarding metformin's molecular mechanisms on glioma, researchers mostly agree that either by Akt inhibition or AMPK activation, mTOR signaling is being inhibited which leads to decreased proliferation (Isakovic *et al.* 2007, Ferla *et al.* 2012, Sato *et al.* 2012, Würth *et al.* 2013, Sesen *et al.* 2015, Yu *et al.* 2015). Metformin partially inhibits complex I of the respiratory chain in mitochondria thus leading to AMPK activation or Redd 1 / DDIT4 activation (DNA damage-inducible transcript 4 protein) and thus mTOR inhibition (Sesen *et al.* 2015). AMPK activation through metformin may also activate c-Jun N-terminal kinase (JNK) and lead to production of reactive oxygen species (ROS) (Isakovic *et al.* 2007) or

cause STAT3 downregulation and Akt inhibition (Ferla *et al.* 2012). Also, both Akt inhibition and AMPK activation can lead to FOXO3 activation, a trigger for differentiation of BTICs (Sato *et al.* 2012). Metformin may as well decrease migration through fibulin-3 downregulation and consequent MMP2 downregulation (Gao *et al.* 2013). These common notions are challenged by Würth *et al.* (2013) who state that Akt inhibition rather than AMPK activation leads to mTOR inhibition and by Liu *et al.* (2014) who report that no AMPK signaling is needed for mTOR inhibition but rather an association of PRAS40 and RAPTOR (Proline-rich Akt substrate of 40 kDa; Regulatory-associated protein of mTOR). Kim *et al.* (2016) observe neither AMPK activation nor mTOR inhibition while Gritti and Würth *et al.* (2014) report a completely independent mechanism of metformin's action: it blocks a chloride ion channel (CLIC1) in its open state thus trapping cells in G1 phase and lowering proliferation. Even though metformin's molecular mechanisms seem manifold, its main signaling axis seems to be AMPK activiation or Akt inhibition leading to mTOR inhibition. Metformin seems to selectively affect brain tumor initiating cells more than differentiated tumor cells and this to a greater extent than astrocytes or human stem cells (Isakovic *et al.* 2007; Würth *et al.* 2013, Gritti *et al.* 2014). Accordingly, Würth *et al.* (2013) demonstrated that metformin's anti-proliferative effects are more pronounced in $CD133^+$ cells, making metformin an ideal drug to target cancer initiating cells, which are claimed to be responsible for GBM recurrence.

Several studies exist exploring the *in vitro* possibilities of metformin as a combination partner for other anti-glioma treatments. While Aldea *et al.* (2014) found metformin by itself unable to reduce glioma proliferation, its combination with sorafenib, a RAF inhibitor, attains high apoptotic rates. Kim *et al.* (2016) propose targeting more than one metabolic pathway by blocking oxidative phosphorylation (OXPHOS) using metformin and glycolysis using 2-desoxy-glucose (2DG). This combination is able to reduce cell viability, sphere formation, expression of stemness makers and invasion *in vitro* and prolongs survival in tumor bearing mice. Sesen *et al.* (2015) investigated the effects of combining metformin with TMZ and / or irradiation and found the combination of the three most effective in inducing cell death. Soritau *et al.* (2011) and Yu *et al.* (2015) also found that the combination of TMZ and metformin is more effective in reducing GBM proliferation *in vitro* (Soritau *et al.*) and in tumor bearing mice (Yu *et al.*) than each agent by itself.

According to Würth *et al.* (2013), the IC_{50} for metformin, indicating a 50% proliferation inhibition *in vitro*, is at 10 mM. Below 10 mM, metformin's action is cytostatic, because cell growth recovers after metformin withdrawal. At concentrations higher than 10 mM, however, metformin's effects are cytotoxic and at 50 mM, cells do not recover growth after removal of the drug (Isakovic *et al.* 2007; Würth *et al.* 2013). Therefore, 10 mM metformin was used as

highest dose for this study. Yet, clinically observed concentrations are lower than those used *in vitro*. Generally, concentrations of metformin can be discussed as plasma concentration and tissue concentration. Plasma concentrations in diabetic patients with oral treatment usually range from 8 to 31 µM and even at maximum oral treatment dosage rarely exceed 39 µM (Menendez *et al.* 2014). In acute overdosing, concentrations as high as 300-800 µM were observed and doses between 600-1500 µM were considered fatalities; however, lethal doses have not been clearly defined (Menendez *et al.* 2014).

At present, clinical trials mainly investigate the oral route of metformin application. There are two studies on metformin use in glioblastoma patients (NCT01430351, NCT02780024 on www.clinicaltrials.gov; Nov. 2016). In the first study, 1000 mg metformin twice a day and 150 m/m^2 TMZ are combined for post-radiation treatment. The other study investigates the effects of re-irradiation, metformin and a low carbon diet on recurrent GBM but does not provide information on metformin doses. Two other studies also include lower-grade glioma patients (NCT02149459, NCT02496741 on www.clinicaltrials.gov; Nov. 2016). One study (NCT02149459) combines temozolomide and metformin as treatment before and after radiation therapy for grade 2-4 glioma and the other study (NCT02496741) is a dose-finding study for metformin and chloroquin to treat IDH1/2-mutated solid tumors.

Taking into account current research on metformin's role in GBM, several aspects have not been investigated so far. Firstly, the concentrations of metformin used in GBM experiments were higher than what seems achievable in the human brain tissue raising the question whether lower doses of metformin are effective in lowering proliferation and migration of GBM cells as well. Secondly, the effects of metformin on GBM were mainly explored in one to five cell lines (see Table 2), possibly resulting in bias due to a low case number. And thirdly, the exact molecular mechanisms of metformin's action in GBM are not fully understood to this date especially concerning possible interactions with growth factors such as TGF-β_2.

3.3 The role of TGF-β_2 in glioblastoma

Transforming growth factor beta 2 (TGF-β_2) is a cytokine involved in complex regulations of proliferation, differentiation and the immune response. In healthy tissues, TGF-β controls proliferation; in cancer however, this control is lost and TGF-β becomes oncogenic (Bruna *et al.* 2007). This phenomenon is called the TGF-β paradox and has been explored in different cancerous tissues (Tian *et al.* 2009). In GBM, TGF-β promotes cell growth, migration, invasion, angiogenesis and immunosuppression (Platten *et al.* 2001, Hau *et al.* 2006, Joseph *et al.* 2014).

TGF-β belongs to the TGF-β superfamily which also encompasses other proteins such as bone morphogenic protein (BMP), nodal, activin and inhibin (Aigner and Bogdahn 2008). Three isoforms of TGF-β exist in humans: TGF-β_1, TGF-β_2, and TGF-β_3. All of them are found in GBM, but levels vary. Some researchers have found TGF-β_2 levels to be the highest in glioma (Bodmer *et al.* 1989, Kjellman *et al.* 2000, Leitlein *et al.* 2001), while Frei *et al.* (2015) found mRNA of TGF-β_1 to be highest. Nonetheless, researchers agree that TGF-β_2 plays an important role in GBM (Bruna *et al.* 2007, Aigner and Bogdahn 2008, Hau *et al.* 2011, Frei *et al.* 2015).

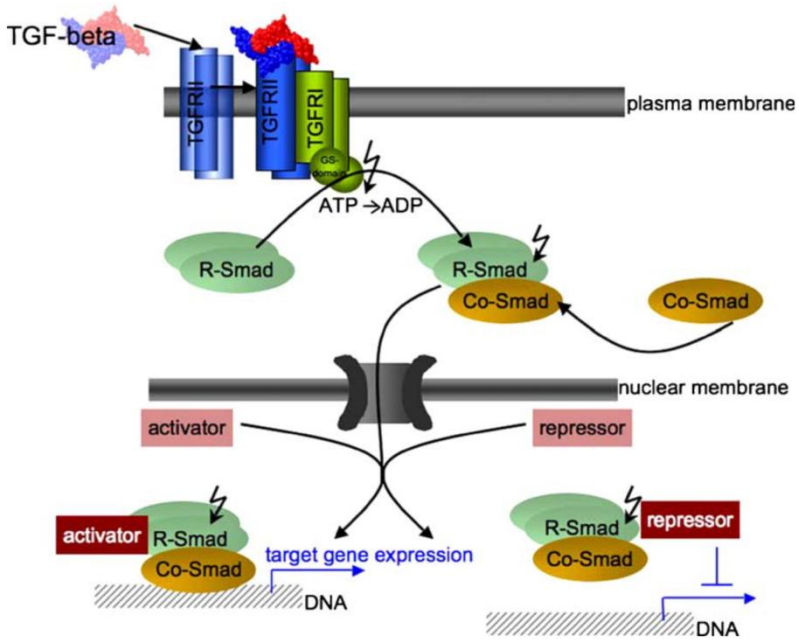

Figure 2: Smad-dependent TGF-β signaling (Aigner and Bogdahn 2008. Republished with author's permission and permission from Springer from "TGF-beta in neural stem cells and in tumors of the central nervous system." Cell and tissue research 2008 (1): 225–241, © 2008. Permission conveyed through Copyright Clearance Center, Sept. 2016). Abbreviations: TGF-beta = transforming growth factor beta; TGFRI and II = TGF- receptor type I and II; R-Smad = regulatory small body size mother of decapentaplegic; ATP = adenosine triphosphate; ADP = adenosine diphoshate; Co-smad = smad4; DNA = deoxyribonucleic acid.

TGF-β proteins are homodimers of 12.5 kD that bind to specific receptor serine/threonine kinases, the TGF-β receptors type I and type II (TGFR-I and II). Seven isoforms have been identified for receptor type I and five for receptor type II (Aigner and Bogdahn 2008, Massagué 2008). After binding the ligand, two TGFR-II units associate with two TGFR-I units to form a complex. A third receptor type, also known as betaglycan, increases the affinity of TGFR-II for TGF-β_2 in GBM (Aigner and Bogdahn 2008). Other membrane proteins such as EMP3 (epithelial membrane protein 3) may increase TGF-β signaling in $CD44^+$ mesenchymal GBM cells (Jun *et al.* 2016). In the receptor complex, TGFR-II activates TGFR-I by phosphorylation and TGFR-I subsequently phosphorylates Smad2 and 3 (small body size mothers against decapentaplegic) (Massagué 2000, Massagué 2008, Dong *et al.* 2015). Smad2 and 3 are receptor substrate smads (Rsmads). Upon activation, they associate with

co-smads (Smad4) and translocate into the nucleus. There, several other DNA-binding cofactors associate with the complex before it binds to specific gene regions. Depending on the type of cell and its environment, different cofactors are present which determine genes and groups of genes targeted by TGF-β signaling. Thus, TGF-β's effects are highly context-dependent and promote or inhibit the expression of a great variety of genes (Massagué 2008). In GBM, several Smads have been identified to play a leading role, namely Smad2 and Smad3. However, there is no clear evidence to date, which one is more important in GBM. In 2007, Bruna *et al.* found mRNA of *smad2* to be highly expressed in GBM while Kjellman *et al.* (2000) found mRNA of *smad2*, *smad3* and *smad4* decreased in GBM specimens.

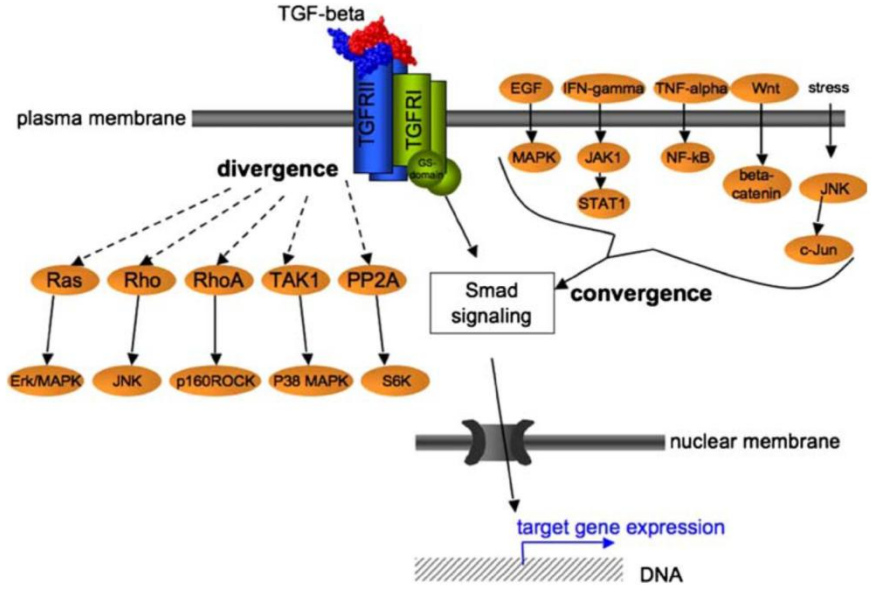

Figure 3: Signaling pathways diverging from and converging on TGF-β signaling (Aigner and Bogdahn 2008. Republished with author's permission and permission from Springer from " TGF-beta in neural stem cells and in tumors of the central nervous system." Cell and tissue research 2008 (1): 225–241, © 2008. Permission conveyed through Copyright Clearance Center, Sept. 2016). Abbreviations: TGF-beta = transforming growth factor beta; TGFRI and II = TGF-receptor type I and II; EGF = epidermal growth factor; IFN-gamma = interferon gamma; TNF-alpha = tumor necrosis factor alpha; Wht = data not found; MAPK = mitogen-activated kinase also known as Ras-Raf-MEK-ERK pathway; JAK1 = Janus kinase 1; NF-kappaB = nuclear factor kappa-light-chain-enhancer of activated B cells; JNK = c-Jun N-terminal kinase; STAT1 = Signal transducer and activator of transcription 1; c-Jun = p39 = Jun Proto-Oncogene; Ras, Rho, RhoA = small GTPaseses of the Ras superfamiliy; TAK1 = TGF-β activated kinase 1; PP2A = protein phosphatase 2; Smad = small body size mother of decapentaplegic; ERK = extracellular signal-regulated kinase = nowadays known as MAPK; MAPK = mitogen-activated kinase also known as Ras-Raf-MEK-ERK pathway; JNK = c-Jun N-terminal kinase; p160ROCK = a serine/threonine protein kinase; S6K = Ribosomal protein S6 kinase; DNA = deoxyribonucleic acid.

Apart from "classic" TGF-β/Smad2/3 signaling, several signaling pathways diverge from and converge to TGF-β signaling in different tissues. For example does TGF-β signaling diverge on:

- the MAPK pathway, either mediated by TAK1 (Massagué 2000, Aigner and Bogdahn 2008) or through Smad2-dependent activation (Moustakas and Heldin 2005)
- the C-Jun-N-terminal kinases (JNK) which are activated by TGF-β in a Smad-independent way (Aigner and Bogdahn 2008)
- p38 signaling (Massagué 2000)
- protein kinase A (PKA) signaling which is activated by Smad3 (Moustakas and Heldin 2005)
- the PI3K / Akt pathway (Aigner and Bogdahn 2008).

The following pathways converge on TGF-β signaling:

- MAPK may activate Smad signaling (Massagué 2000).
- activation of Ras–MEK–ERK may lead to phosphorylation and thus inhibition of smad1, smad2 and smad3 (Massagué 2000, Moustakas and Heldin 2005).

TGF-β signaling is thus embedded in a large network of cell signaling cascades, which is not understood in every aspect today.

There exist several molecules to inhibit TGF-β signaling. In this study, we used SD-208, a TGF-β receptor I kinase inhibitor that has been shown to inhibit TGF-β signaling in glioma tissue *in vitro* and *in vivo* (Uhl *et al.* 2004).

Glioma cells' responses to TGF-β are manifold, heterogeneous and they differ from healthy cells' responses in the sense that TGF-β may act as a tumor suppressor in healthy tissues but as a tumor promoter in glioma. Massagué (2008) proposed that cancer cells evade TGF-β's tumor control either due to mutations in TGF-β's core signaling pathway or because the suppressive arm of the signaling cascade is altered. In glioma, both mechanisms have been found. On the one hand, TGF-β receptor type II may become deficient leading to TGF-β immunity; on the other hand, TGF-β may lose its cytostatic control because of PI3K hyperactivation, loss of p15INK4b (Cyclin-dependent kinase 4 inhibitor B also known as multiple tumor suppressor 2) or mutational inactivation of RB (retinoablastoma protein) (Massagué 2008). Additionally, *p53* mutations in both alleles may lead to enhanced proliferation under TGF-β stimulation in glioma (Kumar *et al.* 2015). But not only does TGF-β produce oncogenic responses in glioma cells, TGF-β production also sustains itself through an autocrine loop (Massagué 2008, Ikushima *et al.* 2009). TGF-β signaling stimulates cAMP responsive element binding protein 1 (CREB1) and Smad3 to induce transcription of TGF-β_2.

This autocrine loop leads to high TGF-β_2 levels in GBM tissue and promotes tumor progression (Rodon *et al.* 2014).

The autocrine loop of TGF-β production has also been shown to conserve stem cell properties of GBM cells. In 2009, Ikushima *et al.* proposed that TGF-β directly alters transcription of sex determining region Y-box 4 (*sox4*) in the nucleus which increases expression of Sox2, a neural marker of stemness. In the same year, Peñuelas *et al.* reported that TGF-β directly induces leukemia inhibitory factor (LIF) and thus sustains self-renewal and prevents differentiation of brain tumor initiating cells. Narushima *et al.* (2016) identified TGFR-II as an important player for GBM cells to retain stemness. Thus, TGF-β inhibits differentiation and helps BTICs to remain tumor initiating cells possessing stem cell properties.

Rapid proliferation and lack of proliferative control is one of GBM BTICs' characteristics and has been partly attributed to TGF-β. However, TGF-β effects on GBM *in vitro* and *in vivo* are heterogeneous. TGF-β may stimulate or attenuate proliferation or leave it unaltered (Rich *et al.* 1999, Piek *et al.* 1999, Bruna *et al.* 2007, Beier *et al.* 2012). Thus, the exact effects of TGF-β seem difficult to predict. Some of the differences might be due to differing receptor set-ups of proneural and mesenchymal cells. *In vitro*, proliferation of proneural BTICs does not increase under stimulation with TGF-β due to TGF-β receptor type II deficiency and consequent failure of Smad-mediated signal transduction (Beier *et al.* 2012). Another predictor might be the methylation status of the *platelet derived growth factor gene B* (*pdgf-b*). In glioma cells with a non-methylated *pdgf-b* gene, TGF-β induces *pdgf-b* expression and thus augments proliferation (Bruna *et al.* 2007).

Phenotype and invasiveness of GBM cells depend on the tumor environment, especially its oxygen content and lactate levels. Hypoxia in tumoric tissues attracts myeloid cells. These release numerous growth factors, especially TGF-β, PDGF, FGF and EGF. In addition to myeloid cells, GBM cells neighboring necrotic areas may produce TGF-β as well. Due to these stimuli, tumor cells can undergo epithelial-mesenchymal transition (EMT), a process in which they acquire a mesenchymal and thus stem cell like phenotype (Iwadate 2016). This type of EMT is called EMT type 3 (Iwadate 2016). In the process, GBM cells lose cell-cell adhesions, because TGF-β represses E-cadherin and cells migrate to invade the surrounding tissue (Odenthal *et al.* 2016). EMT type 3 also plays a role in tumor recurrence: GBM cells evading radiation undergo EMT under TGF-β stimulation and become highly invasive mesenchymal cells leading to an aggressive tumor recurrence (Joseph *et al.* 2014, Iwadate 2016, Iwadate *et al.* 2016). Acidification and elevated lactate levels in the tumor environment may also enhance migration of GBM cells. Tumor cells express lactate dehydrogenase A (LDH-A) catalyzing lactate production. Lactate in turn activates TGF-β_2 in a

thrombospondin 1 (THBS-1)-mediated manner, which then activates MMP2 and MMP9, two matrix enzymes necessary for migration. Also, TGF-β_2 causes the integration of integrin $\alpha_V\beta_3$ into the membrane. Taken together, these processes enhance migration of GBM cells (Wild-Bode *et al.* 2001, Baumann *et al.* 2009, Seliger *et al.* 2013).

Furthermore, TGF-β induces angiogenesis. As TGF-β leads to release of vascular endothelial growth factor (VEGF) by stroma and glioma cells, high TGF-β levels are associated with high vascularity (Aigner and Bogdahn 2008). Some researchers have proposed that the pro-angiogenic effect of TGF-β is more pronounced under hypoxia (Krishnan *et al.* 2015), others have found no such correlation (Seystahl *et al.* 2015). In clinical trials, bevacizumab, a VEGF antibody, showed its potential to improve survival and is hence the only approved molecular therapy for recurrent GBM treatment in the US (Würth *et al.* 2014).

Originally, TGF-β_2 was named GBM cell-derived T cell suppressor factor due to its ability to suppress T cells (Bodmer *et al.* 1989). This fact hints at another very important effect of TGF-β: immunosuppression. TGF-β secretion of GBM leads to downregulation of NKG2D receptors on infiltrating $CD8^+$ T-lymphocytes and $CD8^+$ natural killer (NK)-cells and thus inhibits their proliferation, differentiation and immune infiltration (Friese *et al.* 2004, Aigner and Bogdahn 2008, Crane *et al.* 2010, Beier *et al.* 2012). Thus, GBM escapes the surveillance of the immune system. While mesenchymal tumors do exhibit infiltration with immune cells at the tumor site, very few immune cells are found in proneural GBM tissue, because proneural BTICs impair $CD8^+$ T- and NK-cells through TGF-β secretion (Beier *et al.* 2012). Also, TGF-β downregulates the transcription of important cytolytic genes such as perforin, granzyme A, granzyme B, Fas ligand and interferon γ in $CD8^+$ T-lymphocytes thus hampering their tumor control (Thomas and Massagué 2005).

Clinically, high TGF-β_2 levels in the tumor tissue are correlated with a shorter progression free and overall survival and thus a poorer prognosis (Bruna *et al.* 2007, Hau *et al.* 2011, Frei *et al.* 2015). Furthermore, high TGF-β_2 levels correlate with high pSmad2 activity, which is also associated with poorer prognosis (Bruna *et al.* 2007); however, TGF-β serum levels are no valid predictor for survival of GBM patients (Chiorean *et al.* 2014). As high levels of CAMP-responsive element binding protein 1 (CREB1) are correlated with high levels of TGF-β_2, CREB1 might be valuable as a biomarker to predict tumor sensitivity to anti-TGF-β treatment (Rodon *et al.* 2014).

Reviewing the research that has been conducted on the role of TGF-β_2 in GBM, contradictory reports exist concerning proliferation and migration under TGF-β_2 stimulation and inhibition using SD-208. As TGF-β has been proposed to induce proliferation and migration, but

contrary effects have been reported for metformin, the following section will focus on possible links between the two.

3.4 Possible links between metformin and TGF-β_2

Even though the role of TGF-β_2 in GBM proliferation and migration remains controversial, some of the functional effects of TGF-β seem opposed to those of metformin raising the question of whether the effects of TGF-β and metformin are connected or even antagonistic. Numerous studies have investigated direct links of TGF-β and metformin in tissues other than GBM. Taken together with molecular findings of signaling outlined in previous chapters, the following connections may be postulated.

Possible links between TGF-β and metformin include:

1. functionally opposed effects such as proliferation increase or decrease
2. metformin directly influencing core signaling pathways of TGF-β, especially Smad signaling
3. TGF-β directly influencing core signaling pathways of metformin, namely Akt inhibition or AMPK activation leading to mTOR inhibition
4. metformin changing the tumor environment in a way that TGF-β signaling is impacted
5. metformin and TGF-β converging on the same signaling pathways.

Firstly, functionally opposed effects have been described in GBM as TGF-β_2 has been reported to increase proliferation and migration in numerous cases (view chapter 1.3) while metformin has been found to inhibit these exact processes (view chapter 1.2). In breast cancer tissue, metformin has been found to directly antagonize TGF-β induced EMT (Cufí *et al.* 2010, Vazquez-Martin *et al.* 2010) and TGF-β induced formation of mammospheres (Oliveras-Ferraros *et al.* 2011) indicating a functional antagonism of TGF-β and metformin in this case. Metformin also blocks TGF-β induced EMT in renal tubular epithelial cells (Lee *et al.* 2013). Therefore, a functional antagonism of metformin and TGF-β may be postulated, mostly for non-glioma tissues.

Secondly, metformin has proven to directly impact TGF-β protein levels and Smad signaling. In breast cancer cells, metformin lowers TGF-β levels thus reducing EMT (Vazquez-Martin *et al.* 2010). Similarly, metformin inhibits secretion of TGF-β_1 in cardiomyocytes (Wang *et al.* 2011) and reduces TGF-β_1 levels and vascularization after sponge implantation in mice (Xavier *et al.* 2010). In ovarian and uterine tissue, metformin is also able to reduce TGF-β_1 levels and prevent fibrosis (Zhang *et al.* 2013). In adipocytes, metformin activates Smad7, an inhibitory Smad, thus decreasing TGF-β signaling (Kim *et al.* 2015). In renal fibroblasts,

metformin inhibits Smad3 hence lowering TGF-β-induced collagen I production (Lu *et al.* 2015). Lastly, in nasal polyp-derived fibroblasts, metformin directly inhibits Smad2/3 phosphorylation (Park *et al.* 2014). Hence, metformin is able to lower TGF-β levels or inhibit Smad signaling in different tissues, but no research exists concerning glioma.

Thirdly, direct inhibition of metformin signaling through TGF-β has been described. In renal fibroblasts, TGF-β_1 directly counteracts metformin's signaling via AMPK inhibition thus causing fibrosis (Thakur *et al.* 2015). Again, no data exists for GBM.

Fourthly, metformin lowers glucose levels thus decreasing TGF-β release. Gu *et al.* (2014) found that the glucose content in the culture medium has an effect on TGF-β secretion: the higher the glucose content the higher the TGF-β levels. The glucose induced TGF-β production of renal mesangium cells is impaired by metformin. Similarly, metformin can antagonize diabetes induced increase in TGF-β levels in renal tissue of diabetic rats (Maheshwari *et al.* 2014). On the other hand, impairment of complex I of the respiratory chain may increase lactate levels and lactate has been described as an activator of TGF-β signaling in GBM cells (Baumann and Leukel *et al.* 2009, Seliger *et al.* 2013). Thus, metformin may indirectly activate or inhibit TGF-β depending on cellular context.

Fifthly, metformin and TGF-β are part of complex signaling networks which overlap at certain points. Metformin and TGF-β signaling may converge on FoxO signaling (Moustakas 2005, Sato *et al.* 2012), on JNK signaling (Moustakas and Heldin 2005, Isakovic *et al.* 2007), on Akt signaling (Moustakas and Heldin 2005, Sato *et al.* 2012) or on Sox expression (Ikushima *et al.* 2009, Zhang *et al.* 2014, Kim *et al.* 2016). These links have not been established for identical tissues, but may outline what a great variety of interactions between metformin and TGF-β is conceivable.

The individual effects of metformin and TGF-β_2 have been explored in GBM indicating that their effects might be opposed, but possibly also difficult to predict. Yet, no research exists reviewing functional and molecular effects of both, metformin and TGF-β_2, on glioma cells.

3.5 Research aim

The laboratory group of Molecular NeuroOncology Regensburg investigates brain tumor metabolism, tumor cell invasion, TGF-β-signaling and possible clinical applications for new anti-glioma treatments. This study was designed as a comprehensive approach to analyze the functional responses of proneural and mesenchymal BTICs and TCs to metformin, TGF-β_2 and / or SD-208 treatment.

So far, the effects of metformin on GBM have mainly been explored using concentrations higher than what seems achievable in human brain tissue and have shown various results. These have been attributed to different genetic and metabolic setups of different glioma cells. The reports about TGF-β_2's influence on proliferation and migration of glioma are heterogeneous and again, have been attributed to genetic differences. Lastly, there exists no systematic research reviewing functional effects of both, metformin and TGF-β_2, on GBM cells.

Therefore, this study focused on three main topics:

1. How do different subtypes of GBM cells react to different metformin concentrations? May low concentrations decrease cell proliferation and / or migration? Are there differences in susceptibility?
2. How do TGF-β_2 and SD-208 influence proliferation and migration of different GBM cell lines? Are there differences in susceptibility?
3. Are there any links between the functional effects of metformin and TGF-β_2 on GBM?

In functional assays, changes in proliferation and migration under treatment with different doses of metformin, TGF-β_2, SD-208 and combinations thereof, were examined. Proliferation was mainly assessed in cell counts and exemplarily tested in crystal violet stainings, and migration was mainly assessed in spheroid migration assays and exemplarily explored in scratch migration assays. To investigate whether different susceptibilities to metformin and TGF-β can be predicted based on cell differentiation status or subtype, five BTIC cell lines were maintained at serum-free conditions and compared to their differentiated counterparts (TCs), cultured with serum. BTIC and TC lines were composed of three mesenchymal and two proneural cell lines each.

4 MATERIAL AND METHODS

4.1 Material

4.1.1 Consumables and supplies

Table 3: List of consumable and supplies

Product	Company
6- and 96-well plates	TPP; Trasadingen, Switzerland
96-well plate, round bottom	Costar; Corning, NY, USA
Culture Inserts (Wound-healing-assay)	Ibidi; Martinsried, Germany
Flasks for cell culture (T25 and T75)	TPP; Trasadingen, Switzerland
Neubauer's Hemocytometer	Assistent; Sondheim/Rhön, Germany
Hemocytometer cover glasses (20 x 26 x 0.4 mm)	Hartenstein; Würzburg, Germany
Cell scraper 28 cm	Greiner; Frickenhausen, Germany
Eppendorf tubes (0.5 ml, 1.5 ml, 2 ml)	Eppendorf, Hamburg; Falcon BD, Heidelberg, Germany
Cryo tubes (1.6 and 1.8 ml)	Sarstedt; Nürnbrecht, Germany
Falcon tubes (15 and 50 ml)	Sarstedt; Nürnbrecht, Germany
Pipettes (2, 10, 20, 100, 200, 1000 µl)	Gilson; Middleton, WI, USA
Pipette tips (10, 200, 1000 µl)	Sarstedt; Nürnbrecht, Germany
Step pipette	Eppendorf; Hamburg, Germany
Step pipette tip (5 ml)	Eppendorf; Hamburg, Germany
Transferpette (0-200 µl)	Brand; Wertheim, Germany
Glas pipettes (5, 10, 20 ml)	Brand; Wertheim, Germany
Glas Pasteur pipette	Brand; Wertheim, Germany

4.1.2 Glioblatoma cell lines

All brain tumor initiating cells (BTICs) used for the experiments were obtained during brain tumor surgery at the university hospital Regensburg (UKR) and isolated in the laboratory. After having grown the obtained cells for several passages, some were differentiated using Dulbecco's modified Eagle Medium (DMEM with glucose 1000 mg/L) with 10% fetal calf serum (FCS). Thus, cells from each cell line existed as stem-like cells (BTIC) and as differentiated pair (TC). The following cells were used:

Table 4: List of cell lines used

Proneural cell lines	**BTIC passages**	**TC passages**
RAV19	P25 and P26	P23_3 and P26_6
RAV57	P16 and P18	P17_2 and P20_3

Mesenchymal cell lines	**BTIC passages**	**TC passages**
RAV21	P17, P19 and P24	P24_9 and P24_10
RAV24	P12 and P14	P10_5 and P10_7
RAV27	P16 and P20	P18_5 and P18_6

For differentiated cell lines, Px_y denotes that cells were passaged x times as BTICs and y times as TCs, e.g. RAV19 P23_3 describes that RAV19 BTICs were passaged 23 times before being differentiated and passaged 6 times as TCs. Tumor cell properties for cells in primary tissue and in cell culture as well as patient characteristics are shown in Tables 5,6, and 7.

Table 5: Characteristics of the primary tumors

	Primary Tumors	histology	grade	MGMT-meth.	IDH1 (wt/mut.)
mesenchymal	**RAV 21**	GBM (prim.)	IV	meth.	n.d.
	RAV 24	GS (prim.)	IV	meth.	wt
	RAV 27	GBM (sec.)	IV	unmeth.	p.R132H
proneural	**RAV 19**	GBM (prim.)	IV	unmeth.	wt
	RAV 57	GBM (prim.)	IV	unmeth.	wt

Abbreviations: MGMT-meth. = methylation of the promotor region of the O^6-methylguanine-DNA-methyltransferase; IDH1 (wt/mut.) = isocitrate dehydrogenase wildtype or mutation; prim. = primary; sec. = secondary; meth. = methylated; unmeth. = unmethylated; n.d. = not determined

Table 6: Tumor characteristics in cell culture

	Cell Culture	growth	MGMT -meth.	IDH (wt / mut.)	CD133 (%)	Nestin	Sox2
mesenchymal	**RAV 21**	adherent	meth.	wt	1	pos.	neg.
	RAV 24	adherent	meth.	wt	6	pos.	pos.
	RAV 27	adherent	meth.	wt	62	pos.	neg.
proneural	**RAV 19**	adherent	unmeth.	wt	3	pos.	pos.
	RAV 57	adherent	unmeth.	wt	0	pos.	pos.

Abbreviations: MGMT-meth. = methylation of the promotor region of the O^6-methylguanine-DNA-methyltransferase; IDH1 (wt/mut.) = isocitrate dehydrogenase wildtype or mutation; CD133 = cluster of differentiation; Sox2 = SRY (sex determining region Y)-box 2; meth. = methylated; unmeth. = unmethylated; pos. = positive; neg. = negative

Table 7: Patient characteristics

	Patient data	age	sex	therapy	OS (months)
mesenchymal	**RAV 21**	46	m	radio / chemo	18.75
	RAV 24	55	m	radio / chemo	17.5
	RAV 27	42	m	radio / chemo	8.5
proneural	**RAV 19**	52	f	radio / chemo	4
	RAV 57	49	m	radio / chemo	20.5

Abbreviations: OS = overall survival; m = male; f = female

Table 8: Endogenous TGF-β_2 levels of BTICs

	Cell Culture	TGF-β_2 (ng/ml)	standard deviation
mesenchymal	**RAV 21**	0.2030	0.0250
	RAV 24	0.6655	0.0328
	RAV 27	1.6008	0.1179
proneural	**RAV 19**	0.0773	0.0347
	RAV 57	0.0385	0.0104

Endogenous TGF-β_2 levels were quantified using an ELISA. ELISA was performed with supernatants 48 hs after sowing out 400,000 cells of the respective cell line.

4.1.3 Culture media and supplements

Table 9: List of culture media and supplements

Substance	Company
RHB-A Stem Cell Medium	Stem Cell Technologies; Köln, Germany
Epidermal Growth Factor (EGF)	Miltenyi-Biotec; Bergisch-Gladbach, Germany
Fibroblast Growth Factor (FGF)	Miltenyi-Biotec; Bergisch-Gladbach, Germany

Dulbecco's modified Eagle Medium (DMEM) Low Glucose (1000 mg/l)	Sigma-Aldrich; München, Germany
Fetal Calf Serum (FCS)	Biochrom; Berlin, Germany
Penicillin and Streptomycin (P/S)	Sigma-Aldrich; München, Germany
MEM Non essential amino acids (neAA)	Sigma-Aldrich; München, Germany
MEM - Vitamins	Sigma-Aldrich; München, Germany
Glutamine	Sigma-Aldrich; München, Germany
Cell Dissociation solution	Sigma-Aldrich; München, Germany
Trypsin-EDTA	Sigma-Aldrich; München, Germany
Phosphate Buffer Saline (PBS)	Sigma-Aldrich; München, Germany
Dimethylsulfoxide (DMSO)	Carl Roth; Karlsruhe, Germany
Laminin	Becton Dickinson; Heidelberg, Germany

Table 10: Overview over media ingredients

Medium	**Ingredients**
RHB-A full medium	1% (v/v) Penicillin/Streptomycin 20 ng/ml Epidermal Growth Factor (EGF) 20 ng/ml Fibroblast Growth Factor (EGF)
DMEM full medium	10% (v/v) Fetal Calf Serum (FCS) 1% (v/v) Penicillin/Streptomycin 1% (v/v) Non essential amino acids (neAA) 1% (v/v) MEM-Vitamins 1% (v/v) Glutamine Glucose content = 1000 mg/dl
Cryo conservation medium	RHB-A or DMEM full medium 10% Dimethylsulfoxide (DMSO)

4.1.4 Additional substances and solutions

Table 11: Additional substances used

Substance	Company
Trypan blue stain	Sigma-Aldrich; Taufkirchen, Germany
Metformin Hydrochloride	Fluka, Sigma-Aldrich; Steinheim, Germany
Transforming growth factor beta 2 mammalian (TGF-β_2)	Peprotech; Hamburg, Germany
SD-208 (2-(5-Chloro-2-fluorophenyl)-4-[(4-pyridyl)amino]pteridine)	Tocris; Bristol, UK
Agarose	Biozym; Oldendorf, Germany

Table 12: Additional solutions used

Solution	Ingredients
Crystal violet solution	0.5% crystal violet 20% Methanol
Sodium citrate	0.1 M Sodium citrate 50% Ethanol
Agarose	1% Agrose PBS

4.1.5 Equipment

Table 13: List of equipment

Equipment	Company
Cell Culture Incubator HeraCell (Normoxia)	Thermo Scientific, USA
Cell Culture Hood HeraSafe	Thermo Scientific, USA
Water bath 1083	GFL; Burgwedel, Germany
Light microscope Fluovert Type 090-123.012	Leitz; Wetzlar, Germany

Light microscope Type 090-135.001	Leica; Wetzlar, Germany
Centrifuge Megafuge 10.R	Thermo Scientific, USA
Centrifuge 5417C	Eppendorf; Hamburg, Germany
Vortex-2-Genie	Scientific Industries; Bohemia, NY, USA
Varioscan	Thermo Scientific, USA

4.1.6 Software

Table 14: List of computer software

Programm	**Company**
Microsoft Excel	Microsoft; Redmond, USA
ProgRes CapturePro 2.6, JENOPTIK Laser	Optik Systeme GmbH; Jena, Germany
ImageJ	NIH; Betheada, USA

4.2 Methods

4.2.1 Cell culture

4.2.1.1 Origin of BTICs and differentiated GBM cells

All brain tumor initiating cells (BTICs) used in the experiments were obtained during brain tumor surgery at the University Hospital Regensburg (UKR) and isolated in the laboratory. In the lab group, tumors were broken down physically by use of a scalpel and by being pipetted in PBS for several minutes. In addition, an erythrocyte lysis buffer was used to disintegrate any red blood cells that might still be left in the tumor tissue. After several further steps of washing with PBS and alternating centrifugation, the isolated brain tumor initiating cells were sowed out on 6-well plates for growth under three different conditions:

- RHB-A full medium in a laminin coated well
- RHB-A full medium in a laminin free well
- DMEM + 10% FCS full medium in a laminin free well.

6-well plates were kept in normoxia, at 37°C and 5% CO_2. The serum-free medium RHB-A was supplemented with epidermal growth factor (EGF) and fibroblast growth factor (FGF) to preserve BTICs' stem-like properties. For differentiation, BTICs were cultured in a DMEM (glucose 1000 mg/L) + 10% FCS full medium for at least 2-3 weeks and 1 or 2 passages preferably. After 2-3 weeks, morphological changes were confirmed under the microscope.

4.2.1.2 Maintenance

To culture BTICs and their differentiated pairs, cells were grown in ventilated T25 or T75 flasks according to cell number. They were incubated at 38°C, 80% humidity, 20% oxygen (=normoxia) and 5% CO_2.

In order to preserve stem cell properties of BTICs, they were kept in RHB-A media. It was supplemented with 1 % Penicillin/Streptomycin to prevent bacterial infection as well as 1% EGF and 1% FGF. For differentiated cells, a low glucose DMEM medium (1000 mg glucose/l) with 10% FCS (fetal calf serum) was used. It was supplemented with 1% Penicillin/Streptomycin, 1% vitamins, 1% L-glutamine and 1% non-essential amino acids. 10 ml of medium were used to keep cells in a T75 flask while 5 ml were used for T25 flasks.

All media were changed under sterile conditions on a weekly basis. For adherent cells, half of the medium in the flask was taken out with a glass Pasteur pipette and refilled with fresh medium (e.g. 5 ml of medium were changed in a T75 flask). When adherent cells reached a confluence level between 80 to 90%, they were either split onto several flasks or stored away in a -80°C freezer. In order to split cells, the supernatant medium was taken out of one or several flasks containing the same cell line at the same passage number and put into a 50 ml flask to store. Then, 3ml of cell dissociation solution was added per flask before the flask was put into the incubator. After 5-10 minutes the flask was taken out and shaken moderately (if needed) to increase cell detachment. Next, the flask was rinsed once or twice using the cell dissociation solution already in the flask and then rinsed again once or twice using the stored medium. The resulting suspension was centrifuged at 1200 rpm and 20°C for 5 minutes. After the medium had been carefully taken out with a Pasteur pipette, the cell pellet was redissolved in a required amount of medium (e.g. 30 ml for 3 T75 flasks) and distributed onto the new flasks. Splitting cells in this way increased the passage number by one. After 3 passages, old flasks were replaced.

4.2.1.3 Cryo conservation

In order to store cells, the cell pellet gained as described above was resuspended in a 10% DMSO and medium solution. The suspension was immediately put into a 2 ml cryo conservation cup, which was placed into a container filled with isopropanol for slow temperature reduction. This ensured that the temperature decreased by 1°C per minute

when the isopropanol container was stored in the –80°C freezer. In order to thaw cells, the cryo conservation cup was placed into a 37°C water bath for approximately 1 minute. Next, 2 ml of fresh medium were added to dilute the toxic 10% DMSO solution for centrifugation. The suspension was transferred into a 15 ml falcon tube and centrifuged at 1200 rpm and 20°C for 8 minutes. Afterwards, the supernatant was removed and the pellet was resuspended in 5 mL of fresh medium for transfer into a T25 flask.

4.2.1.4 Cell count

All cell counts were performed on Neubauer's hemocytometers using trypan blue exclusion. Trypan blue is incorporated into the cell membranes of dead cells. Thus, dead cells will appear blue under a light microscope while living cells continue to appear white. To perform a cell count, 40 µl of cell suspension was mixed with 10 µl of trypan blue, resulting in a 1:1.25 dilution. 10 µl of the stained cell suspension was then brought onto a hemocytometer and examined under the microscope at 10x magnification. Since each corner square has the dimensions 1mm x 1mm and a height of 0.1 mm, the resulting volume is 0.1 mm^3 (= 0.1 µl). Therefore, the cell number in 1 ml of cell suspension can be calculated as follows:

$$\frac{\text{cell number}}{\text{ml}} = \frac{\text{number of cells in y corner squares}}{\text{y}} \times 1.25 \times 10 \times \frac{10^3 \mu\text{l}}{\text{ml}} \quad \text{Eqn. 1}$$

y = number of corner squares counted

1.25 = dilution factor

10 = factor to account for the chamber volume of 0.1 µl

4.2.2 Cell Proliferation Assays

The aim of proliferation assays was to determine the effects of metformin, TGF-β_2 and SD-208, a TGF-β_2-I-receptor-kinase-inhibitor, on the proliferation of different GBM cell lines. Metformin was used in different concentrations up to 10 mM, the reported EC_{50} for GBM (Würth *et al.* 2013). TGF-β_2 was used at 10 ng/ml according to prior laboratory experience and 1 µM SD-208 was used, because the EC_{50} for GBM was found at at 0.1 µM (Uhl *et al.* 2004). Counting and comparing the number of living cells to the initial cell number allowed for an estimation of cytostatic effects while the number of dead cells was used as a measure of cytotoxic effects. A proliferation assay was performed over five days. On the first day, cells were sowed out, on the third day, they were treated, on the fourth day, they were retreated and on the fifth day, they were harvested, counted and cell pellets were stored away.

4.2.2.1 Preparation of 6-well plates

For optimum coverage, 150,000 cells were sowed per well on a 6-well plate. Therefore, an average of 3 T75 flasks covered in cells was needed. The flasks were treated with cell dissociation solution and a pellet was gained as described in 2.2.1.2. The pellet was redissolved in approximately 5-10 ml of medium depending on its size. Spheroids of RAV19 P25 and P26 had to be disintegrated by repeated pipetting. Then, 40 µl were taken out for cell counting. After the number of cells had been calculated using Equation 1, a predetermined volume of cell solution required to obtain $5x10^6$ cells was put into a 50 ml falcon tube. Medium was then added to obtain a total volume of 50 ml. Following this, five 6-well-plates were filled with 1.5 ml of cell suspension per well, before being incubated to allow cells to settle and adhere to the well.

4.2.2.2 Treatment

After approximately 48 hs, wells were treated to produce 10 different conditions in replicates of 3. In order to prepare the treatments, the following pipetting scheme was used:

Table 15: Treatments for proliferation assays

condition	end volume	medium	substance
control	7 ml	7 ml	-
DMSO control 1:10,000	7 ml	7 ml	0.7 µl DMSO
0.01 mM metformin	11 ml	9.9 ml	1.1 ml from 0.1 mM metformin
0.1 mM metformin	8 ml	8 ml	0.008 ml stock metformin
1 mM metformin	6 ml	5.94 ml	0.06 ml stock metformin
10 mM metformin	7 ml	6.3 ml	0.7 ml stock metformin
SD-208 1 µM	7 ml	6.93 ml	0.07 ml stock SD-208
TGF-β_2 10 ng/ml	7 ml	6.986 ml	0.014 ml stock TGF-β_2
TGF-β_2 10 ng/ml + 0.01 mM metformin	6 ml	5.388 ml	0.6 ml from 0.1 mM metformin + 0.012 ml stock TGF-β_2
TGF-β_2 10 ng/ml + 10 mM metformin	7 ml	6.286 ml	0.7 ml stock metformin + 0.014 ml stock TGF-β_2

Stock solutions used were:

- Metformin 100 mM in RHB-A or DMEM
- SD208 100 µM in 1% DMSO in RHB-A or DMEM
- TGF-β_2 (mammalian) 5 nM in sterilized water, PBS and 0.1% BSA.

The following example illustrates how to calculate the necessary volume of TGF-β_2 stock for an end volume (V_{end}) of 7 mL and an end concentration of 10 ng/ml:

$$V\ end\ = \frac{V\ end}{df} ml\ stock + \left(V\ end - \frac{V\ end}{df}\right) ml\ medium \quad \text{Eqn. 2}$$

$$7\ ml\ = \frac{7}{500}\ ml\ TGFbeta\ stock + \left(7 - \frac{7}{500}\right) ml\ medium \quad \text{Eqn. 3}$$

$$7\ ml = \ 0.014\ \ ml\ TGFbeta\ stock + 6.986\ ml\ medium \quad \text{Eqn. 4}$$

df = dilution factor

$$df = \frac{end\ concentration}{stock\ concentration} \quad \text{Eqn. 5}$$

$$df = \frac{10\ \text{ng/ml}}{5000\ \text{ng/ml}} = 1 : 500 \quad \text{Eqn. 6}$$

After all treatment solutions had been prepared, the supernatant medium was aspirated and 1.5 ml of treatment solution was added per well. In case of spheroid cell growth (RAV19 P25 and P26), only half the medium was taken out to avoid loss of spheres and treatments in double concentration were added.

4.2.2.3 Re-treatment

Starting after approximately 20 hs, cells growing under the conditions “0.01 mM metformin with 3 re-treatments" as well as “TGF-β_2 + 0.01 mM metformin with 3 re-treatments” were retreated 3 times in approximate 4 h intervals. In order to add a minimal amount of fresh medium and still be able to pipette accurately, 15 µl were taken from the remaining volume of the 1 mM metformin solution from the previous day. Thus, each re-treatment added an identical amount of metformin to that used for initial treatment.

4.2.2.4 Harvest and count

48 hs after treatment, cells were harvested, counted and pellets were stored for Western Blotting. All of these procedures were performed under non-sterile conditions. Using a cell scraper, all cells were detached from the bottom of the well. As they tended to form large aggregates, a Pasteur pipette was used to disseminate cells by pipetting up and down 10-20 times. Afterwards, each well was rinsed with the cell suspension and the entire contents were transferred into a 2 ml Eppendorf tube. After 8 minutes of centrifugation at 2500 rpm and 20°C, supernatant medium was carefully transferred into another 2 ml tube for determination of lactate and glucose concentration. The remaining cell pellet was resuspended in 100 to 500 µl of PBS (phosphate-buffer-saline) by up-and-down-pipetting using a 200 µl (20 times) and a Pasteur pipette (10 times). Then, 40 µl were extracted for

counting while the remaining cell suspensions out of 3 wells were pooled. After centrifugation at 2500 rpm and 20°C for 8 minutes, the supernatant was removed and the pellets were stored in the -80°C freezer. Cells were counted according to the protocol in 2.2.1.4, while both dead and viable cells were noted down. In order to calculate the number of cells per well, a modified formula was used:

$$\frac{\text{cell number}}{\text{ml}} = \frac{\text{number of cells in y corner squares}}{\text{y}} \times 1.25 \times 10 \times \text{z ml} \qquad \text{Eqn. 7}$$

y = number of corner squares counted

1.25 = dilution factor

10 = factor to account for the chamber volume of 0.1 µl

z = number of ml used for resuspension of the cell pellet

4.2.3 Crystal-Violet Staining

Crystal violet assays provide an alternative way to determine cell number and thus proliferation. Crystal violet solutions stain all cells fixed to the well. Since in these experiments dead cells were drained with the supernatant, staining the remaining adherent cells within the well was used to determine only the number of viable cells.

4.2.3.1 Preparation of a 96-well plate

5000, 2500 and 1000 cells per well were distributed in 100 µl of medium on 96-well-plates. 6 blank control were also used.

4.2.3.2 Treatment

To let cells adhere, they were kept in the incubator for 48 hs. Afterwards, each batch of cells was treated in replicates of 3 creating the conditions outlined in Table 15. When a proliferation assay was performed on the same day, one extra milliliter of each treatment solution was prepared and used. In order to treat the cells, the medium was carefully removed using a 100 µl pipette as the suction of a Pasteur pipette could potentially have damaged the integrity of the cell layer in the well. Six wells were thus drained at the same time to prevent the cells from drying out. Following this, 100 µl of treatment solution was carefully pipetted against the wall of the well to avoid cell detachment.

4.2.3.3 Re-treatment

As with the proliferation assay, cells under the conditions “0.01 mM metformin with 3 re-treatments” and “TGF-β_2 + 0.01 mM metformin with 3 re-treatments” had to be retreated starting after 20 hs by adding the initial amount of metformin with every re-treatment. Therefore, 10 µl of left over 0.1 mM metformin solution was applied at time intervals of 4 hs.

4.2.3.4 Staining and Measurements

48 hs after the initial treatment, cells were stained using a 0.5% crystal violet solution in 20% methanol. At first, the supernatant was discarded. Next, 50 µl of crystal violet staining solution was pipetted into each well except for the 6 wells used as blank controls. After 10 minutes of incubation at room temperature, the crystal violet staining solution was thoroughly shaken off. The plate was submerged in water 5 times and rinsed with tab water 5 times to wash off any unspecific staining. In order to fully remove unspecific staining, it was very important to shake off the dye quickly and efficiently and to immediately rinse the plate with water. After the plate had dried for a minimum of 24 hs, 50 µl of 0.1 M sodium citrate in 50% ethanol were added per well, redisssolving the dried crystal-violet dye. The resulting solution was then measured photometrically at a wavelength of 550 nm. The more stained cells there were per well, the higher the photometric value was, which was thus taken as a measure of proliferation.

4.2.4 Spheroid Assay

The aim of spheroid assays is to quantify migration using a light microscope in conjunction with a digital imaging device and *ImageJ*, a computer program to measure spheroid area in photographs. Spheroids form when cells are grown on agarose, which prevents cells from adhering to the bottom of the well. In these experiments, spheroid assays were performed to investigate the effects of metformin, SD-208 and TGF-β_2 on GBM cell migration.

4.2.4.1 Preparation of spheroids

Analogous to the proliferation assay, spheroid assays were carried out on five consecutive days. Firstly, spheroids had to form on an agarose coated 96-well-plate. Agarose was used to prevent cells from adhering to the plate bottom. 1 g of GE LP Biozym Agarose was added to 100 ml of PBS and boiled in the microwave until fully dissolved. After letting the agarose cool for approximately 5 minutes, 100 µl were added per well using a step pipette. While the agarose coated plate cooled off, cells were harvested from flasks and prepared as described in 2.2.1.4 and 2.2.1.4. Following this, a cell suspension in fresh medium was prepared for 65 wells, consisting of a total volume of 7 ml with a total cell number of 280,000 cells. Thus,

adding 100 µl of cell suspension per well resulted in a cell number of 4000 per well. The 96-well-plate was subsequently incubated for approximately 48 h.

4.2.4.2 Treatment

The first step for spheroid treatment involved picking spheroids from their wells and transferring them into a U-bottom plate. In order to pick spheroids, 50 µl of the media were carefully taken out and discarded. Then, the remaining 50 µl were taken out. After checking for a spheroid in the pipette tip, it was carefully pipetted into the U-bottom-plate. Secondly, the treatment solutions had to be prepared. When performing a spheroid assay on the same day as a proliferation assay, the solutions mixed for the proliferation assay could be used as a basis. As each well already contained 50 µl of medium without treatment, the concentration of the 50 µl treatment solutions had to be twice as high as in the proliferation assay. In order to adjust for this fact, the pipetting scheme was modulated as shown below. 50 µL of these treatment solutions were added per well in replicates of 6.

Table 16: Treatment for spheroid migration assays

condition	end volume	from prolif. solution	add
control	0.5 ml	0.5 ml	-
DMSO control 1:10000	0.5 ml	0.5 ml	0.05 µl DMSO
0.01 mM metformin	0.5 ml	0.5 ml	0.05 ml from 0.1 mM metformin
1 mM metformin	0.5 ml	0.5 ml	0.005 ml stock metformin
10 mM metformin	0.5 ml	0.5 ml	0.05 ml stock metformin
SD-208 1 µM	0.5 ml	0.5 ml	0.005 ml stock SD-208
TGF-β_2 10 ng/ml	0.5 ml	0.5 ml	0.001 ml stock TGF-β_2
TGF-β_2 10n g/ml + 10 mM metformin	0.5 ml	0.5 ml	0.05 ml stock metformin + 0.001 ml stock TGF-β_2
TGF-β_2 10 ng/ml + SD-208 1 µM	0.5 ml	0.5 ml	0.002 ml stock TGF-β_2 + 0.01 ml stock SD-208

4.2.4.3 Re-treatment

Cells were retreated as described in section 2.2.3.3.

4.2.4.4 Pictures

In order to monitor spheroid migration, each spheroid was photographed at a set time point at 4x magnification. The time points were 0, 20 and 48 hs after treatment. For photography, a microscope with ProgRes C3B camera was used. The pictures were taken digitally using the

ProgRes Capture Pro2.6, JENOPTIK Laser, Optik Systeme GmbH software at 2080x1542 pixels and an exposure time of 8.64 ms. Each picture was later analyzed using ImageJ. Firstly, the scale was set to 152 pixels/mm using a photograph of a Neubauer's hemocytometer as a reference. This scale was applied to all pictures. Secondly, the area of the spheroid was quantified by drawing along the outer border of the spheroid with the freehand selection tool and then measuring its area. For the images taken after 20 and 48 hs, the outer line of cells migrated furthest was used as spheroid border. Thus, the calculated area represents the entire area covered by cells after migration. The example below demonstrates how the same spheroid was measured after 0, 20 and 48 hs using the freehand selection tool and the measurement function of ImageJ.

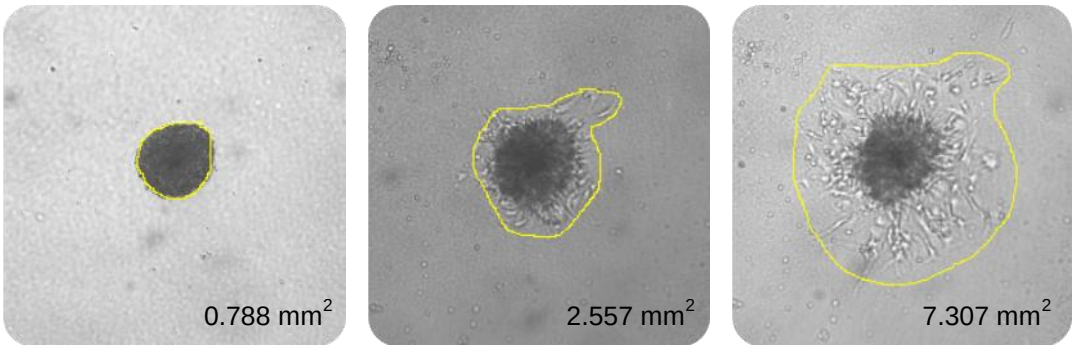

Figure 4: Measuring spheroid areas of RAV19 P23_6 control 1 after 0, 20 and 48 hs.

4.2.5 Scratch Migration Assay

The *scratch migration* assay was performed using special silicon culture inserts to produce a 500 µm cell free gap. Over the course of 48 hs, migration of cells into the gap was documented photographically at different time points to investigate the gap closure time for different cell lines under different conditions.

4.2.5.1 Preparation of 6-well plates

3 culture inserts were glued into each of the six wells by gently pressing them onto the bottom with sterile tweezers. Perfect adhesion is required to form a cell free gap, as cells would otherwise migrate underneath the dividing wall. A solution of 12,500 cells per 70 µl was prepared. Then, they were carefully injected into each culture insert chamber resulting in triplets for the conditions control, 0.01 mM 3x, 0.01 mM, and 10 mM metformin as well as 1 µM SD-208 and 10 ng/ml TGF-β_2.

4.2.5.2 Treatment and re-treatment

After 24 hs of incubation, each well was treated with treatment solutions analogous to proliferation assays (see 2.2.2.2). After the culture inserts had been carefully removed from

the bottom of the well with sterile tweezers, 1.5 ml of treatment solution were pipetted into each well. Starting after 4 hs, the well of “0.01 mM metformin 3x” was retreated 3 times a day at 4 h intervals with 1.5 µl of left over 10 mM metformin solution.

4.2.5.3 Measurements

To monitor cell migration as well as gap closure time, gaps were photographed digitally under the light microscope at 4 h intervals. Pictures were taken at three points of each gap at 10x magnification. In order to accurately reproduce the photo points at each given time point, they were chosen as follows: Firstly, the 'entrance' of the gap was photographed. The second photo was taken of the part directly underneath, avoiding overlap, while the third picture was taken of the 'exit' of the gap. Later, the area of each gap region was determined using the free hand selection tool of the photo program *ImageJ* and measured as described in 2.2.5.4.

4.2.6 Analysis of data

Data obtained in proliferation and migration assays was analyzed using Microsoft Excel. For proliferation assays, values were normalized to the medium control by dividing the number of viable cells per well by the average of viable cells per well in medium controls. Thus, relative proliferation rates were calculated. For migration data, a two-step normalization was performed. At first, values measured after 20 or 48 hs were divided by the initial spheroid size at 0 hs resulting in normalization to 0 hs. Then, these values were divided by the average of the medium control spheroid size at the given time point to obtain relative migration rates. In order to determine statistical significance, relative proliferation rates and relative migration rates under different conditions were compared to the medium control's proliferation/migration rate using a two-tailed heteroscedastic Student's T-Test. The only exemptions were any values obtained for cells treated with SD-208. As SD-208 is dissolved in a solution containing 1% DMSO, a DMSO 1:10,000 control was established to serve as a reference. The following symbols are used to indicate different levels of significance.

Table 17: List of symbols indicating significance

*	p ≤ 0.05 compared to medium control	#	p ≤ 0.05 compared to DMSO-control
**	p ≤ 0.01 compared to medium control	##	p ≤ 0.01 compared to DMSO-control
***	p ≤ 0.001 compared to medium control	###	p ≤ 0.001 compared to DMSO-control

5 RESULTS

5.1 The functional effects of metformin on GBM cells

This work investigated the effects of high and low doses of metformin on different types of GBM cell lines. In 2013, Würth *et al.* were able to show that metformin inhibits proliferation of GBM cells in a dose-dependent manner (Würth *et al.* 2013). Moreover, they calculated that the IC_{50} for metformin is at approximately 10 mM. These findings served as basis for proliferation and migration assays performed with 10 different GBM cells lines. Those cells were treated with 10 mM as well as lower concentrations of metformin. Another aim of the present study was to investigate whether 10 mM metformin reliantly reduces proliferation as well as migration. Concurrently, the susceptibility of certain cell lines towards lower dosages of metformin was of interest.

5.1.1 Overall, high doses of metformin reliably reduced proliferation and migration

As GBM's malignancy is largely due to its rapid proliferation and aggressive migration, these two characteristics were examined in different functional assays. To investigate proliferation, cell counts were carried out, and crystal-violet staining assays were performed to support data exemplarily. Similarly, spheroid migration assays were carried out to examine migration, while scratch migration assays supported the data in selected cases. Proliferation data was obtained in 20 experiments. Two proneural cell lines, RAV19 and RAV57, were used both in the form of brain-tumor-initiating cells (BTICs) and tumor cells (TCs); additionally, three mesenchymal cell lines, RAV21, 24 and 27 were used as BTICs and TCs. Cell counts for each condition were carried out in triplicates; furthermore, each cell count was repeated once with identical cell lines but different passage numbers (n = 6).

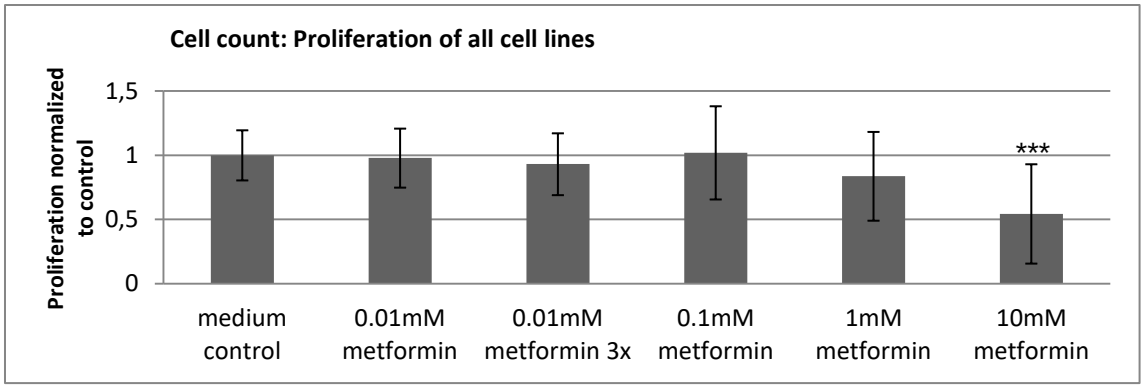

Figure 5: Relative proliferation rates of all cell lines after a 48 h treatment with different concentrations of metformin.

Analysis of the combined proliferation data, demonstrated that only 10 mM metformin produced a significant decrease in proliferation to about 54% compared to the medium control ($p < 0.001$). Lower concentrations of metformin failed to reduce proliferation significantly. Yet, the large standard deviations indicate that different cell lines exhibit varying susceptibility to the anti-proliferative effects of metformin, especially in low doses.

Proliferation and migration assays were performed with cells of the same passage number to ensure comparability. Spheroid migration assays were carried out in sets of 6 for each condition. Again, each experiment was repeated once to ensure a large database to draw from ($n = 12$). Migration was monitored atfter 20 and 48 hs in correlation to proliferation assays with 48 hs as end point. The measured values for spheroid area at each time point were normalized by division by the corresponding initial spheroid size at 0 hs. To compare the differing migratory rates of all cell lines each value was normalized to the average of the non-treated control. As a result, the migratory rate of each condition is shown as relative rate compared to the non-treated control. Figure 9 depicts the average effects of low and high doses of metformin on all cell lines after 20 and 48 hs.

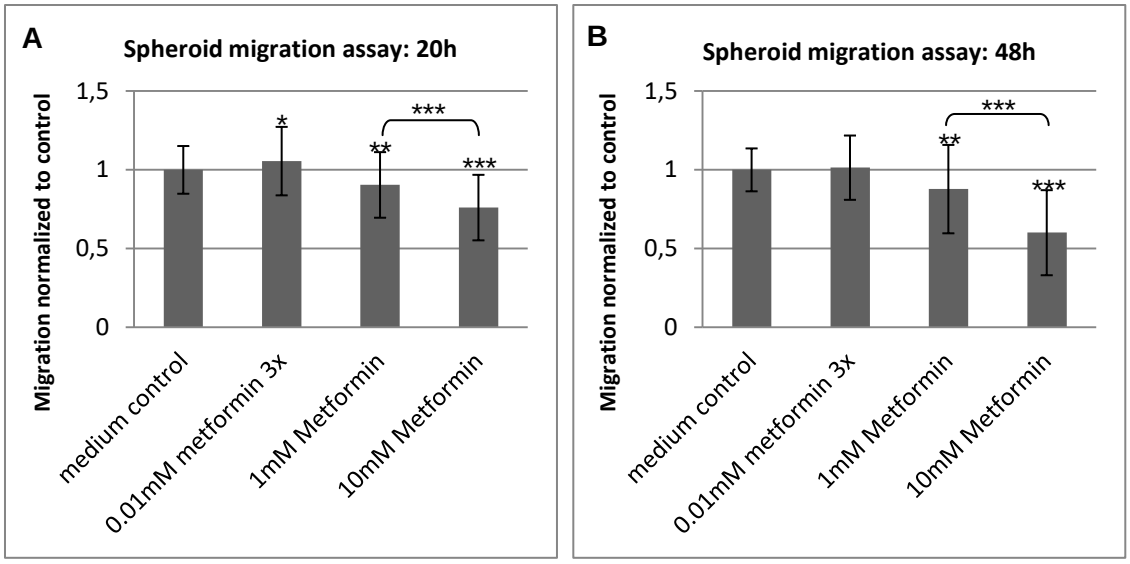

Figure 6: Relative migratory rates of all cell lines after 20 and after 48 hs of treatment with increasing concentrations of metformin: Migration was normalized in two steps: Values of each time point were normalized to initial spheroid size, followed by normalization to the medium control.

At both time points, low concentrations of metformin such as 0.01 mM in triple application showed small effects (migration increased by 5% and 1% respectively). However, intermediate and high concentrations of metformin inhibited migration. As opposed to proliferation assays where 1 mM metformin did not yield a significant reduction, 1 mM metformin reduced migration by 10% after 20 hs and 13% after 48 hs ($p < 0.003$ in both cases). Yet, 10 mM metformin was significantly more effective, decreasing migration by 34% after 20 hours and by 40% after 48 hours ($p < 0.0001$ in both cases).

In summary, high doses of metformin reliably decreased proliferation and migration of GBM cells. Intermediate doses such as 1 mM metformin reduced migration significantly but revealed no consistent anti-proliferative effect. In contrast, low doses of metformin neither decreased proliferation nor migration significantly considering the overall data. Since susceptibility to metformin was heterogeneous, different groups of cells lines as well as individual cell lines were examined more closely as described in the following sections.

5.1.2 Susceptibility to metformin's anti-proliferative and anti-migratory action varied among subgroups of cells

According to cell characteristics and differentiation, cells were grouped into four categories: proneural BTICs, mesenchymal BTICs, proneural TCs, and mesenchymal TCs.

5.1.2.1 Low-dose metformin decreases proliferation of proneural BTICs effectively

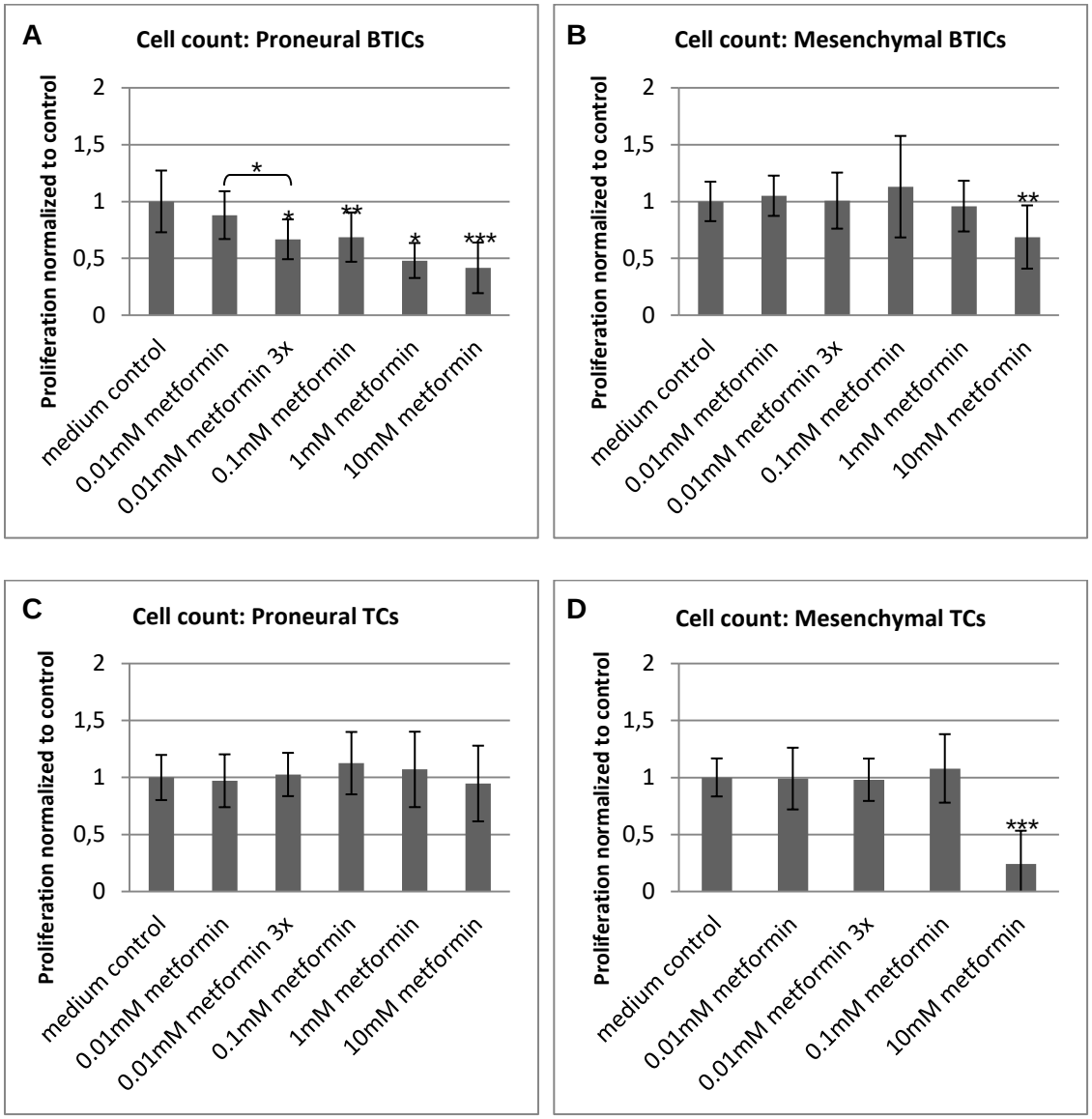

Figure 7: Cell counts after 48 hs of treatment with increasing concentrations of metformin: Absolute numbers of viable cells per well at every condition were divided by the average number of viable cells of the non-treated control.

The anti-proliferative power of even low dosages of metformin becomes evident when looking at different groups of cell lines, especially in proneural BTICs RAV19 and RAV57. Accordingly, triple re-treatment of cells with a very low dose of 0.01 mM metformin resulted in a marked decrease of proliferation (33% decrase) compared to the medium control ($p < 0.003$), see Figure 7 A. Triple re-treatment with 0.01 mM metformin led to a significantly more pronounced decrease in proliferation than single treatment with 0.01 mM metformin ($p < 0.05$). Treatment of proneural BTICs with 0.1 mM metformin decreased proliferation by 31% compared to the medium control ($p < 0.006$). Therefore, treatment and re-treatment of proneural BTICs with low concentrations of metformin was effective to decrease proliferation. However, all other groups of cell lines did not exhibit significant responses to low doses of metformin as depicted in Figure 7 B-D.

As the magnitude of the anti-proliferative effect of metformin is most different between proneural and mesenchymal BTICs, their distinct susceptibilities to metformin are displayed in Figure 8.

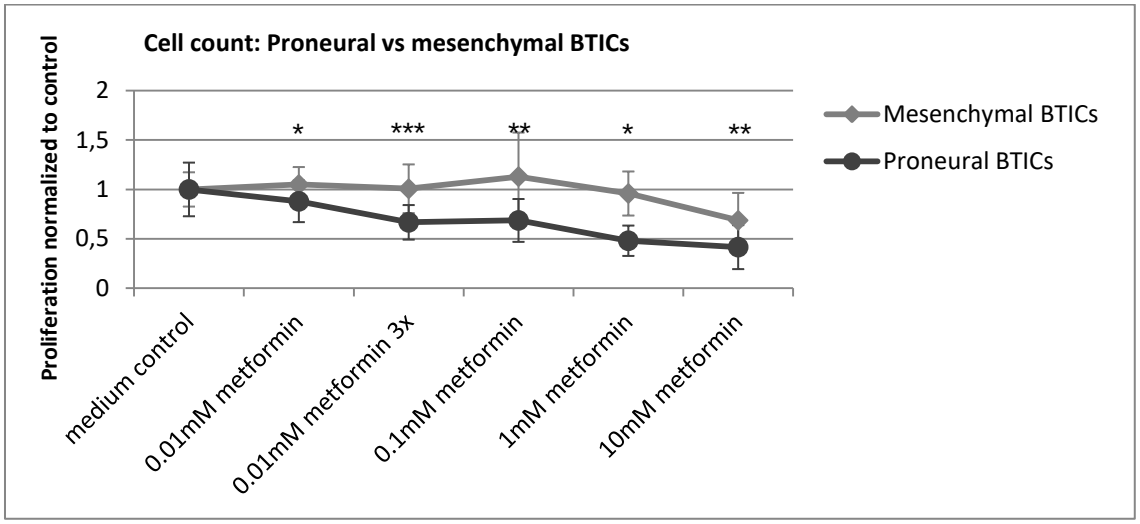

Figure 8: Comparing the different effect sizes of metformin's anti-proliferative action between proneural and mesenchymal BTICs: Symbols of significance are put at a distance to indicate that proliferation rates of proneural cell lines RAV19 and 57 are compared to those of mesenchymal cell lines RAV21, 24 and 27 and not, as usually the case, to the medium control.

For every concentration of metformin used, proneural BTICs' proliferation decreased more than mesenchymal BTICs'. The susceptibility profile can be described as follows: proneural BTICs RAV19 and 57 were highly responsive to metformin whereas mesenchymal BTICs RAV21, 24 and 27 were little responsive.

Figure 7 also shows that susceptibility to anti-proliferative effects of high dose metformin differs considerably. Even though 10 mM metformin were able to reduce proliferation in all except proneural TCs, the comparison of reaction patterns, as detailed in Figure 9, reveals heterogeneous susceptibility to metformin.

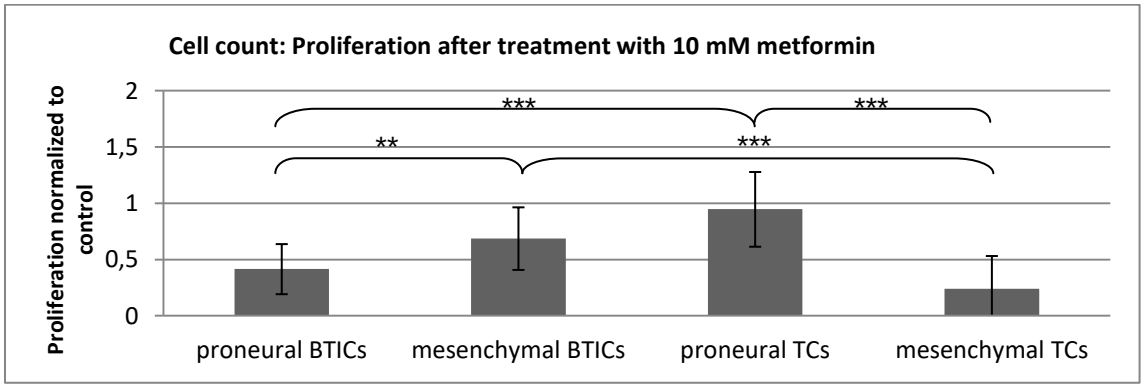

Figure 9: Comparing the effects of 10 mM metformin on different groups of cells.

Mesenchymal TCs showed the strongest reaction to 10 mM metformin. Their proliferation rate was reduced to 0.24 compared to the non-treated control ($p < 0.0001$). Their proneural

counterparts were almost not affected as their relative proliferation decreased to 0.95 (non-significant). These findings were reversed when comparing proneural to mesenchymal BTICs: Whereas 10 mM metformin led to a decrease to 0.68 in mesenchymal BTICs ($p < 0.002$), proliferation was lowered to 0.42 in proneural BTICs ($p < 0.0001$).

5.1.2.2 High dose metformin impaired migration in all groups of cells with proneural BTICs being most susceptible

Analyzing metformin's anti-proliferative effects showed that different groups of GBM cells exhibited different reaction patterns. This was also true when examining migration of GBM cells. In spheroid migration assays, photos were taken after 20 hs and 48 hs to assess the area covered in cells. Figures 10 and 11 compare the relative migratory rates normalized to 0 hs and to the medium control of the four different groups of cells.

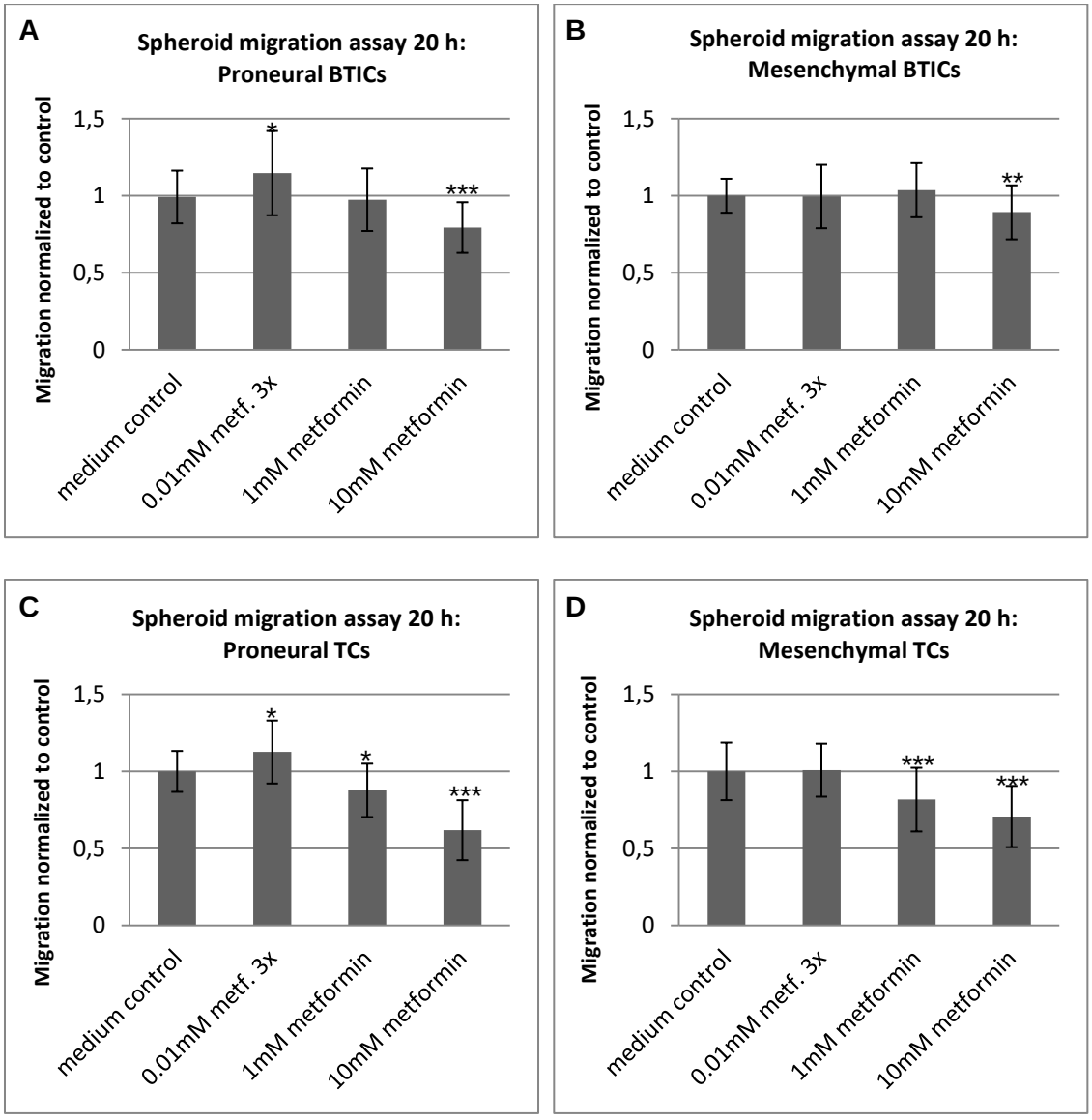

Figure 10: Spheroid migration measured after 20 hs of treatment with different concentrations of metformin: Migration was normalized in two steps: Values of each time point were normalized to initial spheroid size, followed by normalization to the medium control.

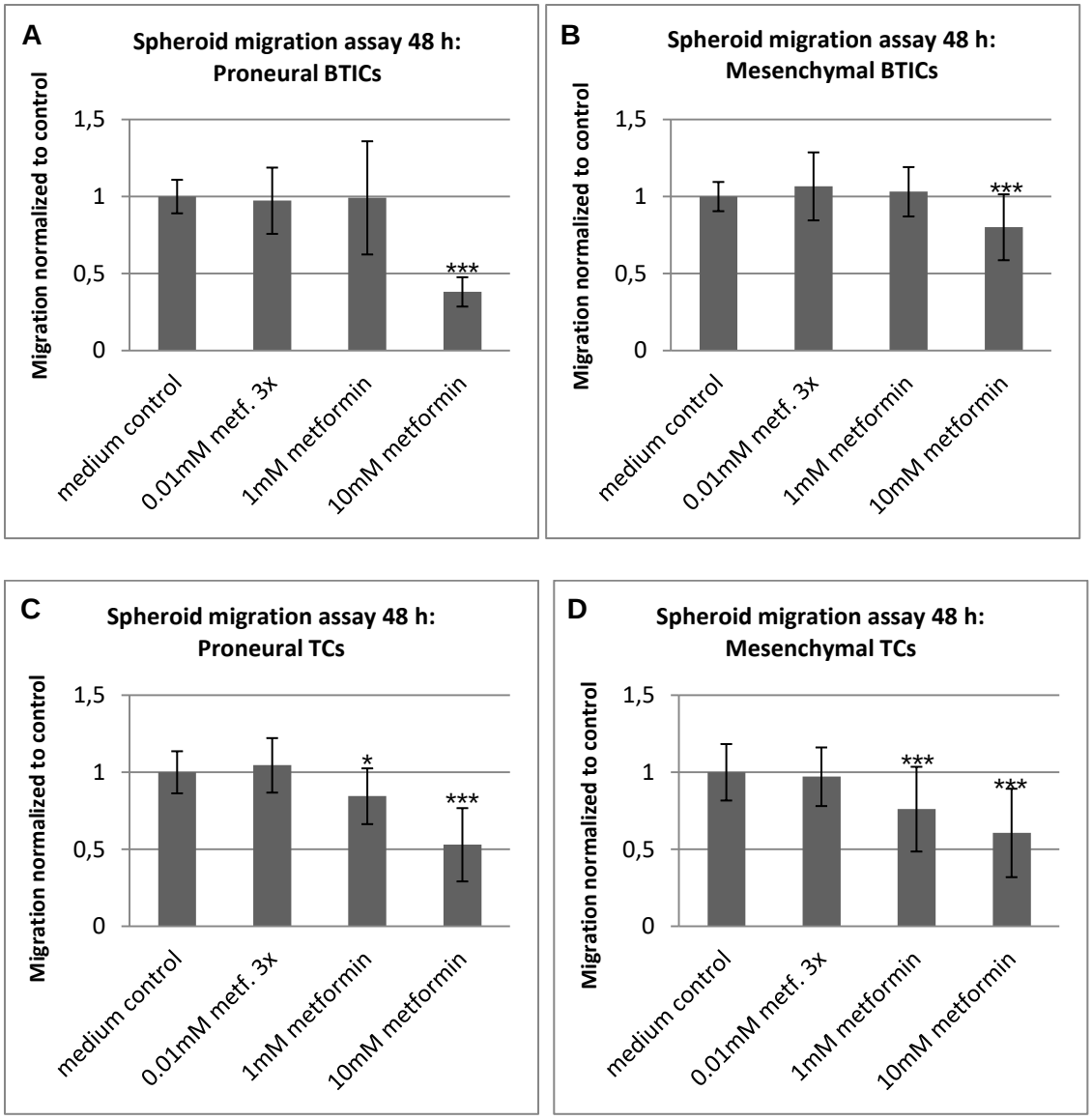

Figure 11: Spheroid migration measured after 48 hs of treatment with different concentrations of metformin: Migration was normalized in two steps: Values of each time point were normalized to initial spheroid size, followed by normalization to the medium control.

Looking at migration after 20 and after 48 hs, three trends were observed. Firstly, low doses of metformin were not able to reduce migratory rates significantly. Even migratory rates of proneural BTICs - which had been very responsive to low-dose metformin's anti-proliferative effects - were not significantly reduced by low doses. Secondly, intermediate doses of metformin consistently diminished migration in TCs but not in BTICs. Thirdly, high doses of metformin clearly reduced migration in all groups of cells. The effect size of 10 mM metformin varied across the four of groups.

Proneural BTICs were most susceptible to 10 mM metformin's action with migration being reduced to 0.38 after 48 hs of treatment ($p < 0.0001$). 10 mM metformin exerted vast anti-proliferative and anti-migratory effects on proneural BTICs. Mesenchymal BTICs on the other hand were less responsive to metformin's anti-migratory action. Migration was decreased by

20% to 0.80 ($p < 0.0001$), resulting in a significant difference in susceptibility when compared to proneural BTICs ($p < 0.001$). For proneural TCs, proliferation was reduced to 0.95 (non-significant) while migration was reduced to 0.53 ($p < 0.0001$). Lastly, 10 mM metformin inhibited both proliferation and migration of mesenchymal TCs: Proliferation was reduced to 0.24 ($p < 0.0001$), and migration was reduced to 0.61 ($p < 0.0001$). Table 18 sums up the differences of susceptibility to metformin regarding proliferation and migration highlighting that low doses of metformin significantly reduced proliferation of proneural BTICs and that high doses of metformin consistently decreased both, migration and proliferation of all GBM cells.

Table 18: Review of the anti-proliferative and anti-migratory effects of different concentrations of metformin after 48 hs of treatment: The left column of each group (dark grey) shows how strongly proliferation was reduced. The right column shaded in light grey depicts contraction of migration at the 48 h time point. Only significant results are shown. Symbols indicate the following: - indicates that proliferation/migration was reduced by up to 25%, - - by 25-50%, - - - by 50-75% and - - - - by more than 75%.

	Pro BTICs		**Mes BTICs**		**Pro TCs**		**Mes TCs**	
	Prolif.	Migra.	Prolif.	Migra.	Prolif.	Migra.	Prolif.	Migra.
0.01 mM	-							
0.01 mM 3x	- -							
0.1 mM	- -							
1 mM	- - -					-		-
10 mM	- - -	- - -	- -	-		- -	- - - -	- -

5.1.3 Unique cellular reaction patterns to metformin

5.1.3.1 Detailed analysis of proliferation and migration of proneural BTICs RAV19 and RAV57

As each group comprised two or three different cell lines, it was important to examine metformin's effects on proliferation and migration on an individual level. The group of proneural BTICs consisted of RAV19 and RAV57. Experiments for each cell line were carried out twice, preferably with cells of comparable passage numbers to avoid changes in reaction patterns due to further passaging.

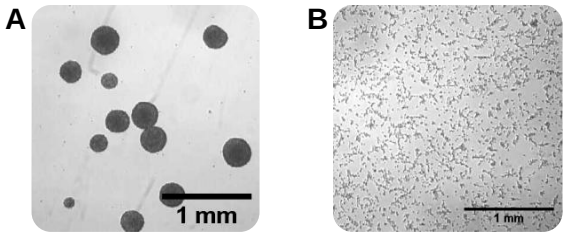

Figure 12: Brain-tumor initiating cells in culture flasks: RAV19 (A) and RAV57 (B).

Figure 13 shows the total number of cells per well as the sum of viable and dead cells.

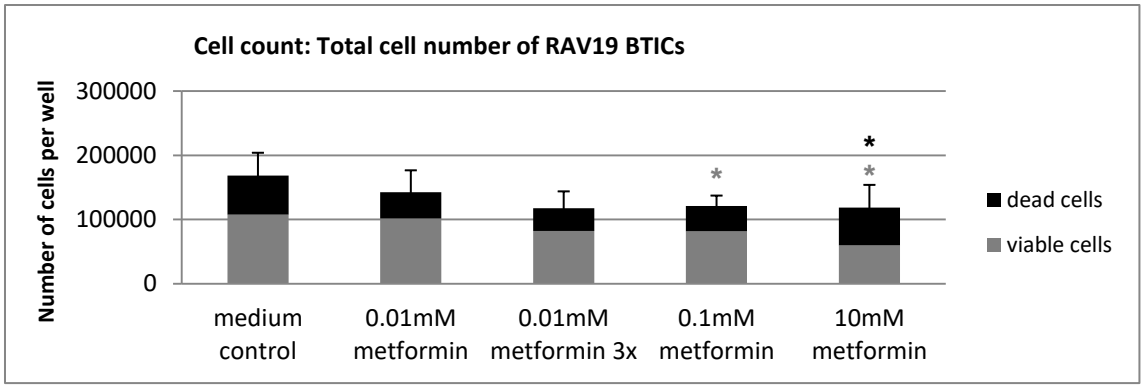

Figure 13: Total cell number per well obtained after treating RAV19 P25 and P26 with different concentrations of metformin for 48 hs: The numbers of viable cells are shown in grey. Accordingly, significant differences between proliferation in treated wells and proliferation in medium control wells are marked with grey stars. Absolute numbers of dead cells are shaded black. Significant differences between the fraction of dead cells in any treated well compared to those in the medium control are marked with a black star.

In line with previous observations of proneural BTICs, RAV19 P25 and P26's proliferation was reduced by low-dose and high-dose metformin. 0.01 mM metformin decreased proliferation by 37% and 10 mM by 46% ($p < 0.05$ and $p < 0.03$). Additionally, the fraction of dead cells in wells treated with 10 mM metformin increased by 13% compared to the medium control ($p < 0.02$) so that 10 mM metformin proved to be a cytotoxic dose to RAV19 BTICs.

RAV57 P16 and P18 grow adherently (see Figure 12). Therefore, cell counts and spheroid migration assays were performed as detailed in 4.2.2 and 4.2.4. Dead and viable cells were counted and results are outlined in the following figure.

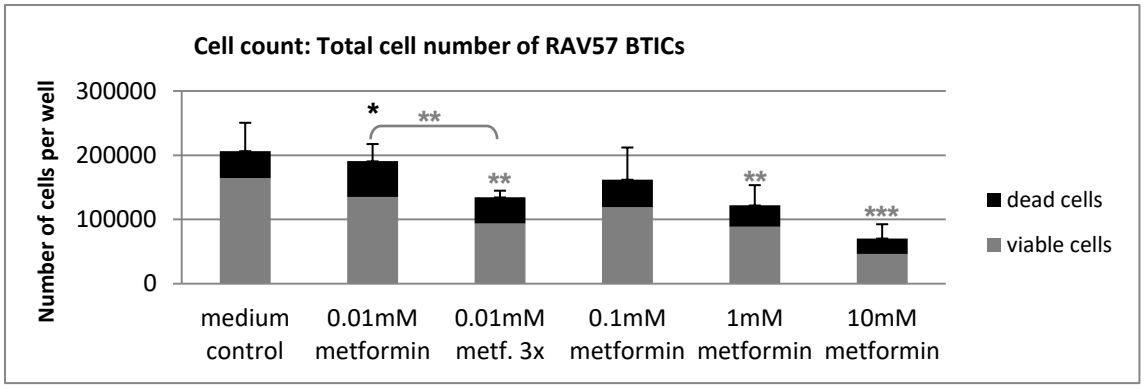

Figure 14: Total cell number per well obtained after treating RAV57 P16 and P18 with different concentrations of metformin for 48 hs: The numbers of viable cells are shown in grey. Accordingly, significant differences between proliferation in treated wells and proliferation in medium control wells are marked with stars. Absolute numbers of dead cells are shaded black. Significant differences between the fraction of dead cells in any treated well compared to the fraction of dead cells in the medium control are marked with black stars.

Proliferation data from RAV57 P16 and P18 coressponded well to the observations seen with RAV19 P25 and P26: Even low doses of metformin were effective to decrease proliferation. Interestingly, 0.01 mM metformin with triple re-treatment lowered proliferation by 43% ($p < 0.006$) while the single treatment reduced proliferation by 18% (non-significant). Thus, the effects of 3x 0.01 mM metformin were almost as pronounced as those of 1 mM metformin, which diminished proliferation by 52% ($p < 0.008$). Hence, both proneural BTICs examined were greatly susceptible to low-dose metformin. In addition, RAV57 P16 and P18 were highly susceptible to high-dose metformin: 10 mM metformin decreased proliferation by 71% ($p < 0.0004$). In summary, proliferation of both proneural cell lines, RAV19 and RAV57, was inhibited by low-dose and high-dose metformin.

Spheroid migration assays with RAV19 P25 and P26 were carried out using laminin-coated U-bottom-wells to enable cell adhesion. As RAV57 P16 and P18 grow adherently, no laminin was required during spheroid migration assays. Figure 15 depicts relative migratory rates of both cell lines.

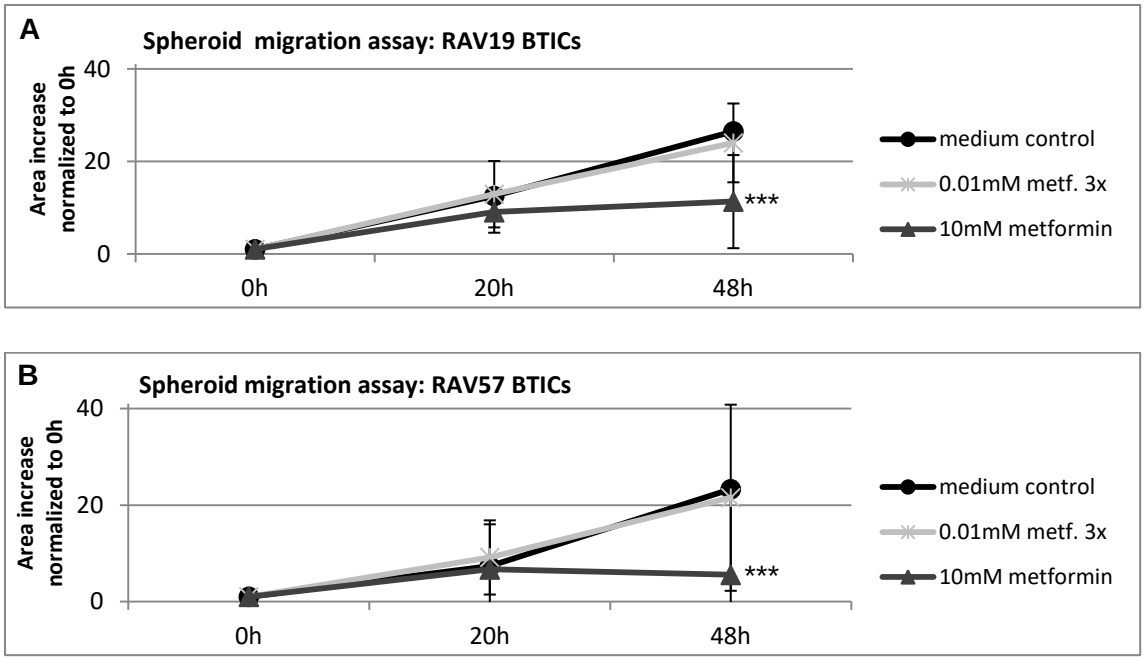

Figure 15: Relative increase of spheroid area of proneural BTICs RAV19 (A) and RAV57 (B) after 48h treatment with different concentrations of metformin: Spheroid sizes were measured after 20 and 48 hs. Migration was normalized in two steps: Values of each time point were normalized to initial spheroid size, followed by normalization to the medium control.

Low doses of metformin were not able to inhibit migration of RAV19 and RAV57 spheroids. Yet, 10 mM proved to exert vast anti-migratory effects on both cell lines. RAV19's spheroid relative migratory rate was more than halved ($p < 0.0001$) and RAV57's was reduced to less than a third ($p < 0.0001$).

Thus, individual examination of proneural BTICs RAV19 and 57 reveals that the effects of metformin within the group are homogeneous: Low and high doses of metformin decreased proliferation while high doses substantially decreased migration.

5.1.3.2 Detailed analysis of proliferation and migration of mesenchymal BTICs RAV21, RAV24 and RAV27

In the group of mesenchymal brain-tumor initiating cell lines, experiments were performed with RAV21 P19, RAV24 P12 and P14 as well as RAV27 P16 and P20.

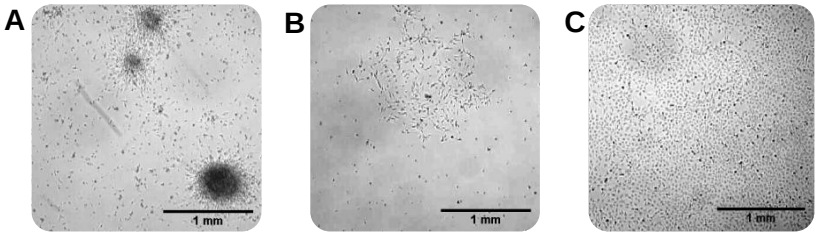

Figure 16: Brain-tumor initiating cells in culture flasks: RAV21 (A), RAV24 (B) and RAV27 (C).

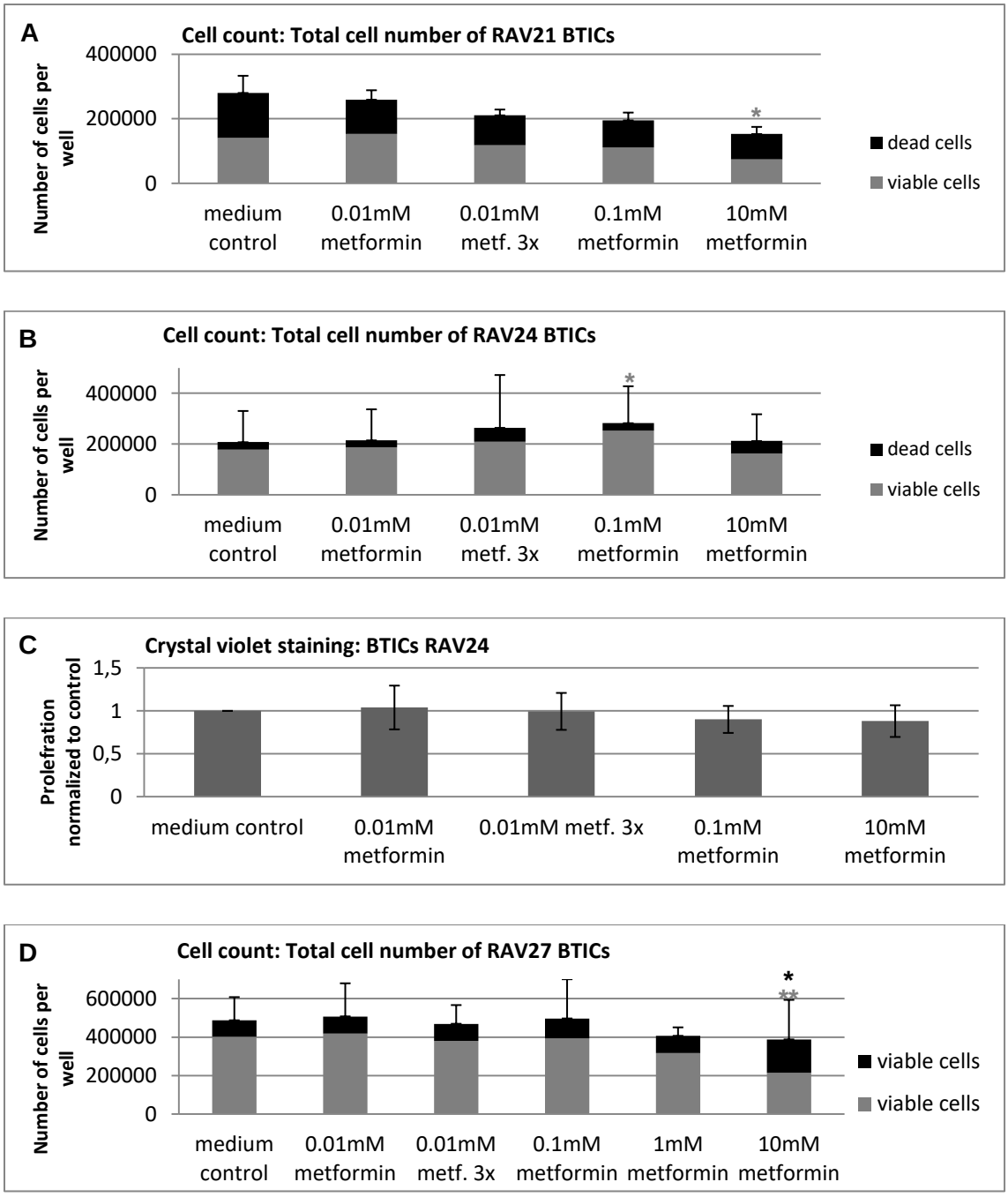

Figure 17: Total cell number per well obtained after treating RAV21 P19 (A), RAV24 P12 and P14 (B and C) and RAV27 P16 and P20 (D) with different concentrations of metformin: For (A), (B) and (D), the numbers of viable cells are shown in grey. Accordingly, significant differences between proliferation with treatment and at medium control conditions are marked with grey stars. Absolute numbers of dead cells are shaded black. Significant differences between the fraction of dead cells in any treated well compared to the fraction of dead cells at medium control conditions are marked with black stars. In (C), proliferation relative to the medium control from a crystal violet assay is shown. Here, the amount of viable cells was determined, only.

Mesenchymal brain tumor initiating cell lines RAV21 and RAV27 responded to high-dose metformin. Proliferation decreased by 48% in RAV21 ($p < 0.05$) and by 49% in RAV27 ($p < 0.03$) when cells were treated with 10 mM metformin for 48 hs. For RAV27, the fraction of dead cells in wells treated with 10 mM metformin was 27% higher than in the medium control ($p < 0.05$). Lower concentrations of metformin (0.01 mM) resulted in a 48% increase

in proliferation in RAV24 ($p < 0.04$). To validate cell-counting data, a crystal violet staining assay was exemplarily performed with RAV24. It also showed that metformin did not alter proliferation of RAV24 significantly.

Proliferation and spheroid migration assays were preferably performed with mesenchymal cell lines of identical passage number to ensure comparability. Solely in the case of RAV21 this was not possible, thus RAV21 P17 and P24 were investigated for migration assessment.

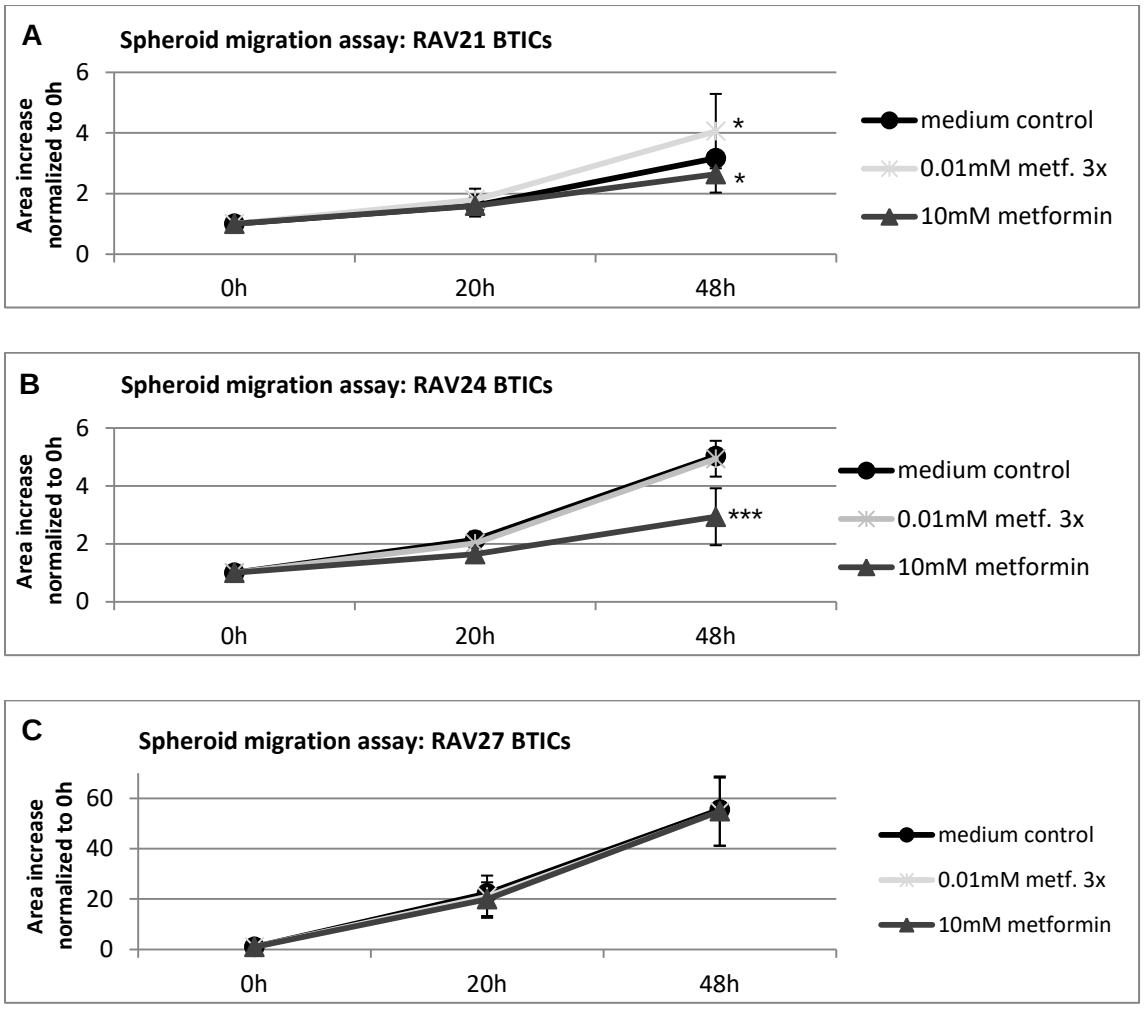

Figure 18: Relative increase of spheroid area in mesenchymal BTICs RAV21 (A), RAV24 (B) and RAV27 (C) after 48h treatment with different concentrations of metformin: Spheroid sizes were measured after 20 and 48 hs. Migration was normalized in two steps: Values of each time point were normalized to initial spheroid size, followed by normalization to the medium control.

Migratory rates of mesenchymal BTICs were influenced by metformin to a different extent. After 48 hs, migration of RAV21 P17 and P24 increased to 1.27 due to 0.01 mM metformin in triple re-treatment ($p < 0.02$); however, 10 mM metformin caused a decline to 0.83 ($p < 0.02$). Migratory rates of RAV24 P12 and P14 dropped to 0.58 with 10 mM metformin treatment ($p < 0.0001$) while those of RAV27 P16 and P20 remained unaffected by any concentration of metformin. RAV27 P16 and P20 showed aggressive migration. After 48 hs spheroid sizes were 55 times larger than initial spheroid sizes, regardless of any treatment (medium control

or 10 mM metformin). Spheroid sizes of RAV21 and RAV24 on the other hand quintupled, indicating a less aggressive migratory behavior.

En masse, metformin exerted the following effects on mesenchymal BTICs: (i) 10 mM reduced proliferation and migration in RAV21, (ii) RAV24's proliferation remained unaffected while migratory rates declined, and (iii) RAV27's proliferation has halved, but its migratory rates did not change significantly.

5.1.3.3 Detailed analysis of proliferation and migration of proneural TCs RAV19 and RAV57

As illustrated in Figure 19, cells of RAV19 changed their morphology upon differentiation. While BTICs grew as spheres, RAV19 TCs grew adherently. Cells of RAV57 continued to grow adherently but changed morphology to a more spindle-like shape.

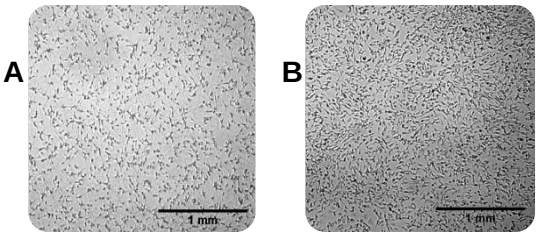

Figure 19: Differentiated GBM cells in culture flasks: RAV19 (A) and RAV57 (B).

Due to the low proliferation rate of differentiated RAV 19 and 57, the usual 150,000 cells/well were not obtained. Therefore, 60,000 cells/well of RAV19 P23_6 were sowed out, 70,000 cells/well of RAV57 P17_2 and 30,000 cells/well of RAV57 P20_3 were used.

Consequently, the average number of cells per well obtained during cell counts decreased. Compared to an average of 100.000 to 200.000 cells/well counted for proneural BTICs, there was only an average of 20.000 to 40.000 cells/well to be determinded after differentiation.

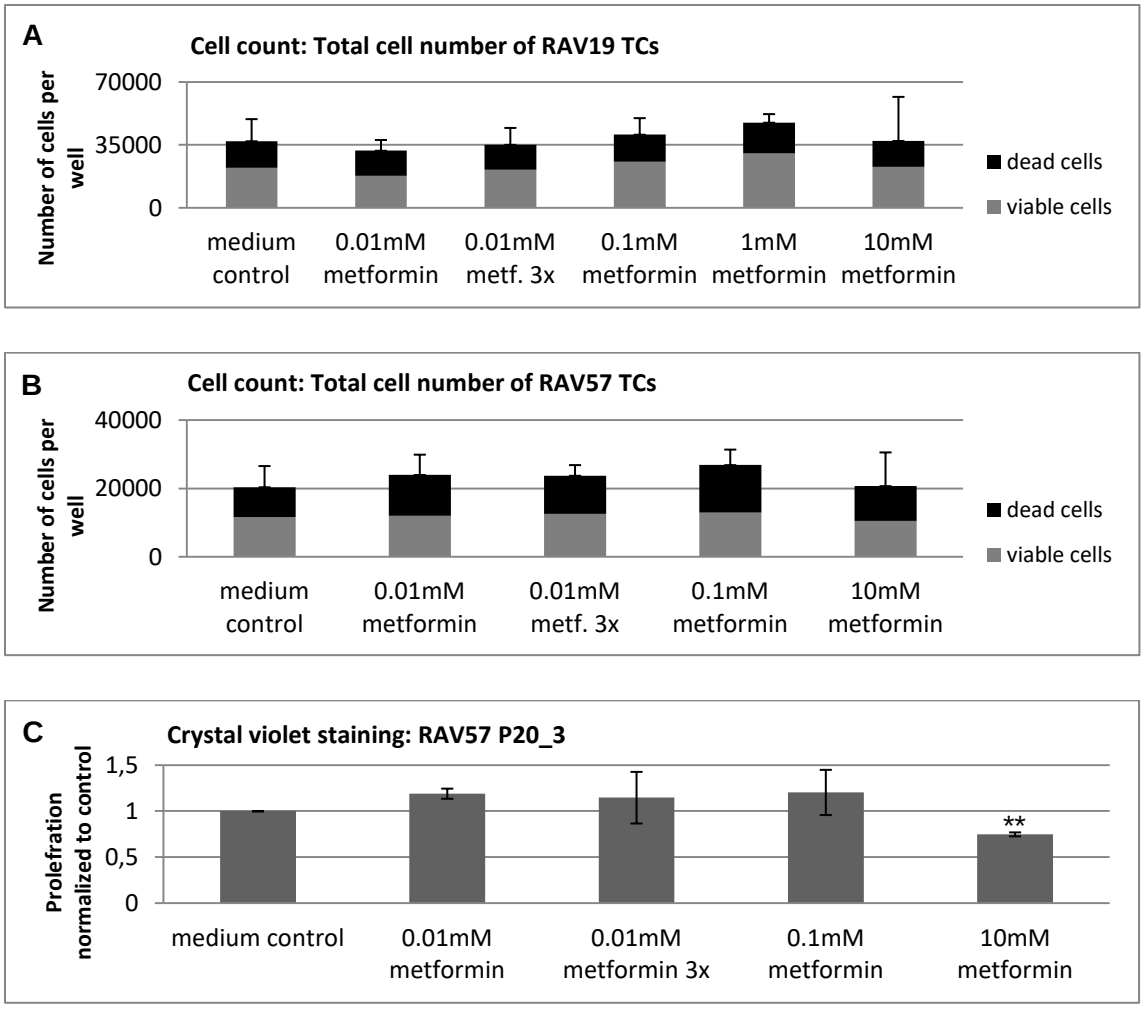

Figure 20: Cell count with total number of cells per well after treatment of RAV19 P23_3 and P23_6 (A) and RAV57 P17_2 and P20_3 (B) with different concentrations of metformin and crystal violet staining assay of RAV57 P20_3 (C): For (A) and (B), the numbers of viable cells are shown in grey. Accordingly, significant differences between proliferation with treatment and at medium control conditions are marked with grey stars. Absolute numbers of dead cells are shaded black. Significant differences between the fraction of dead cells in any treated well compared to the fraction of dead cells at medium control conditions are marked with black stars. In (C), proliferation relative to the medium control from a crystal violet assay is shown. Here, the amount of viable cells was determined, only.

During cell counts, neither RAV19 P23_3 and P23_6 nor RAV57 P17_2 and P20_3 showed significant changes in numbers of viable and dead cells after 48 hs of treatment with metformin. Alternative data obtained in a crystal violet staining assay performed with RAV57 P20_3 showed that proliferation modestly decreased to 0.75 when treated with 10 mM metformin ($p < 0.003$).

Spheroid migration assays were performed with proneural tumor cells of identical passage numbers as those used for cell counts.

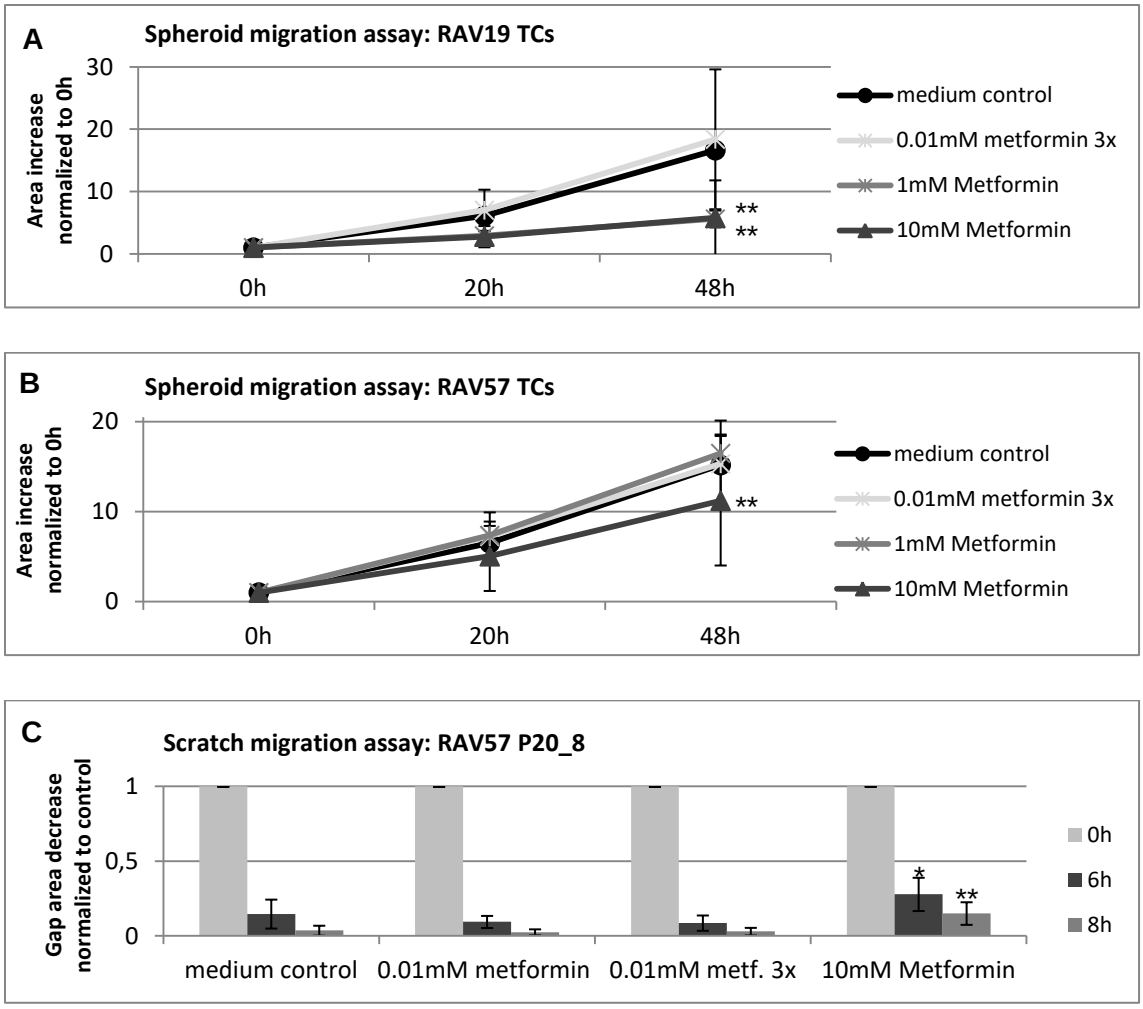

Figure 21: Relative increase of spheroid area in proneural TCs RAV19 (A) and RAV57 (B) with additional data from a scratch migration assay performed with RAV57 P20_8 (C): For (A) and (B), spheroid sizes were measured after 20 and 48 hs. Migration was normalized in two steps: Values of each time point were normalized to initial spheroid size, followed by normalization to the medium control. For reasons of clarity, significances are only marked for the end point of 48 hs. For (C), gap areas were measured at 0, at 6 and at 8 hs. Values for 6 and 8 hs were then divided by values obtained at 0 hs. In a second step, the gap area relative to initial gap size was divided by the average of relative gap area of the controls resulting in data showing gap area decrease relative to 0 hs and to the medium control.

As opposed to proliferation rates, migratory rates of proneural TCs were lowered by high-dose metformin. After 48 hs, RAV19 TC spheroids had quintupled in size when 1 mM or 10 mM metformin was present while spheroids in medium control wells had expanded to an average of 16 times their initial size ($p < 0.003$ in both cases). 10 mM metformin impaired RAV57 TC spheroids' expansion significantly but less pronounced: After 48 hours, it was 11 times the initial size while spheroids in medium control wells had reached 15 times their initial size ($p < 0.005$). A scratch migration assay performed with RAV57 P20_8 supported these results. After 6 hours and after 8 hs, the cell free gaps in wells treated with 10 mM metformin were larger than those of the medium control wells measuring twice the size of control wells after 6 hs ($p < 0.02$) and four times the size after 8 hs ($p < 0.002$). Hence, metformin exerts anti-migratory effects on individual proneural TC lines.

5.1.3.4 Detailed analysis of proliferation and migration of mesenchymal TCs RAV21, RAV24 and RAV27

All mesenchymal TCs grew adherently. Yet, in some cases, proliferation of mesenchymal TCs was slower than that of BTICs. Due to these diminished proliferation rates, less than the usual 150,000 cells/well were sowed out for RAV21 P24_10 (60,000 cells/ well), RAV24 P10_5 (70,000 cells/well) and RAV24 P10_7 (100,000 cells/well).

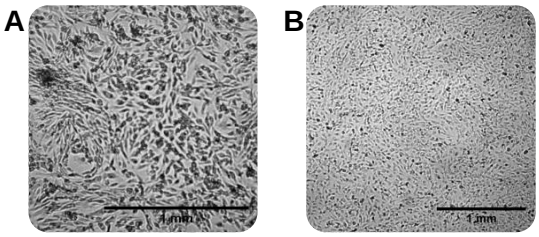

Figure 22: Differentiated GBM cells in culture flasks: RAV24 (A) and RAV27 (B).

Proliferation after treatment with metformin was assessed after 48 hs using cell counts and investigated exemplarily by crystal violet staining assays.

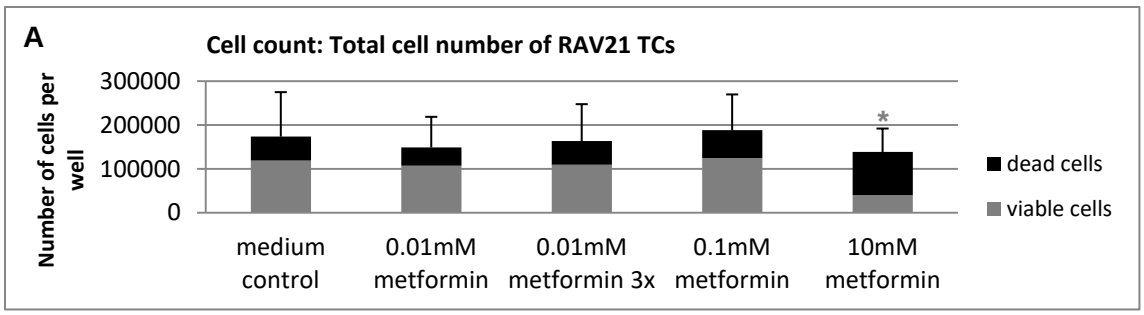

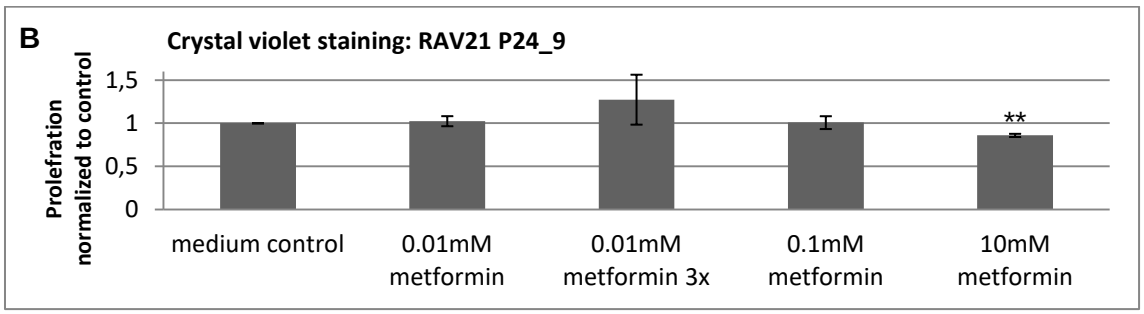

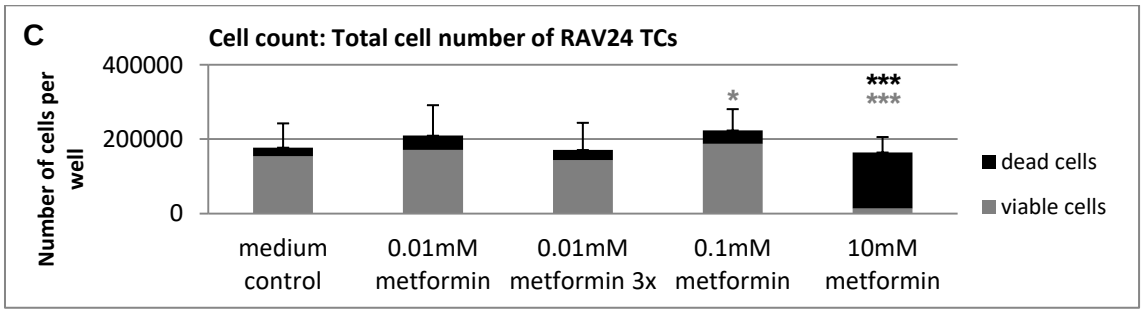

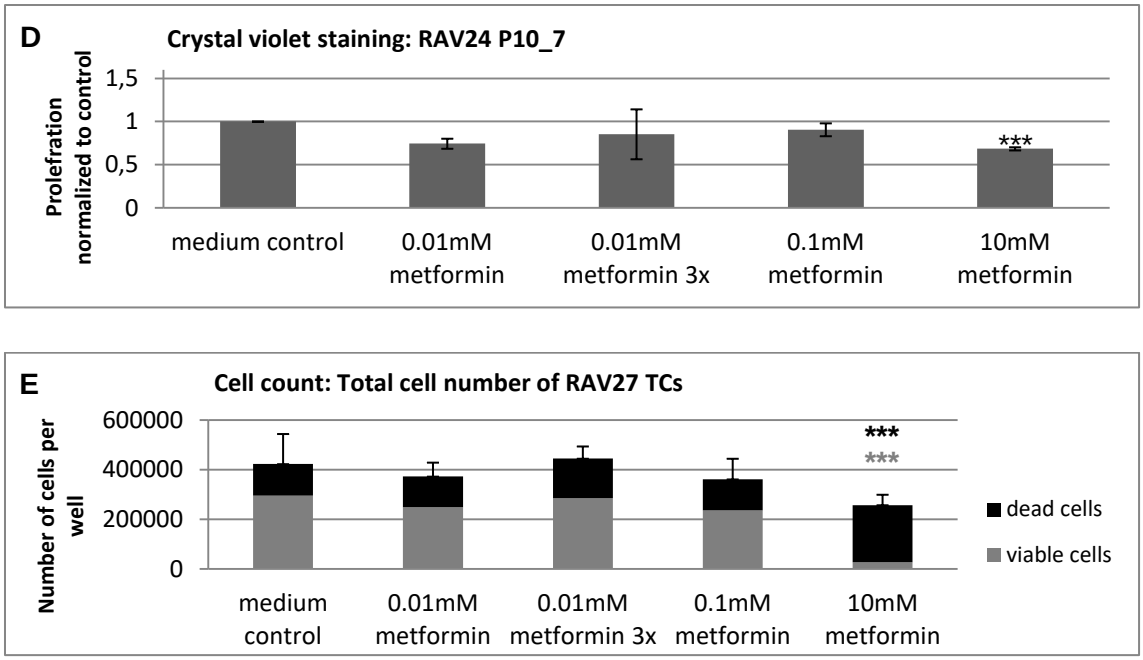

Figure 23: Cell counts with absolute number of cells and crystal violet stainings with proliferation normalized to control: For cell counts of RAV21 P24_9 and P24_10 (A), RAV24 P10_5 and P10_7 (C) and of RAV27 P18_5 and P18_6 (E)**,** the numbers of viable cells are shown in grey. Accordingly, significant differences between proliferation with treatment and at medium control conditions are marked with grey stars. Absolute numbers of dead cells are shaded black. Significant differences between the fraction of dead cells in any treated well compared to the fraction of dead cells at medium control conditions are marked with black stars. For crystal violet staining assays of RAV21 P24_9 (B) and RAV24 P10_7 (D), relative proliferation is shown.

All three mesenchymal TC lines were very susceptible to high-dose metformin's anti-proliferative action: RAV21 TC's proliferation rates decreased by 50% ($p < 0.03$), those of RAV24 TCs decreased by 89% ($p < 0.0001$) and those of RAV27 TCs by 90% ($p < 0.0003$). The anti-proliferative effects that 10 mM metformin exerted on RAV24 TCs and RAV27 TCs were cytotoxic in nature as the fraction of dead cells in metformin treated wells was 7 times higher than in control wells for RAV24 ($p < 0.0007$) and 3 times higher for RAV27 ($p < 0.0001$). To support these findings, crystal violet staining assays were performed. There, the anti-proliferative effects of 10 mM metformin were less pronounced than in cell counts. 10 mM metformin reduced proliferation to 86% in RAV21 TCs ($p < 0.006$) and to 69% in RAV24 TCs ($p < 0.007$). Each mesenchymal tumor cell line exhibited large proliferation decreases due to metformin confirming on an individual level the effects that had been characteristic for the entire group.

Migratory rates of mesenchymal TCs RAV21, RAV24 and RAV27 were assessed in spheroid migration assays using cells of identical passage number as in proliferation assays.

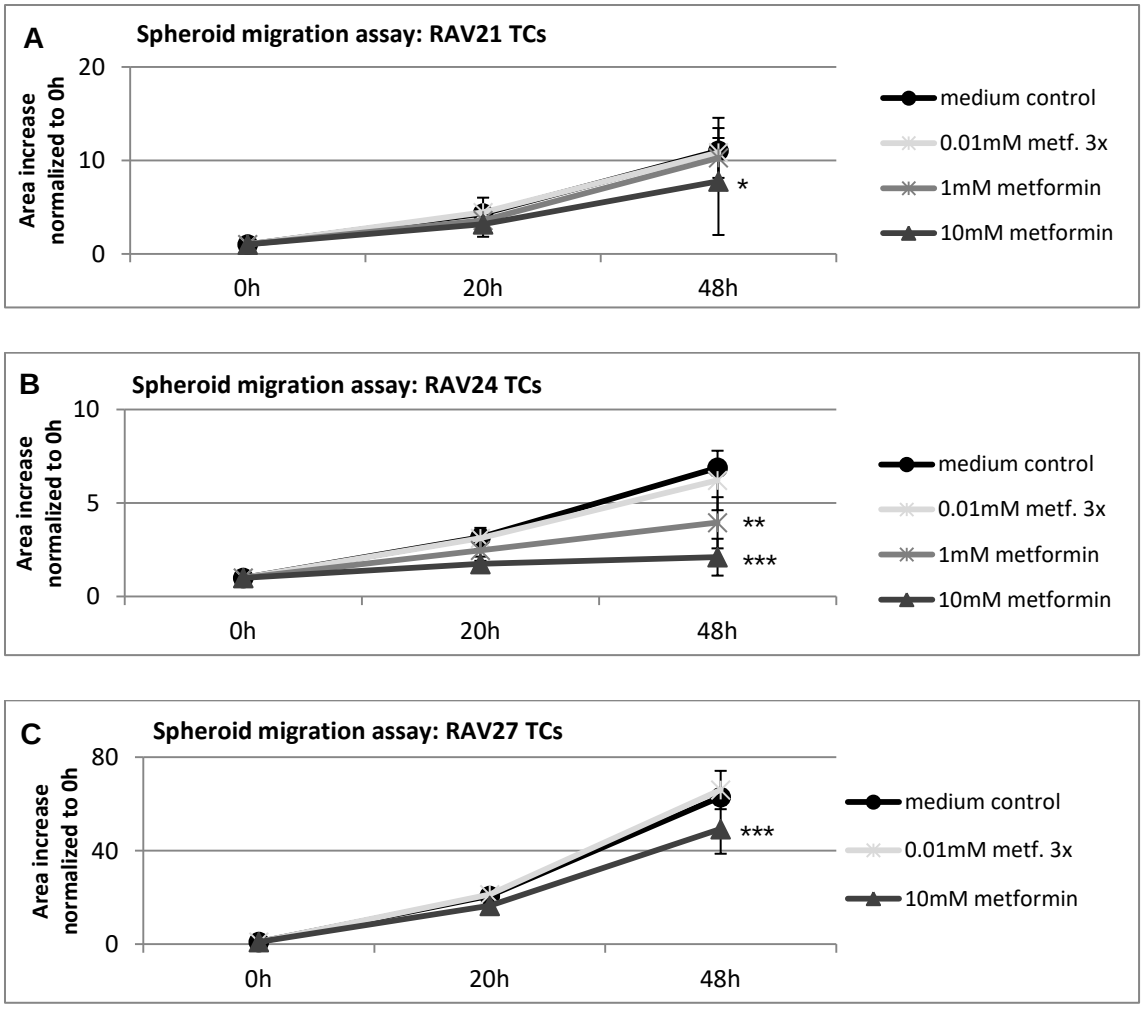

Figure 24: Relative increase of spheroid area in mesenchymal TCs RAV21 (A), RAV24 (B) and RAV27 (C) after 48h treatment with different concentrations of metformin: Spheroid sizes were measured after 20 and 48 hs. Migration was normalized in two steps: Values of each time point were normalized to initial spheroid size, followed by normalization to the medium control. For reasons of clarity, significances are only marked for the end point of 48 hs.

Mesenchymal TCs RAV21, RAV24 and RAV27 migrated at different rates: After 48 hs, RAV21's average spheroid area was 10 times as large as the initial spheroid size, RAV24's average spheroid area expanded 7-fold and RAV27's was 63 times as large as initially. Migratory rates were significantly lowered by 10 mM metformin. RAV21 TCs' migration diminished to 0.73 ($p < 0.02$). RAV24 TCs' migratory rates were decreased to 0.56 ($p < 0.0002$) by 1 mM metformin and to 0.30 ($p < 0.0001$) by 10 mM metformin. RAV27 TCs' migration, being very rapid in the first place, was diminished to 0.79 ($p < 0.0001$).

Overall, differentiated mesenchymal GBM cell lines RAV21, RAV24 and RAV27 were highly susceptible to the anti-proliferative power of 10 mM metformin, while lower concentrations did not decrease proliferation significantly. Also, migration of RAV21, 24 and 27 TCs was noticeably lowered by 10 mM metformin and in case of RAV24 TCs, also by 1 mM metformin.

5.2 The functional effects of TGF-β_2 on GBM cells

TGF-β is described as a tumorigenic cytokine inducing proliferation, migration, invasion, angiogenesis and suppressing the immune response. Several studies have explored the effects of TGF-β on glioma proliferation and have found heterogeneous results. Apart, TGF-β_2 is described as a key inducer of migration in GBM. Hence, this study aimed to analyze the effects of TGF-β_2 on glioma proliferation and migration to establish similarities and differences between BTICs, TCs, proneural and mesenchymal cells.

Experiments to investigate the effects of TGF-β_2 and SD-208 were performed analogous to those with different concentrations of metformin. There were 10 cell lines for cell counts and spheroid migration assays and each experiment was repeated once with the same cell line. During cell counts, triplicates were examined for each condition and during spheroid migration assays each condition had six replicates.

5.2.1 TGF-β_2's effects were anti-proliferative and anti-migratory

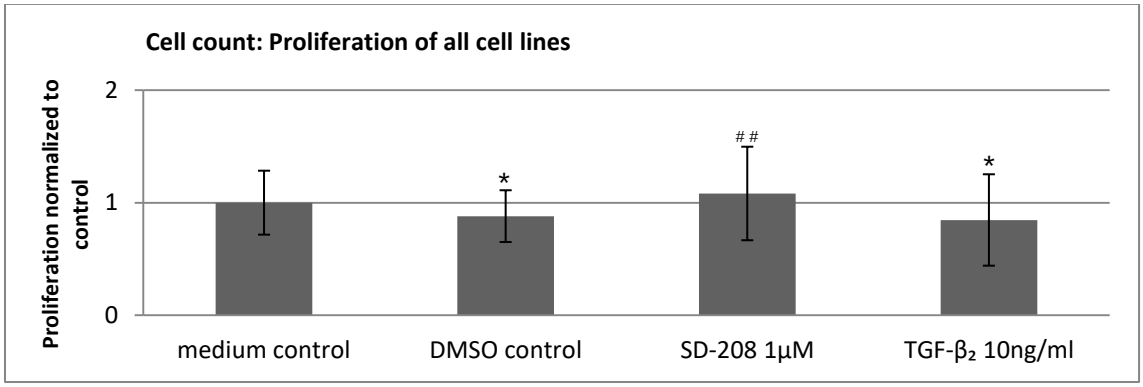

Figure 25: Effects of TGF-β_2 and its receptor antagonist, SD-208, on proliferation: The symbol # # indicates that the increase of proliferation caused by SD-208 was significant compared to the DMSO-control as SD-208 is dissolved in 1% DMSO.

TGF-β_2's action on GBM cells was slightly but significantly anti-proliferative reducing proliferation by 15% compared to the medium control ($p < 0.02$). SD-208 increased proliferation by 20% compared to the DMSO-control ($p < 0.005$). Hence, on a grand scheme, TGF-β_2 and SD-208 had opposite effects on proliferation.

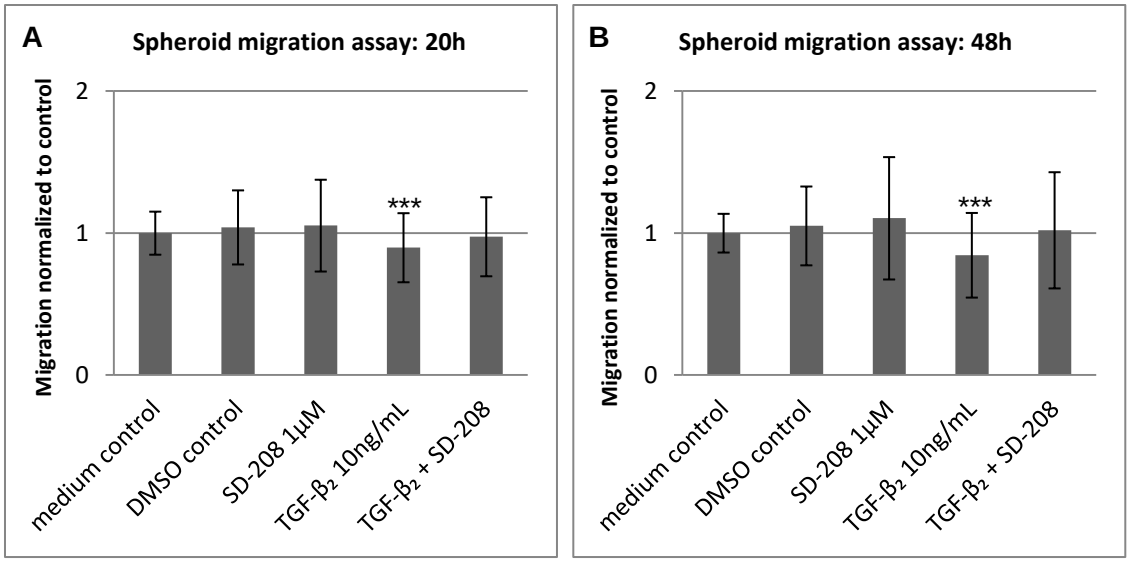

Figure 26: Effects of TGF-β_2 and its antagonist, SD-208, on migration: Migration was assessed after 20 hs (A) and 48 hs (B). Here, data is shown for all cell lines after two steps of normalization to initial spheroid size and then to relative increase in size of medium control spheroids.

TGF-β_2 reduced migration to 0.90 after 20 hs ($p < 0.0002$) and to 0.84 ($p < 0.0001$) after 48 hs compared to the medium control. For SD-208, no significant effects were observed. Similarly, the combination of TGF-β_2 and SD-208 did not influence migration significantly hinting that SD-208 might have nullified TGF-β_2's anti-migratory effects.

5.2.2 Mesenchymal GBM cell lines were most susceptible to TGF-β_2

TGF-β_2 and SD-208 affected different groups of cells to a different extent. The following section details differences in proliferation and migration after 20 and 48 hs.

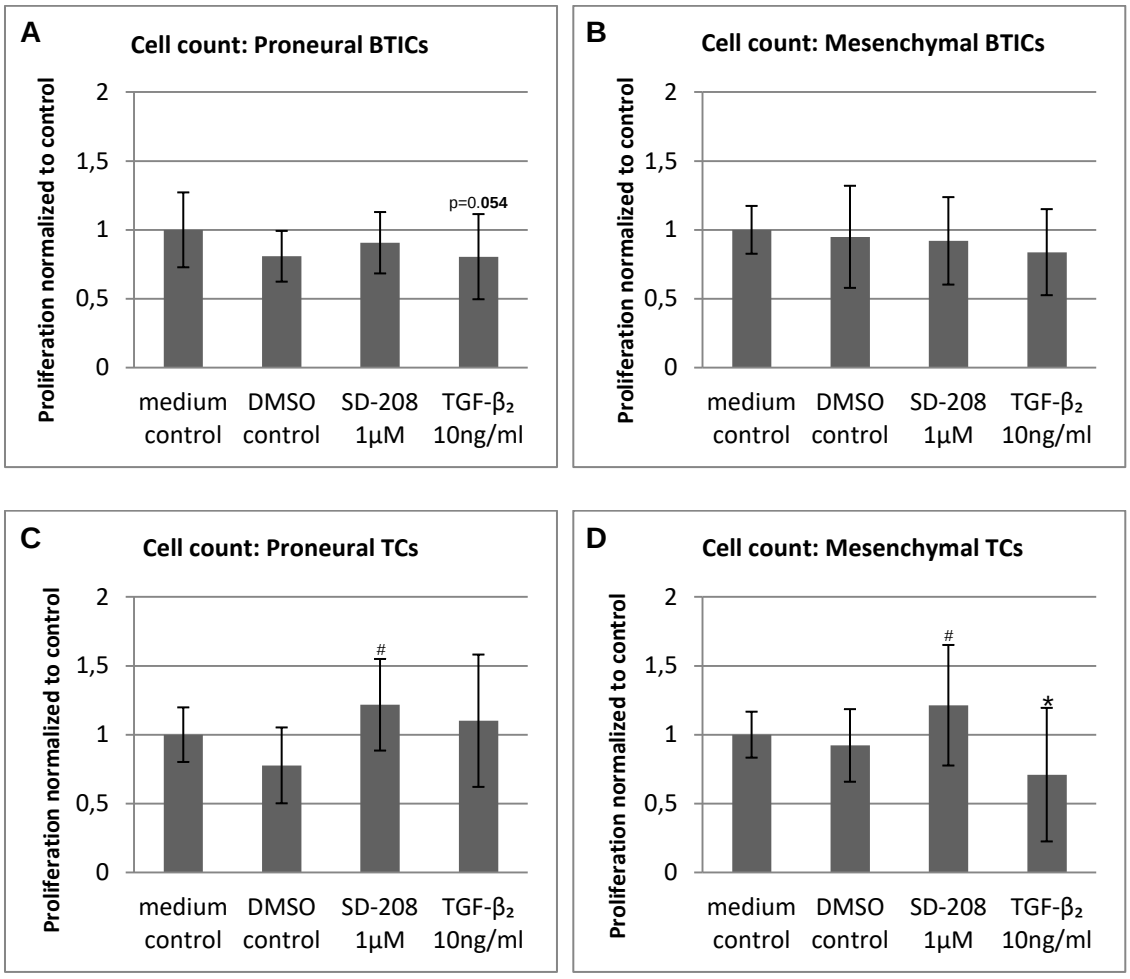

Figure 27: Cell counts after 48 hs of treatment: The absolute numbers of viable cells per well of any condition were divided by the average number of viable cells in the medium control wells.

TGF-β_2 decreased proliferation in all but proneural TCs. Firstly, in proneural BTICs, proliferation was reduced to 0.8 bordering significance ($p = 0.054$). Significant anti-proliferative effects were observed in mesenchymal TCs where proliferation decreased to 0.71 ($p < 0.03$). Compared to proliferation rates in DMSO-treated wells, SD-208 enhanced proliferation in differentiated cell lines: proneural TCs' proliferation increased by 44% and that of mesenchymal TCs by 29%. Here, TGF-β_2 and SD-208 had antagonistic effects. TGF-β_2 was also able to inhibit proliferation in proneural BTICs where SD-208 did not show significant effects and SD-208 was able to increase proliferation in proneural TCs where TGF-β_2 's effects were non-significant.

Figures 28 and 29 illustrate whether these findings are in line with the migratory data.

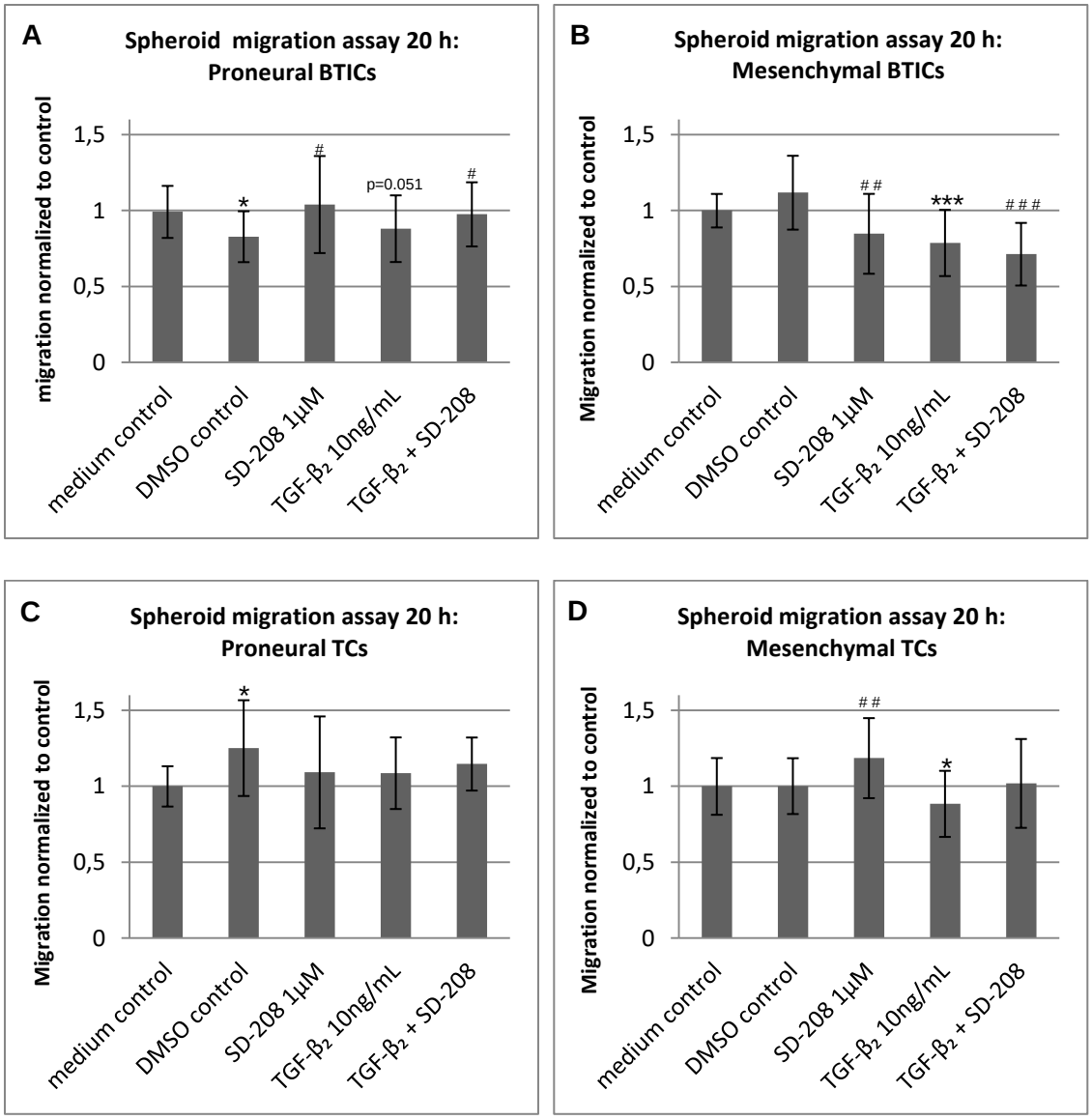

Figure 28: Spheroid migration after 20 hs of treatment: Relative migratory rates were calculated by double normalization. Therefore, values for each 20 h time point were first divided by the corresponding value at 0 hs and secondly by the average of the medium control.

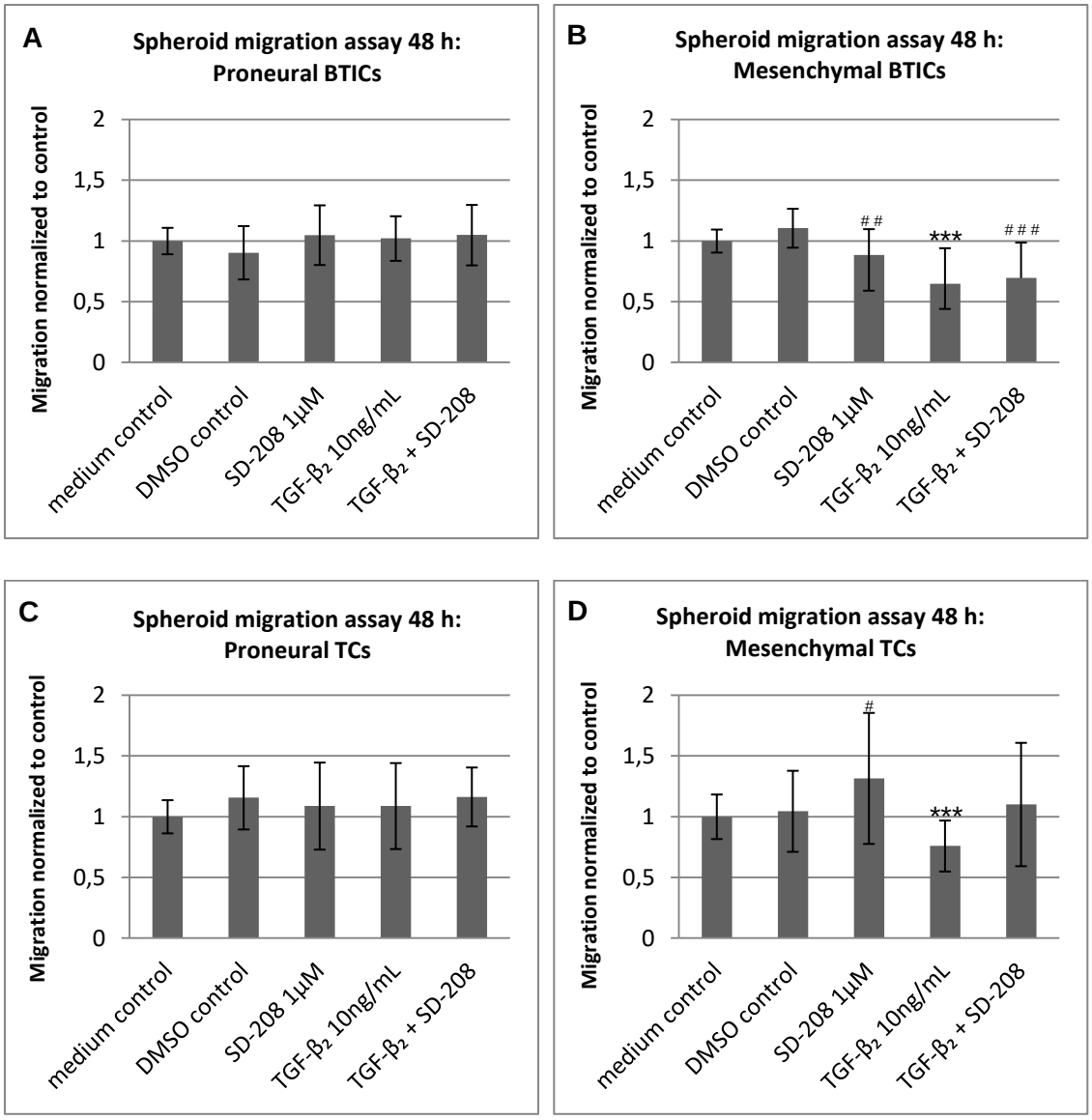

Figure 29: Spheroid migration after 48 hs of treatment: Relative migratory rates were calculated by double normalization. Therefore, values for each 20 h time point were first divided by the corresponding value at 0 hs and secondly by the average of the medium control.

Regarding the role of TGF-β_2 in migration, two trends could be distinguished: Proneural cell lines - whether stem-like or differentiated - only scarcely reacted to TGF-β_2 with migration being reduced in proneural BTICs at the 20 h time point only (0.88 with $p = 0.051$). Apart, no significant effects were observed. Migratory rates of mesenchymal BTICs decreased to 0.79 after 20 hs and to 0.65 after 48 hs of treatment ($p < 0.0001$ in both cases) making mesenchymal BTICs very responsive to TGF-β_2's anti-migratory actions. Similarly, migratory rates of mesenchymal TCs were lowered to 0.89 after 20 hs ($p < 0.02$) and to 0.76 after 48 hs ($p < 0.0001$). Hence, the anti-migratory power of TGF-β_2 was more pronounced in mesenchymal cell lines than in proneural cell lines.

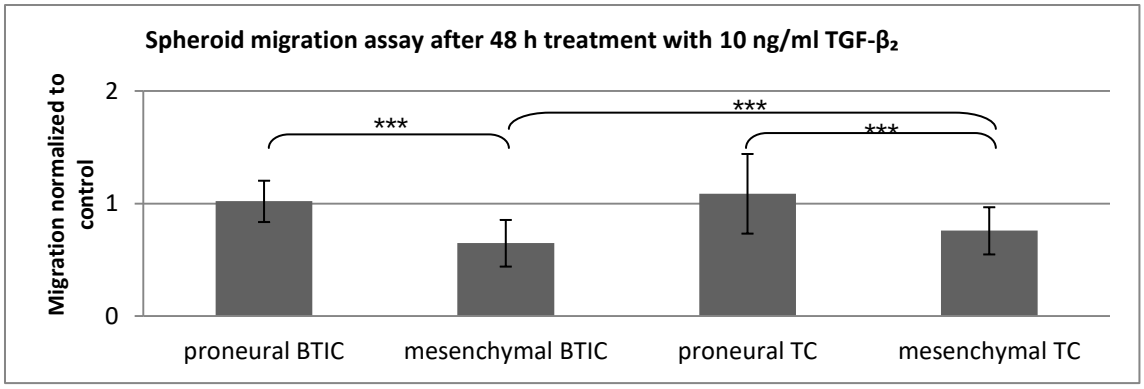

Figure 30: Comparing the effects of 10 ng/ml TGF-β_2 on relative migratory rates of different groups of cells: Significances between different groups of cells are marked.

Reviewing Figures 28 and 29, SD-208 exerted no effects on migration of proneural cell lines except on proneural BTICs after 20 hs. In mesenchymal cell lines, the effects were heterogeneous: Migration was impaired by SD-208 in mesenchymal BTICs (relative migratory rate was reduced by 22% with $p < 0.005$), but it was enhanced by 27% compared to the DMSO-control in mesenchymal TCs ($p < 0.02$).

In summary, TGF-β_2's effects were anti-proliferative and anti-migratory especially in mesenchymal cell lines. In mesenchymal TCs, TGF-β_2 reduced both proliferation and migration while SD-208's effects were opposite. In all the other cell lines, the anti-proliferative and anti-migratory effects were only partially detectable: In proneural BTICs for example, TGF-β_2 only reduced proliferation; in mesenchymal BTICs it only reduced migration. SD-208 raised proliferation in proneural TCs but reduced migration in mesenchymal ones.

Table 19: Overview over the effects of 10 ng/ml TGF-β_2 and 1 µM SD-208 on proliferation and migration of different groups of GBM cells: The left column in dark grey shows how strongly proliferation is reduced after 48 hs of treatment. The right column shaded in light grey depicts contraction of migration at the 48 h time point. Only significant results are shown. Symbols indicate the following: - indicates that proliferation/migration is reduced by up to 25%, - - by 25-50%, - - - by 50-75% and - - - - by more than 75%. If proliferation or migration are increased, +'s are used for indication.

	Pro BTICs		Mes BTICs		Pro TCs		Mes TCs	
	Prolif.	Migra.	Prolif.	Migra.	Prolif.	Migra.	Prolif.	Migra.
TGF-β_2 10 ng/ml	-			-			- -	-
SD-208 1 µM				-	++		++	++

Table 20: Overview over functional effects (48 h) of TGF-β_2 and SD-208 on all GBM cell lines

Effect after 48 h	TGF-β_2	SD-208
Proliferation decrease	20%	20%
Proliferation increase	0%	0%
Migration decrease	60%	20%
Migration increase	10%	30%

5.2.3 Unique cellular reaction patterns to TGF-β_2 and SD-208

5.2.3.1 Detailed analysis of proliferation and migration of proneural BTICs RAV19 and RAV57

Figure 31 shows results for cell counts and spheroid migration assays of proneural BTICs RAV19 P25 and P26 as well as RAV57 P16 and P18.

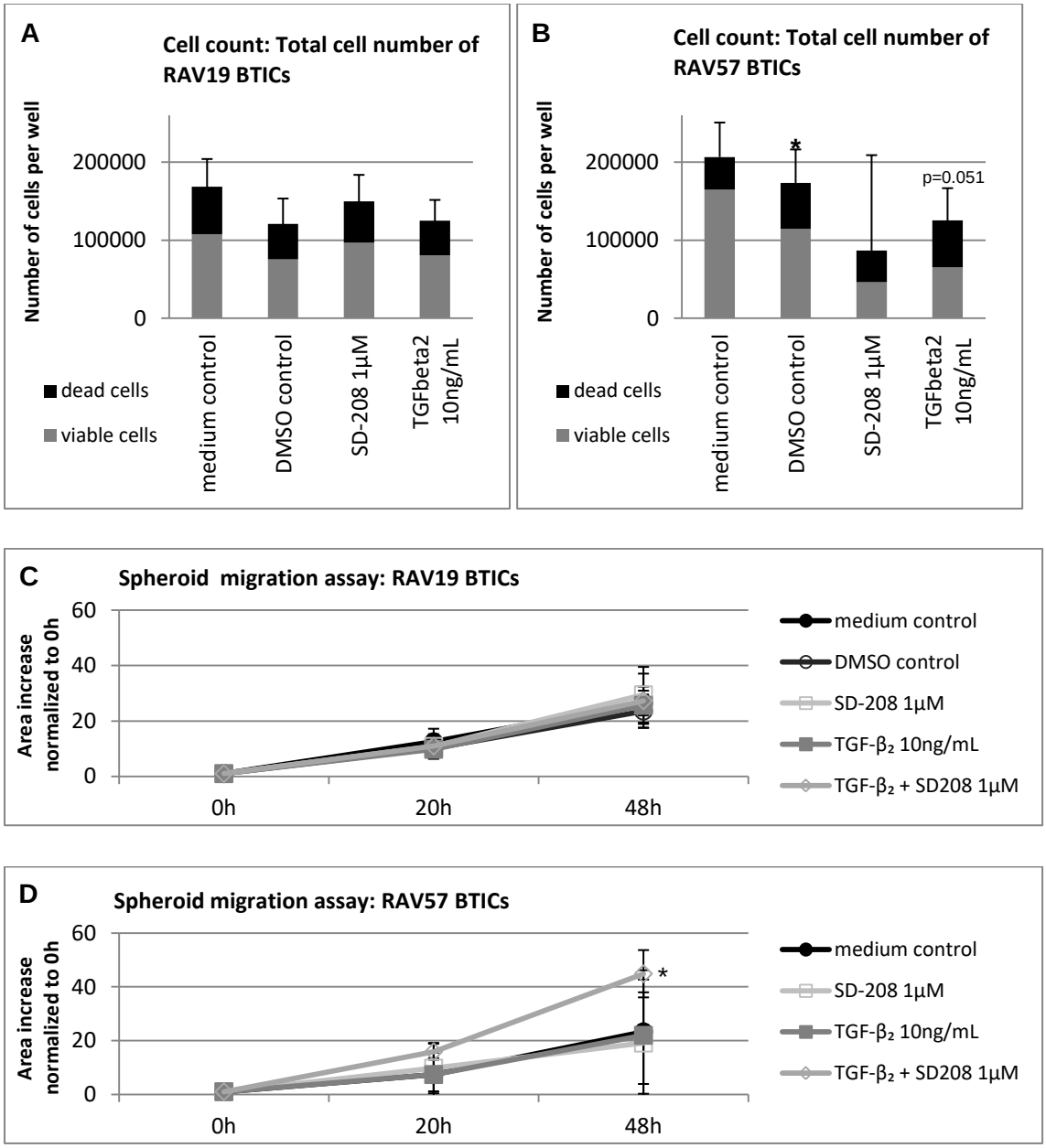

Figure 31: Cell count with total number of cells per well (A and B) and spheroid migration assays (C and D) after treatment with 10 ng/ml TGF-β_2 or with 1 µM SD-208: In (A) and (B), absolute numbers of viable cells are colored grey. Accordingly, significant differences between relative proliferation in treated wells and the medium control wells are marked with grey stars. Absolute numbers of dead cells are shaded black. Significant differences between the fraction of dead cells in any treated well compared to the fraction of dead cells in the medium control are marked with black stars. To create line-plot diagrams (C) and (D), spheroid sizes were measured after 20 and 48 hs. Migration was normalized in two steps: Values of each time point were normalized to initial spheroid size, followed by normalization to the medium control. For reasons of clarity, significance is only marked for the end point of 48 hs.

The proliferation decrease after treatment with TGF-β_2 was neither significant in RAV19 BTICs nor in RAV57 BTICs. Yet, the fraction of dead cells of RAV57 BTICs increased by 10% compared to the medium control in a suggestively significant manner ($p = 0.0507$) implying that TGF-β_2 might be cytotoxic to RAV57 BTICs. Migration also remained mostly unaffected by TGF-β_2 and SD-208. Solely the combination of TGF-β_2 and SD-208 produced an increase in relative migratory rates of RAV57 BTICs. Proneural BTICs RAV19 and RAV57 were mildly affected in their proliferation and migration after TGF-β_2 or SD-208 treatment.

5.2.3.2 Detailed analysis of proliferation and migration of mesenchymal BTICs RAV21, RAV24 and RAV27

In proliferation assays, RAV21 P19, RAV24 P12 and P14 and RAV27 P16 and P20 were assessed 48 hs after treatment with 10 ng/ml TGF-β_2 or 1 µM SD-208. To support data from cell counts, crystal violet staining assays were performed with RAV24 P12 and P14.

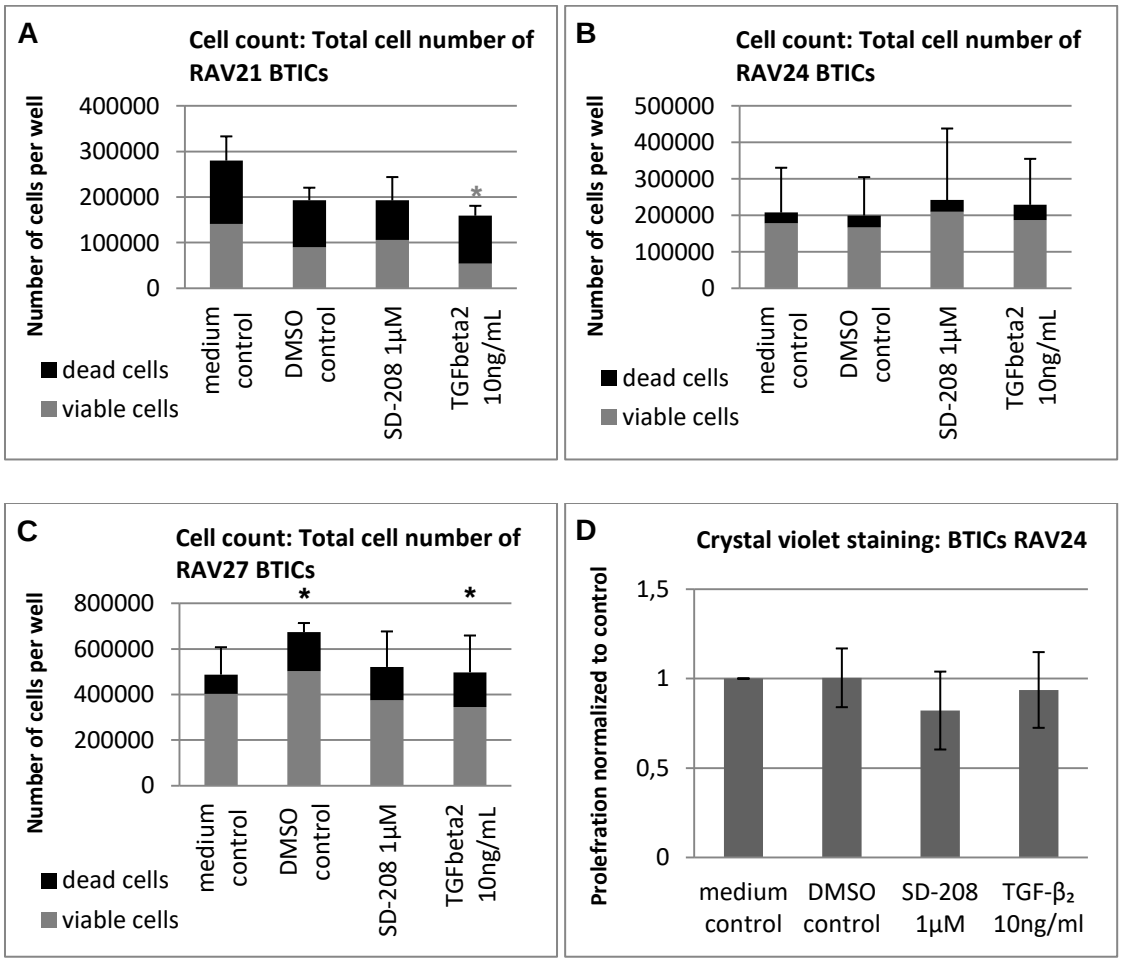

Figure 32: Total cell number per well obtained after treating RAV21 P19 (A), RAV24 P12 and P14 (B and D) and RAV27 P16 and P20 (C) with 10 ng/ml TGF-β_2 or with 1 µM SD-208: For (A), (B) and (C), the numbers of viable cells are shown in grey. Accordingly, significant differences between proliferation with treatmeant and at medium control conditions are marked with grey stars. Absolute numbers of dead cells are shaded black. Significant differences between the fraction of dead cells in any treated well compared to the fraction of dead cells at medium control conditions are marked with black stars. In (D), proliferation relative to the medium control from a crystal violet assay is shown. Here, the amount of viable cells was determined, only.

In mesenchymal BTICs, TGF-β_2 and SD-208 affected proliferation heterogeneously. As indicated in Figure 32 A, proliferation of RAV21 was lowered to 0.38 when 10 ng/ml TGF-β_2 was present ($p < 0.03$). RAV24 did not react to TGF-β_2 and SD-208, in neither cell counts nor in crystal violet staining assays. Lastly, in RAV27, proliferation was not influenced by TGF-β_2 nor SD-208; however, the fraction of dead cells increased when TGF-β_2 or DMSO were present, hinting that these substances are cytotoxic to RAV27 BTICs. Thus, SD-208 did not exert significant influences while TGF-β_2's action was either non-existent (RAV24), cytostatic (RAV21) or cytotoxic (RAV27).

Migration was assessed using cells of identical passage numbers as proliferation. In case of RAV21, P17 and P24 were utilized.

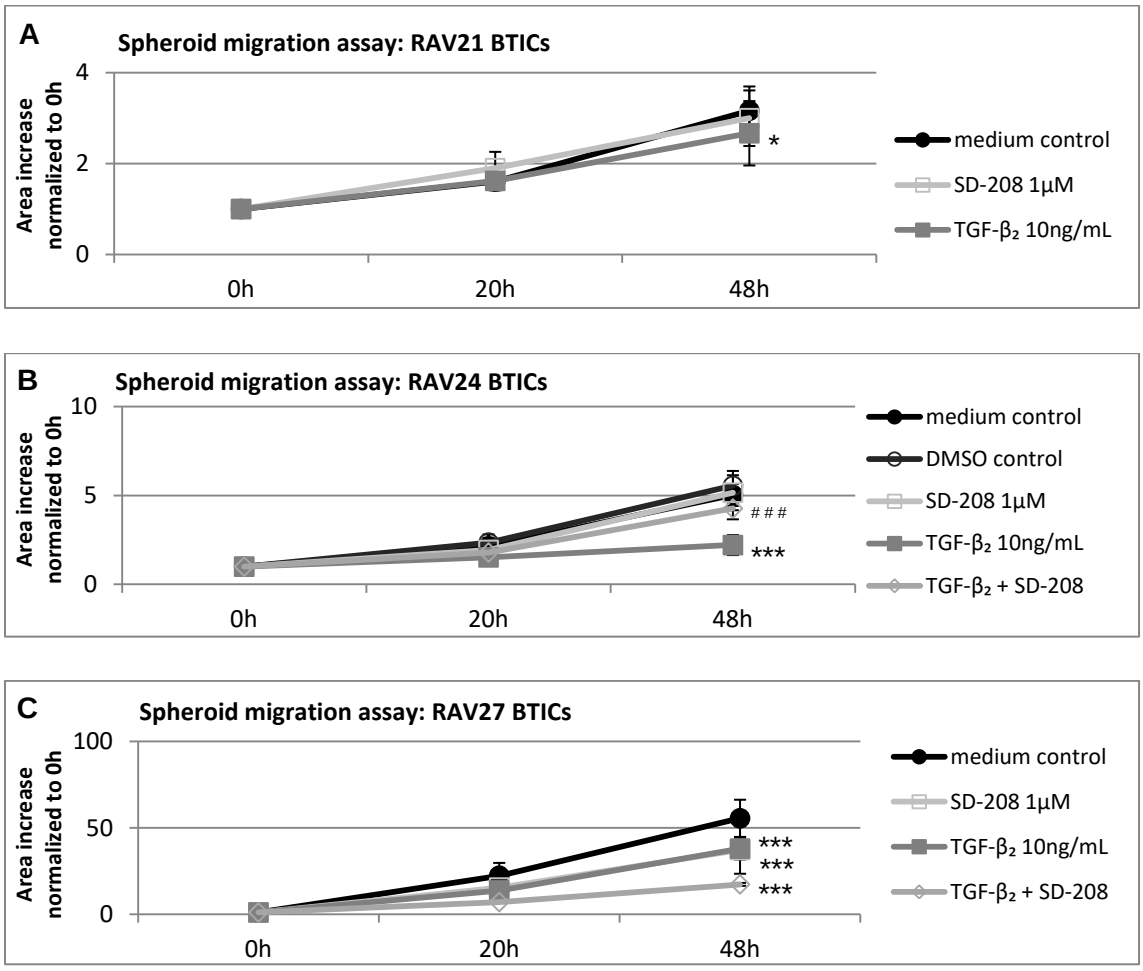

Figure 33: Relative increase of spheroid area for mesenchymal BTICs RAV21 P17 and 24 (A), RAV24 P12 and P14 (B) and RAV27 P16 and P20 (C) after 48 hs of treatment with 10ng/ml TGF-β_2 or with 1µM SD-208: Spheroid sizes were measured after 20 and 48 hs. Migration was normalized in two steps: Values of each time point were normalized to initial spheroid size, followed by normalization to the medium control. For reasons of clarity, significances are only marked for the end point of 48 hs. Preferably, values for SD-208 were compared to those of the DMSO control to determine significance (symbol: #); yet, where DMSO controls were missing, values for SD-208 were compared to the medium control (symbol: *).

In all three mesenchymal BTIC lines, 10 ng/ml of TGF-β_2 reduced migration. Spheroid migration of RAV21 was lowered to 0.83 after 48 hs ($p < 0.01$) by TGF-β_2, but SD-208

exerted no significant effects. RAV24 BTICs' migratory rates were decreased to 0.45 after 48 hs ($p < 0.0001$) even though their proliferation rates had not been affected by TGF-β_2 and SD-208. When TGF-β_2 and SD-208 were combined, migratory rates were 25% lower than those of the DMSO control suggesting that in RAV24 BTICs, 1 µM SD-208 was not able to antagonize 10 ng/ml TGF-β_2. In RAV27, TGF-β_2's and SD-208's abilities to reduce migration were comparable: TGF-β_2 decreased it to 0.70 and SD-208 to 0.65 ($p < 0.0001$ in both cases). Combining TGF-β_2 and SD-208 resulted in a 63% decrease of migration of RAV27 BTICs. Overall, TGF-β_2 lowered migration of all mesenchymal BTIC lines.

5.2.3.3 Detailed analysis of proliferation and migration of proneural TCs RAV19 and RAV57

Cell counts and spheroid migration assays were performed with RAV19 P23_3 and P23_6 along with RAV57 P17_2 and P20_3.

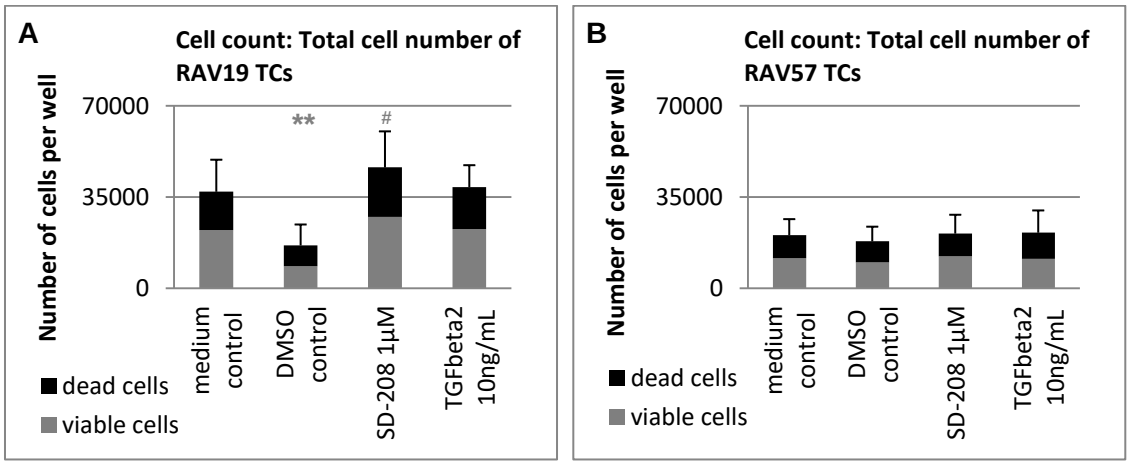

Figure 34: Cell counts with total number of cells per well after treatment with 10 ng/ml TGF-β_2 or with 1 µM SD-208: RAV19 P23_3 and P23_6 (A) and RAV57 P17_2 and P20_3 (B) were used.The numbers of viable cells are shown in grey. Accordingly, significant differences between proliferation with treatment and at medium control conditions are marked with grey stars. Absolute numbers of dead cells are shaded black. Significant differences between the fraction of dead cells in any treated well compared to the fraction of dead cells at medium control conditions are marked with black stars

RAV19 and RAV57 TCs proliferated slowly. Therefore, instead of the standard 150,000 cells/well, 60,000 cells/well of RAV19 P23_6, 70,000 cells/well per well of RAV57 P17_2 and 30,000 cells/well of RAV57 P20_3 were sowed out for cell counts. An increase in proliferation of RAV19 P23_3 and P23_6 by 78% was observed when 1 µM SD-208 was present ($p < 0.04$ compared to the DMSO control). TGF-β_2 did not alter proliferation of RAV19 TCs. Neither SD-208 nor TGF-β_2 had significant impact on the proliferation of RAV57 TCs. Thus, proliferation of proneural TCs reactet scarcely to treatment with TGF-β_2 and SD-208.

In addition to spheroid migration assays, which were performed with cells of identical passage number as proliferation assays, a scratch migration assay was performed for RAV57 P20_8 to support results from spheroid migration assays.

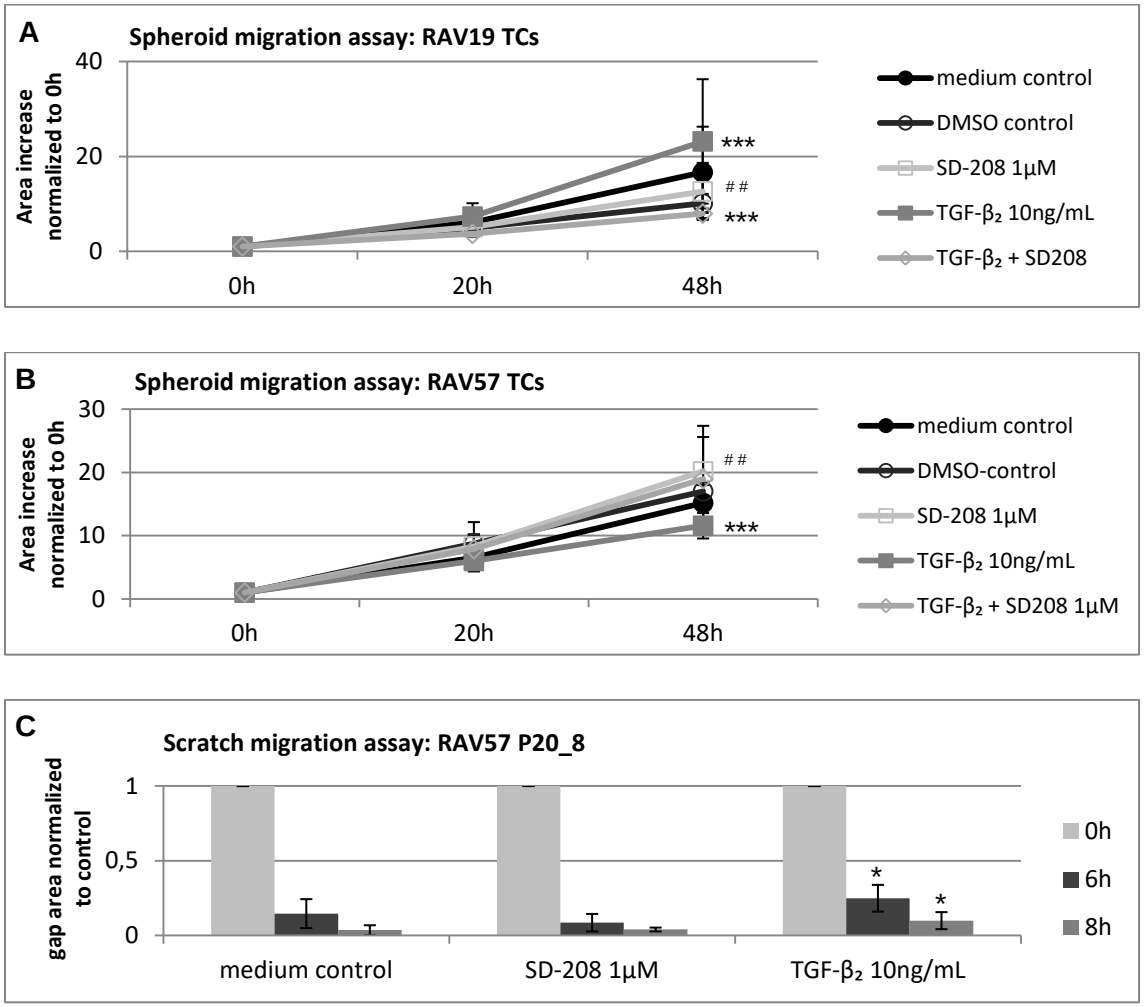

Figure 35: Spheroid migration assays (A and B) and scratch migration assay (C) after treatment with 10 ng/ml TGF-β_2 or with 1 µM SD-208: For spheroid migration assays with RAV19 P23_3 and P23_6 (A) and with RAV57 P17_2 and 20_3 (B), spheroid sizes were measured after 20 and 48 hs. Migration was normalized in two steps: Values of each time point were normalized to initial spheroid size, followed by normalization to the medium control. For reasons of clarity, significances are only marked for the end point of 48 hs. In (C), results from a scratch migration assay with RAV57 P20_8 are shown. Gap area at 6 and at 8 hs were normalized to the corresponding 0 h values and afterwards normalized to the medium control. No DMSO control was used.

Migration of RAV19 and RAV57 TCs was significantly altered by SD-208 and TGF-β_2. Interestingly, migration of RAV19 P23_3 and 23_6 after 48 hs increased under TGF-β_2 to 1.41 ($p<0.0001$). SD-208 lowered migration by 45% compared to the DMSO-control ($p < 0.008$). RAV19 TCs was the only cell line in which TGF-β_2 increased and SD-208 decreased migration. For RAV57 TCs, TGF-β_2 inhibited migration to 0.76 of the average medium control migration rates (48 hs; $p < 0.0002$) while SD-208 enhanced migration by 32% compared to the DMSO control ($p < 0.004$). Scratch migration assays further demonstrated TGF-β_2's ability to decrease migratory rates in RAV57 TCs. In TGF-β_2 treated

wells, the cell free gap was almost twice the size of the medium control after 20 hs ($p < 0.04$) and approximately three times the size after 48 hs ($p < 0.02$).

In summary, the effects of TGF-β_2 and SD-208 on proneural TCs were heterogeneous. While SD-208 increased proliferation of RAV19 TCs, it decreased migration, and TGF-β_2 increased migration. RAV57 TCs' proliferation rates were not affected by TGF-β_2, but their migratory rates decreased after 48 hs. Thus, there is no homogenous group trend that could be postulated for proneural TCs. Hence, it is important to note that RAV19 TCs were the only cell line in which migration was increased by TGF-β_2.

5.2.3.4 Detailed analysis of proliferation and migration of mesenchymal TCs RAV21, RAV24 and RAV27

Proliferation and migration were assessed using RAV21 P24_9 and P24_10, RAV24 P10_5 and P10_7 as well as RAV27 P18_5 and P18_6. Proliferation was mostly assessed in cell counts and supported exemplarily by a crystal violet staining assay of RAV24 P10_7.

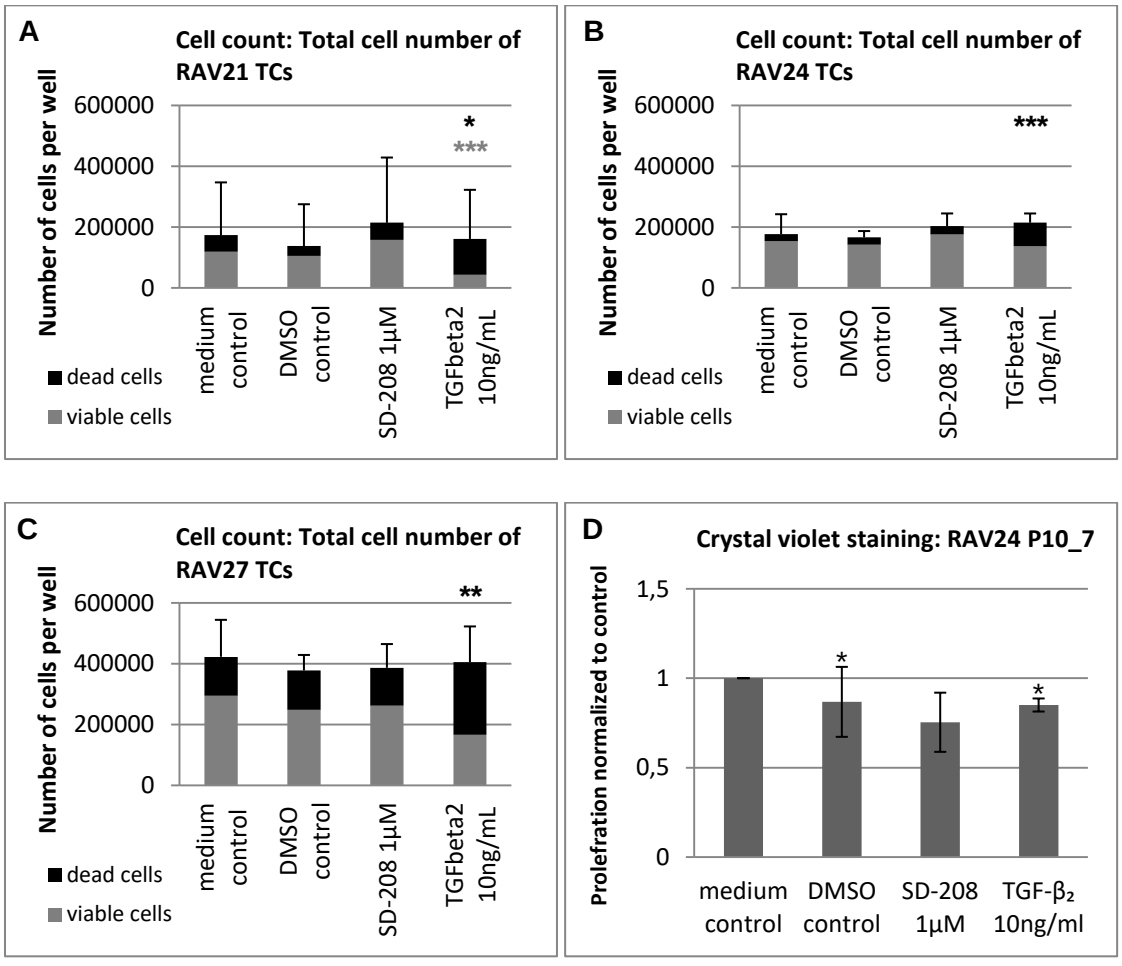

Figure 36: Total cell number per well obtained after a 48 h treatment with 10 ng/ml TGF-β_2 or with 1 µM SD-208: For cell counts of RAV24 P24_9 and P24_10 (A), of RAV24 P10_5 and P10_7 (B) and of RAV27 P18_5 and P18_6 (C), the numbers of viable cells are shown in grey. Accordingly, significant differences between

proliferation with treatment and at medium control conditions are marked with grey stars. Absolute numbers of dead cells are shaded black. Significant differences between the fraction of dead cells in any treated well compared to the fraction of dead cells at medium control conditions are marked with black stars. In (D), proliferation relative to the medium control from a crystal violet assay is shown for RAV24 P10_7. Here, the amount of viable cells was determined, only.

Compared to proneural TCs, mesenchymal TCs exhibited higher 48 h proliferation rates with an average number of 200.000 cells/well for RAV21 and RAV24 and approximately 400.000 cells/well for RAV27. SD-208 did not influence proliferation significantly. TGF-β_2, decreased proliferation of all mesenchymal TCs: In RAV21 TCs proliferation dropped to 0.40 ($p < 0.0001$) and in a crystal violet staining performed with RAV24 P10_7 it decreased to 0.85 ($p < 0.02$). The fraction of dead cells significantly increased in all mesenchymal TCs: For RAV21 TCs, it rose by 42% ($p < 0.03$), for RAV24 TCs by 23% ($p < 0.0003$) and for RAV27 TCs by 28% ($p < 0.009$). Thus, TGF-β_2's effect on mesenchymal TCs's proliferation was cytotoxic.

Migratory rates of mesenchymal TCs under treatment with 10 ng/ml TGF-β_2 and 1 µM SD-208 were investigated in spheroid migration assays.

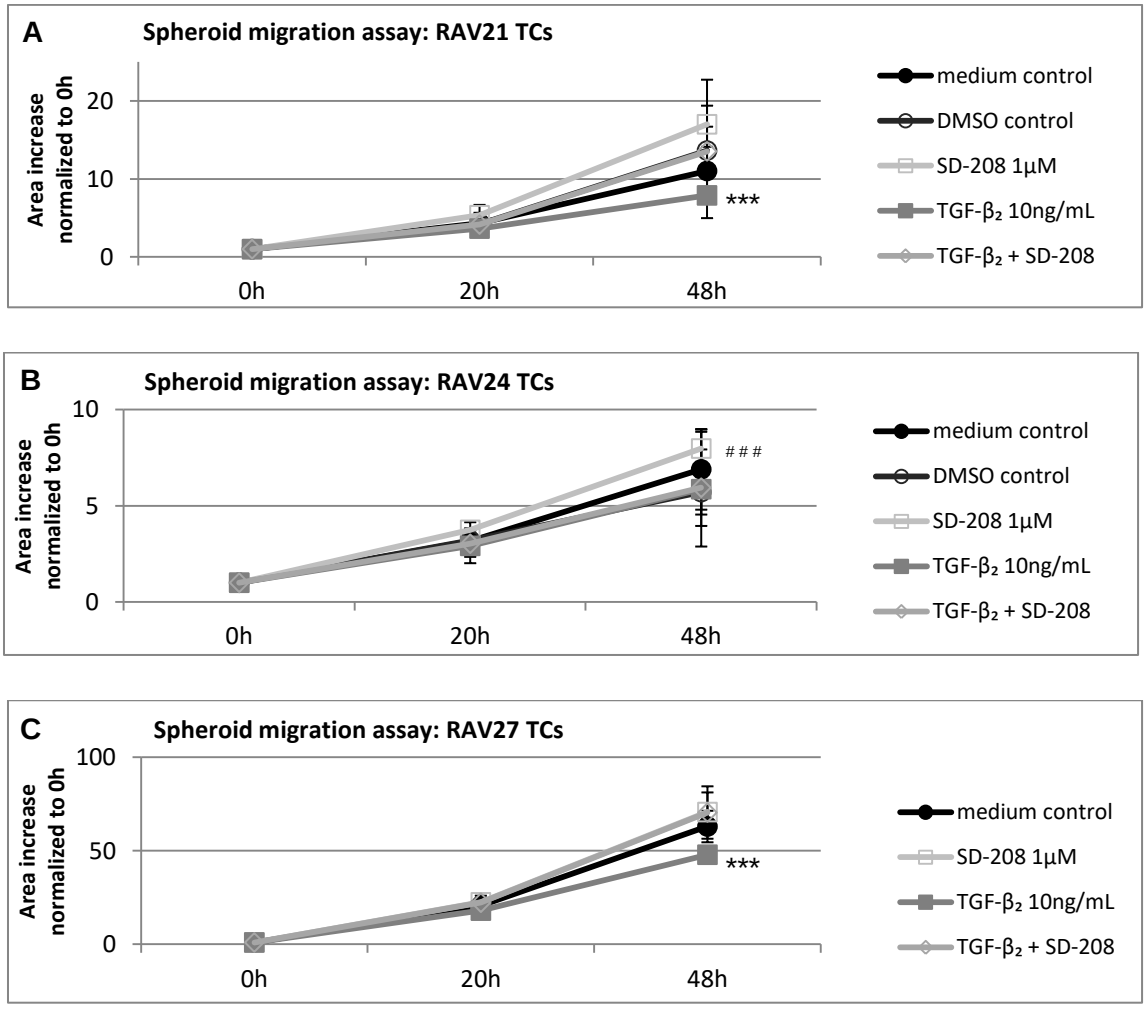

Figure 37: Relative increase of spheroid area for mesenchymal TCs RAV21 P24_9 and P24_10 (A), RAV24 P10_5 and P10_7 (B) and RAV27 P18_5 and P18_6 (C) after 48 hs of treatment with 10 ng/ml TGF-β_2 or

with 1 µM SD-208: Spheroid sizes were measured after 20 and 48 hs. Migration was normalized in two steps: Values of each time point were normalized to initial spheroid size, followed by normalization to the medium control. For reasons of clarity, significances are only marked for the end point of 48 hs. Preferably, values for SD-208 were compared to those of the DMSO control to investigate significance (symbol: #); yet, where DMSO controls were missing, values for SD-208 were compared to the medium control (symbol: *).

Migratory rates within the group of mesenchymal TCs varied. At 48 hs, a spheroid of RAV24 TCs had an average of 7 times the initial size, a spheroid of RAV21 TCs was at approximately 10 times the initial size, and a spheroid of RAV27 TCs measured about 60 times the initial size. SD-208 increased migration; yet, only the 36% increase of RAV24 TCs' migration rate was significant. TGF-β_2 decreased migration; RAV21 TCs' migratory rates were reduced by 30% ($p < 0.0009$), those of RAV24 TCs by 20% (non-significant) and those of RAV27 TCs by 23% ($p < 0.0001$). Combinations of 10 ng/ml TGF-β_2 and 1 µM SD-208 resulted in migratory rates that were approximately equal to those of the DMSO control except in RAV27 TCs. Here, migration after individual SD-208 treatement was at 1.12 ($p < 0.0001$) and after treatment with TGF-β_2 + SD-208 it equaled 1.13 ($p < 0.007$).

Thus, mesenchymal GBM cell lines RAV21, RAV24 and RAV27 formed a homogeneous group which was highly susceptible to the anti-proliferative and anti-migratory effects of TGF-β_2.

5.3 The functional effects of metformin and TGF-β_2 on GBM cells

Having examined the effects of low and high doses of metformin as well as of 10 ng/ml TGF-β_2 individually, the third aim was to investigate if the effects of metformin and TGF-β_2 are functionally linked.

5.3.1 Metformin and TGF-β_2 were anti-proliferative and anti-migratory

To determine the overall effects of metformin and TGF-β_2 on proliferation and migration of GBM cells, relative proliferation rates from 20 experiments with 10 different cell lines were summed up.

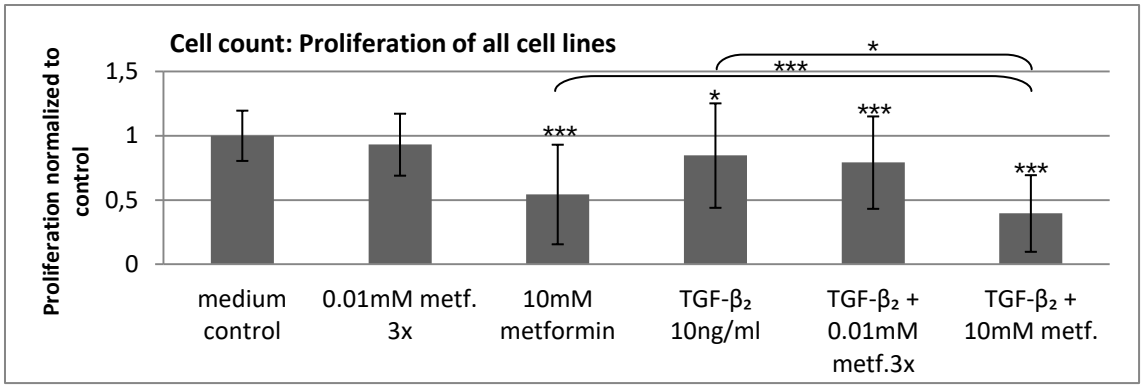

Figure 38: Relative proliferation rates of all cell lines after 48 hs of treatment: After cell count of viable cells, each value was divided by the average of the medium control to normalize proliferation.

Both, 10 mM metformin and 10 ng/ml TGF-β_2, decreased proliferation. While 10 mM metformin reduced proliferation to 0.54 ($p < 0.0001$), TGF-β_2 reduced it to 0.85 ($p < 0.03$). When GBM cells were treated with TGF-β_2 and 0.01 mM metformin in triple treatment, proliferation equaled 0.79. The anti-proliferative effects of TGF-β_2 + 0.01 mM metformin seemed largely due to the action of TGF-β_2. The combination of TGF-β_2 and 10 mM metformin reduced proliferation significantly more than both agents administered individually. Combined treatment reduced proliferation to 0.40 ($p < 0.0001$).

The results for spheroid migration assays are summed up in Figure 39.

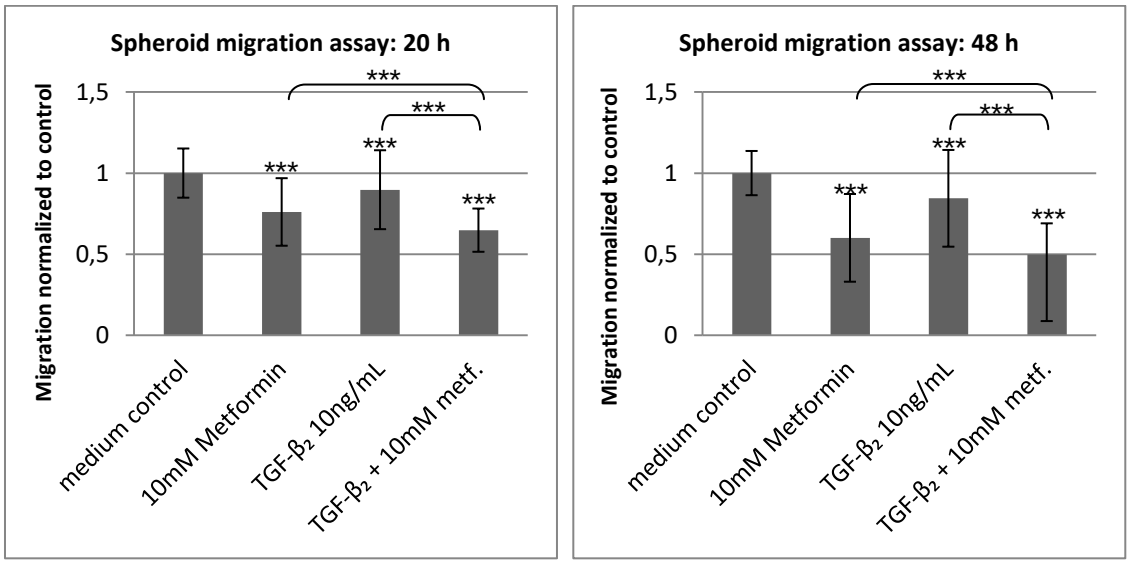

Figure 39: Relative migratory rates for all cell lines after 20 and after 48 hs of treatment: Values for all cell lines were normalized to initial spheroid size and to relative migratory rates of the medium control.

Firstly, 10 mM metformin inhibited migration which was at 0.76 after 20 hs ($p < 0.0001$) and at 0.60 after 48 hs ($p < 0.0001$). Also, TGF-β_2 diminished spheroid migration to 0.90 at 20 hs ($p < 0.0002$) and to 0.84 after 48 hs ($p < 0.0001$). The combination of 10 mM metformin and 10 ng/ml TGF-β_2 decreased migration to 0.65 at 20 hs ($p < 0.0001$) and to 0.50 at 48 hs

($p < 0.0001$). The anti-migratory effects of the combination were significantly more pronounced than 10 mM metformin's and TGF-β_2's individual effects.

Metformin and TGF-β_2 reduced proliferation and migration of GBM cells. When combined, their anti-proliferative and anti-migratory effects were greater than those of the individual agents.

5.3.2 The combination of 10 mM metformin and 10 ng/ml TGF-β_2 reduced proliferation and migration especially in mesenchymal cell lines

The anti-proliferative and anti-migratory effects of the combination of metformin and TGF-β_2 were different for each group of cells. The groups comprised proneural BTICs RAV19 and RAV57, mesenchymal BTICs RAV21, RAV24 and RAV27, proneural TCs RAV19 and RAV57 and mesenchymal TCs RAV21, RAV24 and RAV27.

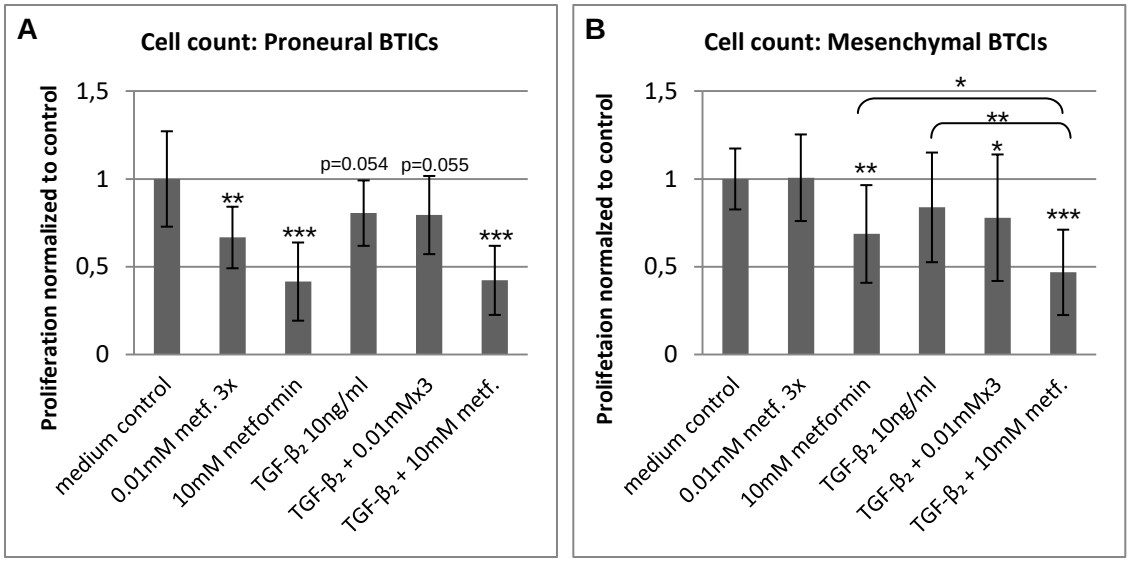

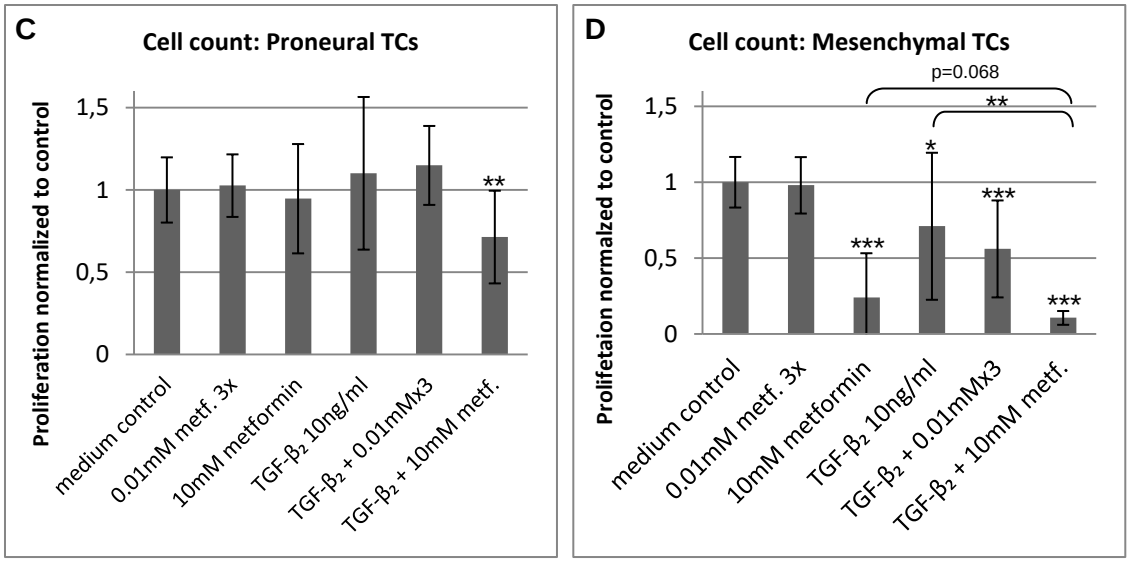

Figure 40: Cell counts after a 48 h treatment: The absolute numbers of viable cells per well of any condition were divided by the average number of viable cells in medium control wells to calculate proliferation rates normalized to control.

The combination of 10 mM metformin and 10 ng/ml TGF-β_2 reliably reduced proliferation rates of GBM cells. In proneural BTICs, this effect was likely due to their high sensitivity to metformin. Both, 10 mM metformin and the combination of 10 mM metformin and TGF-β_2 reduced proliferation by 58% ($p < 0.0001$ in both cases). The anti-proliferative effects of TGF-β_2 itself and in combination with 0.01 mM metformin in triple treatment were suggestively significant: Proliferation was decreased to 0.81 ($p = 0.054$) and 0.79 ($p = 0.055$) respectively. TGF-β_2 did neither increase nor decrease the anti-proliferative effects of 0.01 mM metformin in triple re-treatment. In proneural TCs, the addition of 10 ng/ml TGF-β_2 enhanced the effects of 10 mM metformin: 10 mM metformin did not reduce proliferation in proneural TCs, but the combination of 10 mM metformin and TGF-β_2 decreased it to 0.71 ($p < 0.01$).

Mesenchymal BTICs and TCs resembled each other: In both, the anti-proliferative effects of 10 mM metformin and TGF-β_2 were more pronounced than those of the individual treatments. In mesenchymal BTICs, 10 mM metformin reduced proliferation by 31% ($p < 0.002$), TGF-β_2 by 16% (non-significant) and their combination by 53% ($p < 0.0001$). Similarly, proliferation rates of mesenchymal TCs declined by 76% due to 10 mM metformin ($p < 0.0001$), by 29% for 10 ng/ml TGF-β_2 ($p < 0.03$) and by 89 % when the two substances were combined ($p < 0.0001$).

In summary, the effects of the combination treatment were different for each group. In proneural BTICs, the anti-proliferative effects of 10 mM metformin and the combination treatment were very similar, in proneural TCs, only the combination treatment decreased proliferation, and in mesenchymal BTICs and TCs, the anti-proliferative effects of 10 mM

metformin and TGF-β_2 in combination were more pronounced than those of the individual agents.

Having explored the reaction patterns of different groups of GBM cells regarding proliferation, the upcoming section will examine alterations in migration.

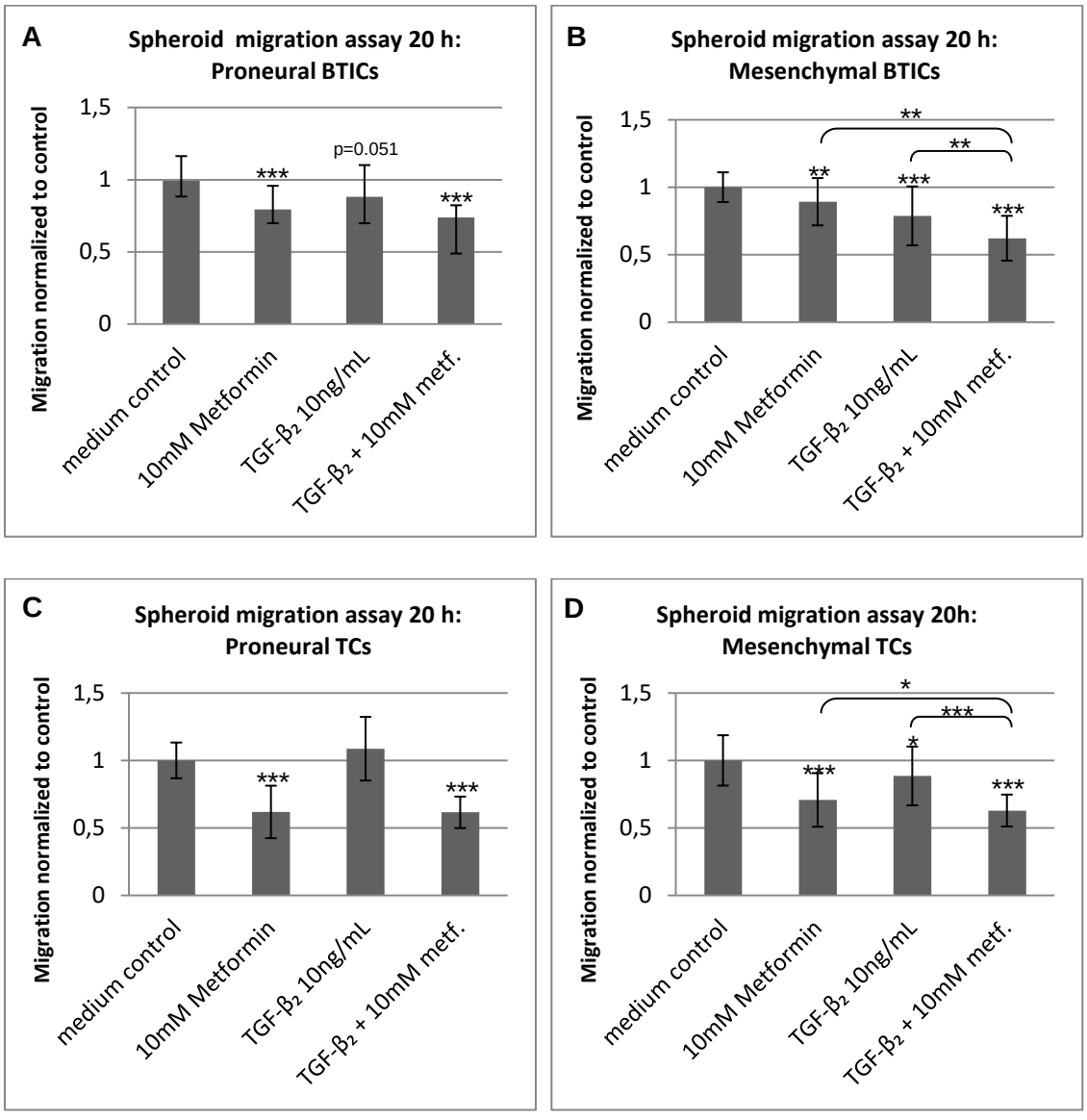

Figure 41: Relative migratory rates after 20 hs of treatment: Values for all cell lines were normalized to initial spheroid size and to relative migratory rates of the medium control and finally summed up in the four groups.

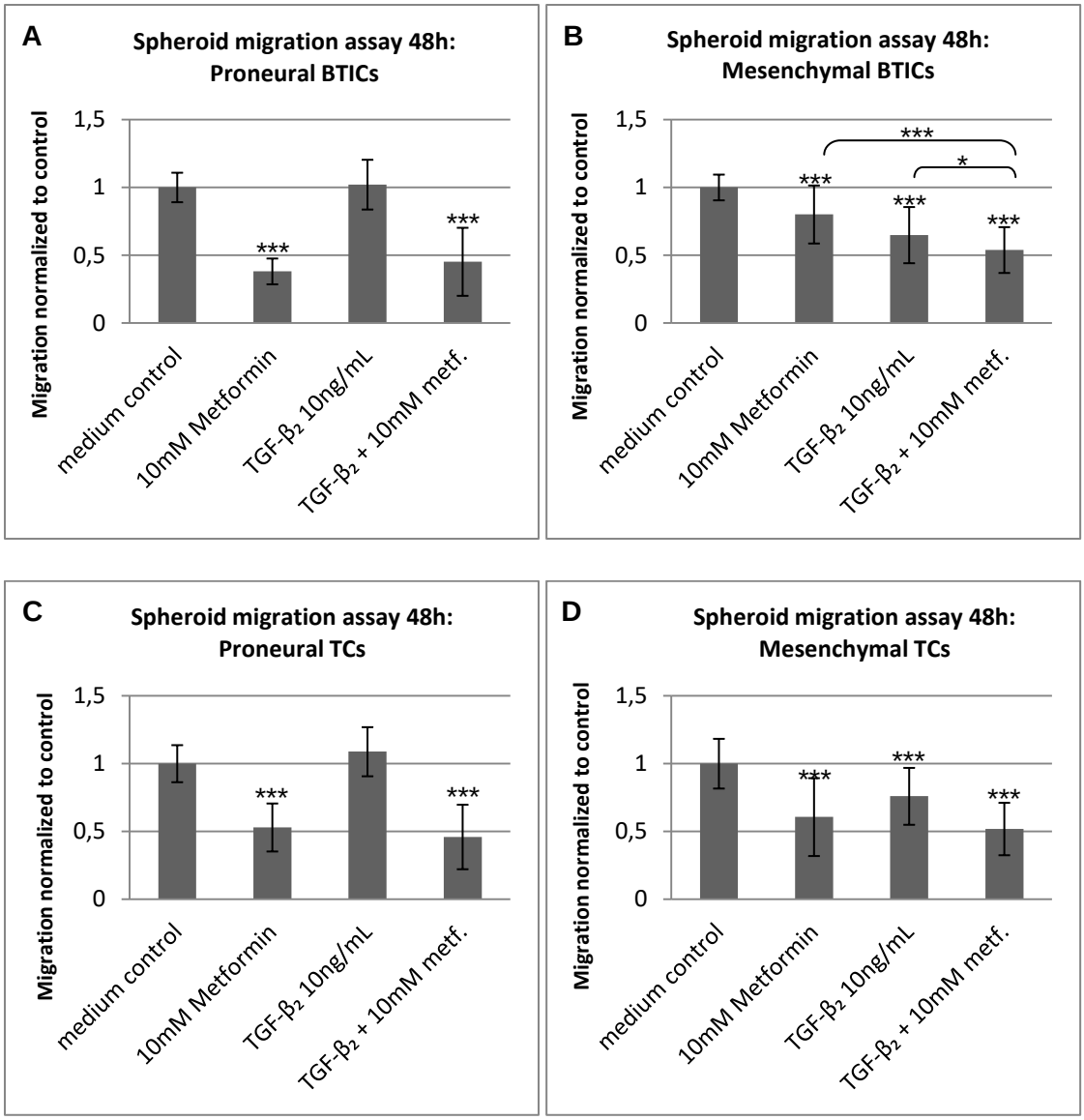

Figure 42: Relative migratory rates after 48 hs of treatment: Values for all cell lines were normalized to initial spheroid size and to relative migratory rates of the medium control and finally summed up in the four groups.

In proneural BTICs, 10 mM metformin but not TGF-β_2 diminished migration. Consequently, combined treatment did not decrease migration to a significantly greater extent than 10 mM metformin (5% difference after 20 hs and 7% difference after 48 hs).

For proneural TCs, TGF-β_2 showed no significant influence on migration after 20 h or 48 hs. At 20 hs, there was no difference between the anti-migratory effects of 10 mM metformin or its combination with TGF-β_2 (0.62 vs 0.61, $p < 0.0001$ in both cases). After 48 hs, 10 mM metformin reduced migration to 0.53 and the combination to 0.46 ($p < 0.0001$ in both cases), but the difference was not significant. Therefore, the effects seemed largely due to metformin's action.

For mesenchymal BTICs, the combination treatment decreased migration significantly more than the individual treatments. After 20 hs, mesenchymal BTICs' migratory rate compared to

the medium control was at 0.89 under 10 mM metformin ($p < 0.004$), at 0.79 under TGF-β_2 ($p < 0.0001$), and at 0.62 under combined treatment ($p < 0.0001$). Similarly, after 48 hs, mesenchymal BTICs' migration was reduced to 0.80 under 10 mM metformin, to 0.65 under TGF-β_2 and to 0.56 under combined treatment ($p < 0.0001$ in all cases).

Mesenchymal TCs resembled their stem-like counterparts especially at the 20 h time point. After 20 hs, 10 mM metformin reduced migration to 0.70 ($p < 0.0001$), TGF-β_2 to 0.89 ($p < 0.02$) and their combination to 0.63 ($p < 0.0001$) compared to the medium control. The anti-migratory effects of the combination of 10 mM metformin and 10 ng/ml TGF-β_2 were greater than those of the single treatments. After 48 hs, 10 mM metformin diminished migration to a similar extent compared to the combined treatment: 10 mM metformin yielded a decline to 0.60, TGF-β_2 to 0.76 and in combination, they produced a decline to 0.52 ($p < 0.0001$ in all cases).

Table 21 gives an overview of the anti-proliferative and anti-migratory effects of metformin, TGF-β_2 and their combinations.

Table 21: Review of the anti-proliferative and anti-migratory effects of metformin, TGF-β_2 and their combinations after 48 hs of treatment: The left column of each group (dark grey) shows how strongly proliferation was reduced. The right column shaded in light grey depicts contraction of migration at the 48 h time point. Blank spaces signify that there is not data for these conditions. Only significant results are shown. Symbols indicate the following: - indicates that proliferation/migration is reduced by up to 25%, - - by 25-50%, - - - by 50-75% and - - - - by more than 75%.

	Pro BTICs		**Mes BTICs**		**Pro TCs**		**Mes TCs**	
	Prolif.	Migra.	Prolif.	Migra.	Prolif.	Migra.	Prolif.	Migra.
0.01 mMx3 metf.	- -							
10 mM metformin	- - -	- - -	- -	-		- -	- - - -	- -
10 ng/ml TGF-β_2				- -			- -	-
TGF-β_2+0.01 mMx3			-				- -	
TGF-β_2+10 mM	- - -	- - -	- - -	- -	- -	- - -	- - - -	- -

5.3.3 Unique cellular reaction patterns to the combination of TGF-β_2 and metformin

This section examines the effects of the combination of 10 mM metformin and TGF-β_2 on an individual cell line level. Pictures of spheroid migration assays will be shown exemplarily together with close-up shots to investigate morphological changes after treatment.

5.3.3.1 Detailed analysis of proneural BTICs RAV19 and RAV57

Cell counts and spheroid migration assays were performed with RAV19 P25 and P26 and RAV57 P16 and P18.

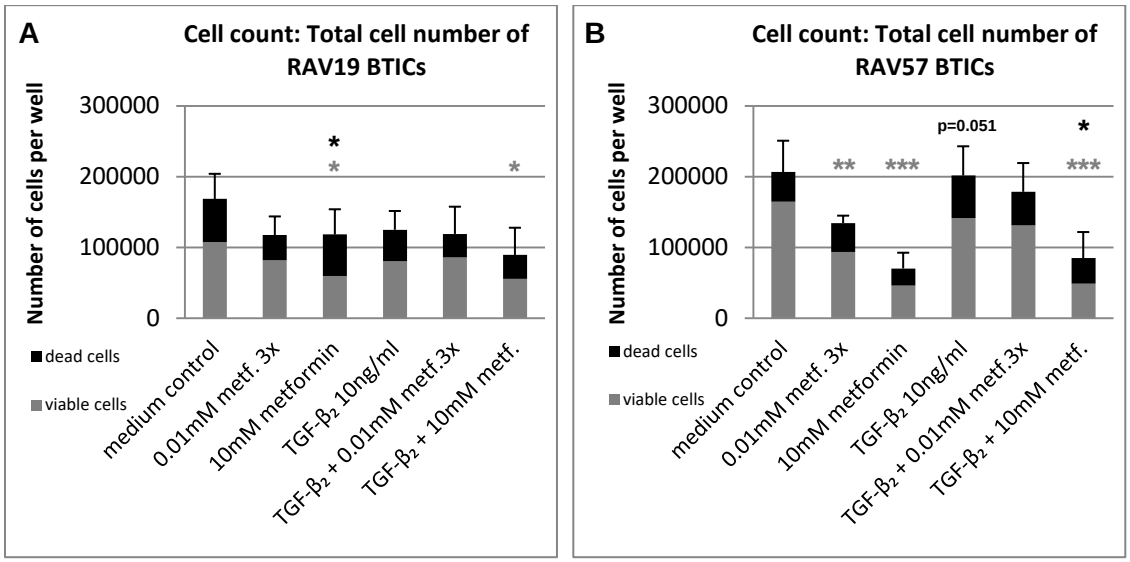

Figure 43: Total cell number per well obtained after 48 hs treatment: For cell counts of RAV19 P25 and P26 (A) and of RAV57 P16 and P18 (B), the numbers of viable cells are shown in grey. Accordingly, significant differences between proliferation with treatment and at medium control conditions are marked with grey stars. Absolute numbers of dead cells are shaded black. Significant differences between the fraction of dead cells in any treated well compared to the fraction of dead cells at medium control conditions are marked with black stars.

RAV19 BTICs' proliferation was reduced to 0.54 by 10 mM metformin ($p < 0.03$) and to 0.53 by the combination of 10 mM metformin and TGF-β_2. Thus, the anti-proliferative effect was likely due to metformin.

Similar results were obtained for RAV57 BTICs. The proliferation reduction of 10 mM metformin to 0.29 ($p < 0.0004$) was virtually equal to that of the combination of 10 mM metformin and 10 ng/ml TGF-β_2 (0.32; $p < 0.0004$). Thus, proneural BTICs were highly susceptible to metformin, but TGF-β_2 left their proliferation largely unaffected.

For spheroid migration, pictures of RAV57 BTICs are shown exemplarily.

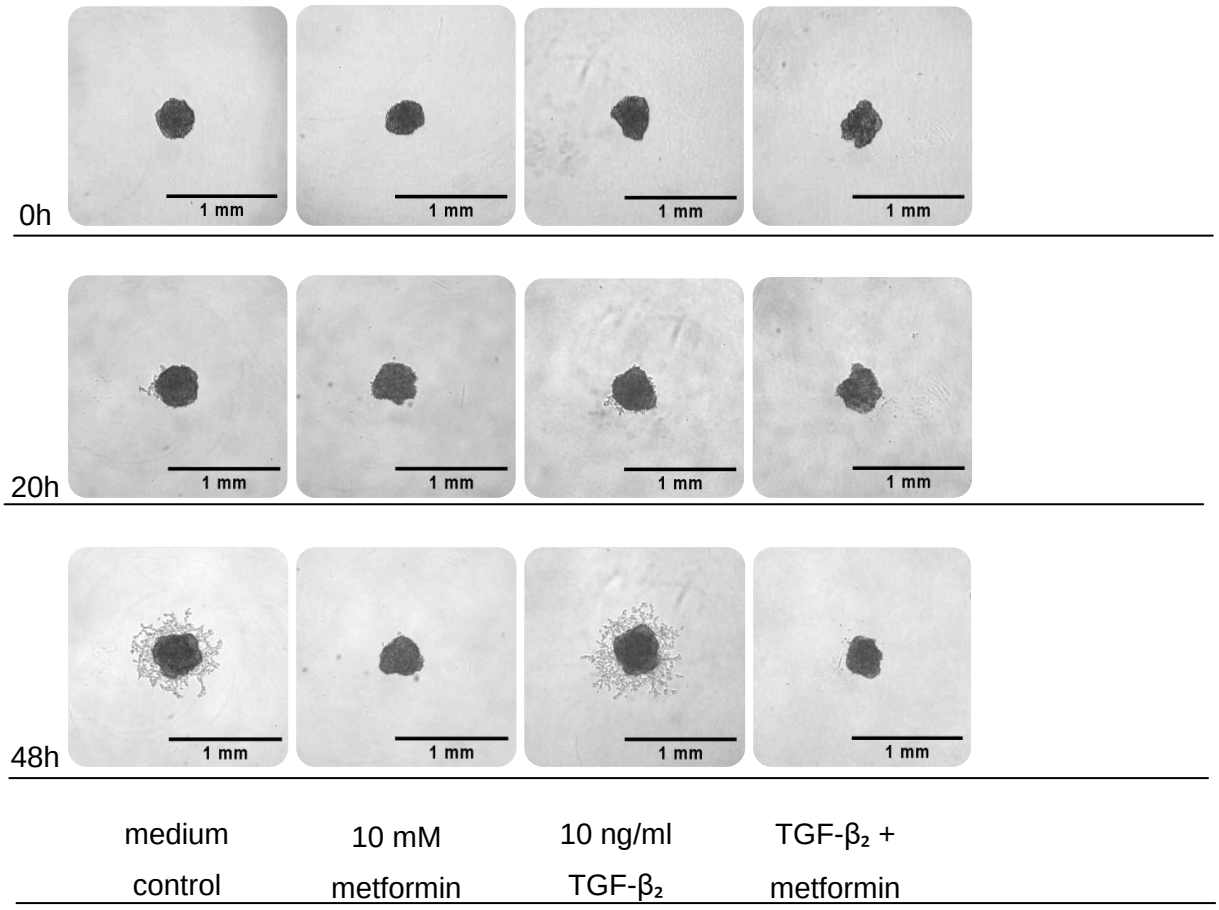

Figure 44: Spheroid migration of RAV57 BTICs: Pictures were taken 0, 20 and 48 hs after treatment with metformin, TGF-β_2 and their combination at 5x magnification.

Both, 10 mM metformin and its combination with TGF-β_2 inhibited spheroid migration. Under TGF-β_2, RAV57 BTICs migrated at approximately the same rate as in the medium control.

Figure 45 outlines the results of spheroid migration assays.

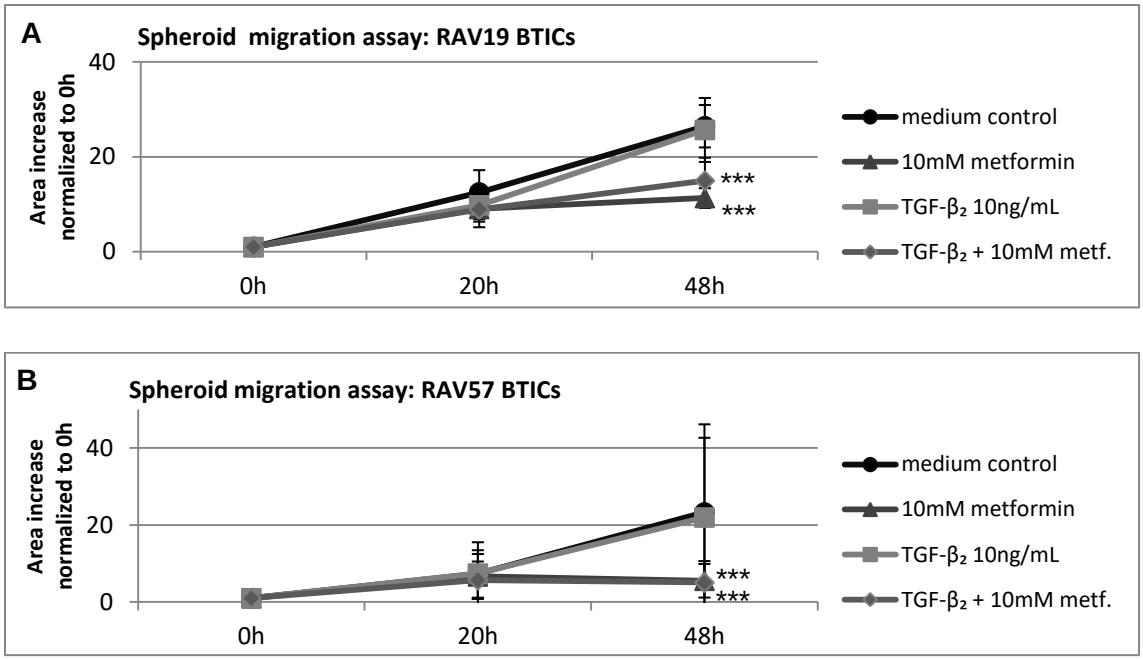

Figure 45: Relative increase of spheroid area of proneural BTICs RAV19 P25 and P26 (A) and RAV57 P16 and P18 (B): Spheroid sizes were measured after 20 and 48 hs. Migration was normalized in two steps: Values of each time point were normalized to initial spheroid size, followed by normalization to the medium control. For reasons of clarity, significances are only marked for the end point of 48 hs.

Spheroid migration of RAV19 and of RAV57 remained mostly unaffected by TGF-β_2. While 48 h treatment with 10 mM metformin decreased migration to 0.43 in RAV19 ($p < 0.0001$) and to 0.33 in RAV57 ($p < 0.0001$), the effects of combined treatment differed. The combination reduced migration of RAV19 BTICs to 0.60 ($p < 0.0002$) and that of RAV57 BTICs to to 0.29 ($p < 0.0001$).

Finally, the effects of 10 mM metformin, TGF-β_2 and the combination thereof on cell morphology are examined in Figure 46.

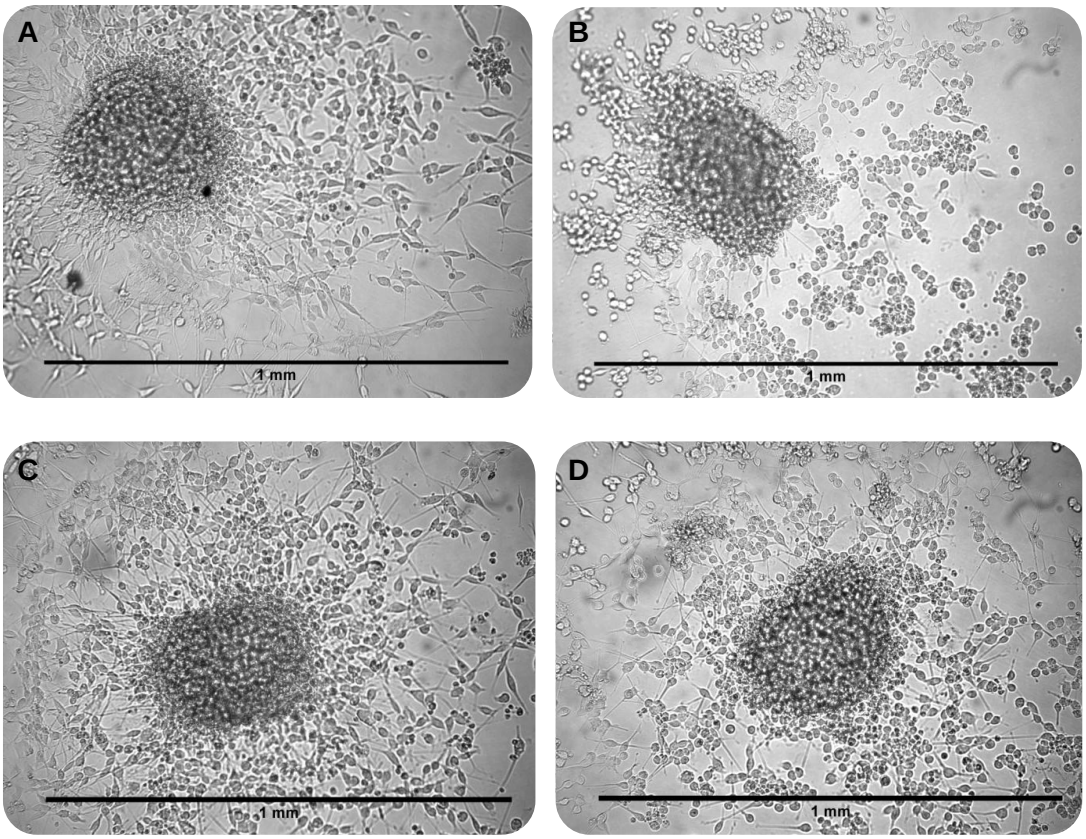

Figure 46: Spheroid photographs of RAV19 BTICs after 48 hs at 10x magnification: Medium control (A), 10 mM metformin (B), 10 ng/ml TGF-β_2 (C) and the combination of 10 mM metformin and 10 ng/ml TGF-β_2 (D).

When 10 mM metformin was present in a well (B), cell morphology changed as cells appeared to be more spherical compared to the medium control (A) where cells appeared spindle-shaped. Spindle-shaped cell morphology was also seen in TGF-β_2 treated wells (C). When closely examining wells treated with the combination of 10 mM metformin and TGF-β_2 (D) it seems as if BTICs exhibit more protrusions than in metformin treated wells (B) hinting that possibly, the addition of TGF-β_2 attenuated not only the effects of 10 mM metformin on migration but also on cell morphology.

5.3.3.2 Detailed analysis of mesenchymal BTICs RAV21, RAV24 and RAV27

To investigate proliferation, cell counts were carried out with RAV21 P19, RAV24 P12 and P14 and RAV27 P16 and P20 and a crystal violet staining was performed with RAV24.

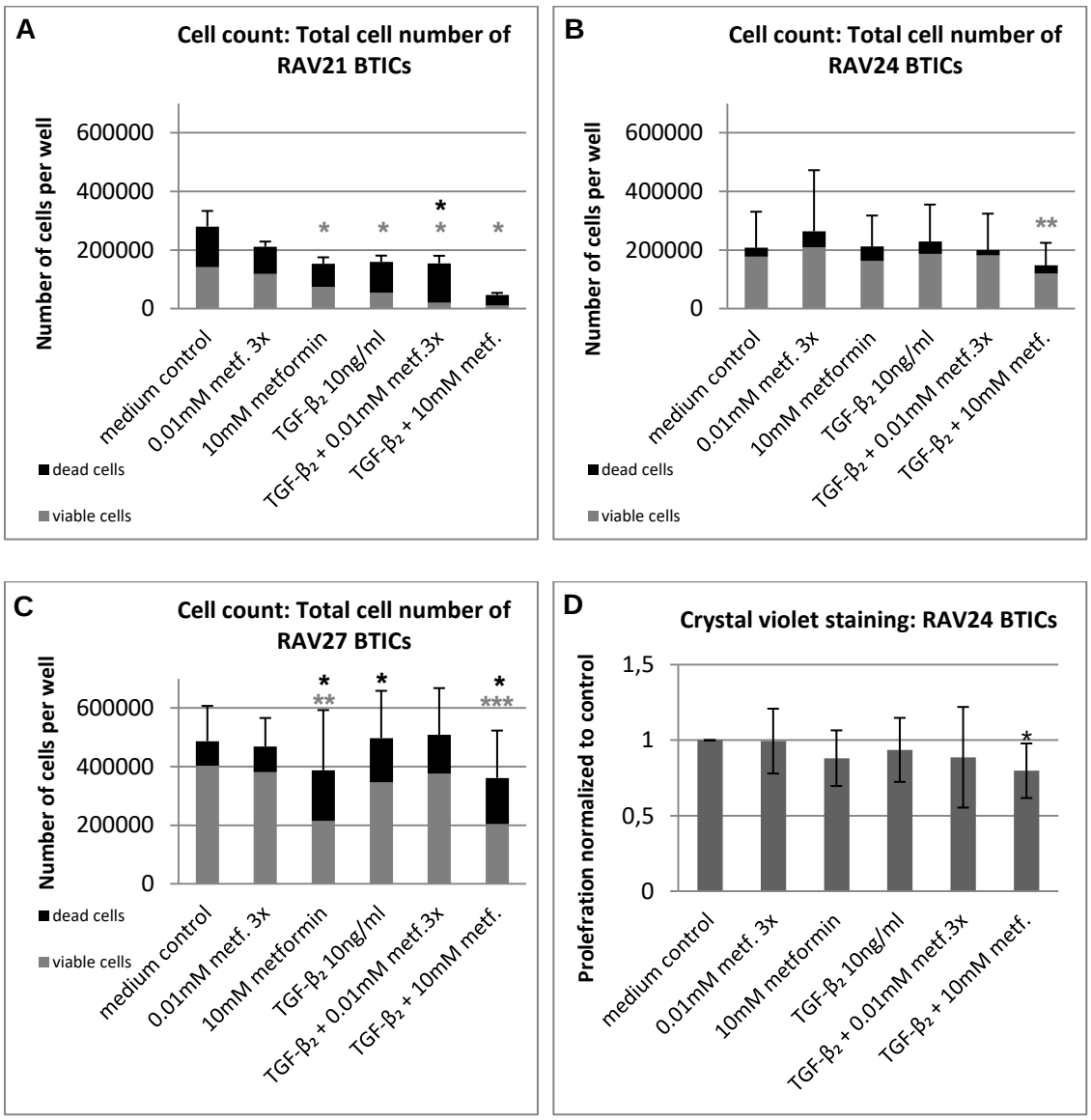

Figure 47: Total cell number per well obtained after 48 hs treatment: For cell counts of RAV21 P19 (A), of RAV24 P12 and P14 (B) and of RAV27 P16 and P20 (C), the numbers of viable cells are shown in grey. Accordingly, significant differences between proliferation with treatment and at medium control conditions are marked with grey stars. Absolute numbers of dead cells are shaded black. Significant differences between the fraction of dead cells in any treated well compared to the fraction of dead cells at medium control conditions are marked with black stars. (D) depicts results of a crystal violet staining assay performed with RAV24 BTICs. Values were normalized to control.

Among mesenchymal cell lines, reaction patterns to the combination of metformin and TGF-β_2 were heterogeneous. Concerning RAV21 P19, the effects of combined metformin and TGF-β_2 were more pronounced as proliferation was reduced to 0.84 by 0.01 mM metformin with triple re-treatment (non-significant), to 0.38 by TGF-β_2 ($p < 0.03$) but to 0.14 ($p < 0.02$) when both substances were present. Similarly, 10 mM metformin reduced proliferation to 0.53 ($p < 0.05$), and the combination with TGF-β_2 decreased it to 0.08

($p < 0.02$). Therefore, anti-proliferative effects on RAV21 P19 of combined treatment were greater than single applications' effects of low and high doses of metformin. TGF-β_2 + 0.01 mM metformin x3's fraction of dead cells was 1.66 times as large as the medium control's ($p < 0.05$) suggesting cytotoxicity. The combination treatment of TGF-β_2 + 10 mM metformin decreased proliferation by 83% ($p < 0.02$), revealing cytostatic properties.

RAV24, non-responsive to individual treatment with metformin or TGF-β_2, reacted to the combination. It reduced migration to 0.63 ($p < 0.003$) in cell counts (B), a result which was supported by a crystal violet staining assay (D) in which proliferation was diminished to 0.80 by combined metformin and TGF-β_2 ($p < 0.05$).

In RAV27, a rapidly proliferating mesenchymal cell line, two major trends were observed. Firstly, the fraction of dead cells compared to the medium control was 2.65 times larger under 10 mM metformin ($p < 0.05$), 1.76 times larger under 10 ng/ml TGF-β_2 ($p < 0.02$) and 2.59 times larger under combined treatment ($p < 0.02$). Hence, all three conditions appeared cytotoxic. Secondly, proliferation reduction was likely due to metformin, because both, 10 mM metformin and combined treatment approximately halved proliferation ($p < 0.003$; $p < 0.0007$), but TGF-β_2 by itself did not alter proliferation rates significantly.

In summary, the anti-proliferative effects of combined metformin and TGF-β_2 were more pronounced in RAV21; in RAV24, only their combination resulted in a proliferation decrease; and in RAV27, proliferation rate reduction was likely due to metformin.

To investigate migration, spheroid migration assays were performed. Figure 48 depicts migration photographs of RAV24 BTICs exemplarily.

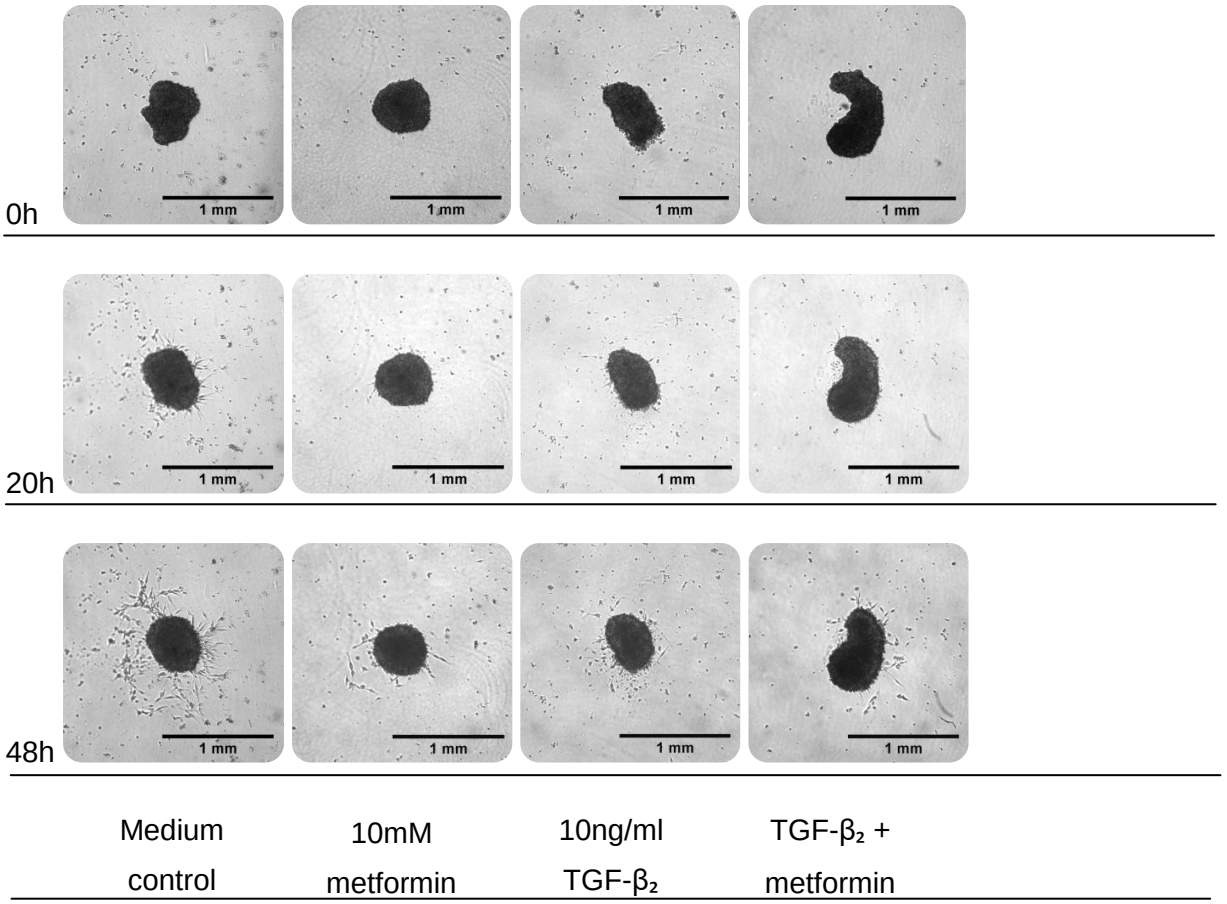

Figure 48: Spheroid migration of RAV24 BTICs: Pictures were taken 0, 20 and 48 hs after treatment with metformin, TGF-β_2 and their combination at 5x magnification.

Judging from the photographs, 10 mM metformin, 10 ng/ml TGF-β_2 and the combination thereof impaired migration of RAV24 BTICs to a similar extent. The following figure displays the results from quantitative assessment of migratory rates of RAV21, RAV24 and RAV27 BTICs.

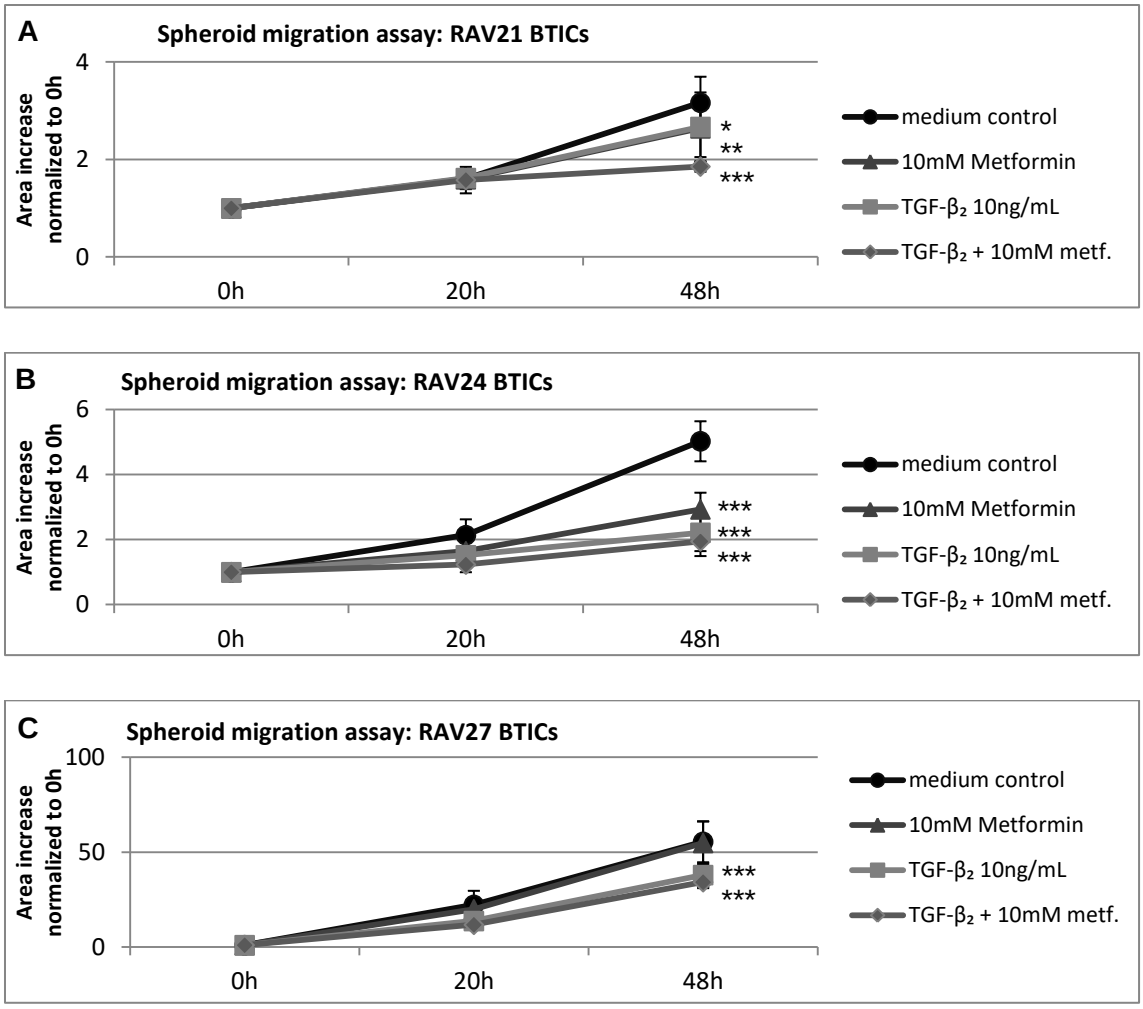

Figure 49: Relative increase of spheroid area of mesenchymal BTICs RAV21 P17 and P24 (A), RAV24 P12 and P14 (B) and RAV27 P16 and P20 (C): Spheroid sizes were measured after 20 and 48 hs. Migration was normalized in two steps: Values of each time point were normalized to initial spheroid size, followed by normalization to the medium control. For reasons of clarity, significances are only marked for the end point of 48 hs.

After 48 hs, 10 mM metformin as well as TGF-β_2 reduced migration of RAV21 BTICs to 0.83 ($p < 0.02$, $p < 0.009$), and to 0.70 by their combination ($p < 0.0001$). The anti-migratory effects of the combination were more pronounced than those of the individual agents.

The migratory rates of RAV24 BTICs after 48 hs were reduced to 0.58 by 10 mM metformin, to 0.45 by TGF-β_2 and to 0.38 by their combination ($p < 0.0001$ in all cases) whereas proliferation was only influenced by the combined treatment.

RAV27 BTICs' migration was not influenced by metformin while 10 ng/ml TGF-β_2 decreased migration after 48 hs to 0.70 by itself ($p < 0.0001$) and to 0.64 when combined with 10 mM metformin ($p < 0.0001$).

To conclude, RAV21 displayed vast sensitivity to anti-proliferative and anti-migratory effects of combined 10 mM metformin and 10 ng/ml TGF-β_2. In RAV24, proliferation was only reduced by their combination, but migration was impaired under all three conditions. RAV27's

proliferation was diminished by metformin, but not by TGF-β_2; yet, TGF-β_2 lowered migration. Overall, the anti-proliferative and anti-migratory effects of the combination treatment were most pronounced.

How the agents by themselves and in combination influenced cell morphology after 105 hs is exemplarily shown for RAV24 BTIC.

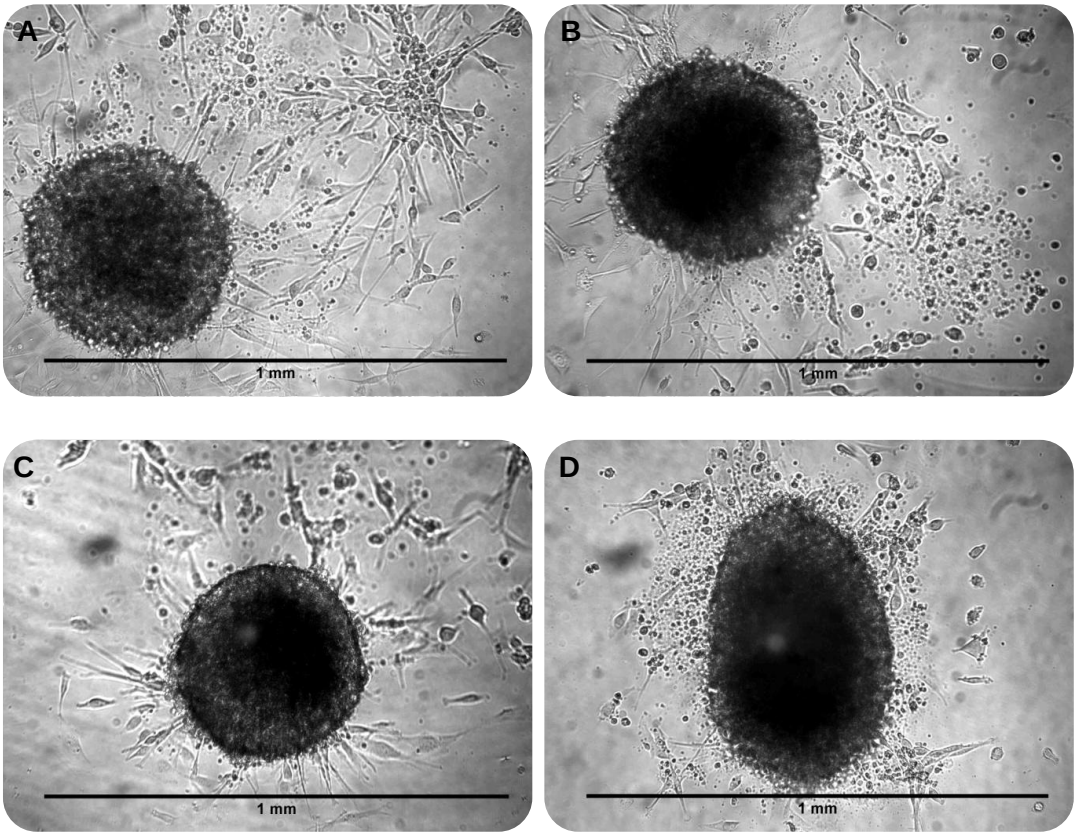

Figure 50: Spheroid photographs of RAV24 BTICs after 105 hs at 10x magnification: Medium control (A), 10 mM metformin (B), 10 ng/ml TGF-β_2 (C) and the combination of 10mM metformin and 10ng/ml TGF-β_2 (D).

RAV24 BTICs changed to a more spherical shape under 10 mM metformin (B). TGF-β_2 did not attenuate these effects (D). Thus, morphological changes align well with results from functional assays as the combination treatment produced the largest anti-proliferative, anti-migratory and cell morphology changing effects.

5.3.3.3 Detailed analysis of proneural TCs RAV19 and RAV57

Proliferation was assessed in cell counts with RAV19 P23_3 and P23_6 and RAV57 P17_2 and P20_3.

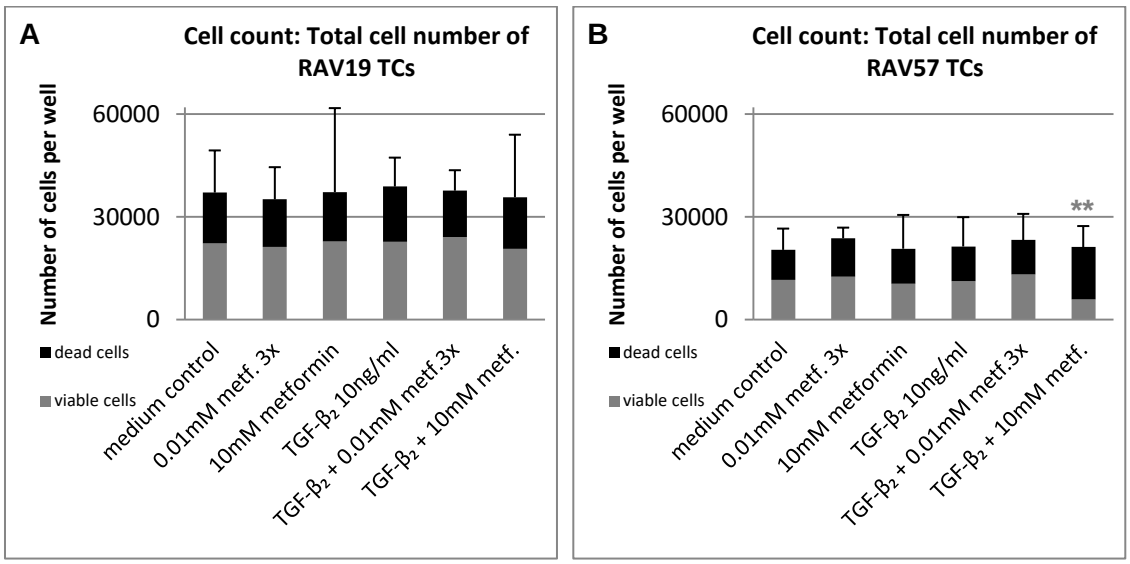

Figure 51: Total cell number per well obtained after 48 hs treatment: For cell counts of RAV19 P25 and P26 (A) and of RAV57 P16 and P18 (B) the numbers of viable cells are shown in grey. Accordingly, significant differences between proliferation with treatment and at medium control conditions are marked with grey stars. Absolute numbers of dead cells are shaded black. Significant differences between the fraction of dead cells in any treated well compared to the fraction of dead cells at medium control conditions are marked with black stars.

Neither RAV19 nor RAV57 TCs reacted much to any given substance. In RAV57, only 10 ng/ml TGF-β_2 + 10 mM metformin decreased proliferation to 0.55 ($p < 0.002$).

Figure 52 illustrates migratory behavior of RAV19 TCs at 0, 20 and 48 hs.

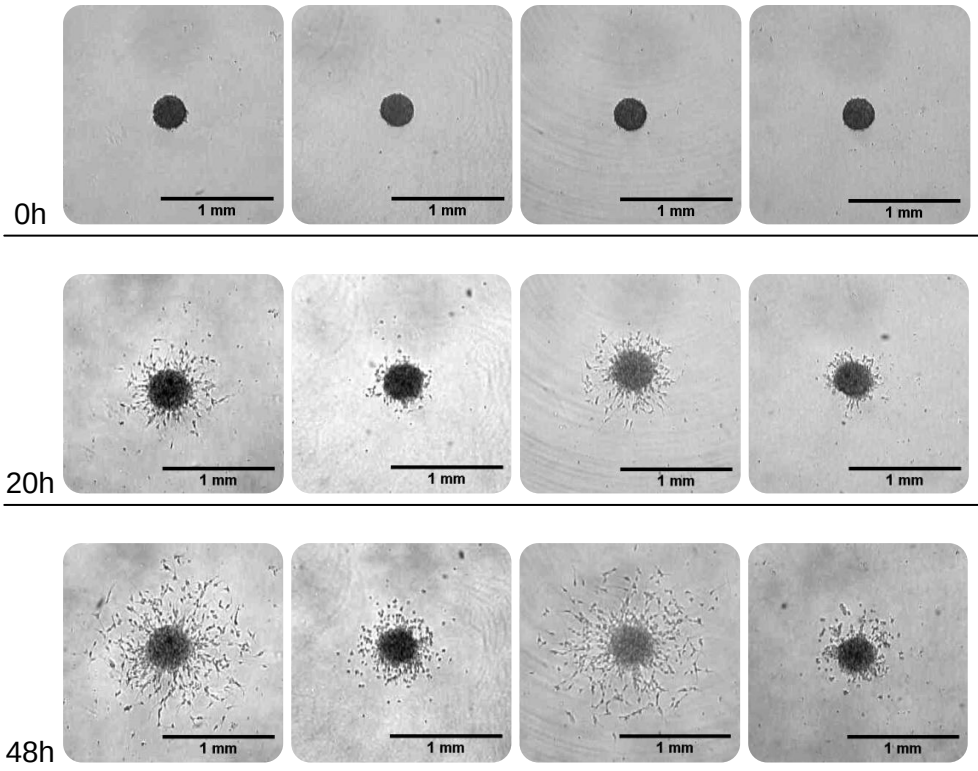

Figure 52: Spheroid migration of RAV19 TCs: Pictures were taken 0, 20 and 48 hs after treatment with metformin, TGF-β_2 and their combination at 5x magnification.

Here, the anti-migratory effects of 10 mM metformin on RAV19 TCs become apparent. Even at 5x magnification, morphological changes can be detected which will be further illustrated by Figure 54. However, 10 ng/ml TGF-β_2's effects were not anti-migratory which will be further assessed in Figure 53.

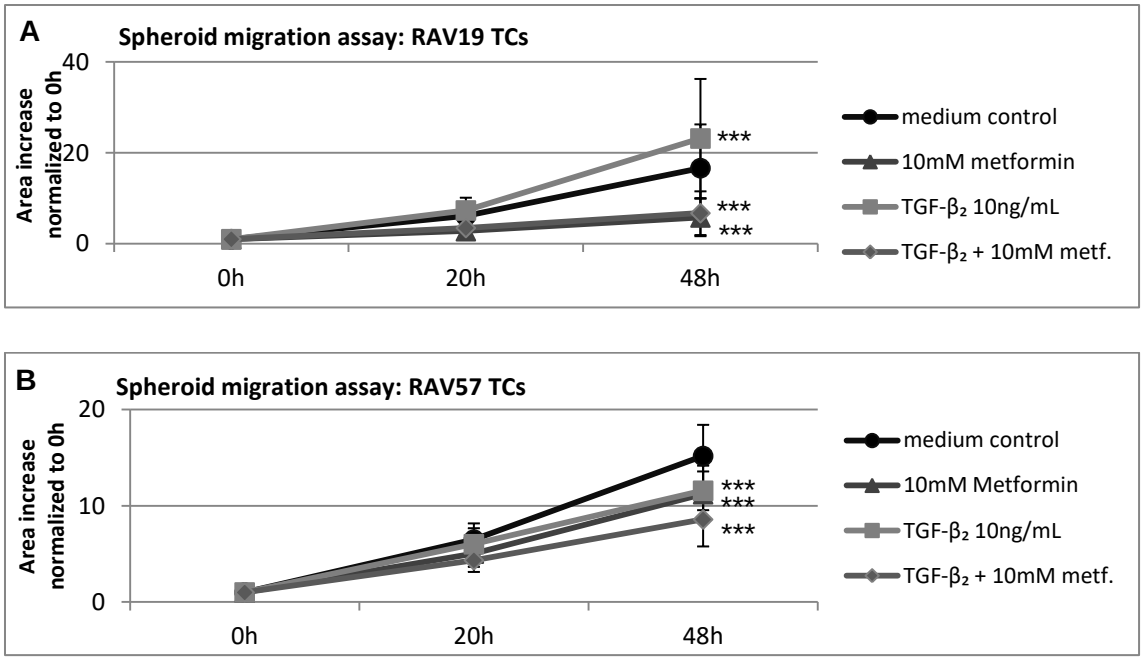

Figure 53: Relative increase of spheroid area of proneural TCs RAV19 P23_3 and P23_6 (A) and RAV57 P17_2 and P20_3: Spheroid sizes were measured after 20 and 48 hs. Migration was normalized in two steps: Values of each time point were normalized to initial spheroid size, followed by normalization to the medium control. For reasons of clarity, significances are only marked for the end point of 48 hs.

As Figure 52 suggested, anti-migratory effects were observed in RAV19 BTICs under 10 mM metformin treatment. After 48 hs, migration was reduced to 0.32 by 10 mM metformin ($p < 0.0001$) and to 0.36 in combination with 10 ng/ml TGF-β_2 ($p < 0.0001$), even though 10 ng/ml TGF-β_2 increased migration to 1.41 ($p < 0.0001$). Thus, the anti-migratory effects obtained by the combined treatment were likely due to metformin.

After 48 hs, migration of RAV57 was lowered to 0.73 by 10 mM metformin ($p < 0.0002$), to 0.76 by 10 ng/ml TGF-β_2 ($p < 0.0002$) and to 0.56 by their combination ($p < 0.0001$). In this case, the anti-migratory effects of metformin and TGF-β_2 were greater than for single agents.

Figure 54 displays morphological changes in RAV19 TCs induced by 120 hs of treatment with high dose metformin.

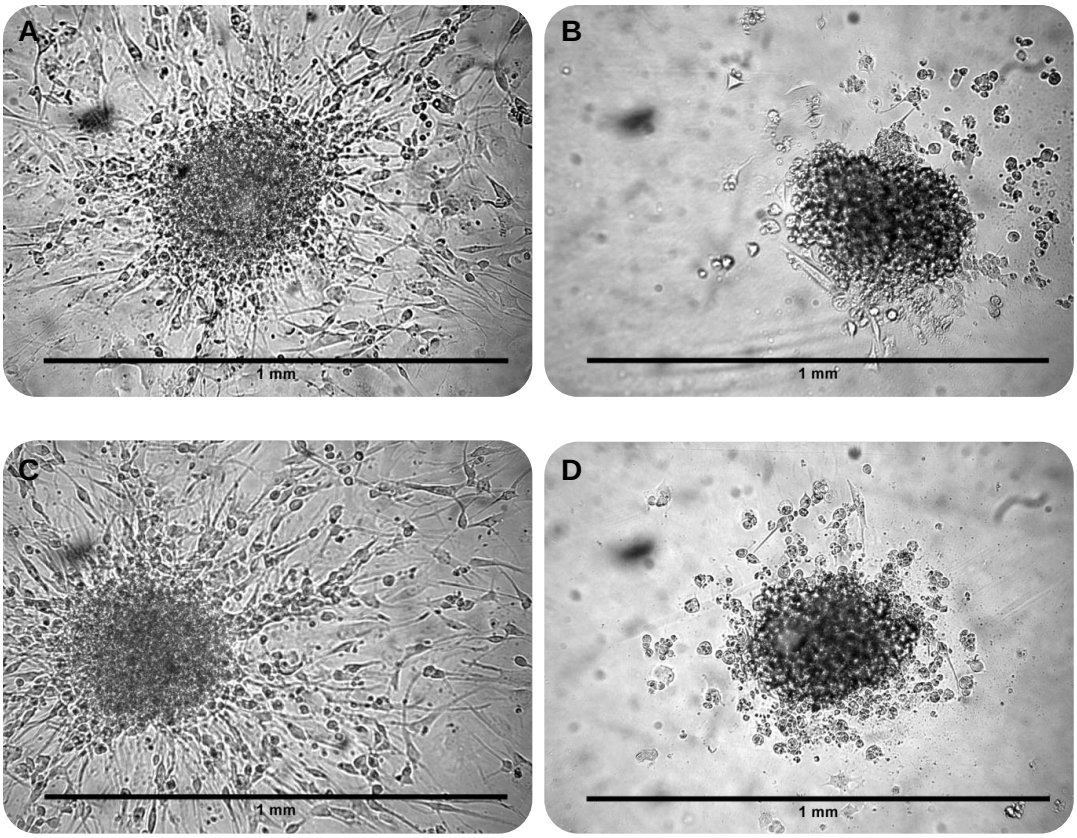

Figure 54: Spheroid photographs of RAV19 TCs after 120 hs at 10x magnification: Medium control (A), 10 mM metformin (B), 10 ng/ml TGF-β_2 (C) and the combination of 10 mM metformin and 10 ng/ml TGF-β_2 (D).

Compared to tumor cells rich in protrusions as seen in medium control wells (A) and TGF-β_2 treated wells (C), tumor cells in metformin treated wells 10 mM metformin (B and D) lost almost all of their protrusions and adopted a spherical shape. Morphological changes are thus in line with results from functional assays.

5.3.3.4 Detailed analysis of mesenchymal TCs RAV21, RAV24 and RAV27

In proliferation assays, RAV21 P24_9 and P24_10 were used along with RAV24 P10_5 and P10_7 as well as RAV27 P18_5 and P18_6.

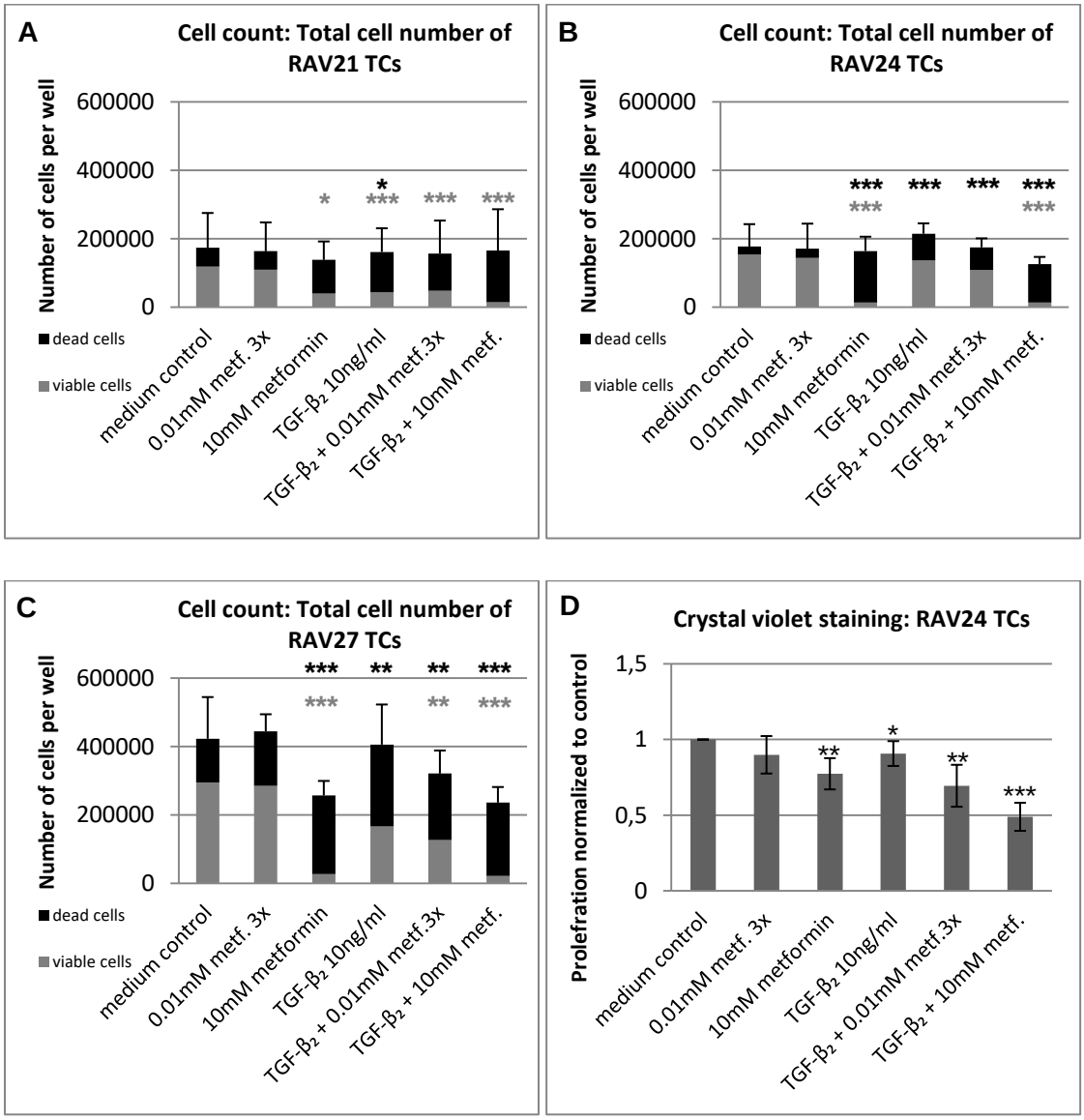

Figure 55: Total cell number per well obtained after 48 hs treatment: For cell counts of RAV21 P24_9 and 24_10 (A), of RAV24 P10_5 and P10_7 (B) and of RAV27 P18_5 and P18_6 (C), the numbers of viable cells are shown in grey. Accordingly, significant differences between proliferation with treatment and at medium control conditions are marked with grey stars. Absolute numbers of dead cells are shaded black. Significant differences between the fraction of dead cells in any treated well compared to the fraction of dead cells at medium control conditions are marked with black stars. (D) depicts proliferation normalized to non-treated controls.

Mesenchymal TCs reacted to metformin and to TGF-β_2. RAV21's proliferation rates decreased to 0.51 under 10 mM metformin ($p < 0.03$), to 0.4 under 10 ng/ml TGF-β_2, to 0.38 under TGF-β_2 + 0.01 mM metformin with triple re-treatment and to 0.14 under the combined treatment of 10 mM metformin and 10 ng/ml TGF-β_2 ($p < 0.0001$ in the latter three instances). Thereby, the effects of combined treatment were suggestively significant when comparing effects of 10 ng/ml TGF-β_2 + 10 mM metformin to those of 10 mM metformin

$p < 0.002$ and to those of TGF-β_2 $p = 0.069$). Also, TGF-β_2 increased the fraction of dead cells 2.35-fold compared to the medium control ($p < 0.03$).

RAV24's proliferation was diminished by 90% through 10 mM metformin and by 92% through combined treatment ($p < 0.001$ in both cases). These effects appeared cytotoxic as the fraction of dead cells multiplied times 7 in both cases ($p < 0.001$). The effects of TGF-β_2 by itself and in combination with 0.01 mM metformin triple treatment were also cytotoxic with the fraction of dead cells approximately tripling ($p < 0.0003$ in both cases); yet their ability to reduce proliferation was not significant. A crystal violet staining assay underlined these trends. Here, proliferation was reduced to 0.77 by 10 mM metformin ($p < 0.004$), to 0.90 by TGF-β_2 ($p < 0.05$), to 0.69 by TGF-β_2 + 0.01 mM metformin x3 ($p < 0.003$) and to 0.49 by TGF-β_2 + 10 mM metformin ($p < 0.0001$). Thus, the effects of the combination of metformin and TGF-β_2 were more pronounced than those of single agents for low and high doses.

Proliferation of RAV27 was reduced by high-dose metformin and its combination with TGF-β_2. It was decreased by 90% by 10 mM metformin ($p < 0.0003$), by 34% through TGF-β_2 (non significant), by 54% through TGF-β_2 + 0.01 mM x3 ($p < 0.002$) and by 92% by TGF-β_2 + 10 mM metformin ($p < 0.0003$). Under all of these conditions the fraction of dead cells was significantly larger than in the medium control. It tripled for 10 mM metformin or TGF-β_2 + 10 mM metformin treatment ($p < 0.0003$ in both cases) and it doubled under treatment with TGF-β_2 or TGF-β_2 + 0.01 mM metformin x3 ($p < 0.009$ in both cases).

Concluding, TGF-β_2's effects were cytotoxic to mesenchymal TCs RAV21, RAV24 and RAV27. The combination of TGF-β_2 and 10 mM metformin consistently decreased proliferation.

To compare these findings to spheroid migration, Figures 56 and 57 give an overview.

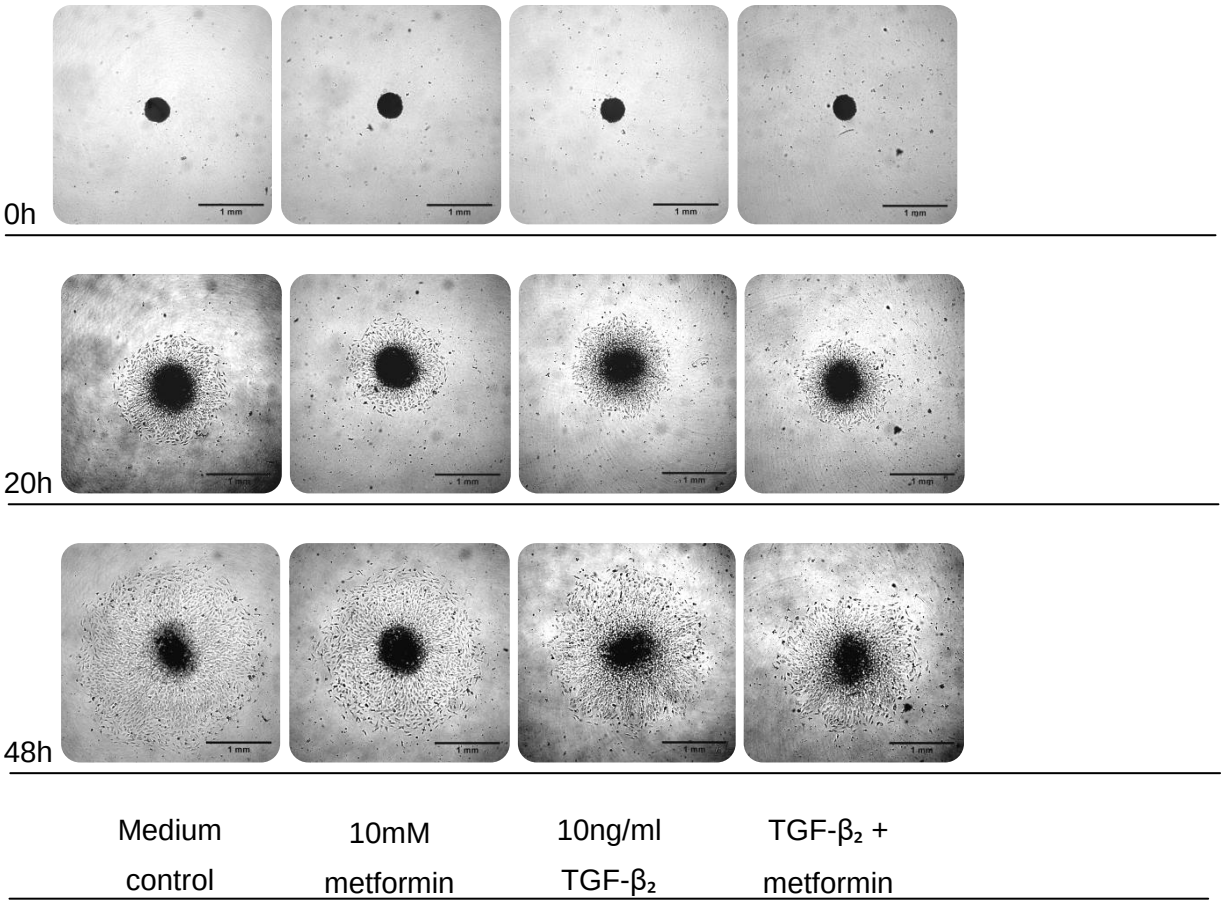

Figure 56: Spheroid migration of RAV27 TCs: Pictures were taken 0, 20 and 48 hs after treatment with metformin, TGF-β_2 and their combination at 5x magnification.

From photographs presented in Figure 56, it seems that migration of RAV27 TCs was inhibited mostly by the combination of 10 mM metformin and TGF-β_2. Quantitative results are outlined in Figure 57.

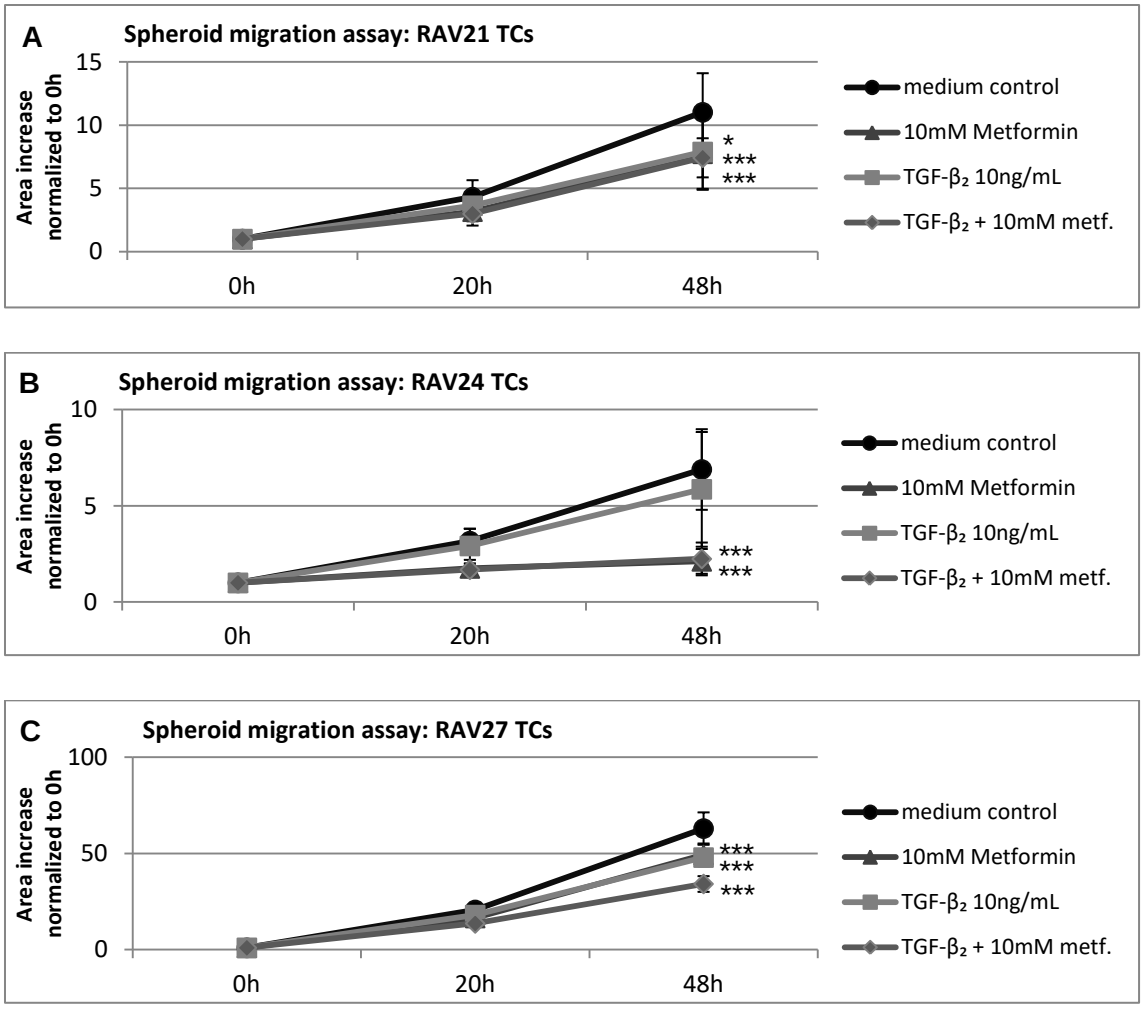

Figure 57: Relative increase of spheroid area of mesenchymal TCs RAV21 P24_9 an P24_10 (A), RAV24 P10_5 and P10_7 (B) and RAV27 P18_5 and P18_6 (C): Spheroid sizes were measured after 20 and 48 hs. Migration was normalized in two steps: Values of each time point were normalized to initial spheroid size, followed by normalization to the medium control. For reasons of clarity, significances are only marked for the end point of 48 hs.

Migration of RAV21 after 48 hs was lowered by metformin, TGF-β_2 and combinations thereof and the effects were comparable (A). 10 mM metformin lowered migration to 0.73 ($p < 0.02$), TGF-β_2 to 0.71 ($p < 0.0009$) and their combination to 0.69 ($p < 0.0005$).

Migratory rate reduction in RAV24 after 48 hs was likely due to 10 mM metformin. Migration was decreased to 0.3 by 10 mM metformin ($p < 0.0001$), to 0.8 by 10 ng/ml TGF-β_2 (non-significant) and to 0.32 by their combination.

TGF-β_2 reduced migration of RAV27 TCs to 0.77 ($p < 0.0001$), 10 mM metformin reduced migration to 0.79 ($p < 0.0001$).

Hence, the combination of TGF-β_2 and 10 mM metformin consistently decreased migration. Reaction patterns ranged from equal anti-migratory power of TGF-β_2 and metformin in RAV21 TCs, over no significant effect of TGF-β_2 but vast decrease through 10 mM metformin

in RAV24 TCs to pronounced anti-migratory effects in RAV27 TCs. These three mesenchymal TC lines showed heterogeneous reaction patterns.

Pictures taken of RAV21 TCs serve as an example to show how metformin and TGF-β_2 influenced cell morphology.

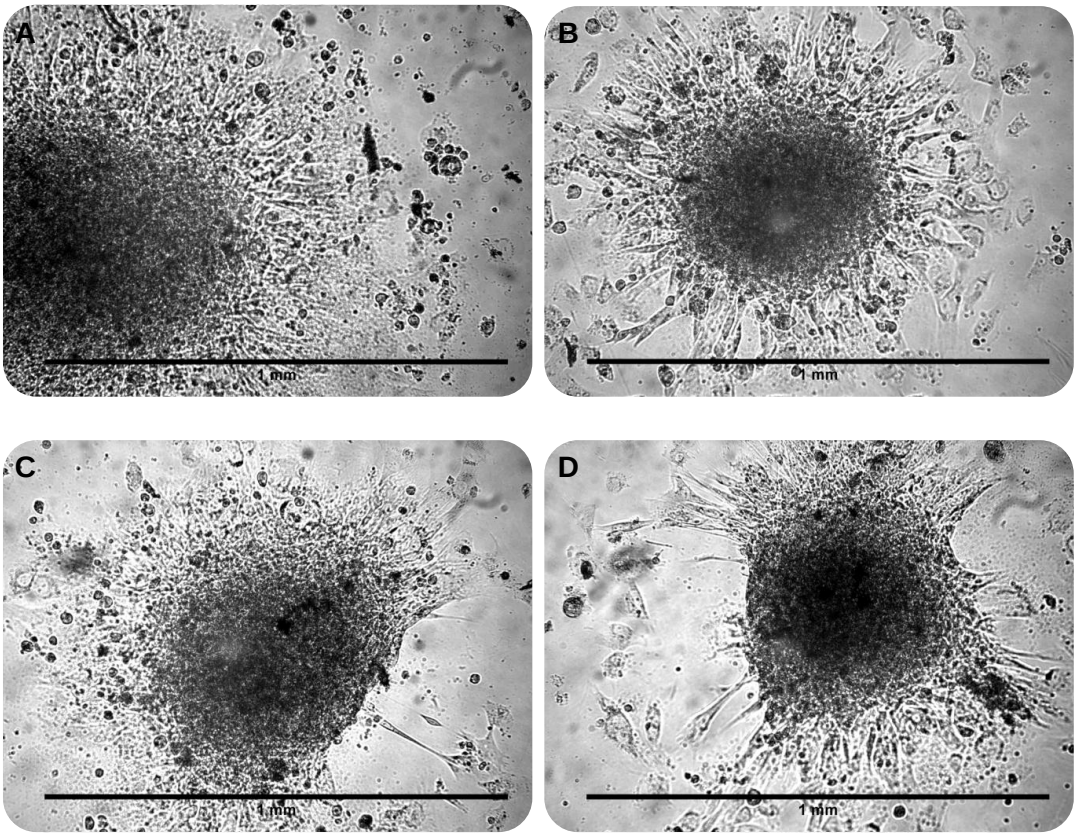

Figure 58: Spheroid photographs of RAV21 TCs after 48 hs at 10-fold magnification: Medium control (A), 10 mM metformin (B), 10 ng/ml TGF-β_2 (C) and the combination of 10 mM metformin and 10 ng/ml TGF-β_2 (D).

As outlined in Figure 58, 10 mM metformin (B) resulted in discrete cell swelling. The presence of TGF-β_2 led to cell free areas immediately next to the initial spheroid into which only few cells migrated.

5.4 Synopsis of the functional effects of metformin, TGF-β_2 and SD-208

Table 22 summarizes all significant changes in proliferation and migration of all cell lines and for all conditions at the 48 h time point.

Table 22: Summary of all treatment conditions and their effects on proliferation and migration of all cell lines after 48 h: Proliferation (dark grey) and migration (light grey) are depitcted after 48 h. Blank spaces signify that there is not data for these conditions. Only significant results are shown. Symbols indicate the following: - indicates that proliferation/migration is reduced by up to 25%, - - by 25-50%, - - - by 50-75% and - - - - by more than 75%. Accordingly, + indicates a proliferation / migration increase by up to 25% and ++ by up to 50%.

Cell line	Results after 48 h	0.01 mM metformin	0.01 mM metformin x3	0.1 mM metformin	1 mM metformin	10 mM metformin	SD-208 1 µM	TGF-β_2 10 ng/ml	TGF-β_2 10 ng/ml + 0.01 mM metformin x3	TGF-β_2 10 ng/ml + 10 mM metformin	TGF-β_2 10 ng/ml + SD-208 1 µM
RAV19 BTIC	Proli.			- -		- -				- -	
	Migra.					- - -				- -	
RAV57 BTIC	Proli.		- -		- - -	- - -				- - -	
	Migra.					- - -				- - -	
RAV21 BTIC	Proli.					- -		- - -	- - - -	- - - -	
	Migra.		++			-		-		- -	
RAV24 BTIC	Proli.			++						- -	
	Migra.					- -		- - -		- - -	-
RAV27 BTIC	Proli.					- -				- - -	
	Migra.						- -	- -		- -	- - -
RAV19 TC	Proli.						++				
	Migra.				-	- - -	-	++		- - -	
RAV57 TC	Proli.									- -	
	Migra.					-	+	-		- -	+
RAV21 TC	Proli.					- -	++	- - -	- - -	- - - -	
	Migra.					- -		- -		- -	
RAV24 TC	Proli.			++		- - - -				- - - -	
	Migra.				- -	- - -	+			- - -	
RAV27 TC	Proli.					- - - -			- - -	- - - -	
	Migra.					-	+	-		- -	+

Apart from effects on proliferation and migration, changes in morphology were also observed. They were exemplarily shown for RAV19 BTICs, RAV24 BTICs, RAV19 TCs and RAV 21 TCs as they best exemplified group trends and had the best picture quality. Changes in morphology can be summed up as follows:

- 10 mM metformin:
    - spherical, non-spindle like, smaller: RAV19 BTICs, RAV24 BTIC
    - small, irregular, no protrusions: RAV19 TCs
    - bigger, less spindle-like: RAV21 TCs.
- 10 ng/ml TGF-β_2:
    - unaltered compared to control: RAV19 BTICs, RAV19 TCs,
    - less spindle-like: RAV24 BTICs
    - lower density and cell free areas: RAV21 TCs.
- 10 mM metformin + 10 ng/ml TGF-β_2:
    - effects cancel out RAV19 BTICs
    - more spherical and smaller than after 10 mM metformin: RAV24 BTICs
    - equal morphology compared to metformin-treated cells: RAV19 TCs
    - bigger, less spindle-like and cell free areas: RAV21 TCs.

6 DISCUSSION

Proliferation and migration are two of the main tumor characteristics of GBM. Both are influenced by TGF-$\beta_{2,}$ which has been described as a tumor suppressor and tumor promotor in glioma, and by metformin, a potential anti-glioma drug. While previous data on TGF-β_2's effects on glioma is heterogenous showing increased, decreased and steady proliferation rates (see Table 23) and possibly reduced migratory rates, data concerning metformin (see Table 2) more consistently indicates that overall, metformin reduces proliferation and migration of GBM *in vitro*. This study aimed to investigate functional effects of the two agents on primary tumor cells obtained in brain surgery at the University Hospital Regensburg and uncovering possible links.

6.1 The role of metformin in GBM

Several researchers have explored metformin's effects on GBM's proliferation and migration. Mostly, doses of 10 mM and higher were used, because Würth *et al.* (2013) calculated the IC_{50} for metformin at approximately 10 mM. Lower doses often failed to produce an effect (see Table 2). However, doses as high as 10 mM seem hardly achievable in the human brain, so this study explored whether 10 mM consistently reduces proliferation and migration and whether lower doses are effective in some GBM cell lines as well.

In this study, 10 mM metformin decreased proliferation by 46% or, on an individual level, in 7 / 10 cases. Looking at proliferation inhibition in detail, cytostatic and cytotoxic effects were identified. High-dose metformin (10 mM) was cytostatic in 3 / 7 cases and revealed its cytotoxic properties in 4 / 7 cases, meaning that the amount of dead cells in metformin treated wells significantly exceeded the amount of dead cells in control wells. No effects on proliferation were observed in 3 / 10 cases. These results align with pertinent literature. Würth *et al.* (2013), Gao *et al.* (2013), Liu *et al.* (2014) and Sesen *et al.* (2015) observed proliferation reduction after treatment with 10 mM metformin. Ferla *et al.* (2012) observed a dose-dependent proliferation reduction between 2 and 16 mM metformin treatment. Sesen *et al.* (2015) established a timeline of cytotoxicity. After 12 hs, the earliest cell cycle arrests could be detected, and after 48 hs consistent cell death can be found. Thus, 48 hs generally seems to be acceptable to investigate alterations in proliferation. Liu *et al.* (2014) also observed cytostatic effects in the three cell lines examined while Isakovic *et al.* (2007) and Sesen *et al.* (2015) describe apoptosis and autophagy.

Cytotoxic effects of metformin were described only for doses higher than 10 mM (Würth *et al.* 2013). However, in this study, cytotoxic effects were observed at 10 mM metformin, suggesting that glioma cell lines considerably differ in their sensitivity to metformin. Two of the cases in which cytotoxic effects were observed, were in mesenchymal TC lines. Here, results from cell counts differed from a crystal violet assay. The observed difference between the amount of proliferation reduction in cell counts versus crystal violet staining could be due to different procedures. Cell counts involved several steps of scraping the cells off the well with a sterile cell scraper, washing them with PBS multiple times and pipetting them up and down to avoid the formation of lumps which would have distorted cell count results. These procedures were carried out identically for each cell line, but metformin may have weakened RAV24 and RAV27 TCs in a way that cell count procedures, especially pipetting, led to cell death. Figure 55 shows that the total amount of dead and viable cells was only slightly or moderately lower than that of the control wells after 10 mM metformin treatment supporting that RAV24 and RAV27 became fragile after metformin treatment and died during cell count procedures. In this case, the magnitude of proliferation decrease may be more accurately reflected by the crystal violet staining assay, as the procedures of staining and washing were more gentle. Determining whether 10 mM metformin was cytotoxic in mesenchymal TCs or whether effects were actually cytostatic but distorted by cell count procedures, remains difficult. Certainly, the amount of dead cells in mesenchymal TC cell counts impressively proves that metformin weakens GBM cells which might be why metformin increases sensitivity to irradiation treatment (Sesen *et al.* 2015).

In 3 / 10 cases, cell lines did not respond to 10 mM metformin at all. One of the cell lines was RAV24 BTIC, a cell line which in general did not respond to metformin treatment neither in cell counts nor in a crystal violet staining assay. This leads to the assumption that either, doses were too low for an effect, treatment time was too short, or RAV24 BTIC simply resists metformin's action. The other two cell lines which did not respond to high-dose metformin treatment were RAV19 TC and RAV57 TC. As outlined in section 5.3.3.3, proneural TCs proliferation rates were 10-times slower than the average proliferation rate, making gauging alterations in proliferation after 48 hs difficult. Sesen *et al.* (2015) propose that some glioma cells, namely those with PTEN mutations, respond only after treatment times of 96 hs. Würth *et al.* (2010) observed maximum anti-proliferative effects after 72 h. Most likely, longer treatment duration is needed to accurately investigate metformin's anti-proliferative effects on slowly proliferating cell lines.

Low doses of metformin yielded anti-proliferative results in only proneural BTICs. They reacted to doses as low as 0.01 mM metformin in triple re-treatment and the effect of

0.01 mM metformin in triple re-treatment was significantly more pronounced than that of 0.01 mM metformin alone.

Some caution is advisable regarding the results for RAV19 BTIC (see Figures 12 and 13). Their responsiveness to low dose metformin could have been because they grew in spheres, and in cell counts, spheres may distort results. The aggregation of cells leads to unrealistically high numbers in one count and unrealistically low numbers in another. To disintegrate spheres, RAV19 BTICs were pipetted up and down more extensively than other cell lines. The results for all conditions are in a similar range, as each condition had a total of six replicates. As standard deviation is small, the results are probably accurate despite RAV19 BTIC's spherical growth. This is especially interesting as spherical growth may impede metformin reaching cells located at the center of a sphere. Metformin's ability to decrease proliferation of a cell line growing spherically underlines its anti-glioma potential. Very low doses of metformin may exert anti-proliferative effects in certain glioma cell lines, while re-treatment may increase metformin's power.

Metformin in a concentration of 0.01 mM (= 10 µM) may actually be reached in the brain of a human diabetic. Given that a concentration of 44 µM can be reached in rat brain tissue after 3 weeks of 300 mg/kg metformin administered orally per day (Łabuzek *et al.* 2010) and that 12 µM were measured in a mouse brain after oral administration of 50 mg/kg metformin (Wilcock and Bailey 1994), the metformin concentration in the brain of a 70 kg patient with an oral intake of 3000 mg metformin (which equals around 43 mg/kg) could be 10 µM. Therefore, if rat data is applicable to humans, 0.01 mM metformin may actually be achieved in human diabetics.

Another way of calculating metformin concentrations in human brains considers plasma to brain ratios of metformin. In mice models, metformin concentration in the brain is about 10% of the plasma concentration (Kim *et al.* 2016). Studies of human patients show that the plasma concentration of metformin is commonly found between 8 and 31 µM (Menendez *et al.* 2014). Therefore, levels between 0.8 and 3.1 µM could be attained in human brain tissue. Now, the maximum daily intake of 3000 mg metformin was established as a safe dose for long-term diabetic treatment (Pollak 2013). Hence, clinical trials exploring maximum tolerable doses of metformin for cancer patients and using alternative administration routes (e.g. intraperitoneal administration) should be conducted (Menendez *et al.* 2014, Pollak *et al.* 2013). The first study to explore tolerable doses is a phase I trial investigating doses of metformin and chloroquine in IDH1/2-mutant gliomas (NCT02496741). Alternatively, the use of phenformin, another biguanide exerting strong anti-neoplastic effects on BTICs, should be considered (Pollak *et al.* 2013, Jiang *et al.* 2016). As lactic acidosis was observed more often in phenformin treatment than in metformin treatment, phenformin is not used to treat diabetes

anymore (Jiang *et al.* 2016). However, Jiang *et al.* 2016 argue that only very low doses of phenformin are needed to treat GBM bearing mice rendering side effects less probable. In summary, the effects of low-dose metformin on proneural BTICs observed in this study set the rationale to explore more aggressive dosing of metformin or alternative application of phenformin.

Looking at pooled data from all cell lines, migration was reliably reduced. After 20 hs, 10 mM metformin reduced migration by 34% and after 48 h by 40%. Looking at individual cell lines, migration was lowered in 9 / 10 cases. Overall, 1 mM metformin also reduced migration significantly after 20 h and after 48 h (10% and 20% respectively); yet individual analysis shows that this was true for only 2 / 10 cell lines. These results correspond well with other researchers' findings who report migration inhibition at different dosages: 0.3 - 3 mM (Gao *et al.* 2013), 2 - 16 mM metformin (Ferla *et al.* 2012) and 5 - 50 mM metformin (Würth *et al.* 2013). However, Kim *et al.* (2016) found no migration reduction with 5 mM or 15 mM metformin. Of note, they did not examine proneural cell lines, but classic, mesenchymal and neural cell lines. Hence, susceptibility to metformin's anti-migratory effects seems to vary considerably among GBM.

For any concentration of metformin given, proneural BTICs were more sensitive to metformin's anti-proliferative power than mesenchymal BTICs. Several factors may account for these differences. Firstly, proliferation rate and confluence levels influence the effectiveness of metformin. Isakovic *et al.* (2007) noted that 4 mM metformin induces cell cycle arrest in non-confluent cells but induces apoptosis in confluent cells. Thus, cells proliferating at a high rate, reaching confluence while being treated with metformin, may be affected more severely. The reverse was observed in proneural TCs proliferating 10-times slower than the rest and not responding to metformin.

Secondly, the mutational background plays an important role as it affects the expression of regulatory and metabolic genes. Among proneural cells' characteristic mutations are *idh*-mutations and PDGFRA alterations; *p53* mutations are also found frequently (Verhaak *et al.* 2010). According to Viollet *et al.* (2012) and Buzzai *et al.* (2007), colon cells with *p53* mutations are at a selective disadvantage when being treated with metformin, because metformin depletes energy levels leading to a metabolic shift that *p53* (-/-) cells are unable to perform. Thus, proneural glioma cells carrying *p53* mutations might be more responsive to metformin, because they are unable to react to metformin-induced energy depletion. Another predictor may be *pten* mutational status. Sesen *et al.* (2015) observed that GBM cells carrying *pten* wild-type are more sensitive to metformin, because 10 mM metformin reduces proliferation within 48 hs. PTEN mutated GBM cells' proliferation, on the other hand, is affected only after 96 hs. They explain that in PTEN wild type cells, Akt is not constitutively

active and may be inhibited by metformin whereas cells with *pten* mutations exhibit constitutive Akt activity which is not influenced by metformin treatment (Sesen *et al.* 2015). Thus, proneural cell lines' sensitivity to metformin may be due to their *p53* (-/-) and/ or *pten* wt mutational status which would need to be confirmed for the cell lines used in this study.

Thirdly, metabolic reactions reflected in oxygen consumption vary. Earlier this year, we were able to show that proneural BTICs RAV57 heavily rely on oxidative phosphorylation, while mesenchymal BTICs RAV27 did not to such an extent. Oxygen consumption of RAV57 was therefore reduced by 1 mM metformin and drastically impaired by 10 mM metformin while RAV27's respiration did not change after treatment with 1mM metformin (Seliger and Meyer *et al.* 2016). Correspondingly, mesenchymal cells rely more heavily on glycolysis than proneural cells (Mao *et al.* 2013). Overall, *p53* and PTEN mutational status and also proneural subtype and reliance on oxidative phosphorylation (OXPHOS) may present valuable markers to predict GBM's sensitivity to metformin. The finding that proneural cells seem more sensitive to metformin is important, because Verhaak *et al.* (2010) noted that the proneural subtype does not respond to aggressive chemotherapy treatment whereas the mesenchymal subtype does. Additionally, Patel *et al.* (2014) found that proneural subsets of cells are present in all tumors of investigation regardless of their overall classification. Thus, metformin may present a drug to specifically target omnipresent chemotherapy-resistant proneural tumor cells.

Proneural TCs were less sensitive to metformin than mesenchymal TCs. This result again might have been due to very slow proliferation of proneural TCs, making gauging proliferation after 48 hs nearly impossible. In a crystal violet staining assay, exemplarily performed for RAV57 TC, 10 mM metformin decreased proliferation suggesting that longer observation periods would help detect anti-proliferative effects in proneural TCs as well.

Proneural TCs were also less sensitive to metformin's anti-proliferative effects than proneural BTICs. Another reason might be that the stem-cell like subset of tumor cells called BTICs relies on oxidative phosphorylation more than their differentiated counterparts (Janiszewska *et al.* 2012). As metformin targets oxidative phosphorylation by (partially) blocking complex I of the mitochondrial respiratory chain, this might explain why metformin selectively affects BTICs (Kim *et al.* 2016). Gritti *et al.* (2014) explain that the difference in sensitivity to metformin is due to differentiated expression of the ion channel CLIC1. The chloride ion channel is normally stored in the cytosol and is inserted into the plasma membrane during G1 phase preceding transition into S phase. The expression of CLIC1 is higher in BTICs than in TCs. Metformin specifically blocks CLIC1 in its open state, which traps GBM cells in their G1 phase, leading to apoptosis and reduced proliferation rates. Aldea *et al.* (2015) confirm metformin's selective cytotoxicity for cancer stem cells but not for differentiated cells. Würth

et al. (2013) ascribe BTICs' sensitivity to metformin to the fact that Akt inhibition is possible in these cells. On the contrary, Akt is continuously active in TCs thus rendering them resistant to metformin. In summary, BTICs seem more susceptible to metformin due to their reliance on OXPHOS, their high expression of CLIC1 and discontinuous Akt activation.

Strikingly, differentiation of BTICs to TCs through the use of a different medium (DMEM + 10% FCS instead of RHB-A + EGF + FGF) changed sensitivity to metformin. While proneural cells became less sensitive to 10 mM metformin after being differentiated in DMEM and FCS, mesenchymal cells became markedly more sensitive to 10 mM metformin. The seeming resistance to metformin of slowly proliferating proneural TCs was most likely due to a short observation interval.

Concerning mesenchymal cell lines, glucose content of different media might account for the increase in sensitivity towards metformin upon differentiation. Analysis of glucose content of RHB-A in the lab group revealed that it contains 30 mM glucose while DMEM contains 5.6 mM. Sato *et al.* (2012) found that the sensitivity to metformin depends on the availability of glucose. In their experiments they showed that lower concentrations of glucose (17.5 mM instead of 26 mM) help metformin activate AMPK and FOXO3 more effectively. Thus, metformin's anti-proliferative effects may have been stronger in mesenchymal TCs, because they were kept in 5.6 mM glucose instead of 30 mM. Except for Würth *et al.* (2013), all researchers examining the effects of metformin on glioma used DMEM supplemented with 5-10% FCS as media (see Table 2). According to our laboratory standards, DMEM and 10% FCS is used as differentiating media, while serum-free and growth factor supplemented RHB-A is used to maintain stem cell properties. Therefore, only the results of Würth *at al.* (2013) describe metformin's effects on BTICs, while all other results would be describing effects on TCs. Examening media and cell lines when comparing results is important, because as shown for our cell lines, media may considerably change responses to different treatments. This is also true for tumor environment *in vivo*. As the tumor environment plays a very important role, cell media should imitate these conditions as realistically as possible. For future experiments with metformin or any other drug influencing tumor metabolism, careful attention should be paid to the selection of cell media, their glucose contents and supplements. Identical glucose concentrations should be used for BTICs and TCs to attain comparable results. Preferably, these concentrations should be low to better reflect *in vivo* conditions where glucose levels are at 0-3 mM in tumor tissue and 2-5 mM in healthy brain tissue (Markus *et al.* 2010). To maintain consistently low glucose concentrations without glucose depletion, a Nutrostat setup may be advisable (Birsoy *et al.* 2014). Fresh media with respective glucose concentration is added at the same rate as old media is removed without

cell loss (Birsoy *et al.* 2014). Nutrient concentrations in removed media may be measured to determine, among others, the rate of conversion of glucose into lactate (Birsoy *et al.* 2014).

This study shows for the first time that low doses of metformin are able to lower proliferation of proneural BTICs. These concentrations may actually be achievable in brain tissues of GBM patients. Potential markers to predict susceptibility to metformin treatment may be *p53* and *pten* mutational status and proneural subtype. This study confirms the anti-proliferative and anti-migratory effects of 10 mM metformin on almost all GBM cell lines examined and shows that differences in reaction patterns may be predicted based on subtype. Proneural BTICs examined in this study appear sensitive to metformin while mesenchymal cells and TCs might be less sensitive. Investigation of further cell lines is needed to prove whether proneural subtype is a valid predictor for GBM's sensitivity to metformin. Then, metformin may present a drug to specifically target chemotherapy-resistant proneural cells as well as a drug that specifically targets BTICs, the cell subpopulation responsible for rapid tumor recurrence of GBM. However, further characterization of protein expression (CLIC1), signaling pathways (constitutive Akt activity), mutational background (*p53*, *pten*) and metabolic properties (reliance on oxidative phosphorylation) in used cell lines is needed to link functional results to molecular characteristics and identify reliable markers for sensitivity to metformin in patient treatment.

6.2 The role of TGF-β_2 in GBM

The cytokine TGF-β_2 has been found to exert multiple effects on GBM, namely induction of proliferation, migration and invasion, angiogenesis and immunosuppression (Platten *et al.* 2001, Hau *et al.* 2006, Joseph *et al.* 2014). As TGF-β_2 may act as a tumor promoter or inhibitor depending on tissue context, previous findings related to proliferation have been ambiguous (see Table 23) indicating an increase in proliferation in 22%, a decrease in 37% and no effects in 41% of the cases. Thus, the effects of TGF-β_2 on proliferation seem difficult to predict. This study aimed at elucidating GBM's migratory and proliferative response to TGF-β_2. TGF-β_2 was used as it seems to be the most important isoform in glioma (Bruna *et al.* 2007, Aigner and Bogdahn 2008, Hau *et al.* 2011, Frei *et al.* 2015). More specifically, TGF-β_2 and SD-208, a TGFR-I inhibitor, were used according to prior laboratory experience and pertinent literature (Uhl *et al.* 2004, Seliger and Meyer *et al.* 2016). As SD-208 was dissolved in DMSO, respective DMSO controls were used to calculate significance.

Summarizing all data, TGF-β_2 decreased proliferation by 15% ($p < 0.02$) compared to medium controls and SD-208 increased proliferation by 20% compared to DMSO controls ($p < 0.005$). TGF-β_2 also decreased migration by 10% after 20 hs and by 16% after 48 hs

($p < 0.0002$), but SD-208 treatment yielded no effect. Examined in more detail, TGF-β_2 inhibited proliferation in 2 / 10 cases. It reduced migration in 6 / 10 cases, in all three mesenchymal BTIC lines, in two mesenchymal TC lines and in one proneural TC line. Lastly, TGF-β_2 increased migration in 1 / 10 cases, RAV19 TC. Its antagonist SD-208 increased proliferation in 2 / 10 cases, one proneural and one mesenchymal TC line, and migration in 3 / 10 cases, one proneural and two mesenchymal TC lines, while it reduced migration in 2 / 10 cases, one mesenchymal BTIC line and one proneural TC line. Of the seven cases where SD-208 showed an effect, four showed an opposite effect to TGF-β_2, two cases exhibited no TGF-β_2 effect and in one case the combination of SD-208 and TGF-β_2 yielded the strongest migration inhibition (RAV27 BTIC).

Comparing these results to pertinent literature reveals that they match only to a certain extent. Table 23 summarizes research on TGF-β_2's effects on GBM cell proliferation.

Table 23: The effects of TGF-β on proliferation of different glioma cells

Study	**Human glioma cell lines**	**Medium & Treatment**	**Prol. ↑**	**Prol. ↓**	**Prol. =**
Rich *et al.* 1999	U87, T98G, U373, D54, U251, D259, D270, D409, D423, D538, D566, D645	Improved zinc option medium + 10% FCS TGF-β_1 + TGF-β_2	2 / 12	6 / 12	4 / 12
Piek *et al.* 1999	U-178 MG, U-343 MG, U-343 MGa 31L, U-343 MGa 35L, U-251 MGAgCl1, U-1242 MG	DMEM + 5 % FCS + 5% NCS TGF-β_1	2 / 6	2 / 6	2 / 6
Bruna *et al.* 2007	U87MG, U373MG, A172, T98G, hs683, U251, C3, C4, C52	DMEM + 10% FCS TGF-β	4 / 10	2 / 10	4 / 10
Beier *et al.* 2012	R8, 11, 18, 28, 44, 49, 53, 54, 58; GS01, 04, 05, 07	DMEM-F12 + 20 ng/mL EGF + bFGF + LIF + B27 TGF-β_1 + TGF-β_2	1 / 13	5 / 13	7 / 13

Abbreviations: Prol. = proliferation; FCS = fetal calf serum; TGF-β = transforming growth factor beta; DMEM = Dulbecco's modified Eagle's medium; NCS = newborn calf serum; EGF = epidermal growth factor; bFGF = basic fibroblast growth factor; LIF = leukemia inhibitory factor

Firstly, prior research has shown that proliferation increases in 20% of the cases, but in this study, no single case showed increased proliferation after treatment with TGF-β_2. While a

proliferation decrease was observed in 20% of the cases in this study, it was reported in 37% of all cases in pertinent literature. With only 10 cell lines examined in this study and 41 in the literature reviewed, data on GBM's proliferative response to TGF-β_2 is still scarce, challenging the significance of a 17% deviation. However, this study noted no proliferation increase due to TGF-β_2 at all, which challenges that TGF-β_2 acts as a tumor promoter by increasing proliferation.

Secondly, migration data seems to deviate as well. In this study, a migration decrease was seen in 60% of the cases and an increase in 10%, while pertinent literature mostly elaborates on TGF-β_2's pro-invasive stimuli (Wild-Bode *et al.* 2001, Baumann and Leukel *et al.* 2009, Seliger *et al.* 2013, Joseph *et al.* 2014, Iwadate 2016, Iwadate *et al.* 2016). Thus, TGF-β_2's effects remain heterogeneous. This study shows that if TGF-β_2 has an effect at all, it is more likely to be anti-proliferative and anti-migratory. Bruna *et al.* (2007) argue that TGF-β induces proliferation in glioma cells with an unmethylated *pdfg-b* gene. Consequent gene expression increases proliferation. Here, further investigating *pdfg-b* methylation status to determine whether used GBM cell lines only exhibited methylated *pdfg-b* genes and whether the hypothesis of Bruna *et al.* (2007) is applicable would be worthwhile.

Generally, mesenchymal cell lines were more sensitive to TGF-β_2's influence because all cell lines in which proliferation was inhibited and 5 / 6 of the cases of migration inhibition concerned mesenchymal cell lines. Interestingly, endogenous TGF-β_2 levels in mesenchymal BTICs were already between 2.5 and 40 times higher than in proneural BTICs (see Table 8). TGF-β_2 signaling seems to be more important in mesenchymal cells than in proneural cells. Additionally, differences in susceptibility to TGF-β_2 may be due to different receptor setups in proneural and mesenchymal cell lines. On the one hand, Beier *et al.* (2012) showed that proneural cells possess deficient TGF-β receptors type II. As TGF-β_2 normally binds to the TGFR-II before it can associate with TGFR-I and activate the Smad-signaling cascade (Aigner and Bogdahn 2008), TGF-β_2 signaling is impaired in proneural cells. Conversely, Jun *et al.* (2016) report that TGF-β signaling is enhanced in mesenchymal cell lines. Mesenchymal cells are characterized by high CD44 expression. In these cells, epithelial membrane protein 3 (EMP3) interacts with the TGF-β receptor type II and thus enhances TGF-β_2 signaling. Differences in sensitivity may be caused by higher endogenous TGF-β_2 levels, and enhanced EMP3-mediated TGF-β signaling in mesenchymal cell lines as well as TGFR-II deficiency of proneural cell lines.

However, TGFR-II deficiency does not mean that proneural GBM cells do not use TGF-β as a tumor promoter. Proneural cells profit from TGF-β as an immunosuppressor. In vivo, proneural tumor sites exhibit less immune infiltration through $CD8^+$ T- and NK-cells than mesenchymal tumor sites (Beier *et al.* 2012). Apparently, proneural cells inhibit NK2D

expression on $CD8^+$ T- and NK-cells through TGF-β signaling thus escaping immune surveillance even more effectively than mesenchymal cells (Beier *et al.* 2012). Because of this, the results of this study should be viewed with caution. Even though TGF-β_2 exhibited far less tumorigenic characteristics than expected, it is by no means a general tumor suppressor in GBM. TGF-β's abilities to suppress the immune response and induce angiogenesis remain important hallmarks *in vivo*.

In the majority of cases, TGF-β_2 and SD-208 exerted independent or opposite effects. In 4 / 20 cases, TGF-β_2 exerted an anti-migratory effect, but these effects were no longer observed when TGF-β_2 and SD-208 treatments were combined. In 2 / 20 cases, only SD-208 exerted an effect, and in migration assays, this was not present for combined treatment. In 4 / 20 cases, one case regarding proliferation and 3 cases regarding migration, effects were observed for both agents. The effects on migration of combined treatment canceled out in 1 / 3 cases, or the effects of SD-208 remained in 2 / 3 cases. In RAV27 BTIC, both TGF-β_2 and SD-208, reduced migration and the effect became more pronounced for combined treatment (see Table 22). TGF-β_2 and SD-208 acted as functional antagonists as described by Uhl *et al.* (2004), but in two cases the effects of SD-208 remained more pronounced when treatment was combined, and in RAV27 BTIC, effects of both agents were anti-migratory. As the experiments with RAV27 BTIC were the first performed for this study, the role of DMSO was not clear and no DMSO controls were performed for migration assays. Consequently, migration under SD-208 was compared to medium controls. Possibly, the anti-migratory effect observed under SD-208 treatment was due to an anti-migratory influence of DMSO. In conclusion, the results obtained for RAV27 BTIC's migration should be viewed with caution.

Apart from RAV27's data, the data obtained for RAV19 TCs seems contradictory. It was the only cell line in which migration was increased by TGF-β_2 and fittingly, SD-208 decreased migration. However, SD-208 also seemingly increased proliferation. Here, the results from the proliferation assay should be interpreted with extreme caution. Unfortunately, only three instead of the standard six replicates were carried out for DMSO controls, and they all showed a strong proliferation decrease. The values obtained for SD-208 in six replicates showed great deviations (values between 0.76 and 2.55). While migration data seems reliable due to many replicates (12) and small standard deviations (view Figure 35), proliferation data might not be reliable, because RAV19 TC proliferated slowly and data obtained in cell counts might not sufficiently support any statement about their proliferation behavior under TGF-β_2 stimulation. A longer observation period is needed to evaluate slow proliferating cell lines' responses to treatment. As migration data seems reliable, however, the question remains why RAV19 TC was the only cell line in which TGF-β_2 increased migration. *pdfg-b* methylation status would be of interest to define whether this marker could

reliably predict proliferation increase caused by TGF-β_2. In most cases the effects of TGF-β_2 and SD-208 were the opposite of expected. Cases of contradictory data with an insufficient number of DMSO controls performed further underline the need to pay attention to media and components that might lead to bias. Lastly, the example of migration increase in RAV19 TC indicates that responses to TGF-β_2 remain heterogeneous and not fully predictable.

With the exception of RAV27 BTIC, all effects of SD-208 were observed in TCs, not in BTICs. This might have been due to different media used for BTICs and TCs. TGF-β_2 ELISAs performed in the laboratory group revealed that RHB-A contains 0.02 ng/ml TGF-β_2 while DMEM + 10% FCS contains 0.23 ng/ml. Different concentrations of TGF-β_2 in the media may affect how TGF-β_2 and SD-208 influence proliferation and migration. When media contain high levels of TGF-β_2, adding more might be cytotoxic or SD-208 might exert vast effects. TCs cultured in DMEM +10 % FCS were exposed to TGF-β_2 concentrations 10 times higher than those for BTICs in RHB-A. This could explain why SD-208 exerted vast effects on TCs but not on BTICs and why TGF-β_2 had cytotoxic effects on all mesenchymal TCs when effects on mesenchymal BTICs were mainly anti-migratory. Another hypothesis would be that mesenchymal TCs were more fragile, because 10 mM metformin was also cytotoxic for them.

Evidence suggesting that RHB-A media might enhance TGF-β_2 signaling comes from that EGF concentrations and glucose content of media may influence TGF-β_2 signaling. RHB-A media were supplemented with 20 ng/ml EGF. As Aigner and Bogdahn (2008) point out, EGF-signaling converges on Smad-signaling via MAPK. Maybe, Smad-signaling was activated by EGF independently of TGFR interactions. As SD-208 acts on TGFR-I but not on Smad-signaling, it may have been unable to counteract this TGFR-independent activation. This might account for the fact that in 9 / 10 cases, SD-208 treatment did not change proliferation nor migration of BTICs. However, RHB-A contained six times more glucose than DMEM. Gu *et al.* (2014) describe a linear correlation between media glucose content and TGF-β production by renal epithelial cells: the higher the glucose content the higher the TGF-β levels. If GBM followed the same pattern, then RHB-A would have led to increased autocrine TGF-β_2 production. Yet, as TGF-β_2 concentrations of serum-containing DMEM were already 10 times higher than those of RHB-A, a possible increase of autocrine TGF-β_2 production of BTICs was probably less pronounced and not influencing results as much as different TGF-β_2 contents of the culture media. Therefore, future experiments need to be conducted with identical media for both BTICs and TCs to exclude bias due to different TGF-β_2 levels in culture media, bias due to TGFR-independent Smad-activation through EGF and bias due to different glucose contents.

Recapitulating the findings of this study, TGF-β_2's effects were far more anti-proliferative and anti-migratory than previously expected (8 / 9 cases in which an effect was observed). Fittingly, in many cases, SD-208 proved to induce proliferation and migration especially in TCs (5 / 7 cases). Interestingly, mesenchymal cell lines were more sensitive to TGF-β_2 while proneural cell lines were almost resistant. This might be attributed to TGFR-II deficiency in proneural cell lines and the expression of EMP3 in mesenchymal cell lines. Overall, the role of TGF-β_2 remains ambiguous. On the one hand, TGF-β_2 levels in brain tumors seem lower than expected and are subject to a high degree of inter-individual variation (Riemenschneider *et al.* 2015). On the other hand, this *in vitro* study only examined two GBM properties influenced by TGF-β_2, proliferation and migration. *In vivo*, TGF-β_2 also induces angiogenesis and suppresses the immune response (Friese *et al.* 2004, Hau *et al.* 2006, Aigner and Bogdahn 2008, Crane *et al.* 2010, Beier *et al.* 2012). Therefore, TGF-β_2 should not be considered a tumor suppressor in GBM. However, TGF-β_2 seems to promote proliferation and migration of GBM cells to a lesser extent than previously expected.

6.3 Possible links between metformin and TGF-β_2 in GBM

Previous research has described TGF-β_2's ability to increase proliferation and migration of GBM cells (Rich *et al.* 1999, Piek *et al.* 1999, Wild-Bode *et al.* 2001, Bruna *et al.* 2007, Baumann *et al.* 2009, Beier *et al.* 2012, Seliger *et al.* 2013, Iwadate 2016) and it has been suggested that metformin lowers both (Beckner *et al.* 2005, Isakovic *et al.* 2007, Sato *et al.* 2012, Ferla *et al.* 2012, Würth *et al.* 2013, Gao *et al.* 2013, Liu *et al.* 2014, Sesen *et al.* 2015, Kim *et al.* 2016). This study addressed the question of whether metformin exerts opposite effects compared to TGF-β_2 and whether TGF-β_2's effects can be attenuated through metformin use. To determine whether the effects of two or more treatments are synergistic, additive or antagonistic, a combination index (CI) needs to be calculated according to the method of Chou-Talalay (Chou 2010). The Chou-Talalay combination index is calculated with a formula based on the mass-action law principle. However, results of equimolar concentrations of the drugs themselves and their combination are needed (Chou 2010). Unfortunately, respective data did not exist for this study. Chou (2010) explains, that neither the arithmetic sum nor P values may accurately define synergistic, additive or antagonistic effects. Hence, this study avoids these terms.

Overall, relationships between TGF-β and metformin may be functional, but signaling pathways may also be interconnected. As mentioned in chapter 3.4., possible links between TGF-β and metformin include:

1. functionally opposed effects such as proliferation increase or decrease

2. metformin directly influencing core signaling pathways of TGF-β, especially Smad-signaling
3. TGF-β directly influencing core signaling pathways of metformin, namely inhibition of complex I of the mitochondrial respiratory chain and subsequent AMPK activation and mTOR inhibition or Akt activation and mTOR inhibition
4. metformin changing the tumor environment in a way that TGF-β signaling is impacted
5. metformin and TGF-β converging on the same signaling pathways.

As this study examined the functional effects of metformin and TGF-β_2, the first possible link will be addressed in detail before literature on the latter four possible links will be discussed to give an outlook for future experiments.

The combination of 10 mM metformin and 10 ng/ml TGF-β_2 reduced proliferation in 9 / 10 cases and migration in 10 / 10 cases. Compared to treatment with single agents, the following scenarios were observed:

1. the combined treatment reduced proliferation to a greater extent than each of the single agents: 5 / 10

2. the combined treatment reduced migration to a greater extent than the single agents: 3 / 10

3. the combined treatment reduced migration to a lesser extent than the single agents: 1 / 10

4. the combined treatment had no greater influence on proliferation than metformin by itself: 4 / 10

5. the combined treatment had no greater influence on migration than metformin by itself: 4 / 10

6. the combined treatment had no greater influence on proliferation than TGF-β_2 by itself: 1 / 10.

Hence, metformin and TGF-β_2 exerted similar effects on GBM cells or did not influence their respective effects.

Scenarios 1-3 describe situations in which the combination treatment exerted greater effects than the single agents. Reviewing scenario 1, in three cases, TGF-β_2 did not influence proliferation by itself but it augmented metformin's anti-proliferative action, demonstrating its anti-proliferative potential. In the other two cases, TGF-β_2 had already proven its anti-proliferative power as a single agent, but combined treatment with metformin increased the

effect. In all cases of scenario 2, TGF-β_2 had already demonstrated its anti-migratory power as a single agent, but combined with metformin the effect increased. In only one case (scenario 3) did TGF-β_2 attenuate metformin's anti-migratory capacity: for RAV19 BTIC. Therefore, the first three scenarios show that with only one exception, metformin's and TGF-β_2's effects were not only consistently anti-migratory and anti-proliferative, but also increased when both agents were combined.

Scenarios 4-6 describe those 9 / 20 cases in which proliferation and migration were not altered by combined treatment. In most cases, these effects were due to metformin and did not change when treatment was combined with TGF-β_2. However, in one case, the anti-migratory effects were more likely due to TGF-β_2 (scenario 6). Thus, approximately half of the cases in which treatments of metformin and TGF-β_2 were combined, displayed uniform and enhanced effects of the two agents and the other half exhibited no mutual influence on existing anti-proliferative and anti-migratory actions.

Mesenchymal cells were more susceptible to TGF-β_2, which is why the combination was more effective in lowering proliferation or migration than metformin itself mostly in mesenchymal cells. Contrarily, proneural BTICs and TCs showed virtually no response to TGF-β_2 treatment with the exception of proliferation of RAV57 TC which was reduced by only the combination of metformin and TGF-β_2.

The effects of the combination of 0.01 mM metformin in triple re-treatment and 10 ng/ml TGF-β_2 were only investigated concerning proliferation due to technical reasons. It reduced proliferation in 3 / 10 cases. Compared to treatment with single agents, the following two scenarios were observed:

1. the combined treatment reduced proliferation to a greater extent than each of the single agents: 2 / 10
2. the combined treatment had no greater influence on proliferation than TGF-β_2 by itself: 1 / 10.

Interestingly, this combination affected only mesenchymal cells. Moreover, 0.01 mM metformin in triple re-treatment exerted no effect on any of the three cell lines when given as a single agent. In one case (scenario 2), the anti-proliferative effect was most probably due to TGF-β_2's action. Regarding scenario 1, the cell lines affected were RAV21 BTIC and TC. In one case, TGF-β_2 by itself had already shown an anti-proliferative effect and it was enhanced by the addition of 0.01 mM metformin in triple re-treatment. Yet, in another case, neither of the agents had shown any effect individually, but the combination clearly reduced proliferation. As discussed before, low dose metformin did not affect mesenchymal cells

when given by itself. Interestingly, it was still able to increase TGF-β_2's anti-proliferative effects on RAV21 cells. Apparently, these cells were weakened by TGF-β_2 to an extent that the addition of even low dose metformin could further inhibit their multiplication.

Although there were instances in which the combined treatment of TGF-β_2 and either 10 mM or 0.01 mM x3 metformin reduced proliferation and migration of GBM cells to a greater extent than metformin by itself, TGF-β_2 and metformin treatment should not be combined to treat GBM patients. TGF-β_2 weakenes the immune response and may induce angiogenesis (Friese *et al.* 2004, Hau *et al.* 2006, Aigner and Bogdahn 2008, Crane *et al.* 2010, Beier *et al.* 2012) and thus enhance tumor growth. Unless when treating GBM with oncolytic viruses (Han *et al.* 2015), the immuno-suppressive effect of TGF-β in GBM remains undesired in treatment of GBM.

As TGF-β_2 neither produced pro-proliferative / pro-migratory stimuli by itself nor attenuated metformin's anti-proliferative / anti-migratory effects, the hypothesis that metformin might counteract TGF-β_2's impact on proliferation and migration of GBM is disproved. As a recent publication from our laboratory group (Seliger and Meyer *et al.* 2016) is the only existing literature on possible links between TGF-β_2 and metformin in GBM, putting this study into scientific context is difficult. Direct functional interactions of metformin and TGF-β have only been described for EMT and mammosphere formation in breast cancer tissue (Cufí *et al.* 2010, Vazquez-Martin *et al.* 2010, Oliveras-Ferraros *et al.* 2011) and TGF-β-induced EMT in renal epithelial cells (Lee *et al.* 2013) all of which have found metformin to directly antagonize TGF-β's functional effects. However, results obtained from tissues other than GBM and from the investigation of functional effects other than proliferation and migration seem very difficult to compare to the results of this study, because (as this study demonstrates) TGF-β's effects are highly dependent on context and cell lines. To further explore functional connections between TGF-β_2 and metformin, data should be obtained in a manner that allows for calculations of CI according to Chou-Talalay. This requires at least five data points: two different concentrations of metformin, two different concentrations of TGF-β_2 and one of the combination (Chou 2010). Preferably, more data points should be employed, e.g. using concentrations below and above the EC_{50} (Chou 2010). Thus, the effects of metformin and TGF-β_2 could be accurately described as synergistic or antagonistic.

Apart from effects on proliferation and migration, changes in morphology were also observed (see section 5.4). Metformin, TGF-β_2 and the two combined changed morphology, and some of the changes reflect the results obtained in functional assays. Firstly, RAV19 BTIC is an example of how the effects of metformin and TGF-β_2 may be opposed: While metformin treatment caused changes towards a smaller spherical morphology characteristic of apoptosis (Elmore 2007), TGF-β_2 did not change morphology (see Figure 46). The

combination treatment led to a varied picture with more protrusions than after 10 mM metformin treatment but less than in control wells. The effects seem to attenuate each other. This serves as an example of the opposite effects of metformin and TGF-β_2 emphasizing again that other functional characteristics investigated in this study were consistent. RAV24 BTICs demonstrate the opposite: combined treatment enhanced apoptotic effects of metformin and TGF-β_2 as indicated by very small spherical cells (Elmore 2007) (see Figure 50). This was very much in line with results of cell counts where only combined treatment lowered proliferation (see Figure 47). Judging from the images of RAV19 TCs taken after 120 hs (see Figure 54), metformin and metformin + TGF-β_2 could lower proliferation, an effect not observed in cell counts due to the relatively short 48-h observation period. Morphological changes after metformin treatment indicated cytostatic and cytotoxic effects leading to apoptosis while TGF-β_2 did not alter morphology. The latter underlines that proneural cells seem virtually resistant to TGF-β_2 treatment. Mesenchymal cell lines such as RAV21 TCs, on the contrary, were sensitive to TGF-β_2. Metformin treatment rendered RAV21 TCs fragile and the proliferation decrease caused by all three, metformin and TGF-β_2 individually and their combination, can be made out (see Figure 58). Cell swelling as observed in RAV21 TCs is a sign of necrosis or "oncotic cell death" (Elmore 2007) and could indicate that metformin's and TGF-β_2's effects were cytotoxic. In cell counts, the fraction of dead cells in wells treated with single 10 mM metformin +/- 10 ng/ml TGF-β_2 was not quite significant ($p = 0.09$), but after TGF-β_2 treatment, a significant amount of cells died ($p = 0.024$) underlining the impression of cell images. Cell-free areas were observed in some images of TGF-β_2 treated RAV21 TCs. Their significance remained unknown. Overall, morphological changes were mostly consistent with results from cell counts concerning cytotoxicity and may represent an alternative to assessing cytostatic and cytotoxic effects. Results from this study align with pertinent literature: Isakovic *et al.* (2007) also describe morphological changes induced by 4 mM metformin either to a more spindle-like shape or to a granular shape. Taking into account that Sato *et al.* (2012) found that 1 mM reduces sphere formation and induces differentiation, more spindle-like shapes might represent differentiation while granular shapes represent either apoptosis (smaller cell size) or oncotic cell death (larger cell size) (Elmore 2007). Hence, morphological changes in GBM cells already point to important cell events such as differentiation, apoptosis or oncotic cell death; yet, verifying these events using appropriate differentiation or apoptosis markers is helpful.

Apart from functional effects on proliferation, migration and cell morphology, metformin and TGF-β_2 may also influence each other's signaling pathways or lead to indirect effects which can alter signaling. To understand signaling interactions of metformin and TGF-β_2 in glioma, metformin signaling in GBM has to be scrutinized. Table 24 summarizes current research on metformin's molecular mechanisms on glioma:

Table 24: Proposed mechanisms for metformin's effects on GBM

Study	Cell lines	Proposed mechanisms of metformin
Isakovic *et al.* 2007	C6 (rat)*; U251	• AMPK activation and downstream JNK activation (member of the MAPK family) • in confluent glioma cell cultures: AMPK activation --> permanent mitochondrial depolarization and ROS production --> caspase-dependent apoptosis • in low-density glioma cell cultures: AMPK activation --> temporary mitochondrial depolarization and absence of ROS production --> cell cycle arrest • ROS does not cause mitochondrial depolarization, but might be its consequence. • Pan-caspase inhibitors prevent apoptosis in confluent glioma cell cultures hinting that caspases play a crucial role in apoptosis of glioma cells.
Ferla *et al.* 2012	LN18, LN229	• AMPK activation --> STAT3 downregulation and Akt inhibition
Sato *et al.* 2012	dnf.	• Normally, Akt and ERK phosphorylate FOXO3, thus keeping it inactive. Hence, Akt inhibition results in FOXO3 activation. • AMPK activation --> FOXO3 activation (transcription factor) --> increased gene expression of *p21* --> proliferation reduction • FOXO3 activation --> differentiation of BTICs (reduced stem-cell marker expression of Nestin, Musashi and Bmi1 and increased differentiation marker expression of neural βIII-tubulin and astrocyte GFAP) • FOXO3 activation --> reduction of BTICs' tumorigenic potential after transplantation • lower glucose levels in the culture medium (17.5 mM instead of 26 mM) --> more effective AMPK and FOXO3 activation --> enhanced differentiation of BTICs
Würth *et al.* 2013	GBM1-4	• in BTICs: prevention of EGF-induced activation of Akt --> net inhibition of Akt --> mTOR inhibition --> decreased proliferation • in differentiated cells: continuous activation of Akt --> no mTOR inhibition --> no effect of metformin • No AMPK-activation is observed after treatment with

		metformin, demonstrating that mTOR inhibition results from Akt inhibition and not from AMPK activation, both of which would be possible pathways to mediate mTOR signaling.
Gao *et al.* 2013	U251	• downregulation of fibulin-3 --> downregulation of MMP2 --> lowered migration
Gritti and Würth *et al.* 2014	3 GBM cell lines	• GBM cells express CLIC1, a chloride ion channel, which is normally stored in the cytosol and inserted into the plasma membrane during G1 phase preceding transition into S phase • CLIC1 expression: higher in BTICs than in TCs • specific CLIC1 blockage in its open state when located within the plasma membrane --> GBM cells trapped in G1 phase --> lowered proliferation • dose- and time-dependency --> high-dose and long-term applications of metformin favorable
Liu *et al.* 2014	T98G, A172, U87	• neither ATP-depletion nor AMPK signaling are necessary for metformin's anti-proliferative action • metformin increases PRAS40's association with RAPTOR --> mTOR inhibition --> proliferation reduction
Sesen *et al.* 2015	U87, U251, LN18, SF767	• partial block of complex I of the respiratory chain (12-31%) • AMPK activation or Redd1 / DDIT4 activation --> mTOR inhibition • in *pten* wt cells: Akt inhibition • in *pten* mutated cells: Akt is not affected by metformin • --> AMPK-dependent and AMPK-independent effects
Yu *et al.* 2015	U87, U251	• Akt inhibition • AMPK activation --> mTOR inhibition
Kim *et al.* 2016	TS13-20, TS15-88, TS09-03, GSC11, U87	• no AMPK activation nor mTOR inhibition

* If not otherwise stated, cell lines were derived from humans. Abbreviations: AMPK = AMP-activated kinase; JNK = c-Jun N-terminal kinase; MAPK = Mitogen-activated protein kinase; ROS = Reactive oxygen species; STAT3 = Signal transducer and activator of transcription 3; Akt = refers to a mouse named "Ak", expressing spontaneous lymphomas and "t" thymoma, also Akt = PKB = protein kinase B; ERK = Extracellular signal-regulated kinase = nowadays known as MAPK; FOXO3 = Forkhead box protein O3; p21 = Protein 21; Bmi1 = Polycomb complex protein; BTICs = Brain tumor initiating cells; GFAP = Glial fibrillary acidic protein; EGF = Epidermal growth factor; mTOR = mammalian Target of rapamycin; MMP2 = Matrix metalloproteinase 2;

TCs = Tumor cells (differentiated); CLIC1 = Chloride intracellular channel1; G1 phase = gap phase one; S phase = synthesis phase; ATP = Adenosine triphosphate; PRAS40 = Proline-rich Akt substrate of 40 kDa; RAPTOR = Regulatory-associated protein of mTOR; Redd1 = Regulated in development and DNA damage responses 1; DDIT4 = DNA damage-inducible transcript 4 protein; PTEN = Phosphatase and tensin homolog.

As outlined in Table 24, metformin has a multitude of molecular mechanisms. One of the main axes seems to be via AMPK activation and subsequent mTOR inhibition. In our study (Seliger and Meyer *et al.* 2016), we showed that TGF-β_2 does not activate AMPK nor inhibit mTOR. Therefore, we could demonstrate that TGF-β_2 does not act on metformin's main signaling axis. However, a multitude of other pathways such as Akt, JNK, FOXO3, RAPTOR and CLIC1 remain to be explored to confirm that metformin signaling is not influenced by TGF-β_2.

The question is whether metformin could alter TGF-β_2's main signaling axis which is Smad-mediated. We revealed that metformin neither increases levels of TGF-β_2 mRNA nor protein levels, nor does it alter Smad2-signaling (Seliger and Meyer *et al.* 2016). Thus, no direct influence of metformin on Smad signaling was observed in two GBM cell lines. Also, indirect effects such as an increase in lactate levels due to metformin treatment and a subsequent activation of TGF-β_2 could play a role (Seliger and Leukel *et al.* 2013). These were not observed in the two cell lines utilized in our study (Seliger and Meyer *et al.* 2016). Yet, further research is needed to validate these results for a greater number of cell lines.

Lastly, metformin and TGF-β are part of complex signaling networks which overlap at certain points. Metformin and TGF-β signaling converge on FOXO signaling exerting similar effects: TGF-β-activates Smad signaling and several other factors including FoxO that are able to activate *p21* transcription and thus inhibit proliferation (Moustakas 2005). In GBM, metformin activates AMPK which activates FOXO3 which increases gene expression of *p21* and thus reduces proliferation (Sato *et al.* 2012). Hence, FOXO mediated *p21* induction may represent a common pathway for TGF-β and metformin. Also, TGF-β and metformin resemble each other in their ability to induce apoptosis mediated by either JNK- or Akt. Both converge on JNK, a member of the MAPK family. TGF-β-induced JNK activation can either activate Smad3 signaling or inhibit Smad2 signaling and ultimately lead to apoptosis (Moustakas and Heldin 2005). Metformin, correspondingly, activates JNK in GBM which leads to apoptosis (Isakovic *et al.* 2007). Similar effects are described for Akt: Moustakas and Heldin (2005) state that TGF-β inhibits Akt in a Smad-dependent way, which leads to apoptosis. Metformin also inhibits Akt and induces apoptosis in GBM (Sato *et al.* 2012), so that TGF-β and metformin show similar capabilities to induce apoptosis. Contrary effects of TGF-β and metformin are observed concerning Sox expression. TGF-β alters transcription of *sex determining region Y-box 4* (*Sox4*) in the nucleus of GBM cells which increases expression of Sox2 and helps BTICs retain their stemness and their self-renewing capacities (Ikushima *et al.* 2009). Metformin, however, may upregulate microRNA30a in prostate cancer cells,

which decreases Sox4 and thus inhibits proliferation and EMT (Zhang *et al.* 2014). In GBM, a combination of 2-desoxy-glucose and metformin consistently reduces Sox2 expression (Kim *et al.* 2016), showing that TGF-β and metformin act as direct signaling antagonists on Sox2 expression. The pathways outlined above indicate possible intersections of metformin and TGF-β signaling. However, most results regarding the molecular mechanisms of TGF-β do not originate from the examination of GBM tissue. As the effects of TGF-β are highly context- and cell line-dependent and as cancerous tissues exhibit great heterogeneity concerning genetic and metabolic characteristics, these possible intersections of metformin's and TGF-β_2's signaling networks need to be investigated for GBM to allow for legitimate conclusions.

6.4 Outlook

Culture media are *in vitro* imitations of the tumor environment. Methodically, this study showed that culture media have to be chosen very carefully. As the tumor environment strongly influences GBM's metabolism and its hallmarks of cancer, the culture media need to realistically reflect conditions from tumor environment *in vivo* or at least be controlled for any substance influencing results. Thus, for studies investigating metformin and TGF-β_2, glucose content, lactate content, pH, TGF-β_2 content, autocrine TGF-β_2 secretion, EGF levels, or any other substance influencing metabolisms or TGF-β_2 signaling need to be identical to make results of different cell lines comparable and also need to be as realistic as possible to reflect *in vivo* conditions. Also, any future study investigating the effects of two substances in terms of possible synergism or antagonism should be planned to yield data sets applicable for the Chou-Talalay method to calculate the CI. Any study further exploring the interactions of metformin and TGF-β_2 on a molecular level should use signaling networks established in other tumor models as an example to test for interactions in GBM. Hence, exploration of signaling pathways of Akt and JNK, FOXO3 and *p21* expression, RAPTOR, and Sox2 expression could prove valuable.

To establish ties between fundamental research and clinical applications of metformin in cancer treatment, several steps are needed. Firstly, the functional results obtained in this study should be linked to molecular and genetic properties of GBM cells. To further understand the exact mechanisms of metformin's and TGF-β_2's action, results from other laboratory groups should be validated including but not limited to differential investigation of respiratory chain inhibition, apoptosis markers, CLIC1 expression, Redd1 / DDIT4 expression, to determine if certain mechanisms apply to certain subgroups of cells and may eventually be used as markers for susceptibility. Also, proposed susceptibility markers for metformin such as reliance on OXPHOS, or *p53* and *pten* mutations need to be linked to

functional results of this study. Similarly, markers of susceptibility to TGF-β_2, such as TGFR-II deficiency of proneural cells and EMP3 expression of mesenchymal cells, should be tested. The establishment of reliable markers will help to stratify GBM patients according to their potential benefit from metformin treatment. Also, reliable markers set the rationale for more aggressive metformin administration in patients with susceptible GBM subtypes. This more aggressive treatment may use higher oral doses of metformin, alternative application routes (e.g. intraperitoneal), alternative medication such as phenformin, combinations such as metformin and 2DG or even different approaches yet to be discovered. Thus, further fundamental and clinical research is needed to improve treatment of GBM patients and improve their progression-free and overall survival.

7 LITERATURE

Adamson, Cory; Kanu, Okezie O.; Mehta, Ankit I.; Di, Chunhui; Lin, Ningjing; Mattox, Austin K.; Bigner, Darell D. (2009): GBM multiforme: a review of where we have been and where we are going. In *Expert opinion on investigational drugs* 18 (8), pp. 1061–1083. DOI: 10.1517/13543780903052764.

Adeberg, Sebastian; Bernhardt, Denise; Ben Harrabi, Semi; Bostel, Tilman; Mohr, Angela; Koelsche, Christian *et al.* (2015): Metformin influences progression in diabetic GBM patients. In *Strahlentherapie und Onkologie : Organ der Deutschen Rontgengesellschaft … [et al]* 191 (12), pp. 928–935. DOI: 10.1007/s00066-015-0884-5.

Aigner, Ludwig; Bogdahn, Ulrich (2008): TGF-beta in neural stem cells and in tumors of the central nervous system. In *Cell and tissue research* 331 (1), pp. 225–241. DOI: 10.1007/s00441-007-0466-7.

Aldea, Mihaela D.; Petrushev, Bobe; Soritau, Olga; Tomuleasa, Ciprian I.; Berindan-Neagoe, Ioana; Filip, Adriana G. *et al.* (2014): Metformin plus sorafenib highly impacts temozolomide resistant GBM stem-like cells. In *Journal of B.U.ON. : official journal of the Balkan Union of Oncology* 19 (2), pp. 502–511.

Baumann, Fusun; Leukel, Petra; Doerfelt, Anett; Beier, Christoph P.; Dettmer, Katja; Oefner, Peter J. *et al.* (2009): Lactate promotes glioma migration by TGF-beta2-dependent regulation of matrix metalloproteinase-2. In *Neuro-oncology* 11 (4), pp. 368–380. DOI: 10.1215/15228517-2008-106.

Beckner, Marie E.; Gobbel, Glenn T.; Abounader, Roger; Burovic, Fatima; Agostino, Naomi R.; Laterra, John; Pollack, Ian F. (2005): Glycolytic glioma cells with active glycogen synthase are sensitive to PTEN and inhibitors of PI3K and gluconeogenesis. In *Laboratory investigation; a journal of technical methods and pathology* 85 (12), pp. 1457–1470. DOI: 10.1038/labinvest.3700355.

Beier, Christoph P.; Kumar, Praveen; Meyer, Katharina; Leukel, Petra; Bruttel, Valentin; Aschenbrenner, Ines *et al.* (2012): The cancer stem cell subtype determines immune infiltration of GBM. In *Stem cells and development* 21 (15), pp. 2753–2761. DOI: 10.1089/scd.2011.0660.

Beier, Dagmar; Schulz, Joerg B.; Beier, Christoph P. (2011): Chemoresistance of GBM cancer stem cells--much more complex than expected. In *Molecular cancer* 10, p. 128. DOI: 10.1186/1476-4598-10-128.

Bhat, Krishna P. L.; Balasubramaniyan, Veerakumar; Vaillant, Brian; Ezhilarasan, Ravesanker; Hummelink, Karlijn; Hollingsworth, Faith *et al.* (2013): Mesenchymal differentiation mediated by NF-kappaB promotes radiation resistance in glioblastoma. In *Cancer cell* 24 (3), pp. 331–346. DOI: 10.1016/j.ccr.2013.08.001.

Birsoy, Kivanc; Possemato, Richard; Lorbeer, Franziska K.; Bayraktar, Erol C.; Thiru, Prathapan; Yucel, Burcu *et al.* (2014): Metabolic determinants of cancer cell sensitivity to glucose limitation and biguanides. In *Nature* 508 (7494), pp. 108–112. DOI: 10.1038/nature13110.

Bodmer, S.; Strommer, K.; Frei, K.; Siepl, C.; Tribolet, N. de; Heid, I.; Fontana, A. (1989): Immunosuppression and transforming growth factor-beta in GBM. Preferential production of transforming growth factor-beta 2. In *Journal of immunology (Baltimore, Md. : 1950)* 143 (10), pp. 3222–3229.

Bogdahn, U.; Hau, P.; Stockhammer, G.; Venkataramana, N. K.; Mahapatra, A. K.; Suri, A. *et al.* (2011): Targeted therapy for high-grade glioma with the TGF-beta2 inhibitor trabedersen: results of a randomized and controlled phase IIb study. In *Neuro-oncology* 13 (1), pp. 132–142. DOI: 10.1093/neuonc/noq142.

Bruna, Alejandra; Darken, Rachel S.; Rojo, Federico; Ocana, Alberto; Penuelas, Silvia; Arias, Alexandra *et al.* (2007): High TGFbeta-Smad activity confers poor prognosis in glioma patients and promotes cell proliferation depending on the methylation of the PDGF-B gene. In *Cancer cell* 11 (2), pp. 147–160. DOI: 10.1016/j.ccr.2006.11.023.

Bundesärztekammer (BÄK), Kassenärztliche Bundesvereinigung (KBV), Arbeitsgemeinschaft der Wis: tionale VersorgungsLeitlinie Therapie des Typ - 2 - Diabetes – Nationale Versorgungsleitlinie Therapie des Typ-2-Diabetis - Langfassung. 1. Auflage. Version 4. 2013, zuletzt egändert November 2014. DOI: 10.6101/AZQ/000213.

Buzzai, Monica; Jones, Russell G.; Amaravadi, Ravi K.; Lum, Julian J.; DeBerardinis, Ralph J.; Zhao, Fangping *et al.* (2007): Systemic treatment with the antidiabetic drug metformin selectively impairs p53-deficient tumor cell growth. In *Cancer research* 67 (14), pp. 6745–6752. DOI: 10.1158/0008-5472.CAN-06-4447.

Chen, Ruihuan; Nishimura, Merry C.; Bumbaca, Stephanie M.; Kharbanda, Samir; Forrest, William F.; Kasman, Ian M. *et al.* (2010): A hierarchy of self-renewing tumor-initiating cell types in GBM. In *Cancer cell* 17 (4), pp. 362–375. DOI: 10.1016/j.ccr.2009.12.049.

Chiorean, Roxana; Berindan-Neagoe, Ioana; Braicu, Cornelia; Florian, Ioan Stefan; Leucuta, Daniel; Crisan, Doinita; Cernea, Valentin (2014): Quantitative expression of serum biomarkers involved in angiogenesis and inflammation, in patients with GBM multiforme: correlations with clinical data. In *Cancer biomarkers : section A of Disease markers* 14 (2-3), pp. 185–194. DOI: 10.3233/CBM-130310.

Chou, Ting-Chao (2010): Drug combination studies and their synergy quantification using the Chou-Talalay method. In *Cancer research* 70 (2), pp. 440–446. DOI: 10.1158/0008-5472.CAN-09-1947.

Cobbs, Charles S. (2011): Evolving evidence implicates cytomegalovirus as a promoter of malignant glioma pathogenesis. In *Herpesviridae* 2 (1), p. 10. DOI: 10.1186/2042-4280-2-10.

Crane, Courtney A.; Han, Seunggu J.; Barry, Jeffery J.; Ahn, Brian J.; Lanier, Lewis L.; Parsa, Andrew T. (2010): TGF-beta downregulates the activating receptor NKG2D on NK cells and CD8+ T cells in glioma patients. In *Neuro-oncology* 12 (1), pp. 7–13. DOI: 10.1093/neuonc/nop009.

Cufi, Silvia; Vazquez-Martin, Alejandro; Oliveras-Ferraros, Cristina; Martin-Castillo, Begona; Joven, Jorge; Menendez, Javier A. (2010): Metformin against TGFbeta-induced epithelial-to-mesenchymal transition (EMT): from cancer stem cells to aging-associated fibrosis. In *Cell cycle (Georgetown, Tex.)* 9 (22), pp. 4461–4468. DOI: 10.4161/cc.9.22.14048.

DeBerardinis, Ralph J.; Mancuso, Anthony; Daikhin, Evgueni; Nissim, Ilana; Yudkoff, Marc; Wehrli, Suzanne; Thompson, Craig B. (2007): Beyond aerobic glycolysis: transformed cells can engage in glutamine metabolism that exceeds the requirement for protein and nucleotide synthesis. In *Proceedings of the National Academy of Sciences of the United States of America* 104 (49), pp. 19345–19350. DOI: 10.1073/pnas.0709747104.

Den, Robert B.; Kamrava, Mitchell; Sheng, Zhi; Werner-Wasik, Maria; Dougherty, Erin; Marinucchi, Michelle *et al.* (2013): A phase I study of the combination of sorafenib with temozolomide and radiation therapy for the treatment of primary and recurrent high-grade gliomas. In *International journal of radiation oncology, biology, physics* 85 (2), pp. 321–328. DOI: 10.1016/j.ijrobp.2012.04.017.

Dong, Chengyuan; Mi, Ruifang; Jin, Guishan; Zhou, Yiqiang; Zhang, Jin; Liu, Fusheng (2015): Identification of the proliferative effect of Smad2 and 3 in the TGF beta2/Smad signaling pathway using RNA interference in a glioma cell line. In *Molecular medicine reports* 12 (2), pp. 1824–1828. DOI: 10.3892/mmr.2015.3614.

Dubrow, Robert; Darefsky, Amy S. (2011): Demographic variation in incidence of adult glioma by subtype, United States, 1992-2007. In *BMC cancer* 11, p. 325. DOI: 10.1186/1471-2407-11-325.

Elmaci, Ilhan; Altinoz, Meric A. (2016): A Metabolic Inhibitory Cocktail for Grave Cancers: Metformin, Pioglitazone and Lithium Combination in Treatment of Pancreatic Cancer and GBM Multiforme. In *Biochemical genetics* 54 (5), pp. 573–618. DOI: 10.1007/s10528-016-9754-9.

Elmore, Susan (2007): Apoptosis: a review of programmed cell death. In *Toxicologic pathology* 35 (4), pp. 495–516. DOI: 10.1080/01926230701320337.

Esparza, Rogelio; Azad, Tej D.; Feroze, Abdullah H.; Mitra, Siddhartha S.; Cheshier, Samuel H. (2015): GBM stem cells and stem cell-targeting immunotherapies. In *Journal of neuro-oncology. DOI:* 10.1007/s11060-015-1729-x.

Evans, Josie M M; Donnelly, Louise A.; Emslie-Smith, Alistair M.; Alessi, Dario R.; Morris, Andrew D. (2005): Metformin and reduced risk of cancer in diabetic patients. In *BMJ (Clinical research ed.)* 330 (7503), pp. 1304–1305. DOI: 10.1136/bmj.38415.708634.F7.

Ferla, Rita; Haspinger, Eva; Surmacz, Eva (2012): Metformin inhibits leptin-induced growth and migration of GBM cells. In *Oncology letters* 4 (5), pp. 1077–1081. DOI: 10.3892/ol.2012.843.

Forsyth, P. A.; Posner, J. B. (1993): Headaches in patients with brain tumors: a study of 111 patients. In *Neurology* 43 (9), pp. 1678–1683.

Francis, Joshua M.; Zhang, Cheng-Zhong; Maire, Cecile L.; Jung, Joonil; Manzo, Veronica E.; Adalsteinsson, Viktor A. *et al.* (2014): EGFR variant heterogeneity in glioblastoma resolved through single-nucleus sequencing. In *Cancer discovery* 4 (8), pp. 956–971. DOI: 10.1158/2159-8290.CD-13-0879.

Frei, Karl; Gramatzki, Dorothee; Tritschler, Isabel; Schroeder, Judith Johanna; Espinoza, Larisa; Rushing, Elisabeth Jane; Weller, Michael (2015): Transforming growth factor-beta pathway activity in GBM. In *Oncotarget* 6 (8), pp. 5963–5977. DOI: 10.18632/oncotarget.3467.

Friese, Manuel A.; Wischhusen, Jorg; Wick, Wolfgang; Weiler, Markus; Eisele, Gunter; Steinle, Alexander; Weller, Michael (2004): RNA interference targeting transforming growth factor-beta enhances NKG2D-mediated antiglioma immune response, inhibits glioma cell migration and invasiveness, and abrogates tumorigenicity in vivo. In *Cancer research* 64 (20), pp. 7596–7603. DOI: 10.1158/0008-5472.CAN-04-1627.

Furnari, Frank B.; Cloughesy, Timothy F.; Cavenee, Webster K.; Mischel, Paul S. (2015): Heterogeneity of epidermal growth factor receptor signalling networks in glioblastoma. In *Nature reviews. Cancer* 15 (5), pp. 302–310. DOI: 10.1038/nrc3918.

Galli, Rossella; Binda, Elena; Orfanelli, Ugo; Cipelletti, Barbara; Gritti, Angela; Vitis, Simona de *et al.* (2004): Isolation and characterization of tumorigenic, stem-like neural precursors from human GBM. In *Cancer research* 64 (19), pp. 7011–7021. DOI: 10.1158/0008-5472.CAN-04-1364.

Gallo-Oller, Gabriel; Vollmann-Zwerenz, Arabel; Melendez, Barbara; Rey, Juan A.; Hau, Peter; Dotor, Javier; Castresana, Javier S. (2016): P144, a Transforming Growth Factor beta inhibitor peptide, generates antitumoral effects and modifies SMAD7 and SKI levels in human glioblastoma cell lines. In *Cancer letters* 381 (1), pp. 67–75. DOI: 10.1016/j.canlet.2016.07.029.

Gao, Lian-Bo; Tian, Shen; Gao, Hong-Hua; Xu, Yan-Yuan (2013): Metformin inhibits glioma cell U251 invasion by downregulation of fibulin-3. In *Neuroreport* 24 (10), pp. 504–508.

Gao, Lian-Bo; Tian, Shen; Gao, Hong-Hua; Xu, Yan-Yuan (2013): Metformin inhibits glioma cell U251 invasion by downregulation of fibulin-3. In *Neuroreport* 24 (10), pp. 504–508.

Glantz, M. J.; Cole, B. F.; Forsyth, P. A.; Recht, L. D.; Wen, P. Y.; Chamberlain, M. C. *et al.* (2000): Practice parameter: anticonvulsant prophylaxis in patients with newly diagnosed brain tumors. Report of the Quality Standards Subcommittee of the American Academy of Neurology. In *Neurology* 54 (10), pp. 1886–1893.

Gritti, Marta; Wurth, Roberto; Angelini, Marina; Barbieri, Federica; Peretti, Marta; Pizzi, Erika *et al.* (2014): Metformin repositioning as antitumoral agent: selective antiproliferative effects in human GBM stem cells, via inhibition of CLIC1-mediated ion current. In *Oncotarget* 5 (22), pp. 11252–11268.

Gu, Junfei; Ye, Shandong; Wang, Shan; Sun, Wenjia; Hu, Yuanyuan (2014): Metformin inhibits nuclear factor-kappaB activation and inflammatory cytokines expression induced by high glucose via adenosine monophosphate-activated protein kinase activation in rat glomerular mesangial cells in vitro. In *Chinese medical journal* 127 (9), pp. 1755–1760.

Han, Jianfeng; Chen, Xilin; Chu, Jianhong; Xu, Bo; Meisen, Walter H.; Chen, Lichao *et al.* (2015): TGFbeta Treatment Enhances Glioblastoma Virotherapy by Inhibiting the Innate Immune Response. In *Cancer research* 75 (24), pp. 5273–5282. DOI: 10.1158/0008-5472.CAN-15-0894.

Hardie, D. Grahame (2007): AMP-activated/SNF1 protein kinases: conserved guardians of cellular energy. In *Nature reviews. Molecular cell biology* 8 (10), pp. 774–785. DOI: 10.1038/nrm2249.

Hardie, David Grahame (2006): Neither LKB1 nor AMPK are the direct targets of metformin. In *Gastroenterology* 131 (3), 973; author reply 974-5. DOI: 10.1053/j.gastro.2006.07.032.

Hau, Peter; Jachimczak, Piotr; Schlaier, Jurgen; Bogdahn, Ulrich (2011): TGF-β2 Signaling in High-Grade Gliomas. In *CPB* 12 (12), pp. 2150–2157. DOI: 10.2174/138920111798808347.

Hau, Peter; Jachimczak, Piotr; Schlingensiepen, Reimar; Schulmeyer, Frank; Jauch, Tanya; Steinbrecher, Andreas *et al.* (2007): Inhibition of TGF-beta2 with AP 12009 in recurrent malignant gliomas: from preclinical to phase I/II studies. In *Oligonucleotides* 17 (2), pp. 201–212. DOI: 10.1089/oli.2006.0053.

Hawley, Simon A.; Ross, Fiona A.; Chevtzoff, Cyrille; Green, Kevin A.; Evans, Ashleigh; Fogarty, Sarah *et al.* (2010): Use of cells expressing gamma subunit variants to identify diverse mechanisms of AMPK activation. In *Cell metabolism* 11 (6), pp. 554–565. DOI: 10.1016/j.cmet.2010.04.001.

Herbertz, Stephan; Sawyer, J. Scott; Stauber, Anja J.; Gueorguieva, Ivelina; Driscoll, Kyla E.; Estrem, Shawn T. *et al.* (2015): Clinical development of galunisertib (LY2157299 monohydrate), a small molecule inhibitor of transforming growth factor-beta signaling pathway. In *Drug design, development and therapy* 9, pp. 4479–4499. DOI: 10.2147/DDDT.S86621.

Hicks, Martin J.; Chiuchiolo, Maria J.; Ballon, Douglas; Dyke, Jonathan P.; Aronowitz, Eric; Funato, Kosuke *et al.* (2016): Anti-Epidermal Growth Factor Receptor Gene Therapy for Glioblastoma. In *PloS one* 11 (10), e0162978. DOI: 10.1371/journal.pone.0162978.

Houben MP, van Duijn CM, Coebergh JW, Tijssen OC (2005): Gliomas: the role of environmental risk factors and genetic predisposition. In *Tijdschr Geneeskd* (149), pp. 2268–2272.

Idbaih, Ahmed; Ducray, François; Sierra Del Rio, Monica; Hoang-Xuan, Khê; Delattre, Jean-Yves (2008): Therapeutic application of noncytotoxic molecular targeted therapy in gliomas: growth factor receptors and angiogenesis inhibitors. In *The oncologist* 13 (9), pp. 978–992. DOI: 10.1634/theoncologist.2008-0056.

Ikushima, Hiroaki; Todo, Tomoki; Ino, Yasushi; Takahashi, Masamichi; Miyazawa, Keiji; Miyazono, Kohei (2009): Autocrine TGF-beta signaling maintains tumorigenicity of glioma-initiating cells through Sry-related HMG-box factors. In *Cell stem cell* 5 (5), pp. 504–514. DOI: 10.1016/j.stem.2009.08.018.

Isakovic, A.; Harhaji, L.; Stevanovic, D.; Markovic, Z.; Sumarac-Dumanovic, M.; Starcevic, V. *et al.* (2007): Dual antiglioma action of metformin: cell cycle arrest and mitochondria-dependent apoptosis. In *Cellular and molecular life sciences : CMLS* 64 (10), pp. 1290–1302. DOI: 10.1007/s00018-007-7080-4.

Iwadate, Yasuo (2016): Epithelial-mesenchymal transition in GBM progression. In *Oncology letters* 11 (3), pp. 1615–1620. DOI: 10.3892/ol.2016.4113.

Iwadate, Yasuo; Matsutani, Tomoo; Hirono, Seiichiro; Shinozaki, Natsuki; Saeki, Naokatsu (2016): Transforming growth factor-beta and stem cell markers are highly expressed around necrotic areas in GBM. In *Journal of neuro-oncology* 129 (1), pp. 101–107. DOI: 10.1007/s11060-016-2145-6.

Janiszewska, Michalina; Suva, Mario L.; Riggi, Nicolo; Houtkooper, Riekelt H.; Auwerx, Johan; Clement-Schatlo, Virginie *et al.* (2012): Imp2 controls oxidative phosphorylation and is crucial for preserving GBM cancer stem cells. In *Genes & development* 26 (17), pp. 1926–1944. DOI: 10.1101/gad.188292.112.

Jiang, Wei; Finniss, Susan; Cazacu, Simona; Xiang, Cunli; Brodie, Ziv; Mikkelsen, Tom *et al.* (2016): Repurposing phenformin for the targeting of glioma stem cells and the treatment of GBM. In *Oncotarget. DOI:* 10.18632/oncotarget.10919.

Joseph, J. V.; Conroy, S.; Tomar, T.; Eggens-Meijer, E.; Bhat, K.; Copray, S. *et al.* (2014): TGF-beta is an inducer of ZEB1-dependent mesenchymal transdifferentiation in GBM that is associated with tumor invasion. In *Cell death & disease* 5, e1443. DOI: 10.1038/cddis.2014.395.

Joseph, Justin V.; Balasubramaniyan, Veerakumar; Walenkamp, Annemiek; Kruyt, Frank A. E. (2013): TGF-beta as a therapeutic target in high grade gliomas - promises and challenges. In *Biochemical pharmacology* 85 (4), pp. 478–485. DOI: 10.1016/j.bcp.2012.11.005.

Jun, Fu; Hong, Jidong; Liu, Qin; Guo, Yong; Liao, Yiwei; Huang, Jianghai *et al.* (2016): Epithelial membrane protein 3 regulates TGF-beta signaling activation in CD44-high GBM. In *Oncotarget. DOI:* 10.18632/oncotarget.11102.

Kasznicki, Jacek; Sliwinska, Agnieszka; Drzewoski, Józef (2014): Metformin in cancer prevention and therapy. In *Annals of translational medicine* 2 (6), p. 57. DOI: 10.3978/j.issn.2305-5839.2014.06.01.

Kim, Byung-Hak; Han, Songhee; Lee, Haeri; Park, Chi Hye; Chung, Young Mee; Shin, Kyungmin *et al.* (2015): Metformin enhances the anti-adipogenic effects of atorvastatin via modulation of STAT3 and TGF-beta/Smad3 signaling. In *Biochemical and biophysical research communications* 456 (1), pp. 173–178. DOI: 10.1016/j.bbrc.2014.11.054.

Kim, Eui Hyun; Lee, Ji-Hyun; Oh, Yoonjee; Koh, Ilkyoo; Shim, Jin-Kyoung; Park, Junseong *et al.* (2016): Inhibition of GBM tumorspheres by combined treatment with 2-deoxyglucose and metformin. In *Neuro-oncology. DOI:* 10.1093/neuonc/now174.

Kjellman, Christian; Olofsson, Sabine P.; Hansson, Oscar; Schantz, Torbjörn von; Lindvall, Magnus; Nilsson, Ingar *et al.* (2000): Expression of TGF-β isoforms, TGF-β receptors, and SMAD molecules at different stages of human glioma. In *Int. J. Cancer* 89 (3), pp. 251–258. DOI: 10.1002/1097-0215(20000520)89:3<251::AID-IJC7>3.0.CO;2-5.

Kourelis, Taxiarchis V.; Siegel, Robert D. (2012): Metformin and cancer: new applications for an old drug. In *Medical oncology (Northwood, London, England)* 29 (2), pp. 1314–1327. DOI: 10.1007/s12032-011-9846-7.

Krishnan, Shanmugarajan; Szabo, Emese; Burghardt, Isabel; Frei, Karl; Tabatabai, Ghazaleh; Weller, Michael (2015): Modulation of cerebral endothelial cell function by TGF-beta in GBM: VEGF-dependent angiogenesis versus endothelial mesenchymal transition. In *Oncotarget* 6 (26), pp. 22480–22495. DOI: 10.18632/oncotarget.4310.

Kumar P, Naumann U, Aigner L, Wischhusen J, Beier CP, Beier D (2015): Impaired TGF-β induced growth inhibition contributes to the increased proliferation rate of neural stem cells harboring mutant p53. In *Am J Cancer Res*, 5(11):3436-45.

Labuzek, Krzysztof; Suchy, Dariusz; Gabryel, Bozena; Bielecka, Anna; Liber, Sebastian; Okopien, Boguslaw (2010): Quantification of metformin by the HPLC method in brain regions, cerebrospinal fluid and plasma of rats treated with lipopolysaccharide. In *Pharmacol Rep* 62 (5), pp. 956–965.

Lee, Jang Han; Kim, Ji Hyun; Kim, Ja Seon; Chang, Jai Won; Kim, Soon Bae; Park, Jung Sik; Lee, Sang Koo (2013): AMP-activated protein kinase inhibits TGF-beta-, angiotensin II-, aldosterone-, high glucose-, and albumin-induced epithelial-mesenchymal transition. In *American journal of physiology. Renal physiology* 304 (6), F686-97. DOI: 10.1152/ajprenal.00148.2012.

Lee, Nora; Duan, Haichuan; Hebert, Mary F.; Liang, C. Jason; Rice, Kenneth M.; Wang, Joanne (2014): Taste of a pill: organic cation transporter-3 (OCT3) mediates metformin accumulation and secretion in salivary glands. In *The Journal of biological chemistry* 289 (39), pp. 27055–27064. DOI: 10.1074/jbc.M114.570564.

Leitlein, J.; Aulwurm, S.; Waltereit, R.; Naumann, U.; Wagenknecht, B.; Garten, W. *et al.* (2001): Processing of Immunosuppressive Pro-TGF- 1,2 by Human GBM Cells Involves Cytoplasmic and Secreted Furin-Like Proteases. In *The Journal of Immunology* 166 (12), pp. 7238–7243. DOI: 10.4049/jimmunol.166.12.7238.

Liu, Xiaona; Chhipa, Rishi Raj; Pooya, Shabnam; Wortman, Matthew; Yachyshin, Sara; Chow, Lionel M. L. *et al.* (2014): Discrete mechanisms of mTOR and cell cycle regulation by AMPK agonists independent of AMPK. In *Proceedings of the National Academy of Sciences of the United States of America* 111 (4), E435-44. DOI: 10.1073/pnas.1311121111.

Louis, David N.; Ohgaki, Hiroko; Wiestler, Otmar D.; Cavenee, Webster K.; Burger, Peter C.; Jouvet, Anne *et al.* (2007): The 2007 WHO classification of tumours of the central nervous system. In *Acta neuropathologica* 114 (2), pp. 97–109. DOI: 10.1007/s00401-007-0243-4.

Louis, David N.; Perry, Arie; Reifenberger, Guido; Deimling, Andreas von; Figarella-Branger, Dominique; Cavenee, Webster K. *et al.* (2016): The 2016 World Health Organization Classification of Tumors of the Central Nervous System: a summary. In *Acta neuropathologica* 131 (6), pp. 803–820. DOI: 10.1007/s00401-016-1545-1.

Lu, Jiamei; Shi, Jianhua; Li, Manxiang; Gui, Baosong; Fu, Rongguo; Yao, Ganglian *et al.* (2015): Activation of AMPK by metformin inhibits TGF-beta-induced collagen production in mouse renal fibroblasts. In *Life sciences* 127, pp. 59–65. DOI: 10.1016/j.lfs.2015.01.042.

Maheshwari, Rajesh A.; Balaraman, R.; Sen, Ashim K.; Seth, A. K. (2014): Effect of coenzyme Q10 alone and its combination with metformin on streptozotocin-nicotinamide-induced diabetic nephropathy in rats. In *Indian journal of pharmacology* 46 (6), pp. 627–632.

Maile, Edward J.; Barnes, Isobel; Finlayson, Alexander E.; Sayeed, Shameq; Ali, Raghib (2016): Nervous System and Intracranial Tumour Incidence by Ethnicity in England, 2001-2007: A Descriptive Epidemiological Study. In *PLoS ONE* 11 (5), e0154347. DOI: 10.1371/journal.pone.0154347.

Mangani, Davide; Weller, Michael; Seyed Sadr, Emad; Willscher, Edith; Seystahl, Katharina; Reifenberger, Guido *et al.* (2016): Limited role for transforming growth factor-beta pathway activation-mediated escape from VEGF inhibition in murine glioma models. In *Neuro-oncology. DOI:* 10.1093/neuonc/now112.

Mao, Ping; Joshi, Kaushal; Li, Jianfeng; Kim, Sung-Hak; Li, Peipei; Santana-Santos, Lucas *et al.* (2013): Mesenchymal glioma stem cells are maintained by activated glycolytic metabolism involving aldehyde dehydrogenase 1A3. In *Proceedings of the National Academy of Sciences of the United States of America* 110 (21), pp. 8644–8649. DOI: 10.1073/pnas.1221478110.

Marcus, Hani J.; Carpenter, Keri L H; Price, Stephen J.; Hutchinson, Peter J. (2010): In vivo assessment of high-grade glioma biochemistry using microdialysis: a study of energy-related molecules, growth factors and cytokines. In *Journal of neuro-oncology* 97 (1), pp. 11–23. DOI: 10.1007/s11060-009-9990-5.

Massague, J. (2000): How cells read TGF-beta signals. In *Nature reviews. Molecular cell biology* 1 (3), pp. 169–178. DOI: 10.1038/35043051.

Massague, Joan (2008): TGFbeta in Cancer. In *Cell* 134 (2), pp. 215–230. DOI: 10.1016/j.cell.2008.07.001.

Meacham, Corbin E.; Morrison, Sean J. (2013): Tumour heterogeneity and cancer cell plasticity. In *Nature* 501 (7467), pp. 328–337. DOI: 10.1038/nature12624.

Menendez, Javier A.; Quirantes-Piné, Rosa; Rodríguez-Gallego, Esther; Cufí, Sílvia; Corominas-Faja, Bruna; Cuyàs, Elisabet *et al.* (2014): Oncobiguanides: Paracelsus' law and nonconventional routes for administering diabetobiguanides for cancer treatment. In *Oncotarget* 5 (9), pp. 2344–2348.

Moustakas, Aristidis; Heldin, Carl-Henrik (2005): Non-Smad TGF-beta signals. In *Journal of cell science* 118 (Pt 16), pp. 3573–3584. DOI: 10.1242/jcs.02554.

Nakano, Ichiro (2015): Stem cell signature in glioblastoma: therapeutic development for a moving target. In *Journal of neurosurgery* 122 (2), pp. 324–330. DOI: 10.3171/2014.9.JNS132253.

Nana, Andre Wendindonde; Yang, Pei-Ming; Lin, Hung-Yun (2015): Overview of Transforming Growth Factor beta Superfamily Involvement in Glioblastoma Initiation and Progression. In *Asian Pacific journal of cancer prevention : APJCP* 16 (16), pp. 6813–6823.

Narushima, Yuta; Kozuka-Hata, Hiroko; Koyama-Nasu, Ryo; Tsumoto, Kouhei; Inoue, Jun-ichiro; Akiyama, Tetsu; Oyama, Masaaki (2016): Integrative Network Analysis Combined with Quantitative Phosphoproteomics Reveals Transforming Growth Factor-beta Receptor type-2 (TGFBR2) as a Novel

Regulator of GBM Stem Cell Properties. In *Molecular & cellular proteomics : MCP* 15 (3), pp. 1017–1031. DOI: 10.1074/mcp.M115.049999.

Odenthal, Julia; Takes, Robert; Friedl, Peter (2016): Plasticity of tumor cell invasion - governance by growth factors and cytokines. In *Carcinogenesis. DOI:* 10.1093/carcin/bgw098.

Olar, Adriana; Aldape, Kenneth D. (2014): Using the molecular classification of GBM to inform personalized treatment. In *The Journal of pathology* 232 (2), pp. 165–177. DOI: 10.1002/path.4282.

Oliveras-Ferraros, Cristina; Cufi, Silvia; Vazquez-Martin, Alejandro; Torres-Garcia, Violeta Zenobia; Del Barco, Sonia; Martin-Castillo, Begona; Menendez, Javier A. (2011): Micro(mi)RNA expression profile of breast cancer epithelial cells treated with the anti-diabetic drug metformin: induction of the tumor suppressor miRNA let-7a and suppression of the TGFbeta-induced oncomiR miRNA-181a. In *Cell cycle (Georgetown, Tex.)* 10 (7), pp. 1144–1151. DOI: 10.4161/cc.10.7.15210.

Omuro, Antonio; DeAngelis, Lisa M. (2013): GBM and other malignant gliomas: a clinical review. In *JAMA* 310 (17), pp. 1842–1850. DOI: 10.1001/jama.2013.280319.

Ostrom, Quinn T.; Bauchet, Luc; Davis, Faith G.; Deltour, Isabelle; Fisher, James L.; Langer, Chelsea Eastman *et al.* (2014): The epidemiology of glioma in adults: a "state of the science" review. In *Neuro-oncology* 16 (7), pp. 896–913. DOI: 10.1093/neuonc/nou087.

Park, Il-Ho; Um, Ji-Young; Hong, Sung-Moon; Cho, Jung-Sun; Lee, Seung Hoon; Lee, Sang Hag; Lee, Heung-Man (2014): Metformin reduces TGF-beta1-induced extracellular matrix production in nasal polyp-derived fibroblasts. In *Otolaryngology--head and neck surgery : official journal of American Academy of Otolaryngology-Head and Neck Surgery* 150 (1), pp. 148–153. DOI: 10.1177/0194599813513880.

Patel, Anoop P.; Tirosh, Itay; Trombetta, John J.; Shalek, Alex K.; Gillespie, Shawn M.; Wakimoto, Hiroaki *et al.* (2014): Single-cell RNA-seq highlights intratumoral heterogeneity in primary glioblastoma. In *Science (New York, N.Y.)* 344 (6190), pp. 1396–1401. DOI: 10.1126/science.1254257.

Pauleit, Dirk; Floeth, Frank; Hamacher, Kurt; Riemenschneider, Markus J.; Reifenberger, Guido; Muller, Hans-Wilhelm *et al.* (2005): O-(2-18Ffluoroethyl)-L-tyrosine PET combined with MRI improves the diagnostic assessment of cerebral gliomas. In *Brain : a journal of neurology* 128 (Pt 3), pp. 678–687. DOI: 10.1093/brain/awh399.

Penuelas, Silvia; Anido, Judit; Prieto-Sanchez, Rosa M.; Folch, Gerard; Barba, Ignasi; Cuartas, Isabel *et al.* (2009): TGF-beta increases glioma-initiating cell self-renewal through the induction of LIF in human GBM. In *Cancer cell* 15 (4), pp. 315–327. DOI: 10.1016/j.ccr.2009.02.011.

Phase I Factorial Trial of Temozolomide, Memantine, Mefloquine, and Metformin for Post-Radiation Therapy (RT) GBM Multiforme (GBM) - Tabular View - ClinicalTrials.gov. Available online at https://clinicaltrials.gov/ct2/show/record/NCT01430351?term=metformin+AND+glioma&rank=3, checked on 3/6/2015.

Piek, E.; Westermark, U.; Kastemar, M.; Heldin, C. H.; van Zoelen, E. J.; Nister, M.; Dijke, P. ten (1999): Expression of transforming-growth-factor (TGF)-beta receptors and Smad proteins in GBM cell lines with distinct responses to TGF-beta1. In *International journal of cancer* 80 (5), pp. 756–763.

Platten, M.; Wick, W.; Weller, M. (2001): Malignant glioma biology: role for TGF-beta in growth, motility, angiogenesis, and immune escape. In *Microscopy research and technique* 52 (4), pp. 401–410. DOI: 10.1002/1097-0029(20010215)52:4<401::AID-JEMT1025>3.0.CO;2-C.

Pollak, Michael (2013): Potential applications for biguanides in oncology. In *The Journal of clinical investigation* 123 (9), pp. 3693–3700. DOI: 10.1172/JCI67232.

Potten C.S., Loeffler M. (1990): Stem Cells: Attributes, cycles, pitfalls and uncertainties. Lessons for and from the Crypt. In *Development* 110, pp. 1001–1020.

Rich, J. N.; Zhang, M.; Datto, M. B.; Bigner, D. D.; Wang, X. F. (1999): Transforming growth factor-beta-mediated p15(INK4B) induction and growth inhibition in astrocytes is SMAD3-dependent and a

pathway prominently altered in human glioma cell lines. In *The Journal of biological chemistry* 274 (49), pp. 35053–35058.

Riemenschneider, Markus J.; Hirblinger, Maria; Vollmann-Zwerenz, Arabel; Hau, Peter; Proescholdt, Martin A.; Jaschinski, Frank *et al.* (2015): TGF-ss isoforms in cancer: Immunohistochemical expression and Smad-pathway-activity-analysis in thirteen major tumor types with a critical appraisal of antibody specificity and immunohistochemistry assay validity. In *Oncotarget* 6 (29), pp. 26770–26781. DOI: 10.18632/oncotarget.5780.

Riemenschneider, Markus J.; Jeuken, Judith W. M.; Wesseling, Pieter; Reifenberger, Guido (2010): Molecular diagnostics of gliomas: state of the art. In *Acta neuropathologica* 120 (5), pp. 567–584. DOI: 10.1007/s00401-010-0736-4.

Rodon, Laura; Gonzalez-Junca, Alba; Inda, Maria del Mar; Sala-Hojman, Ada; Martinez-Saez, Elena; Seoane, Joan (2014): Active CREB1 promotes a malignant TGFbeta2 autocrine loop in GBM. In *Cancer discovery* 4 (10), pp. 1230–1241. DOI: 10.1158/2159-8290.CD-14-0275.

Sato, Atsushi; Sunayama, Jun; Okada, Masashi; Watanabe, Eriko; Seino, Shizuka; Shibuya, Keita *et al.* (2012): Glioma-initiating cell elimination by metformin activation of FOXO3 via AMPK. In *Stem Cells Transl Med* 1 (11), pp. 811–824. DOI: 10.5966/sctm.2012-0058.

Schebesch, Karl-Michael; Proescholdt, Martin; Hohne, Julius; Hohenberger, Christoph; Hansen, Ernil; Riemenschneider, Markus J. *et al.* (2013): Sodium fluorescein-guided resection under the YELLOW 560 nm surgical microscope filter in malignant brain tumor surgery--a feasibility study. In *Acta neurochirurgica* 155 (4), pp. 693–699. DOI: 10.1007/s00701-013-1643-y.

Schultze, Simon M.; Hemmings, Brian A.; Niessen, Markus; Tschopp, Oliver (2012): PI3K/AKT, MAPK and AMPK signalling: protein kinases in glucose homeostasis. In *Expert reviews in molecular medicine* 14, e1. DOI: 10.1017/S1462399411002109.

Schwartzbaum, Judith A.; Fisher, James L.; Aldape, Kenneth D.; Wrensch, Margaret (2006): Epidemiology and molecular pathology of glioma. In *Nature clinical practice. Neurology* 2 (9), 494-503; quiz 1 p following 516. DOI: 10.1038/ncpneuro0289.

SEER Cancer Statistics Factsheets: Brain and Other Nervous System Cancer. National Cancer Institute. Bethesda, MD, http://seer.cancer.gov/statfacts/html/brain.html. Viewed on Nov. 22nd 2016.

Seliger, Corinna (2013): Auswirkungen der Änderung von LDH-A auf die Funktion der extrazellulären Matrix bei malignen Gliomzellen. Inaugural Dissertation. Universität Regensburg, Regensburg. Lehrstuhl für Neurologie der Fakultät für Medizin.

Seliger, Corinna; Leukel, Petra; Moeckel, Sylvia; Jachnik, Birgit; Lottaz, Claudio; Kreutz, Marina *et al.* (2013): Lactate-modulated induction of THBS-1 activates transforming growth factor (TGF)-beta2 and migration of glioma cells in vitro. In *PLoS ONE* 8 (11), e78935. DOI: 10.1371/journal.pone.0078935.

Seliger, Corinna; Meyer, Anne-Louise; Renner, Kathrin; Leidgens, Verena; Moeckel, Sylvia; Jachnik, Birgit *et al.* (2016): Metformin inhibits proliferation and migration of GBM cells independently of TGF-beta2. In *Cell cycle (Georgetown, Tex.)* 15 (13), pp. 1755–1766. DOI: 10.1080/15384101.2016.1186316.

Sesen, Julie; Dahan, Perrine; Scotland, Sarah J.; Saland, Estelle; Dang, Van-Thi; Lemarie, Anthony *et al.* (2015): Metformin inhibits growth of human GBM cells and enhances therapeutic response. In *PloS one* 10 (4), e0123721. DOI: 10.1371/journal.pone.0123721.

Seystahl, Katharina; Tritschler, Isabel; Szabo, Emese; Tabatabai, Ghazaleh; Weller, Michael (2015): Differential regulation of TGF-beta-induced, ALK-5-mediated VEGF release by SMAD2/3 versus SMAD1/5/8 signaling in GBM. In *Neuro-oncology* 17 (2), pp. 254–265. DOI: 10.1093/neuonc/nou218.

Shu, Yan; Sheardown, Steven A.; Brown, Chaline; Owen, Ryan P.; Zhang, Shuzhong; Castro, Richard A. *et al.* (2007): Effect of genetic variation in the organic cation transporter 1 (OCT1) on metformin action. In *The Journal of clinical investigation* 117 (5), pp. 1422–1431. DOI: 10.1172/JCI30558.

Soritau, O.; Tomuleasa, C.; Aldea, M.; Petrushev, B.; Susman, S.; Gheban, D. *et al.* (2011): Metformin plus temozolomide-based chemotherapy as adjuvant treatment for WHO grade III and IV malignant gliomas. In *Journal of B.U.ON. : official journal of the Balkan Union of Oncology* 16 (2), pp. 282–289.

Stock, Christian; Schwab, Albrecht (2009): Protons make tumor cells move like clockwork. In *Pflügers Archiv : European journal of physiology* 458 (5), pp. 981–992. DOI: 10.1007/s00424-009-0677-8.

Stummer, Walter; Pichlmeier, Uwe; Meinel, Thomas; Wiestler, Otmar Dieter; Zanella, Friedhelm; Reulen, Hans-Jürgen (2006): Fluorescence-guided surgery with 5-aminolevulinic acid for resection of malignant glioma: a randomised controlled multicentre phase III trial. In *The Lancet Oncology* 7 (5), pp. 392–401. DOI: 10.1016/S1470-2045(06)70665-9.

Stupp, Roger; Hegi, Monika E.; Mason, Warren P.; van den Bent, Martin J; Taphoorn, Martin J. B.; Janzer, Robert C. *et al.* (2009): Effects of radiotherapy with concomitant and adjuvant temozolomide versus radiotherapy alone on survival in glioblastoma in a randomised phase III study: 5-year analysis of the EORTC-NCIC trial. In *The Lancet Oncology* 10 (5), pp. 459–466. DOI: 10.1016/S1470-2045(09)70025-7.

Stupp, Roger; Mason, Warren P.; van den Bent, Martin J; Weller, Michael; Fisher, Barbara; Taphoorn, Martin J B *et al.* (2005): Radiotherapy plus concomitant and adjuvant temozolomide for GBM. In *The New England journal of medicine* 352 (10), pp. 987–996. DOI: 10.1056/NEJMoa043330.

Stupp, Roger; Taillibert, Sophie; Kanner, Andrew A.; Kesari, Santosh; Steinberg, David M.; Toms, Steven A. *et al.* (2015): Maintenance Therapy With Tumor-Treating Fields Plus Temozolomide vs Temozolomide Alone for GBM: A Randomized Clinical Trial. In *JAMA* 314 (23), pp. 2535–2543. DOI: 10.1001/jama.2015.16669.

Stupp, Roger; Wong, Eric T.; Kanner, Andrew A.; Steinberg, David; Engelhard, Herbert; Heidecke, Volkmar *et al.* (2012): NovoTTF-100A versus physician's choice chemotherapy in recurrent GBM: a randomised phase III trial of a novel treatment modality. In *European journal of cancer (Oxford, England : 1990)* 48 (14), pp. 2192–2202. DOI: 10.1016/j.ejca.2012.04.011.

Swanson, Kenneth D.; Lok, Edwin; Wong, Eric T. (2016): An Overview of Alternating Electric Fields Therapy (NovoTTF Therapy) for the Treatment of Malignant Glioma. In *Current neurology and neuroscience reports* 16 (1), p. 8. DOI: 10.1007/s11910-015-0606-5.

Thakur, Sachin; Viswanadhapalli, Suryavathi; Kopp, Jeffrey B.; Shi, Qian; Barnes, Jeffrey L.; Block, Karen *et al.* (2015): Activation of AMP-activated protein kinase prevents TGF-beta1-induced epithelial-mesenchymal transition and myofibroblast activation. In *The American journal of pathology* 185 (8), pp. 2168–2180. DOI: 10.1016/j.ajpath.2015.04.014.

Theeler, Brett J.; Gilbert, Mark R. (2015): Advances in the treatment of newly diagnosed glioblastoma. In *BMC medicine* 13, p. 293. DOI: 10.1186/s12916-015-0536-8.

Thomas, Dori A.; Massague, Joan (2005): TGF-beta directly targets cytotoxic T cell functions during tumor evasion of immune surveillance. In *Cancer cell* 8 (5), pp. 369–380. DOI: 10.1016/j.ccr.2005.10.012.

Tian, Maozhen; Schiemann, William P. (2009): The TGF-beta paradox in human cancer: an update. In *Future oncology (London, England)* 5 (2), pp. 259–271. DOI: 10.2217/14796694.5.2.259.

Triscott, Joanna; Lee, Cathy; Hu, Kaiji; Fotovati, Abbas; Berns, Rachel; Pambid, Mary *et al.* (2012): Disulfiram, a drug widely used to control alcoholism, suppresses the self-renewal of GBM and over-rides resistance to temozolomide. In *Oncotarget* 3 (10), pp. 1112–1123.

Tso, Cho-Lea; Freije, William A.; Day, Allen; Chen, Zugen; Merriman, Barry; Perlina, Ally *et al.* (2006): Distinct transcription profiles of primary and secondary GBM subgroups. In *Cancer research* 66 (1), pp. 159–167. DOI: 10.1158/0008-5472.CAN-05-0077.

Uhl, Martin; Aulwurm, Steffen; Wischhusen, Jorg; Weiler, Markus; Ma, Jing Ying; Almirez, Ramona *et al.* (2004): SD-208, a novel transforming growth factor beta receptor I kinase inhibitor, inhibits growth

and invasiveness and enhances immunogenicity of murine and human glioma cells in vitro and in vivo. In *Cancer research* 64 (21), pp. 7954–7961. DOI: 10.1158/0008-5472.CAN-04-1013.

Urbańska, Kaja; Sokołowska, Justyna; Szmidt, Maciej; Sysa, Paweł (2014): GBM multiforme - an overview. In *Contemporary oncology (Poznań, Poland)* 18 (5), pp. 307–312. DOI: 10.5114/wo.2014.40559.

van Meir, Erwin G.; Hadjipanayis, Costas G.; Norden, Andrew D.; Shu, Hui-Kuo; Wen, Patrick Y.; Olson, Jeffrey J. (2010): Exciting new advances in neuro-oncology: the avenue to a cure for malignant glioma. In *CA: a cancer journal for clinicians* 60 (3), pp. 166–193. DOI: 10.3322/caac.20069.

Vander Heiden, M. G.; Plas, D. R.; Rathmell, J. C.; Fox, C. J.; Harris, M. H.; Thompson, C. B. (2001): Growth Factors Can Influence Cell Growth and Survival through Effects on Glucose Metabolism. In *Molecular and Cellular Biology* 21 (17), pp. 5899–5912. DOI: 10.1128/MCB.21.17.5899-5912.2001.

Vander Heiden, Matthew G; Cantley, Lewis C.; Thompson, Craig B. (2009): Understanding the Warburg effect: the metabolic requirements of cell proliferation. In *Science (New York, N.Y.)* 324 (5930), pp. 1029–1033. DOI: 10.1126/science.1160809.

Vazquez-Martin, Alejandro; Oliveras-Ferraros, Cristina; Cufi, Silvia; Del Barco, Sonia; Martin-Castillo, Begona; Menendez, Javier A. (2010): Metformin regulates breast cancer stem cell ontogeny by transcriptional regulation of the epithelial-mesenchymal transition (EMT) status. In *Cell cycle (Georgetown, Tex.)* 9 (18), pp. 3807–3814.

Verhaak, Roel G W; Hoadley, Katherine A.; Purdom, Elizabeth; Wang, Victoria; Qi, Yuan; Wilkerson, Matthew D. *et al.* (2010): Integrated genomic analysis identifies clinically relevant subtypes of GBM characterized by abnormalities in PDGFRA, IDH1, EGFR, and NF1. In *Cancer cell* 17 (1), pp. 98–110. DOI: 10.1016/j.ccr.2009.12.020.

Vescovi, Angelo L.; Galli, Rossella; Reynolds, Brent A. (2006): Brain tumour stem cells. In *Nature reviews. Cancer* 6 (6), pp. 425–436. DOI: 10.1038/nrc1889.

Viollet, Benoit; Guigas, Bruno; Sanz Garcia, Nieves; Leclerc, Jocelyne; Foretz, Marc; Andreelli, Fabrizio (2012): Cellular and molecular mechanisms of metformin: an overview. In *Clinical science (London, England : 1979)* 122 (6), pp. 253–270. DOI: 10.1042/CS20110386.

Wang, Xiao-Fang; Zhang, Jin-Ying; Li, Ling; Zhao, Xiao-Yan (2011): Beneficial effects of metformin on primary cardiomyocytes via activation of adenosine monophosphate-activated protein kinase. In *Chinese medical journal* 124 (12), pp. 1876–1884.

WARBURG, O. (1956): On the origin of cancer cells. In *Science (New York, N.Y.)* 123 (3191), pp. 309–314.

Welch, Mary R.; Grommes, Christian (2013): Retrospective analysis of the effects of steroid therapy and antidiabetic medication on survival in diabetic glioblastoma patients. In *CNS oncology* 2 (3), pp. 237–246. DOI: 10.2217/cns.13.12.

Weller, Michael; Deimling, A. von; Grosu, A.; Hattingen, E.; Hau, P.; Hense, J. *et al.*: S2k-Leitlinie 030/099: Gliome. Stand: 1.3.2014.

Wilcock, C.; Bailey, C. J. (1994): Accumulation of metformin by tissues of the normal and diabetic mouse. In *Xenobiotica* 1994 (24), pp. 49–57. Available online at http://informahealthcare.com/doi/abs/10.3109/00498259409043220, checked on 3/6/2015.

Wild-Bode, C.; Weller, M.; Wick, W. (2001): Molecular determinants of glioma cell migration and invasion. In *Journal of neurosurgery* 94 (6), pp. 978–984. DOI: 10.3171/jns.2001.94.6.0978.

Würth, Roberto; Barbieri, Federica; Florio, Tullio (2014): New molecules and old drugs as emerging approaches to selectively target human GBM cancer stem cells. In *BioMed research international* 2014, p. 126586. DOI: 10.1155/2014/126586.

Würth, Roberto; Pattarozzi, Alessandra; Gatti, Monica; Bajetto, Adirano; Corsaro, Alessandro; Parodi, Alessia *et al.* (2013): Metformin selectively affects human GBM tumor-initiating cell viability: A role for

metformin-induced inhibition of Akt. In *Cell cycle (Georgetown, Tex.)* 12 (1), pp. 145–156. DOI: 10.4161/cc.23050.

Xavier, D. O.; Amaral, L. S.; Gomes, M. A.; Rocha, M. A.; Campos, P. R.; Cota, B D C V *et al.* (2010): Metformin inhibits inflammatory angiogenesis in a murine sponge model. In *Biomedicine & pharmacotherapy = Biomedecine & pharmacotherapie* 64 (3), pp. 220–225. DOI: 10.1016/j.biopha.2009.08.004.

Yu, Yunhu; Ran, Qishan (2015): Nuclear SMAD2 restrains proliferation of GBM. In *Cellular physiology and biochemistry : international journal of experimental cellular physiology, biochemistry, and pharmacology* 35 (5), pp. 1756–1763. DOI: 10.1159/000373987.

Yu, Zhiyun; Zhao, Gang; Xie, Guifang; Zhao, Liyan; Chen, Yong; Yu, Hongquan *et al.* (2015): Metformin and temozolomide act synergistically to inhibit growth of glioma cells and glioma stem cells in vitro and in vivo. In *Oncotarget* 6 (32), pp. 32930–32943. DOI: 10.18632/oncotarget.5405.

Zhang, Jing; Shen, Chengwu; Wang, Lin; Ma, Quanping; Xia, Pingtian; Qi, Mei *et al.* (2014): Metformin inhibits epithelial-mesenchymal transition in prostate cancer cells: involvement of the tumor suppressor miR30a and its target gene SOX4. In *Biochemical and biophysical research communications* 452 (3), pp. 746–752. DOI: 10.1016/j.bbrc.2014.08.154.

Zhang, Xinlin; Zhang, Chengwei; Shen, Shanmei; Xia, Yan jie; Yi, Long; Gao, Qian; Wang, Yong (2013): Dehydroepiandrosterone induces ovarian and uterine hyperfibrosis in female rats. In *Human reproduction (Oxford, England)* 28 (11), pp. 3074–3085. DOI: 10.1093/humrep/det341.

8 APPENDIX

8.1 Table of Abbreviations

°C	Degree Celcius
α	Alpha
$\alpha_V\beta_3$	an Integrin
β	Beta
µ	Micro
µl	Microlitre
µM	Micromolar
2DG	2-desoxy-glucose
4E-BP1	EIf4e Binding Protein
ACC	Acetyl-CoA Carboxylase
Acetyl-CoA	Acetyl-Coenzyme A
ADP	Adenosine Diphoshate
Akt	Refers to a mouse named "Ak", expressing spontaneous lymphomas and "t" thymoma, also Akt PKB protein kinase B
AMP	Adenosine Monophosphate
AMPK	AMP-activated Protein Kinase
Atg13	Autophy-related Protein 13
ATP	Adenosine Triphosphate
bFGF	Basic Fibroblast Growth Factor
Bmi1	Polycomb Complex Protein
BMP	Bone Morphogenic Protein
BTICs	Brain Tumor Initiating Cells
CD	Cluster of Differentiation
CHI3LI	Chitinase 3 like Protein
CI	Combination Index

C-Jun	p39
CLIC1	Chloride Intracellular Channel1
cm	Centimeter
CNS	Central Nervous System
CO_2	Carbon Dioxide
CREB1	CAMP Responsive Element Binding Protein 1
CTLA-4	Cytotoxic T Lymphocyte Antigen
DDIT4	DNA Damage-Inducible Transcript 4 Protein
DEPTOR	DEP Domain-Containing mTOR-Interacting Protein
df	Dilution Factor
DMEM	Dulbecco's Modified Eagle's Medium
DMSO	Dimethylsulfoxide
DNA	Deoxyribonucleic Acid
e.g.	*exempli gratia*
EDTA	Ethylenediaminetetraacetic Acid
EGF	Epidermal Growth Factor
EGFR	Epidermal Growth Factor Receptor
EGFRvIII	Epidermal Growth Factor Receptor Variant III
EIF4e	Eukaryotic Translation Initiation Factor 4E
ELISA	Enzyme-linked Immunosorbent Assay
EMP3	Epithelial Membrane Protein 3
EMT	Epithelial - Mesenchymal Transition
ERK	Extracellular Signal-Regulated Kinase nowadays known as MAPK
et al.	*et alii / et aliae*
f	Female
FCS	Fetal Calf Serum
FET-PET	*O*-(2-[^{18}F]Fluoroethyl)-L-Tyrosine Positron Emission Tomography
FGF	Fibroblast Growth Factor

FOXO3	Forkhead Box Protein O3
G1 Phase	Gap Phase 1
GBM	Glioblastoma
GFAP	Glial Fibrillary Acidic Protein (an Astrocyte Marker)
GFR	Glomerular Filtration Rate
Glc.	Glucose
GβL	G Protein Beta Subunit-Like
h	H(s)
I.p.	Intraperitoneal Administration
IC_{50}	Half Maximal Inhibitory Concentration
IDH	Isocitrate Dehydrogenase
IFN-gamma	Interferon Gamma
IGF	Insulin-like Growth Factor
IgG1	Immunoglobulin G1
IL-8	Interleukin 8
JAK1	Janus Kinase 1
JNK	c-Jun N-Terminal Kinase
kg	Kilogram
LDH	Lactate Dehydrogenase
LIF	Leukemia Inhibitory Factor
LKB1	Liver Kinase 1
LOH	Loss of Heterozygosity
m	Milli / Male / Meter
MAPK	Mitogen-Activated Kinase also known as Ras-Raf-MEK-ERK Pathway

MEK	Raf/Mitogen Activated And Extracellular Signal-Regulated Kinase Kinase
MEM	Minimal Essential Media
MERTK	C-Mer Proto-Oncogene Tyrosine Kinase
Mes.	Mesenchymal
MET	HGFR Hepatic Growth Factor Receptor; CD44 Cluster of Differentiation 44
metf.	Metformin
meth.	Methylated
mg	Milligram
mgmt	O^6-Methylguanine-DNA-Methyltransferase
Migra.	Migration
ml	Milliliter
mm	Millimeter
mM	Millimolar
MMP2	Matrix Metalloproteinase 2
MRI	Magnetic Resonance Imaging
mTOR	Mammalian Target of Rapamycin
mTORC1	Mammalian Target of Rapamycin Complex 1
mut.	Mutated
n.d.	Not Determined
NADPH	Nicotinamide Adenine Dinucleotide Phosphate
NCS	Newborn Calf Serum
neAA	Non Essential Amino Acids
neg.	Negative
NF1	Neuro Fibromatosis 1
NF-kappa B	Nuclear Factor Kappa-Light-Chain-Enhancer of Activated B Cell
ng	Nanogramm
NK	Natural Killer Cells
NKG2D	Natural Killer Group 2D
nM	Nanomolar

OCT	Organic Cation Transporter
Olig2	Oligodendrocyte Transcription Factor 2
OS	Overall Survival
OXPHOS	Oxidative Phosphorylation
P	Passage Number
p	Phosphorylated
P160rock	A Serine/Threonine Protein Kinase
P21	Protein 21
P53	Protein 53
p70s6k	Ribosomal Protein S6 Kinase
PBS	Phosphate Buffer Saline
PD-1	Programmed Cell Death 1
PDGF-B	Platelet Derived Growth Factor B
PDGFRA	Platelet Derived Growth Factor Receptor A
PDL-1	Programmed Cell Death 1 Ligand
PI3K	Phosphoinositide 3-Kinase
PI3KCA	Phosphoinositide 3 Kinase Catalytic Subunit Alpha
PI3KR1	Phosphoinositide 3 Kinase Receptor 1
PIP2	Phosphatidylinositol-4,5-Bisphosphate
PIP3	Phosphatidylinositol-3,4,5-Triphosphate
PKC	Protein Kinase C
PLC	Phospholipase C
pos.	Positive
PP2A	Protein Phosphatase 2
PRAS40	Proline-rich Akt Substrate of 40 kda
prim.	Primary
Pro.	Proneural
Prol.	Proliferation
PTEN	Phosphatase and Tensin Homolog

Ra	Rat Sarcoma
RAF	Rapidly Accelerated Fibrosarcoma
RAG GTPase	Ras-related GTPase
RAPTOR	Regulatory-associated Protein of mTOR
Ras	Rat arcoma
RAV	Regensburg Arabel Vollmann
REDD1	Regulated in Development and DNA Damage Responses 1
RELB	V-Rel Avian Reticulo-Endotheliosis Viral Oncogene Homolog B
Rho	Small GTPases of the Ras Superfamily
ROS	Reactive Oxygen Species
rpm	Rotations per Minute
RPMI1640	Cell Media developed at the Roswell Park Memorial Institute (USA)
R-Smad	Regulatory Small Body Size Mother of Decapentaplegic
S phase	Synthesis Phase
S6K	Ribosomal Protein S6 Kinase
SD-208	2-(5-Chloro-2-Fluorophenyl)-4-[(4-Pyridyl)Amino]Pteridine
Sec.	Secondary
Sox2	Sex Determining Region of Y
STAT1	Signal Transducer and Activator of Transcription 1
STAT3	Signal Transducer and Activator of Transcription 3
T2D	Type 2 Diabetes
TAK1	TGF-β Activated Kinase 1
TCs	Tumor Cells (differentiated);
TGF-β	Transforming Growth Factor Beta
THBS-1	Thrombospondin 1
TIC	Tumor Initiating Cell
TIMP-1	Tissue Inhibitor of Metalloproteinase 1
TMZ	Temozolomide

TNFRSF1A	Tumor Necrosis Factor Receptor Superfamily Member 1A
TNF-α	Tumor Necrosis Factor Alpha
TP53	Tumor Protein 53
TRADD	Gene Encoding for Tumor Necrosis Factor Receptor Type 1-associated DEATH Domain Protein
TSC2	Tuberous Sclerosis Complex Protein 2
TTF	Tumor Treatment Field
UKR	University Hospital Regensburg
unmeth.	Unmethylated
V	Volume
VEGF	Vascular Endothelial Growth Factor
VEGFR	VEGR Receptor
WHO	World Health Organization
wt	Wild-Type

8.2 Table of Figures

Figure 1: Potential mechanisms and sites of metformin's action in cancer cells.....13

Figure 2: Smad-dependent TGF-β signaling.....17

Figure 3: Signaling pathways diverging from and converging on TGF-β signaling 18

Figure 4: Measuring spheroid areas of RAV19 P23_6 control 1 after 0, 20 and 48 hs. 39

Figure 5: Relative proliferation rates of all cell lines after a 48 h treatment with different concentrations of metformin. 42

Figure 6: Relative migratory rates of all cell lines after 20 and after 48 hs of treatment with increasing concentrations of metformin 43

Figure 7: Cell counts after 48 hs of treatment with increasing concentrations of metformin ..44

Figure 8: Comparing the different effect sizes of metformin's anti-proliferative action between proneural and mesenchymal BTICs.....45

Figure 9: Comparing the effects of 10 mM metformin on different groups of cells.....45

Figure 10: Spheroid migration measured after 20 hs of treatment with different concentrations of metformin 46

Figure 11: Spheroid migration measured after 48 hs of treatment with different concentrations of metformin 47

Figure 12: Brain-tumor initiating cells in culture flasks 49

Figure 13: Total cell number per well obtained after treating RAV19 P25 and P26 with different concentrations of metformin for 48 hs.....49

Figure 14: Total cell number per well obtained after treating RAV57 P16 and P18 with different concentrations of metformin for 48 hs.....50

Figure 15: Relative increase of spheroid area of proneural BTICs RAV19 (A) and RAV57 (B) after 48h treatment with different concentrations of metformin.....51

Figure 16: Brain-tumor initiating cells in culture flasks 51

Figure 17: Total cell number per well obtained after treating RAV21 P19 (A), RAV24 P12 and P14 (B and C) and RAV27 P16 and P20 (D) with different concentrations of metformin.....52

Figure 18: Relative increase of spheroid area in mesenchymal BTICs RAV21 (A), RAV24 (B) and RAV27 (C) after 48h treatment with different concentrations of metformin.....53

Figure 19: Differentiated GBM cells in culture flasks.....54

Figure 20: Cell count with total number of cells per well after treatment of RAV19 P23_3 and P23_6 (A) and RAV57 P17_2 and P20_3 (B) with different concentrations of metformin and crystal violet staining assay of RAV57 P20_3 (C). 55

Figure 21: Relative increase of spheroid area in proneural TCs RAV19 (A) and RAV57 (B) with additional data from a scratch migration assay performed with RAV57 P20_8 (C) 56

Figure 22: Differentiated GBM cells in culture flasks. 57

Figure 23: Cell counts with absolute number of cells and crystal violet stainings with proliferation normalized to control.....58

Figure 24: Relative increase of spheroid area in mesenchymal TCs RAV21 (A), RAV24 (B) and RAV27 (C) after 48h treatment with different concentrations of metformin.....60

Figure 26: Effects of TGF-β_2 and its antagonist, SD-208, on migration.....61

Figure 27: Cell counts after 48 hs of treatment 62

Figure 28: Spheroid migration after 20 hs of treatment 63

Figure 29: Spheroid migration after 48 hs of treatment 64

Figure 30: Comparing the effects of 10 ng/ml TGF-β_2 on relative migratory rates of different groups of cells 65

Figure 31: Cell count with total number of cells per well (A and B) and spheroid migration assays (C and D) after treatment with 10 ng/ml TGF-β_2 or with 1 µM SD-208 66

Figure 32: Total cell number per well obtained after treating RAV21 P19 (A), RAV24 P12 and P14 (B and D) and RAV27 P16 and P20 (C) with 10 ng/ml TGF-β_2 or with 1 µM SD-208.....67

Figure 33: Relative increase of spheroid area for mesenchymal BTICs RAV21 P17 and 24 (A), RAV24 P12 and P14 (B) and RAV27 P16 and P20 (C) after 48 hs of treatment with 10ng/ml TGF-β_2 or with 1µM SD-208.....68

Figure 34: Cell counts with total number of cells per well after treatment with 10 ng/ml TGF-β_2 or with 1 µM SD-208.....69

Figure 35: Spheroid migration assays (A and B) and scratch migration assay (C) after treatment with 10 ng/ml TGF-β_2 or with 1 µM SD-208.....70

Figure 36: Total cell number per well obtained after a 48 h treatment with 10 ng/ml TGF-β_2 or with 1 µM SD-208.....71

Figure 37: Relative increase of spheroid area for mesenchymal TCs RAV21 P24_9 and P24_10 (A), RAV24 P10_5 and P10_7 (B) and RAV27 P18_5 and P18_6 (C) after 48 hs of treatment with 10 ng/ml TGF-β_2 or with 1 µM SD-208.....72

Figure 38: Relative proliferation rates of all cell lines after 48 hs of treatment.....74

Figure 39: Relative migratory rates for all cell lines after 20 and after 48 hs of treatment 74

Figure 40: Cell counts after a 48 h treatment.....76

Figure 41: Relative migratory rates after 20 hs of treatment 77

Figure 42: Relative migratory rates after 48 hs of treatment 78

Figure 43: Total cell number per well obtained after 48 hs treatment.....80

Figure 44: Spheroid migration of RAV57 BTICs.....81

Figure 45: Relative increase of spheroid area of proneural BTICs RAV19 P25 and P26 (A) and RAV57 P16 and P18 (B).....82

Figure 46: Spheroid photographs of RAV19 BTICs after 48 hs at 10x magnification 83

Figure 47: Total cell number per well obtained after 48 hs treatment.....84

Figure 48: Spheroid migration of RAV24 BTICs.....86

Figure 49: Relative increase of spheroid area of mesenchymal BTICs RAV21 P17 and P24 (A), RAV24 P12 and P14 (B) and RAV27 P16 and P20 (C).....88

Figure 51: Total cell number per well obtained after 48 hs treatment.....89

Figure 52: Spheroid migration of RAV19 TCs.....90

Figure 53: Relative increase of spheroid area of proneural TCs RAV19 P23_3 and P23_6 (A) and RAV57 P17_2 and P20_3.....91

Figure 54: Spheroid photographs of RAV19 TCs after 120 hs at 10x magnification.....92

Figure 55: Total cell number per well obtained after 48 hs treatment.....93

Figure 56: Spheroid migration of RAV27 TCs.....95

Figure 57: Relative increase of spheroid area of mesenchymal TCs RAV21 P24_9 an P24_10 (A), RAV24 P10_5 and P10_7 (B) and RAV27 P18_5 and P18_6 (C).....96

Figure 58: Spheroid photographs of RAV21 TCs after 48 hs at 10-fold magnification.....97

8.3 Table of Tables

Table 1: Molecular and genetic characteristics of proneural and mesenchymal GBM cells (Verhaak 2010)..... 8

Table 2: Functional effects of metformin on glioma cells.....11

Table 3: List of consumable and supplies.....25

Table 4: List of cell lines used.....26

Table 5: Characteristics of the primary tumors.....27

Table 6: Tumor characteristics in cell culture.....27

Table 7: Patient characteristics.....28

Table 8: Endogenous TGF-β_2 levels of BTICs.....28

Table 9: List of culture media and supplements.....28

Table 10: Overview over media ingredients.....29

Table 11: Additional substances used.....30

Table 12: Additional solutions used.....30

Table 13: List of equipment.....30

Table 14: List of computer software.....31

Table 15: Treatments for proliferation assays.....34

Table 16: Treatment for spheroid migration assays.....38

Table 17: List of symbols indicating significance.....40

Table 18: Review of the anti-proliferative and anti-migratory effects of different concentrations of metformin after 48 hs of treatment.....48

Table 19: Overview over the effects of 10 ng/ml TGF-β_2 and 1 µM SD-208 on proliferation and migration of different groups of GBM cells.....65

Table 20: Overview over functional effects (48 h) of TGF-β_2 and SD-208 on all GBM cell lines.....65

Table 21: Review of the anti-proliferative and anti-migratory effects of metformin, TGF-β_2 and their combinations after 48 hs of treatment.....79

Table 22: Summary of all treatment conditions and their effects on proliferation and migration of all cell lines after 48 h 98

Table 23: The effects of TGF-β on proliferation of different glioma cells 107

Table 24: Proposed mechanisms for metformin's effects on GBM.....116

8.4 Table of Equations

Eqn. 1: Calculation of the cell number in 1 ml of cell suspension..... 33

Eqn. 2: Calculation of the needed volume of treatment solution, step 1..... 35

Eqn. 3: Calculation of the needed volume of treatment solution, step 2..... 35

Eqn. 4: Calculation of the needed volume of treatment solution, step 3..... 35

Eqn. 5: Calculation of the dilution factor, step 1..... 35

Eqn. 6: Calculation of the dilution factor, step 1..... 35

Eqn. 7: Calculation of the cell number in x ml of cell suspension..... 36

8.5 Acknowledgments

I would like to express my gratitude towards all people who contributed to my dissertation:

- My advisor, Prof. Dr. med. Peter Hau, for giving me the opportunity to work on my dissertation in your laboratory group, for our weekly discussion of results and further improvements and your helpful advice.
- My supervising tutor, Dr. med. Corinna Seliger, for your never ending interest in science, for your help and your questions that always motivated me to think further.
- The director of the department of Neurology, Prof. Dr. med. Ulrich Bogdahn, for the opportunity to complete my dissertation at the department of Neurology at the University of Regensburg.
- The head of the laboratory group “NeuroOncology”, Dr.rer.nat Arabel Vollmann-Zwerenz, for your support and your advice in difficult situations.
- Birgit Jachnik, for teaching me with great patience and support, for your help in any situation, for the many tricks you showed to me and for frequent fits of laughter.
- The entire laboratory work group “NeuroOncology”, especially Dr. Verena Leidgens, Dr. Sylvia Möckel, Judith Proske, Patrizia Weigell, Ina Weig-Meckl, Anne Tasler, Suomi Sponton, Ulrieke Tischler, Lisa Rauer and Gabriel Gallo- Oller for your help, your advice, your great work ethic and all the fun we had.
- My flatmate and my friends for always listening and helping me out.
- My family for your consistent interest in the well-being of my cells and the progress of my experiments. Thank you for your unconditional love!